Conservation of Earthen Vernacular Architecture in Ireland

Study of the Mechanical Properties and the Structural Behaviour of Cob

Trinity College Dublin
Coláiste na Tríonóide, Baile Átha Cliath
The University of Dublin

Alejandro Jiménez Rios

Supervisor: Dermot O'Dwyer

Dissertation submitted to the Department of Civil, Structural and Environmental Engineering at Trinity College Dublin in partial fulfilment of the requirements to obtain the degree of:

Doctor of Philosophy

2020

Declaration

I declare that this thesis has not been submitted as an exercise for a degree at this or any other university and it is entirely my own work.

I agree to deposit this thesis in the University's open access institutional repository or allow the library to do so on my behalf, subject to Irish Copyright Legislation and Trinity College Library conditions of use and acknowledgement.

_____

Alejandro Jiménez Rios

2020

Abstract

Cultural heritage is increasingly threatened not only by traditional causes of decay, but also by changing social, economic and environmental conditions. The deterioration or disappearance of any cultural item constitutes a harmful impoverishment of our heritage. Besides, culture has been recognized as an enabler and driver of sustainable development, peace and economic progress, which highlights the necessity of fostering its documentation, protection, and promotion. For all these reasons, working in the conservation of our cultural heritage should not only be justified but encouraged.

The general objective of this PhD thesis is to contribute with the efforts to achieve Target 11.4 of the Sustainable Development Goals (SDG), adopted by the United Nations (UN) in 2015, by strengthening the efforts to protect and safeguard the world's cultural and natural heritage. The aim of the research is to increase awareness regarding the importance of vernacular architecture and its intrinsic values, as identified on the International Council of Monuments and Sites (ICOMOS) Action Plan for the Future. It specifically focuses on the improvement of earthen architectural heritage conservation, as this group of structures is particularly vulnerable to environmental and anthropologic threats.

The thesis presents a summarized and concise picture of the present situation of the remaining earthen buildings in Ireland, identifies their main characteristics, the values that make such buildings important, evaluates their vulnerability as vernacular architectural style and therefore, allows to understand and better approach any future intervention on such kinds of structures.

Within the context of current conservation practice, which is based on a scientific approach and implements a cyclic method of research, diagnosis, intervention and control activities, the thesis contributes to the development of quantitative research methods. A first contribution is presented on the structural analysis of cob by evaluating the suitability of available constitutive material to model its non-linear structural behaviour using two of the most commonly used Finite Element Method (FEM) software in the market, ANSYS and ABAQUS.

A second contribution is concerned with the experimental testing of cob. A Minor Destructive Test (MDT) known as the flat jack test, has been experimentally validated by testing it in a series of cob wallettes built in the laboratory of Civil, Structural and Environmental Engineering (CSEE) at Trinity College Dublin (TCD). The purpose of the experimental campaign was to assess the feasibility of the technique to measure the average compressive levels of stress in existent cob walls and estimate their mechanical properties. The principal results show that effectively the test can be applied in cob walls but it tends to overestimate the stress values by a factor of approximately two. As conclusion, it is advised to correct the average compressive stress, f_m, by using a value for the dimensionless geometrical efficiency constant, K_e, of 0.51. The use of a more realistic value would prevent the design and application of over invasive interventions that may place in danger the value of the historical fabric. The double flat jack tests allowed to estimate the mechanical parameters of the material to a good degree of certainty.

Finally, a parametric analysis of cob walls is presented with the aim of providing conservation practitioners with rule of thumb guidance to assess the safety of existent cob buildings under seismic actions. The methodology presented in this regard is not limited to the Irish context but could as well be implemented in different countries where the seismic hazard represents an actual threat for the structural safety of remaining vernacular cob buildings.

Para Don Abel…

Acknowledgements

Thank you to my supervisor, Dermot O'Dwyer, for have given me the required freedom to perform this PhD and for helping me getting some of the funding needed to cover the corresponding expenses.

Mil gracias a las Profesoras Sara Pavia y Maria Nogal. Sin su guía, ayuda, consejos, motivación y amistad a todo lo largo de estos tres años este proyecto nunca se hubiera llevado a cabo. En especial, gracias por haber organizado y facilitado la estancia de investigación que lleve a cabo en el verano del 2018 en la Universidad de Cantabria en Santander, España.

De igual forma gracias a los Profesores Luis Villegas e Ignacio Lombillo quienes amablemente me recibieron en la Universidad de Cantabria. El conocimiento compartido por el Profesor Lombillo fue de suma importancia para el excito alcanzado en la campaña experimental realizada durante este proyecto de investigación.

The completion and success of the experimental campaign performed during this PhD would never had been achieved without the help and support of all staff from the Department of Civil, Structural and Environmental Engineering at Trinity College Dublin. Thanks a million to Mary Curley and Daniel Warren for all the help they provided me to deal with the numerous bureaucratic issues I came across. How could I not thank the invaluable help of all technical staff? I am in debt with David McAuley, Michael Grimes, Patrick Veale, Eoin Dunne and Mark Gilligan for all the patience, understanding, advice, and good moments they shared with me during my laboratory work, which, despite had been the most enjoyable part of my PhD, I must admit was also the one that gave me the bigger number of sleepless nights.

Thank you as well to Becky Little, Francois Streiff and to all the organizers of the International BASEhabitat Summer School in which I participated and learned the amazing traditional skills needed to prepare the specimens of my experimental campaign. I tried to transmit such skills to other people as well, thus, thank you to all the people that participated in the workshops and visits I organized during my PhD.

Special acknowledgements go to all my colleagues. The people with whom I shared almost every single day of the last three years of my life and were always there in the good moments and, more importantly, the bad ones. Thanks as well to other friends, especially to my former SAHC classmates, with whom I regularly shared and discussed the progress of my PhD and always helped and supported me.

Finalmente me gustaría agradecer el apoyo de mi familia que, desde lejos, nunca dejo de motivarme y darme razones para seguir adelante. Los amo.

Table of contents

List of figures

Chapter 1

Chapter 2

Chapter 3

Chapter 4

Chapter 5

Chapter 6

Chapter 7

List of tables

Chapter 1

Chapter 2

Chapter 3

Chapter 4

Chapter 5

Chapter 6

Chapter 7

List of acronyms

Analysis of Variance	ANOVA
American Society for Testing and Materials	ASTM
Central Composite Design	CCD
Concrete Damage Plasticity	CDP
Compressed Earthen Blocks	CEB
European Committee for Standardization	CEN
Confidence Interval	CI
International Scientific Committee on Vernacular Architecture	CIAV
Coefficient of Variation	COV
International Centre on Earthen Architecture	CRATerre
Cob Research Institute	CRI
Concrete Smeared Cracking	CSC
Civil, Structural and Environmental Engineering	CSEE
Central Statistics Office	CSO
Department of Culture, Heritage and the Gaeltacht	DCHG
Department of Transport, Tourism and Sport	DTTS
Discontinuity Layout Optimization	DLO
Discrete Element Method	DEM
Damage Evolution	DMGE
Damage Initiation	DMGI
Design of Experiments	DOE
Destructive Test	DT
Dublin Technical University	DTU
Earthen Architecture Initiative	EAI
Embodied Carbon	EC
Equilibrium Moisture Content	EMC
European Macroseismic Scale	EMS
Inventory of Carbon and Energy	ICE

National Superior School of Architecture of Grenoble	ENSAG
Finite Element Method	FEM
Free Vibration Tests	FVT
Gross Value Added	GVA
International Council on Monuments and Sites	ICOMOS
International Centre for the Study of the Preservation and Restoration of Cultural Property	ICCROM
International Residential Code	IRC
International Scientific Committees	ISC
International Scientific Committee on Analysis and Restoration of Structures of Architectural Heritage	ISCARSAH
International Scientific Committee on Earthen Architectural Heritage	ISCEAH
International Organization for Standardization	ISO
International Union for Conservation of Nature	IUCN
Linear Programming	LP
Linear Variable Differential Transformer	LVDT
List of World Heritage in Danger	LWHD
Minor Destructive Test	MDT
Multilinear Isotropic Hardening	MISO
Non-Destructive Test	NDT
National Inventory of Architectural Heritage	NIAH
New Integrated Knowledge based approaches to the protection of cultural heritage from Earthquake–induced Risk	NIKER
National Monuments Service	NMS
Over Consolidation Ratio	OCR
Office of Public Works	OPW
Particle Size Distribution	PSD
Reunion Internationale des Laboratoires et Experts des Materiaux	RILEM
Serviceability Limit State	SLS
Standard Deviation	SD
Sustainable Development Goals	SDG
Seismic Hazard Harmonization in Europe	SHARE
Smooth Particle Hydrodynamics	SPH

Seismic Retrofitting Project	SRP
Trinity College Dublin	TCD
Total Strain Rotating Crack Model	TRSCM
Unconfined Compressive Strength	UCS
Ultimate Limit State	ULS
Universal Beam	UB
University of British Columbia	UBC
University of Cantabria	UC
University College Dublin	UCD
United Kingdom	UK
United Nations	UN
United Nations Educational, Scientific and Cultural Organization	UNESCO
UNESCO World Heritage Centre	UWHC
Volumetric Heat Capacity	VHC
Vernacular Heritage National Scientific Committee	VHNSC
Variance Inflation Factor	VIF
World Heritage Committee	WHC
World Heritage Earthen Architecture Programme	WHEAP
World Heritage Fund	WHF
World Heritage List	WHL

List of symbols

a	Ground acceleration
a_{CCD}	Axial spacing of the design points
c	Cohesion
d	Distance from wall edge to the idealised location of N
d'_t	Regularised damage variable at the end of the last sub step
$d_{t+\Delta t}$	Non-regularised current damage variable
$d'_{t+\Delta t}$	Regularised damage variable at current time
f	Fundamental frequency of vibration
f_1	Ultimate compressive strength for a state of biaxial compression superimposed on hydrostatic stress state
f_2	Ultimate compressive strength for a state of uniaxial compression superimposed on hydrostatic stress state
f_c	Compressive strength
f_{cb}	Ultimate biaxial compressive strength
f_m	Average compressive stress in the fabric
f_{mi}	Cumulative stress at a point i
f_s	Shear strength
f_t	Tensile strength
f_y	Yielding strength
g	Gravity acceleration
g_v	Energy dissipated per unit volume
h	Crack-band width or equivalent length
k	Number of factors
p	Pressure in the flat jack required to restore the initial distance between gauge points
t	Distance from wall edge to idealised support
u	Pore water pressure
u_0	Characteristic crack length

w	Moisture content
w_L	Liquid limit
w_P	Plastic limit
$\bar{A}_{je}$	Average of the effective area of both slots
$\bar{A}_{slot}$	Average area of the two slots
A	Flat jack width
A_{elem}	Element area
A_{je}	Effective area of the slot
A_{slot}	Area of slot
B	Flat jack linear depth
C	Vertical distance between flat jacks
$C1$	Energy dissipated per unit area from tensile fiber damage
$C2$	Viscous damping coefficient for tensile fiber damage
$C3$	Energy dissipated per unit area from compressive fiber damage
$C4$	Viscous damping coefficient for compressive fiber damage
$C5$	Energy dissipated per unit area from tensile matrix damage
$C6$	Viscous damping coefficient for tensile matrix damage
$C7$	Energy dissipated per unit area from compressive matrix damage
$C8$	Viscous damping coefficient for compressive matrix damage
C_C	Coefficient of curvature
C_U	Uniformity coefficient
$D60, D50, D30, D10$	PSD percentages
E	Young's modulus
E_{si}	Secant (RILEM) or Chord (ASTM) modulus at a point i
E_t	Tangent modulus
F	Function of principal stress state
F_{CCD}	Number of points in the factorial part of the design
F_{us}	Ultimate safety factor
F_{ys}	Yielding safety factor
G_c	Fracture energy in compression

G_f	Fracture energy per unit area
${G_f}^I$	Fracture energy in tension
H_0	Null hypothesis
H_{wall}	Wall Height
I_C	Consistency index
I_L	Liquidity index
I_P	Plasticity index
K	Ratio of the second invariant on the tensile meridian to that on the compressive meridian
K_a	Ratio of the area of the flat jack to the measured area of the slot
K_e	Dimensionless geometrical efficiency constant
K_m	Dimensionless constant based on the geometrical deformability properties of the flat jack
L	Gauge length (distance between control points for the flat jack test)
L_e	Characteristic length of the element
L_{wall}	Wall length
N	External loads transferred from the roof
P	Wall self-weight
R	Flat jack radius
R^2	Coefficient of determination
R^t	Reduced secant modulus
S	Failure surface expressed in terms of principal stresses
S_r	Restoring stress value
S_{ut}, S_{uc}	Material ultimate tensile and compressive strengths
S_{yt}, S_{yc}	Material yielding tensile and compressive strengths
T_c	Tensile stress relaxation multiplier
T_{wall}	Wall thickness
U_e	Equivalent displacement
U_e^f	Ultimate equivalent displacement
α	Seismic mass multiplier

β_c	Shear transfer coefficient for a closed crack
β_t	Shear transfer coefficient
γ	Weight density
γ_{cob}	Cob's density
δf_m	Increment of stress
$\delta \varepsilon_m$	Increment of strain
ϵ	Eccentricity
ε^{max}	User defined maximum strain
ε_{0c}^{el}	Elastic strain
ε_c	Total strain
ε^{ck}	Strain corresponding to the tensile strength of the material
ε_{mi}	Cumulative strain at a point i
ε_{pl}	Plastic strain
$\tilde{\varepsilon}_c^{in}$	Inelastic strain
ε_{ult}	Ultimate crack strain
ε_y	Yield strain
ζ	Equivalent viscous damping ratio
η	Viscous damping coefficient
μ_1, μ_2	Group means
ν	Poisson's ratio
ξ_4	Hashin's fibre failure criterion
ξ_5	Hashin's matrix failure criterion
ρ	Bulk density
ρ_{CSC}	CSC multiplying factor
ρ_d	Dry density
ρ_s	Particle density or specific gravity
σ	Total stress
σ'	Effective stress
$\sigma_1, \sigma_2, \sigma_3$	Principal stresses
σ_{b0}	Initial equibiaxial compressive yield stress
σ_{c0}	Initial uniaxial compressive yield stress
σ_e	Equivalent stress

σ_p'	Pre-consolidation pressure
σ_t^u	Failure stress
σ_{v0}'	Effective overburden pressure
$\sigma_x, \sigma_y, \sigma_z$	Normal stresses
$\sigma_{xc}^f, \sigma_{yc}^f$	Failure stress in compression for the x and y directions
$\sigma_{xt}^f, \sigma_{yt}^f$	Failure stress in tension for the x and y directions
$\sigma_{xy}^f, \sigma_{yz}^f$	Failure shear stresses in the xy and yz directions
$\sigma_{xy}, \sigma_{xz}, \sigma_{yz}$	Shear stresses
τ	Shear strength of a soil
φ	Macroscopic angle of friction
φ'	Effective macroscopic angle of friction
ψ	Dilation angle
Δt	Time increment

Chapter 1: Introduction

1.1 Context

On October 25th, 2015 the General Assembly of the United Nations (UN) adopted a resolution aiming at transforming our world: the 2030 Agenda for Sustainable Development. The resolution envisaged the creation of 17 interrelated Sustainable Development Goals (SDG) and 169 specific targets based on the economic, social and environmental dimensions of sustainable development. SDG 11 aims at making cities and human settlements inclusive, safe, resilient and sustainable. Within this framework, Target 11.4 has as objective strengthening the efforts to protect and safeguard the world's cultural and natural heritage (United Nations, 2015b).

> *Cultural heritage refers to monuments, groups of buildings and sites with historical, aesthetic, archaeological, scientific, ethnological or anthropological value (UNESCO WHC, 2008).*

The United Nations Educational, Scientific and Cultural Organization (UNESCO) is the worldwide organisation in charge of promoting the equal dignity of all cultures and the conservation of cultural heritage. In 1972, the adoption of the Convention Concerning the Protection of the World Cultural and Natural Heritage led to the establishment of the World Heritage Committee (WHC), the World Heritage Fund (WHF) and to the creation of the World Heritage List (WHL) in which the first twelve sites were inscribed in 1978 (UNESCO, 1972). The number of inscribed sites on the WHL has been increasing each year ever since. In 2010, there were 890 sites enlisted (UNESCO, 2010) and at the time this thesis was written (July 2019) the list comprised 1121 sites in 167 countries (UNESCO, 2019).

The creation of a second heritage list was also previewed by the 1972 Convention. The aim of this second list is to identify world heritage sites in danger. Known as the List of World Heritage in Danger (LWHD), it lists the sites that require major interventions

to ensure their conservation (UNESCO, 1972). The number of sites inscribed in the LWHD has been constantly increased. In July 2019 a total of 36 cultural sites were considered in danger (UNESCO, 2019).

By adopting the World Heritage Convention in 1972 the Member States of UNESCO, Ireland among them, acquired the responsibility of identifying, protecting, conserving and presenting the world's heritage. To guide the Member States, the WHC published and periodically revises a series of Operational Guidelines (UNESCO WHC, 2016). Moreover, in 1992 the UNESCO World Heritage Centre (UWHC) was created. The UWHC is responsible for the day-to-day management of the Convention and the administration of the WHF.

The WHC is advised by three bodies; the International Union for Conservation of Nature (IUCN), the International Council on Monuments and Sites (ICOMOS) and the International Centre for the Study of the Preservation and Restoration of Cultural Property (ICCROM). ICCROM, founded in 1956 (UNESCO, 1956), provides expert advice on how to conserve sites on the WHL, as well as on training in restoration techniques (UNESCO WHC, 2016). ICOMOS, established in 1965 after the adoption of the Venice Charter (ICOMOS, 1964), promotes the doctrine and the techniques of conservation. ICOMOS provides the WHC with evaluations of properties proposed for inscription on the WHL, as well as with comparative studies, technical assistance and reports on the state of conservation of inscribed properties (UNESCO WHC, 2016).

In 2008, during the 15th ICOMOS General Assembly, a series of principles were adopted to define the role and goals of International Scientific Committees (ISC) (ICOMOS, 2008). ISC contribute to the protection and management of the world heritage by gathering, studying and disseminating information related to principles, techniques and policies on conservation. There are 28 ISC (ICOMOS, 2018). Of special interest for this thesis is the work carried out by the International Scientific Committee on Analysis and Restoration of Structures of Architectural Heritage (ISCARSAH), the International Scientific Committee on Earthen Architectural Heritage (ISCEAH) and the International Scientific Committee on Vernacular Architecture (CIAV).

In 1998, UNESCO established a Chair on Earthen Architecture, Construction Cultures and Sustainable Development to foster the dissemination of scientific and technical know-how on earthen architecture focusing mainly in two different areas:

environment and world heritage, and environment and human settlements/housing. This Chair is led by the International Centre on Earthen Architecture (CRATerre) located at the National Superior School of Architecture of Grenoble (ENSAG) (Guillaud, 2010).

1.1.1 World Heritage Earthen Architecture Programme (WHEAP)

A specific group of heritage structures is particularly vulnerable: structures built using earthen construction techniques. This group of buildings is greatly threatened by both natural and human impacts. Earthen architecture sites account for up to 25 % of the enlisted sites on the LWHD (UNESCO, 2007). The main factors affecting world heritage earthen architecture include:

- Floods and earthquakes.
- Industrialization.
- Urbanization.
- Modern building technologies.
- Disappearance of traditional conservation practices.

Aiming at developing policies for the conservation, revitalization and increased awareness of earthen architecture properties in 2001, the WHC approved the establishment of the WHEAP. The WHEAP had the enhancement of the conservation, presentation and management of earthen architectural heritage as mission. The main technical partners involved with the WHEAP were CRATerre-ENSAG, ICCROM and ICOMOS (UNESCO, 2007).

One of the deliverables of this project was an inventory of world heritage earthen architecture. The inventory identified the presence of earth materials in 150 buildings on the WHL (as for 2012). Furthermore, an investigation was carried out as a collaboration between WHC, ISCEAH and CRATerre-ENSAG with the managers of those sites, which was based on a questionnaire structured around four subjects: types and methods of construction, current status of the property, threats affecting the property, and priorities of action (Gandreau and Delboy, 2012).

The inventory also highlighted the use in percentage of the four main earthen construction techniques studied; namely, rammed earth, adobe, wattle and daub, and cob

(a description of these and other earthen construction techniques is provided in section 2.2). As shown in Figure 1. 1, cob was present in 6 % of the 150 WHL earthen architecture sites of the inventory, but in reality, the use of cob was mentioned by 29 of the managers that replied to the survey. Hence, almost 20 % of WHL earthen architecture sites involve cob. Those sites are listed in Table 1. 1 and their worldwide distribution is presented in Figure 1. 2.

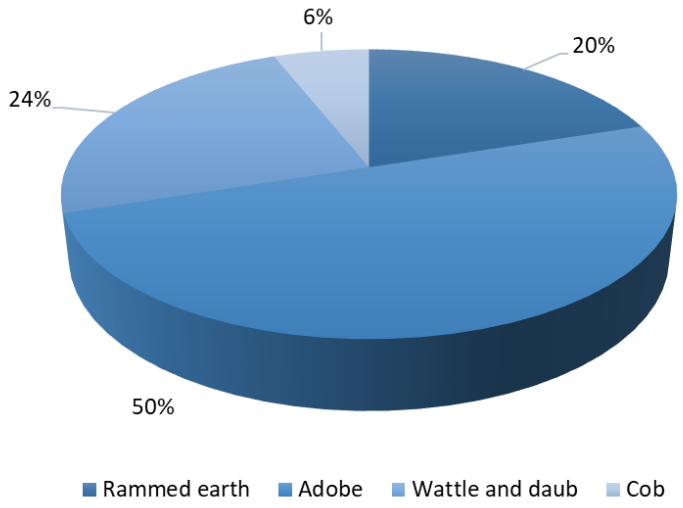

Figure 1. 1. Percentage of use of the different earthen construction techniques on the listed sites studied on the inventory of world heritage earthen architecture (Gandreau and Delboy, 2012).

1.1.2 The Irish context

Ireland is a Member State of the UN and of UNESCO. As such, it has adopted the 1972 Convention and agreed to embrace the concept of sustainable development and also to identify, protect, conserve, present and transmit to future generations the cultural and natural heritage of the world (UNESCO WHC, 2016).

An ICOMOS National Committee was founded in 1984 in Ireland (ICOMOS Ireland, 1984). Of special interest for this thesis is the Vernacular Heritage National Scientific Committee (VHNSC) created in 2012 following the Dubrovnik-Valletta principles (ICOMOS, 2009).

At a regional level, Ireland has acknowledged the Convention for the Protection of the Architectural Heritage of Europe, signed in Granada Spain on October 1985 (Council of Europe, 1985). In this document, the principles and obligations of the signatories concerned with the identification of properties for their preservation and with the implementation of established statutory protection procedures are detailed.

Table 1. 1. List of Earthen Architecture UNESCO Sites in which cob is present (Gandreau and Delboy, 2012).

Country	Site name	# of sites
Benin	Royal Palaces of Abomey	1
Burkina Faso	Ruins of Loropéni	1
Ghana	Asante Traditional Buildings	1
Madagascar	Royal Hill of Ambohimanga	1
Mali	Cliff of Bandiagara (Land of the Dogons)	1
Nigeria	Osun-Osogbo Sacred Grove	2
	Sukur Cultural Landscape	
Libya	Old Town of Ghadamès	1
Yemen	Old City of Sana'a	1
Iran	Bam and its Cultural Landscape	2
	Soltaniyeh	
Tajikistan	Proto-urban Site of Sarazm	1
Japan	Historic Monuments of Ancient Kyoto (Kyoto, Uji and Otsu Cities)	2
	Historic Monuments of Ancient Nara	
Republic of Korea	Haeinsa Temple Janggyeong Panjeon, the Depositories	2
	Historic Villages of Korea: Hahoe and Yangdong	
Uzbekistan	Itchan Kala	1
France	Historic Site of Lyons	1
Brazil	Historic Centre of Sao Luís	4
	Historic Centre of the Town of Diamantina	
	Historic Centre of the Town of Goiás	
	Historic Town of Ouro Preto	
El Salvador	Joya de Cerén, Archaeological Site	1
Colombia	Coffe Cultural Landscape of Colombia	1
Cuba	Viñales Valley	1
Mexico	Archaeological Zone of Paquimé, Casas Grandes	4
	Historic Centre of Morelia	
	Historic Town of Guanajuato and Adjacent Mines	
	Historic Centre of Oaxaca and Archaeological Zone of Monte Alban	

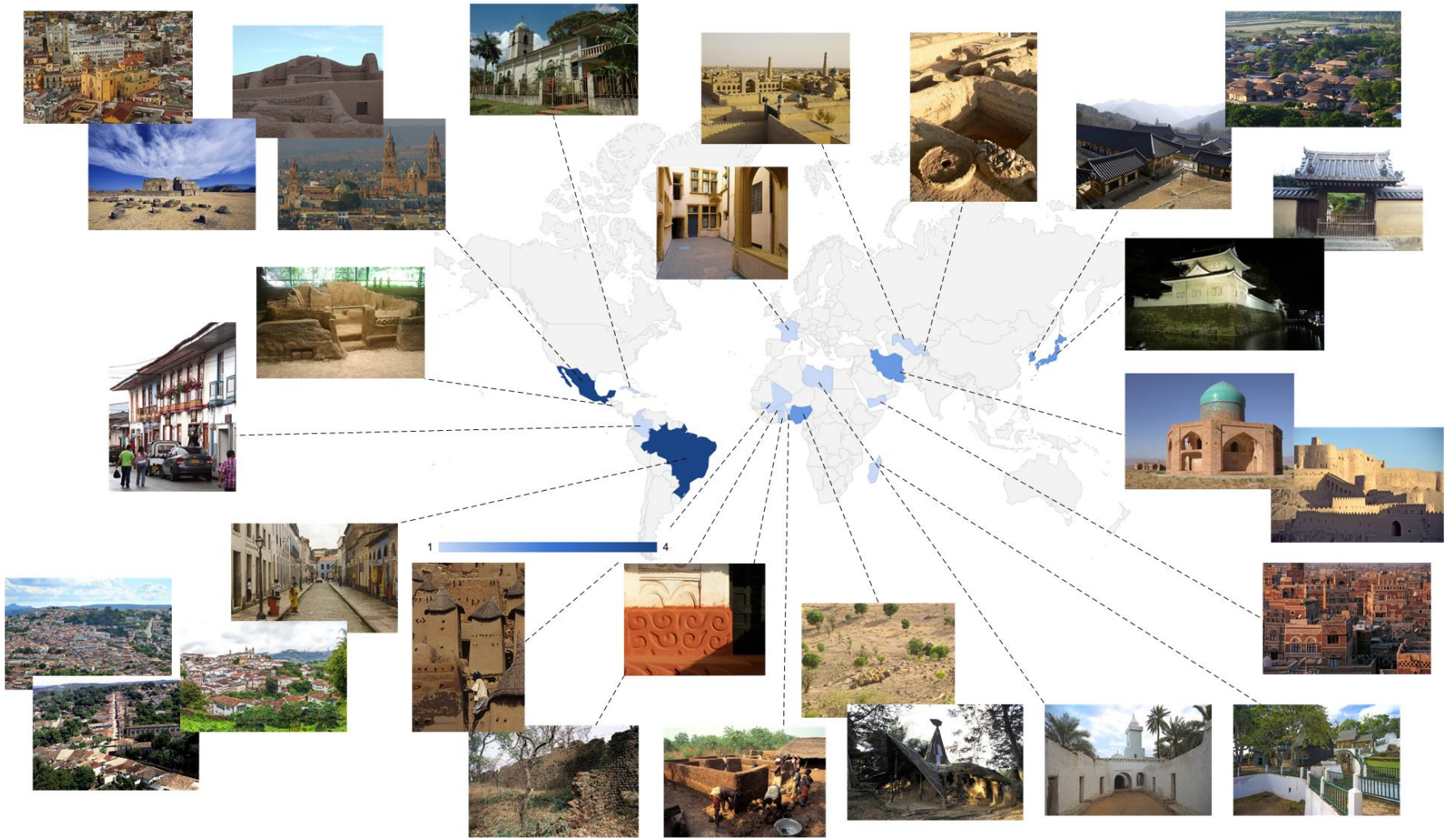

Figure 1. 2. Distribution of Earthen Architecture UNESCO Cultural Heritage Sites in which cob is present (Gandreau and Delboy, 2012). Photos' credits: (UNESCO WHC, 2018).

At a national level, the minister in charge of heritage is the Department of Culture, Heritage and the Gaeltacht (DCHG). This department has adopted two main legislations concerned with historic buildings: the National Monuments Act 1930-2004, which deals with the protection of historic monuments (DCHG, 1954, 1987, 1994, 2004, 2019), and the Planning and Development Acts 2000-2016, where the measures affecting historic buildings are part of a comprehensive framework (Oireachtas, 2000, 2002, 2006, 2010, 2015, 2016).

In Ireland, the Office of Public Works (OPW) oversees the operational functions and the management of the national built heritage which includes 750 national monuments and over 20 historic properties. Its main duty is the ownership, upkeep and maintenance of historic buildings in the country (O'Rourke, 2016).

Another important organization is the National Monuments Service (NMS). This governmental body is responsible of the identification and designation of monuments, the implementation of legislative provisions concerning the protection of monuments and sites, the implementation of protective and regulatory controls, and the provision of heritage input and advice to planning authorities (O'Rourke, 2016).

In 1995, a Heritage Council was created to propose policies and priorities for the protection, preservation and enhancement of the national heritage (Oireachtas, 1995). Moreover, Local Authorities in need of advice and assistance in relation to preservation and protection of monuments can establish their own Historic Monuments Advisory Committee if they consider it appropriate. Finally, in 1999 a National Inventory of Architectural Heritage (NIAH) was formally established to evaluate and record the architectural heritage of Ireland and facilitate sharing such information with planning authorities to inform their choices in the designation of its protection (Oireachtas, 1999).

It is within this context of international organizations' cooperation and of national legislation that the present thesis has been framed. Furthermore, its development has been highly influenced by the philosophies, principles and guidance developed throughout the more than 85 years of efforts aiming at the effective protection of our world cultural heritage.

1.2 Motivation

Cultural heritage is of outstanding interest and, therefore, it needs to be preserved.

> *Heritage is defined as our legacy from the past, what we live with today, and what we pass on to future generations (United Nations, 2018b).*

Cultural heritage is increasingly threatened with destruction not only by traditional causes of decay, but also by changing social and economic conditions. The deterioration or disappearance of any item of cultural heritage constitutes a harmful impoverishment of our heritage. Stakeholders should be motivated to pursuit cultural heritage preservation as it:

- Promotes social cohesion and intercultural dialogue.
- Creates a collective identity and sense of belonging.
- Encourages participation in political and cultural life.
- Empowers marginalised groups.
- Promotes economic development.
- Supports planning, infrastructure and the making of public spaces.
- Contributes to placemaking, understanding of city's history and the valorisation of urban spaces.
- Contributes to climate change resilience.

Gradually, culture has been recognized as an enabler and driver of sustainable development, peace and economic progress (UNESCO, 2013). The emergence of the creative economy demonstrates its relevance for the economic and social well-being of countries. The cultural and creative industries account for over 30 million jobs worldwide. The creative economy contributes to 6.1 % of the global economy, representing USD 4.3 trillion per year (United Nations, 2018b). Moreover, safeguarding cultural traditions can also help to revive local economies and to create job opportunities in rural settlements (United Nations, 2018b).

This thesis is mainly concerned with the conservation of earthen vernacular cultural heritage. One of the reasons that motivated the study of vernacular architecture in this thesis came from the results published by the 2005 ICOMOS report on The World

Heritage List, Filling the Gaps – an Action Plan for the Future (ICOMOS, 2005). As can be seen in Figure 1. 3, vernacular architecture in Europe is greatly underrepresented in comparison with monumental architecture. Therefore, part of this work aims at researching and identifying vernacular heritage in Ireland to increase awareness of its value and of the efforts required for its preservation. This motivation is in alignment with the objective of creating a more representative, balanced and credible WHL in accordance with the WHC's Global Strategy.

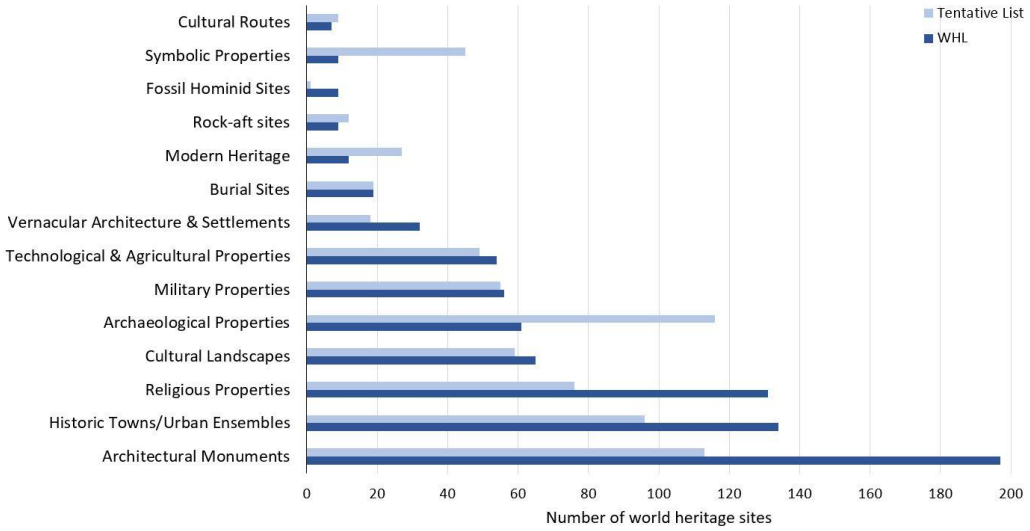

Figure 1. 3. Typological comparison of WHL and Tentative Lists on Europe and North America (ICOMOS, 2005).

Another incentive that influenced the scope of the thesis is the fact that earth is not always recognized as an important element of heritage. As highlighted on the World Heritage Inventory of Earthen Architecture:

> *"… on some archaeological sites, built elements in earth were sometimes entirely removed, leaving only meagre traces (as is the case with the upper terrace of the palace of Persepolis)" (Gandreau and Delboy, 2012).*

According to the Inventory, the state of conservation of earthen properties in Europe is insufficient. This is attributed mainly to the lack of staff, and more specifically, to the lack of knowledge and specialized personnel that could implement better adapted strategies and restoration techniques. To deal with the natural degradation phenomena and with the negative climate change effects that affect 47 % and 37 % of the assets

respectively, efforts need to be made to increase the education and training of both conservators and technical staff on the conservation of earthen structures.

The objectives of the thesis were also motivated by the research needs identified by the WHEAP (UNESCO, 2007); namely, the need to develop new assessment and conservation methods for earthen architectural heritage. To satisfy those needs WHEAP advised to perform:

a) Laboratory research on raw materials, stabilization and damp migration.

b) Applied research and documentation.

c) Experimentation using prototype samples and other methods.

d) Thematic seminars with site managers and earthen architectural conservation specialists.

Finally, it was decided to develop a project on the conservation of earthen vernacular buildings in Ireland, as the conservation of cultural heritage is desirable as it represents an important segment of the national economy. The historic environment directly supports around 25,000 jobs and 40,000 indirect or induced jobs (ECORYS, 2011). Heritage, both natural and cultural, in Ireland contributes annually with around €1.5 billion of its Gross Value Added (GVA) (ECORYS, 2011). Cultural heritage contributes 1 % of the total Irish GVA and about 2 % of its overall employment (ECORYS, 2011).

1.3 Objectives

1.3.1 General objective

The general objective of this thesis is to contribute with the efforts to achieve Target 11.4 of the SDG adopted by the UN in 2015. The scope of the project is limited to the study of the conservation of Irish earthen vernacular buildings. Within this framework the aim is to increase awareness regarding the value of vernacular architecture, as identified on the ICOMOS Action Plan for the Future (ICOMOS, 2005), and to improve the conservation of earthen architectural heritage, as this group of structures is particularly vulnerable to environmental and anthropologic impacts. More precisely, this thesis aims at contributing to a better understanding of the mechanical properties and the structural

behaviour of cob and to enhance the structural assessment and diagnosis of existent cob buildings in Ireland.

1.3.2 Specific objectives

To achieve the general objective of this thesis a series of specific objectives were set:

- To present a summarised and concise picture of the present situation of the remaining earthen buildings in Ireland, identify their main characteristics, the values that make such buildings important, evaluate their vulnerability as a vernacular architectural style and, therefore, understand and better approach any future intervention on such structures.
- To evaluate the available constitutive material models' suitability for the modelling of cob's structural behaviour in two of the most commonly used Finite Element Method (FEM) programs in the market.
- To experimentally validate the use in cob walls of a Minor Destructive Test (MDT) known as the flat jack test, performed to determine in-situ the levels of stress in the structure and the mechanical properties of the material of existent walls.
- To develop a parametric analysis of cob walls to provide conservation practitioners with rule-of-thumb guidance on the level of safety assessment of existent cob buildings subjected to seismic loads.

1.4 Thesis outline

The present thesis is divided into seven chapters. A summary of the information presented in each one of them is given hereafter:

Chapter 1: Details the context within which the thesis has been framed. It describes the institutional development of the field of conservation from the beginning of the 20th century until today. It lists the main organisations dealing with the conservation of cultural heritage. The facts that justify the development of the thesis are also highlighted in the motivation section. The general and specific objectives that the thesis tries to accomplish are indicated. Finally, a summarised description of the content of each chapter is provided.

Chapter 2: Presents the literature review and state of the art in the fields of conservation, earthen construction techniques and vernacular architecture. Current practice in the field of conservation is explained at the beginning of the chapter. In the second section, a general description of the different earthen construction techniques used around the world is given. A more detailed description is dedicated to cob, as this is the main construction technique used to build the surviving earthen buildings in Ireland. Cob is also one of the construction methods used in Irish earthen buildings being built in recent years. Research published on the mechanical properties and the structural behaviour of cob is of special interest for this thesis and thus is deal with in more detail. Finally, a description of vernacular architecture is provided and the main factors affecting its survival are highlighted.

Chapter 3: This chapter contains the results of a thorough literature review process on the remaining earthen vernacular buildings in Ireland. Historical context, social, cultural and economic aspects are described. Based on this information, the authenticity of this group of historical buildings is defined.

Chapter 4: Contains part of the new contributions of this thesis to the state of knowledge. This chapter presents the results obtained of the simulation of cob's non-linear monotonic behaviour using two well-known FEM commercial packages. Furthermore, a mesh size sensitivity analysis was performed following a mesh refinement approach. Pros and cons of different available constitutive material models are identified and discussed.

Chapter 5: Another important contribution of this thesis is presented in chapter 5. Here the experimental campaign carried out on the use of the flat jack test and the methodology adopted are presented. The construction process of the cob wallettes, the procedure of the tests and the data obtained are presented and discussed. The suitability of this technique to determine the levels of stress in cob walls and to obtain the mechanical properties of the material is assessed.

Chapter 6: This chapter contains the last contribution of the thesis to the field of conservation of earthen structures. Here a parametric analysis is presented where the effect of the values of certain parameters in the response of existent cob walls subjected to seismic loads is evaluated. A series of rules for easy application on a day-to-day basis

is presented. This may represent an attractive option for conservation practitioners and researchers to obtain an initial approximation of the safety level of existent cob walls.

Chapter 7: Finally, chapter 7 contains the conclusions obtained from the work presented on this thesis. Moreover, a list of proposed future work to continue developing the knowledge on the conservation of cob structures is included. During the PhD period several publications were produced, both in scientific journals and international conferences. These are listed at the end of this chapter.

Chapter 2: State of the art and literature review

This chapter includes state of the art information and current practice concepts about the fields of conservation, earthen construction techniques and vernacular architecture based on the literature review process performed. Within each section, a general explanation of the topic is provided. More importantly, those concepts directly related to the contributions presented in this thesis are treated in more detail and respective gaps in the knowledge are highlighted.

2.1 Conservation approach

The practice of monuments and historical buildings conservation is based on a set of principles and guidelines broadly accepted and applied by the international community. The Venice Charter, adopted in 1964 by the 2nd International Congress of Architects and Technicians of Historic Monuments, is the main reference document of the present conservation approach. After its adoption, a series of other Charters complementing the Venice Charter and addressing specific subjects have also been developed and adopted. The main concepts related to the conservation of earthen vernacular buildings are found within the following documents:

- The Venice Charter (ICOMOS, 1964).
- The Nara Document on Authenticity (ICOMOS, 1994).
- The Charter on the Built Vernacular Heritage (ICOMOS, 1999).
- The Principles and Guidelines for the Analysis, Conservation and Structural Restoration of Architectural Heritage ((ICOMOS, 2003a, 2003b)).
- The Burra Charter: the Australia ICOMOS Charter for Places of Cultural Significance (ICOMOS, 2013).

2.1.1 The Venice Charter

Two important predecessors of the Venice Charter are the Athens Charter (ICOMOS, 1931) and the 1st International Congress of Architects and Specialists of Historic Buildings organized at Paris in 1957 (ICOMOS, 1980). The discussion of those documents is outside of the scope of this thesis but the reader is invited to consult the references provided.

The Venice Charter was adopted at the 2nd Congress of Architects and Specialists of Historic Buildings as a consequence of the acknowledgment of the responsibility to safeguard ancient monuments as a common heritage that represents the unity of human values. It is a revision of the Athens Charter, in which the basic principles of preservation and restoration were defined for the first time.

A historical monument is defined in this charter as any architectural work, urban or rural setting in which is found evidence of a particular civilization, a significant development or a historic event. This document encourages the application of all available sciences and techniques to achieve the conservation and restoration of historical monuments, both as works of art and as historical evidence.

The permanent maintenance of historical monuments is of paramount importance for their conservation. Thus, conservation is better achieved if monuments are kept in use and constantly maintained. Any intervention on a historical monument must preserve and reveal its aesthetic and historical values. New constructions, demolitions, modifications or moving of all or part of a monument must not be allowed unless it is absolutely necessary for the safeguarding of the monument itself or justified by national or international interest of outstanding importance.

The aim of a restoration, which always has to be preceded and followed by a documentation process, is to perpetuate and expose the relevant values of a monument. The use of original construction techniques and materials are preferred but the use of modern materials and techniques to consolidate a monument can be allowed if their efficacy has been proved by scientific data and experience and only if the use of traditional techniques proves to be inadequate. The Venice Charter also recognises the value of the different period contributions of a monument and dictates respect towards them during restorations. In case replacements are necessary for the restoration of a monument, they must be integrated harmoniously with the whole and at the same time be

distinguishable with the aim of facilitating the study of the building´s history. Furthermore, the charter recognises that additions should be forbidden except under very specific conditions were the values of the monument are not compromised.

Finally, the Venice Charter established that all interventions performed on historical monuments should be carefully documented by analytical and critical reports, which should be published and made available for other researchers.

2.1.2 The Burra Charter

This charter provides guidance for the conservation and management of natural, indigenous and historic places of cultural significance. It places special importance on the principle of inter-generational equity, which requires that places of cultural significance must be preserved for present and future generations.

To achieve conservation success, the Burra Charter advises a three-level process in which the significance of the place should be understood first. Once its significance is clear and well defined, a conservation policy is developed and consequently the site has to be managed in accordance with this policy. The significance of a cultural site is defined by its authenticity, which is defined within the Nara Document of Authenticity (ICOMOS, 2013).

2.1.3 The Nara Document on Authenticity

The cultural heritage of each is the cultural heritage of all (ICOMOS, 1994).

The Nara Document on Authenticity, adopted in 1994, extends and complements the Venice Charter. It deals with the concept of authenticity in conservation practice, highlights the importance of cultural and heritage diversity, and provides guidance on how to assess and determine the values of heritage to be safeguarded for future generations.

In conservation practice, authenticity helps to "*clarify and illuminate the collective memory of humanity*" (ICOMOS, 1994) and plays a major role in all scientific studies of the cultural heritage, in its conservation and restoration planning. No fixed criteria to define authenticity can be established since every culture attributes values based on different judgements. To assess authenticity, form and design, materials and

substance, use and function, traditions and techniques, location and setting, spirit and feeling, as well as other external and internal factors must be studied and understood (see Figure 2. 1).

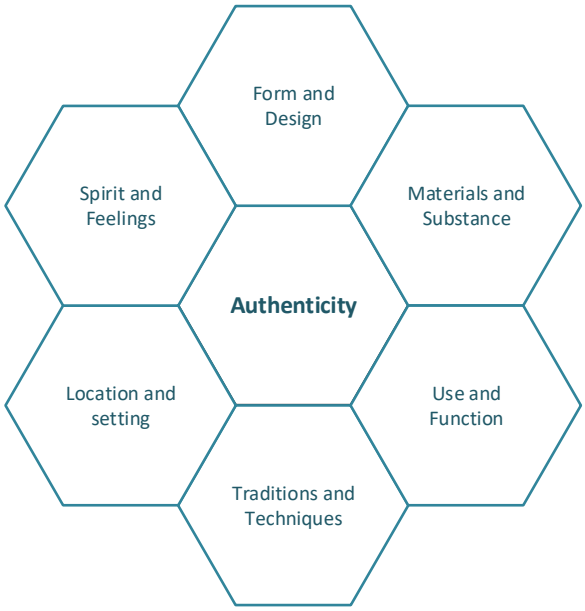

Figure 2. 1. Authenticity values according to the Nara Document (ICOMOS, 1994).

2.1.4 The Charter on the Built Vernacular Heritage

Of special interest for this thesis are the concepts, principles and guidelines defined in the Charter on the Built Vernacular Heritage, ratified in Mexico in 1999. In this Charter, vernacular architecture is defined as:

> *The fundamental expression of the culture of a community, of its relationship with its territory and, at the same time, the expression of the world´s cultural diversity (ICOMOS, 1999).*

Examples of vernacular architecture include different types of community building traditions with a local or regional character, a coherence of style, form and appearance, which effectively satisfy a series of functional, social and environmental needs and for which the know-how is usually transferred from generation to generation. The Charter recognises that the survival of the built vernacular heritage is threatened worldwide by economic, cultural and design homogenisation. To achieve its conservation, the involvement and support of communities, governments and multidisciplinary specialists must foster the continuing use of the vernacular buildings and their permanent maintenance.

The Charter of the Built Vernacular Heritage reinforces the principles of conservation stated in the Venice Charter regarding the multidisciplinary character of the interventions and the respect of their cultural values and traditional character. On the other hand, this Charter differentiates the specific characteristics associated with vernacular architecture in comparison with other heritage typologies. It emphasises the fact that vernacular architecture is better preserved as a regional group or regional settlements, it gives importance to the relationship of such buildings with their cultural landscape and most importantly, it recognises the importance of the intangible values usually attached to vernacular buildings as a result of the way in which they are used and understood.

Conservation guidelines regarding research and documentation, siting, landscape and groups of buildings, the replacement of materials and parts, adaptations, changes and restoration in this Charter are in agreement with the Venice Charter. Complementing guidelines are given regarding the importance of the craft skills and training for the conservation of the built vernacular heritage. It is recognized that the continuity of craft skills is fundamental and essential for the repair and restoration of vernacular structures. The Charter suggests the preservation, recording and transfer of vernacular craftsmanship through education and training. It encourages governments, authorities and organizations to create education, training and information programmes to improve public awareness of the vernacular, assist communities in the conservation of traditional systems, materials and craft skills, and to disseminate the principles of vernacular conservation. It also encourages the creation of regional networks to exchange expertise and experiences on vernacular heritage.

As part of ICOMOS Ireland, the VHNSC was created with the aim of fostering the conservation of vernacular architecture in Ireland by:

- Promoting its documentation assessment, interpretation, conservation and management.
- Encouraging awareness of vernacular architecture among the general public and government institutions.
- Providing a platform for dialogue and cooperation on the conservation of vernacular heritage between professionals, experts, academics and students through meetings, fieldtrips, conferences, workshops and lectures.
- Applying a multidisciplinary conservation approach.

- Integrating the knowledge and expertise of its members to provide expert advice to ICOMOS Ireland on vernacular heritage matters.
- Establishing best practice and standards for the training and qualification of those engaged in vernacular heritage documentation, assessment, conservation and management.
- Collaborating with ICOMOS and CIAV, as well as with other bodies, government agencies or institutions with similar objectives.

Nevertheless, the VHNSC is constituted by only eight members and the last activity reported in its website was carried out in 2014. Moreover, no publications nor a programme of works are available online (ICOMOS Ireland, 2019). These facts testify to a lack of interest at a national level regarding the conservation of the built Irish vernacular architecture and indicate that more efforts should be made in future years in order to achieve the objectives of the VHNSC and an adequate conservation of the vernacular cultural heritage of the country.

Formal educational programmes dealing with vernacular architecture are also very rare in Ireland. The Department of Civil, Structural and Environmental Engineering (CSEE) at Trinity College Dublin (TCD) offers a Postgraduate Diploma in Applied Building Repair and Conservation, which has been approved and accredited by Engineers Ireland and by The Royal Institute of the Architects of Ireland (Trinity College Dublin, 2019b). Despite the fact that the programme covers the topic of vernacular architecture, not enough importance is given to the subject. Only one session out of twenty-four is dedicated to its study. To comply with the recommendation of the Charter of the Built Vernacular Heritage, more courses dealing with the conservation of vernacular architecture should be introduced into the curricula of the universities and colleges of the country both at undergraduate and postgraduate levels.

2.1.5 Principles and Guidelines for the Analysis, Conservation and Structural Restoration of Architectural Heritage

The application of modern codes and building standards in the study of cultural heritage is limited and often leads to excessive measurements of intervention. The Principles for the Analysis, Conservation and Structural Restoration of Architectural Heritage, adopted

by ICOMOS in 2003, were created to provide conservation professionals with suitable guidelines regarding methods of analysis and repair of cultural heritage.

The Principles recognize and reinforce the criterion of a multidisciplinary approach to work on cultural heritage established in the Venice Charter. This document also highlights the importance of values and authenticity of the cultural heritage defined in the Nara Document. The Principles complement previous conservation documents by conferring importance to all the components of the structure and not only to its appearance. Moreover, they prescribed to take into account all previously established conservation requirements and safety conditions whenever a change of use or function is proposed for a historical building. They acknowledge that the restoration of the structure of a historical building is not an end in itself, but a mean to preserve the building as a whole.

An iterative process is prescribed in the Principles to achieve cost effectiveness and minimal impact when working with architectural heritage. This process consists of four phases: research, diagnosis, intervention and control. No intervention should be allowed without having a clear idea of the damage or benefits that it will provoke to the structure. Finally, the Principles allow for the implementation of urgent measurements to safeguard heritage structures from imminent collapse, but advices to avoid modifying in an irreversible way the original fabric of the building.

The conservation process of cultural heritage is usually compared with the study of a patient in medicine (Onsiteformasonry Project, 2005, Lombillo, 2010). The stages usually performed by doctors are the anamnesis, where the patient is directly explored and subjected to a series of tests with the aim of collecting information about the possible causes of his symptoms. The evaluation of all the collected data and its interpretation leads to the diagnosis of the patient when a possible illness is identified. Then, a treatment, where the patient is given medicines or therapy, is set-up. Finally, the patient progress is monitored to assess the efficacy of the treatment. The whole process can be run iteratively in case the treatment is not satisfactory and needs to be improved or in future cases where the patient eventually falls sick with another illness. The recommendations of having a healthy and balanced diet, do exercise, avoiding smoking, etc. are analogous to the permanent maintenance advised for architectural heritage to keep the building in a good state and avoid damage and decay (ICOMOS, 2003a).

Research

The research stage of the conservation process must be done by a multidisciplinary team following an incremental approach. During a first study, basic data and information should be collected and roughly processed. Based on this first information, a more comprehensive plan of activities should be established. An incremental approach allows for an efficient management of available, and very often scarce, resources.

A new two stage research methodology has been recently developed by universities and cultural organizations within the HeritageCare Interreg European project (Heritage Care, 2017b, 2017a, 2017c). The first stage defines the typical damages observed in the built environment and the second stage defines the methodology of inspection, diagnosis and advice to owners in order to achieve a preventive conservation of cultural heritage buildings. Regardless of the south/western European regional scope of the HeritageCare project, this methodology could easily be adopted and applied in any other country, especially Ireland, based on the characteristics it shares with these countries.

The aim of research during the conservation process is to obtain a full understanding of the structural and material characteristics of the building. The necessary information can be collected following three different approaches: historical, qualitative and quantitative. The historical approach involves collecting information on the original and earlier states of the structure, the construction techniques used, past interventions and/or alterations of the building. The qualitative approach is based on direct observation of the structural damage and material decay, together with a comparison of the structure under study with similar ones which have been previously studied. Finally, the quantitative approach is based on material and structural tests, monitoring and structural analysis (see Figure 2. 2).

The main contributions of this thesis address the quantitative approach of the research stage of the conservation process. More specifically, the thesis contains novel material on the material testing and the structural analysis of cob, an earthen construction technique used traditionally in Ireland to build most of the remaining earthen vernacular buildings in the country.

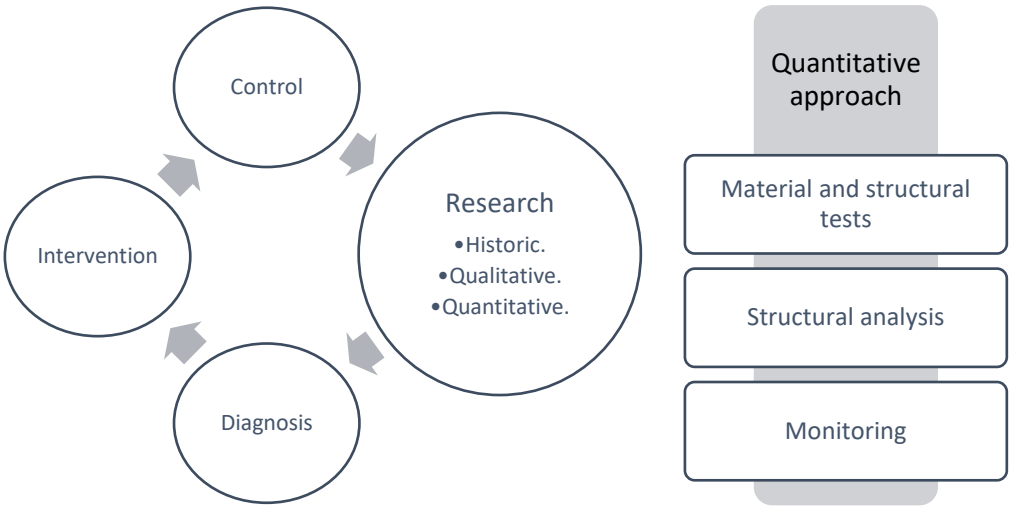

Figure 2. 2. Iterative process for the study of heritage structures.

Diagnosis

The two main objectives of the diagnosis stage are: to determine the causes of damage and to assess the level of safety of the structure. Historic, qualitative and quantitative analysis should be reconciled during diagnosis to achieve such objectives and to prescribe the necessary intervention measurements. The use of different approaches to determine the safety levels of existent structures in comparison to those used for the design of new structures is justified by the use of specific analyses and appropriate considerations. Finally, it is advised that all aspects of the research and diagnosis process should be described in an explanatory report.

Intervention

The best type of intervention on a historical structure is preventive maintenance. In cases were damage has appeared, remedial measures should address its causes rather than its symptoms. Interventions must be based on safety evaluation assessments and be respectful of the authenticity and significance of the structure. Furthermore, interventions should be kept to a minimum, follow an incremental approach, be reversible, maintain compatibility with existing materials and be based on a clear understanding of the kind of actions that were the cause of the damage and decay.

The choice between traditional and innovative techniques should be weighed up on a case-by-case basis, always respecting the distinguishability of the original and/or earlier states of the structure. Interventions should be the result of an overall integrated

plan and must respect the concept, techniques and historical value of the original and earlier states of the structure. Repairing is preferred to replacing. Moreover, dismantling and reassembly should only be taken as an optional measure. No actions should be undertaken without demonstrating that they are indispensable.

Control

Any proposal for intervention must be accompanied by a control program and measures that are impossible to control during execution, should not be allowed. Monitoring should be done during and after interventions to evaluate the efficacy of the works. As for previous stages of the process, all control activities should be documented.

2.1.6 Research (anamnesis)

The research stage of the conservation iterative process is discussed in more detail in this section as the main contributions of this thesis aim at improving the state of knowledge within this topic. Within this context, an overview of the tools currently used for the structural analysis of historic buildings is presented, as well as a detailed description of the flat jack test.

The information collected during the conservation research stage is used to determine the chemical, physical, durability and mechanical properties of the historic fabric. To obtain the mechanical properties of the fabric three different types of test can be performed: Non-Destructive Test (NDT), MDT and Destructive Test (DT). The mechanical properties thus obtained are then used to define the constitutive materials' parameters for the numerical simulation models implemented during the structural analysis stage, which serve to assess the safety level of the structure under study.

NDT are preferred for the investigation of monuments and historical construction, as they do not damage the fabric of the buildings. Unfortunately, NDT techniques can only provide qualitative results that need to be calibrated and require of a lot of experience to be correctly interpreted. On the other hand, some MDT techniques directly provide data and values of the properties of the materials necessary to perform structural analysis and assess the safety level of the structure. MDT cause limited damage to the fabric, but such damage can frequently be easily repaired. The use of DT on architectural heritage is

not desirable, since due to its nature the material employed in the test is destroyed and with it, part of the original fabric and historical value of the building.

The implementation of any research technique should always be justified by a risk-benefit analysis. Table 2. 1 presents a classification of the most common tests available nowadays based on their nature. The use of every test is also shortly described and the reference of the correspondent standard or recommendation for each test is provided in case further reading is desired.

Most of the techniques mentioned in Table 2. 1 have been developed and applied to concrete or different types of masonry. Very few of them have been applied to earthen materials. Research on earthen architecture has been mainly focused on the study of the adobe technique. With a lower frequency, some research has been done on rammed earth buildings. Unfortunately, only few of the techniques presented in Table 2. 1 have been validated or applied to cob structures. This is one of the gaps of knowledge detected during the literature review stage of the thesis. Table 2. 2 summarizes the different available MDT techniques and whether or not they have been applied to research the mechanical properties of earthen historical buildings.

2.1.7 Flat jack test

The flat jack test is one of the most used MDT techniques for the study of historical buildings as it provides information, related to the levels of stress and the deformability properties of the fabric, necessary to assess the structures' current condition. It can also be applied for control purposes while interventions are being carried out (Boffill *et al.*, 2019) and the damage caused by the test can be easily repaired (Gregorczyk and Lourenço, 2000).

Table 2. 1. Common tests available to determine the mechanical properties of materials in historical buildings.

Type	Name	Use	Standard/Recommendation
NDT	Impact-echo	Used to determine wall thickness, to detect leaf detachment, to locate voids and deteriorated areas and to measure cracks. Although limited, the correlation of sonic velocity could give the compressive strength of the material.	(ASTM International, 2015a)
	Thermography	Used to locate voids, irregularities and plaster delamination, to investigate the structure behind plasters and to detect moisture near surfaces.	(ASTM International, 2013b)
	Ultrasonic	Used to determine wall thickness, to locate voids, and in a limited way, to characterize cracks and to correlate the ultrasonic velocity with the compressive strength of the material.	(ASTM International, 2015b)
	Pulse sonic	Used to quantify the material morphology, to detect the presence of voids or flaws and cracks or damage patterns. Also used to assess the effectiveness of repairs.	(RILEM, 1997)
	Ground Penetrator Radar	Used to locate voids or inclusions of different objects within the material.	(ASTM International, 2011)
	Geoelectrical tomography	Used to detect the presence of moisture or voids through anomalies of the resistivity of the material.	(Onsiteformasonry Project, 2005)
	Micro-seismic Shear Waves	Used to describe the elastic dynamic properties of the material.	(Onsiteformasonry Project, 2005)
MDT	Single flat jack	Used to determine the level of stress in the structure. Could also be used to monitor the levels of stress during an intervention.	(ASTM International, 2009) & (RILEM, 2004a)
	Double flat jack	Used to determine Young's modulus, Poisson's ratio and compressive strength of the material.	(ASTM International, 2014) & (RILEM, 2004b)
	Shove	Used to determine the shear strength of the material.	(ASTM INternational, 2016)
	Hole drilling	Used to estimate the stress field in the surface of the structure.	(ASTM International, 2013c)
	Dilatometer	Used to estimate the flexural strength and the pressuremeter modulus of the material.	(Lombillo, 2010)
	Pull off test	Used to determine the tensile strength of the material.	(ASTM International, 2013a) & (British Standard, 2016b)
DT	Simple compression	Used to determine Young's modulus, Poisson's ratio and compressive strength of the material.	(British Standard, 1999) & (RILEM, 1994a)
	Diagonal compression	Used to determine shear modulus and shear strength of the material.	(ASTM International, 2015c)
	Flexural	Used to determine flexural strength of the material.	(British Standard, 2016b) & (RILEM, 1994b)
	Shear-compression	Used to determine shear modulus and shear strength of the material.	(ASTM International, 2012) & (RILEM, 1994c)

Table 2. 2. MDT techniques on earthen buildings.

MDT	Adobe	Rammed earth	Cob
Single flat jack	(Briceño *et al.*, 2018), (Tacas *et al.*, 2019) (Lombillo, 2010), (Rufo, 2010), (Xavier, 2011), (Tacas Guillen, 2018), (Filipe, 2012), (Domingos, 2010)	(Lombillo, 2010), (Lombillo *et al.*, 2013), (Lombillo *et al.*, 2014)	*
Double flat jack	(Briceño *et al.*, 2018), (Lombillo, 2010), (Tacas *et al.*, 2019), (Manzoni *et al.*, 2019), (Rufo, 2010), (Xavier, 2011), (Tacas Guillen, 2018), (Filipe, 2012), (Domingos, 2010),	(Lombillo, 2010), (Giamello *et al.*, 2016), (Parsekian *et al.*, 2019), (Lombillo *et al.*, 2013), (Lombillo *et al.*, 2014)	*
Shove	(Dowling *et al.*, 2004), (Dowling *et al.*, 2005)	*	*
Hole drilling	(Lombillo, 2010)	(Lombillo, 2010), (Lombillo *et al.*, 2013), (Lombillo *et al.*, 2014), (Lombillo *et al.*, 2018)	*
Dilatometer	(Lombillo, 2010)	(Lombillo, 2010), (Lombillo *et al.*, 2013), (Lombillo *et al.*, 2014)	*
Pull off test	(Miccoli *et al.*, 2017)	(Shukla, 2016), (Barroso, 2017)	(Miccoli *et al.*, 2019)

*No results found on the literature.

Originally developed and applied to the field or rock mechanics, the flat jack test was adapted to be applied on historical buildings by Rossi in 1980 (Rossi, 1980). Since then, it has been applied to study structures comprising of brick masonry; (Rossi, 1982a, Rossi *et al.*, 1982, Rossi, 1987a, Epperson and Abrams, 1990, Rossi and Vavassori, 1992, Astudillo and Garcia, 1995, de Vekey, 1995, Rossi, 1995, Binda and Tiraboschi, 1999, Gregorczyk and Lourenço, 2000, Brencich and Sabia, 2008, Carpinteri *et al.*, 2009, Lombillo, 2010, Tecchio *et al.*, 2012, Bartoli *et al.*, 2013, Simões *et al.*, 2016, Della Torre *et al.*, 2019, Saisi *et al.*, 2019), stone masonry; (Rossi, 1987b, Gelmi *et al.*, 1993, Binda and Tiraboschi, 1999, Binda *et al.*, 2003, Bosiljkov *et al.*, 2010, Lombillo, 2010, Almeida *et al.*, 2012, Simões *et al.*, 2016, Casarin *et al.*, 2019, Della Torre *et al.*, 2019, Fanale *et al.*, 2019, Motisi *et al.*, 2019), ashlar masonry; (Abdunur, 1983, Rossi and Zaldivar, 1996, de Vekey and Skandamoorthy, 1997, Binda *et al.*, 2001, Lourenço *et al.*, 2001, Lourenço *et al.*, 2008, Lombillo, 2010), concrete; (Abdunur, 1983, Sumitro *et al.*, 2003, Figueiredo *et al.*, 2010, Chesi *et al.*, 2019), adobe and rammed earth (see Table 2. 2).

As presented in Table 2. 1, two main institutions have developed standards for the application of the flat jack test technique: The American Society for Testing and Materials (ASTM) in the United States and the Reunion Internationale des Laboratoires et Experts des Materiaux, Systemes de Construction et Ouvrages (RILEM) in Europe. Both standards' scopes are limited to the application of the technique to masonry. As there is no specific standard concerned with the application of the flat jacks for cob, the apparatus,

preparation, procedure and calculations available for masonry will be applied as far as possible in this thesis and adapted where necessary.

Flat jacks are manufactured mainly in stainless-steel and are available in different shapes (rectangular, semicircle and eccentric see Figure 2. 3) and sizes (see Table 2. 3). The thickness usually varies from manufacturer to manufacturer going from 3 mm up to 6 mm and their pressure capacity goes from 20 up to 300 bars (2 – 30 N/mm^2).

Table 2. 3. Flat jack sizes.

Shape	Dimensions in mm (A x B x R)
Rectangular	400 x 200 x – [a, b, c] 400 x 120 x – [c] 400 x 50 x – [a] 240 x 120 x – [b, c] 120 x 120 x – [b]
Semicircle	- x – x 200 [a] - x – x 175 [d] - x – x – 150 [b] - x – x 120 [b, c]
Eccentric	- x 85 x 175 [a, c, d] - x 125 x 175 [d] - x 104 x 60 [d]

[a] (GLÖTZL Baumeßtechnik, 2003)
[b] (NOVATEST, 2018)
[c] (BOVIAR, 2012)
[d] (SISGEO, 2015)

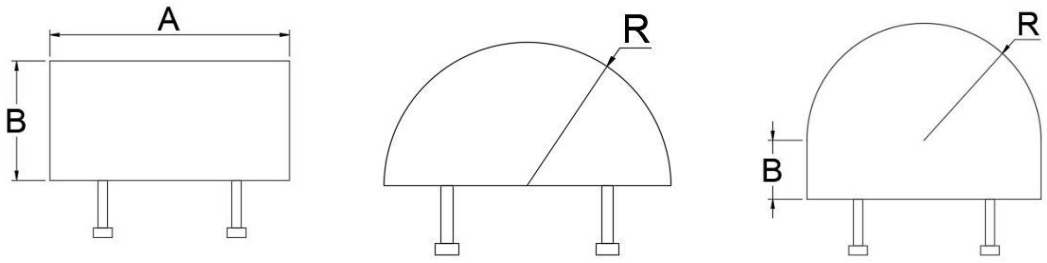

(a) (b) (c)

Figure 2. 3. Flat jack shapes (a) rectangular, (b) semi-circular and (c) eccentric.

The equipment required to perform the single flat jack test consists of:

- Slot cutting equipment.
- Cleaning tools (vacuum, blowers, brushes, etc.).
- Strain measuring equipment.
- Gauge points.
- Flat jack.

- Steel shims (to ensure accurate fit of the jack in the slot).
- Hydraulic pump.
- Pressure meter.
- Slot measurement device.

The procedure consists of fixing a series of vertical gauge points at both sides of the location where the horizontal slot would be performed. The gauge points should be glued equidistant (above and below) from the slot. It is recommended to use four pairs of points with a minimum gauge length, L, of 0.3 times the length A (width of the flat jack), and a maximum gauge length of 0.6 times A. The first and last gauges must be placed within a distance of $A/8$ from either end of the slot (see Figure 2. 4). As the standard has been developed for masonry, it specifies that the slot must be done in a mortar joint and that the gauge points must be glued to the masonry units. This recommendation does not apply for cob as it is a monolithic material.

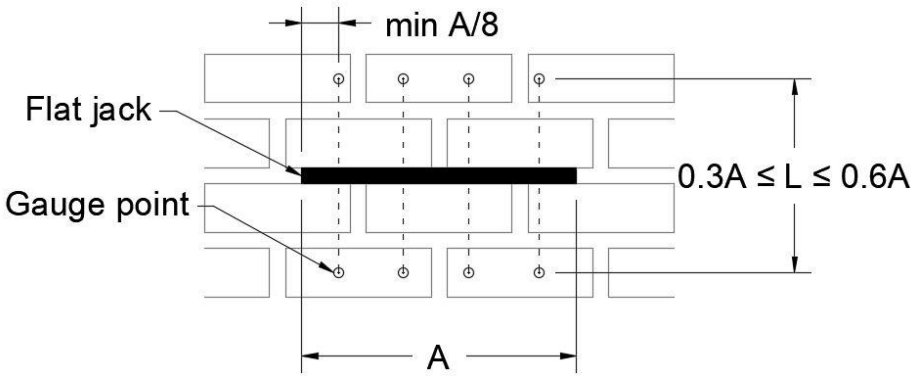

Figure 2. 4. Single flat jack test setup.

Once the glue has dried an initial set of distances between gauge points is taken. Then, a cut is made in the fabric to release local stresses causing the points to move closer in the case where the structural element is being subjected to compression and, conversely, to move further apart when the stresses are of tensile nature. In case tensile stresses are detected the standard practice advises stopping the test and repairing the damaged caused to the fabric, as tensile stresses may lead to a local failure of the structure. Abdunur (1983) on the other hand proposes an interpolation method to determine the tensile stress. The procedure may be applied in cases where it had been deemed that the stability of the structure will not be compromised. The depth of the cut is measured at

every 10-20 mm to determine the actual area of the slot. Dust and material particles have to be removed prior to the insertion of the flat jack.

The distance between gauge points is measured again to determine the initial displacement caused by the release of the stress. After this, a flat jack is introduced into the slot and, if required, shims are placed on the slot to ensure direct contact with the horizontal faces of the cut. The flat jack is connected to the pump and purged.

An initial pressure of about 50 % of the expected maximum pressure is applied to allow the flat jack and the shims to seat. For laboratory tests, the maximum pressure can be easily estimated by dividing the load applied to the wall by its cross section, whereas the estimation of the pressure in a historic building may prove to be quite complicated. In those practical cases, a simplified structural analysis able to describe the load path on the structure may provide an approximate value for the loads acting at the particular location where the test will be performed. After this, the ASTM standard advises that the pressure is completely removed and subsequent increments of pressure are applied to about 25 %, 50 %, and 75 % of the expected maximum pressure. On the other hand, the RILEM standard specifies increments of 1/8 of the maximum pressure expected and not less than 0.5 bars. At each pressure increment, the distance between gauge points must be monitored. According to the ASTM standard the distance between control points should be measured trice.

Pressure is then increased until the original distance between control points is recovered. Average deviations from the original gauge length are limited by the ASTM standard to the greater of ± 0.013 mm or 1/20 of the maximum initial deviation, with no single deviation exceeding the greater of ± 0.025 mm or 1/10 of the maximum deviation. Alternatively, single deviations from the original gauge length are limited to 10 % by the RILEM standard, but it allows for the rejection of the measurements of one of the four gauges used as it considers that gluing the gauges is not 100 % reliable.

Both standards recommended that the pressure increments take place in a time frame of about the same length as the time needed for the preparation of the slot with the aim of minimize effects caused by creep deformations. It is also advised to perform a second series of pressure increments to verify the measurements recorded, but it is acknowledged that the second measurements may be affected by the creep phenomena.

Once all the required measurements have been obtained, the flat jack is depressurised and removed from the slot. The damaged caused to the fabric is then repaired using a material compatible with the existent fabric.

Calculations of the test results are slightly different depending on what standard is adopted. ASTM calculates the average compressive stress in the fabric, f_m, by using EQ. 1:

$$f_m = K_m K_a p \qquad \textit{EQ. 1}$$

Where:

- K_m = Dimensionless constant based on the geometrical and deformability properties of the flatjack provided by the manufacturer or obtained via calibration (ASTM International, 2009).
- K_a = Ratio of the area of the flat jack to the measured area of the slot.
- p = Pressure in the flat jack required to restore the initial distance between gauge points.

On the other hand, RILEM provides EQ. 2 to calculate the restoring stress value, S_r:

$$S_r = K_e p \frac{A_{slot}}{A_{je}} \qquad \textit{EQ. 2}$$

Where:

- p = Pressure in the flat jack required to restore the initial distance between gauge points (as for ASTM).
- A_{slot} = Area of the slot.
- A_{je} = Effective area of the slot obtained via calibration (RILEM, 2004a).
- K_e = Dimensionless geometrical efficiency constant which takes into account the position of the slot in relation to the mortar joints, the relative size of the jack with respect to the units and the geometrical characteristics of the jack. Its value is obtained by means of calibration tests on fabric subjected to a known stress field within a compression testing machine.

Values of K_e for some materials and typologies are available in bibliographical references (Rossi, 1982b, de Vekey, 1995, de Vekey and Skandamoorthy, 1997, Lombillo, 2010) and in cases where data can't be found a value of 1 may be adopted (which will normally give conservative results).

The apparatus required to perform the double flat jack test is similar to the one used for the single test, but in this case two flat jacks are needed instead of just one. After an appropriate location has been chosen as a representative sample of material two horizontal cuts are made in the fabric. The depth of the cuts is measured at every 10-20 mm to determine the actual area of the slot. Dust and material particles have to be removed prior to the insertion of the flat jacks.

The ASTM standard specifies that there should be at least five courses of masonry in between the two slots, but also limits this distance to a maximum value of 1.5 times the width of the flat jack, A (see Figure 2. 5). This standard does not specify what vertical separation between gauge points should be respected, it only advises locating the first and last pair of gauges at a minimum distance of $A/8$ from the edge of the flat jack. On the other hand, the RILEM standard provides a series of sketches based on different masonry typologies (see Figure 2. 6) and specifies that the location of the point gauges should cover 75 to 90 % of the length between the two slots. This standard limits the distance between slots to a maximum of 1 to 1.5 times the width of the jack, A, and to a minimum of 2.5 times the depth of the jack. None of the two standards specifies where the horizontal control points needed to estimate the Poisson's ratio of the material should be glued.

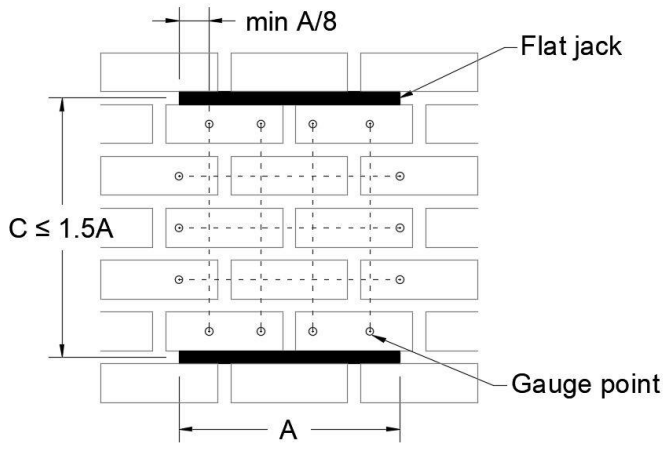

Figure 2. 5. Double flat jack test setup according to ASTM.

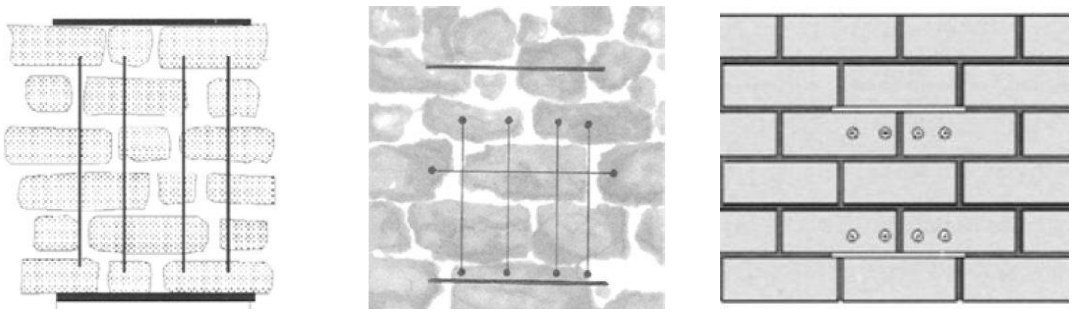

(a) (b) (c)

Figure 2. 6. Double flat jack test setup according to RILEM for: handmade brick masonry (a), irregular stone masonry (b) and modern brickwork (c).

A flat jack is introduced into each one of the respective slots and, if required, shims are placed on the slot to ensure direct contact with the horizontal faces of the cut. The flat jacks are connected to the pump and purged.

ASTM advises applying an initial pressure of about 50 % of the expected maximum pressure to allow the flat jacks and the shims to seat. After this the pressure should be removed and the initial distances between control points recorded. Subsequently, small increments of pressure are applied until a decrease on the flat jack pressure-masonry deformation ratio is detected to prevent the failure of the fabric. The control points' displacements values are measured trice and recorded for the respective increments of pressure. According to the RILEM standard the increments of pressure should correspond to about 10 % of the expected maximum pressure.

Once all the required measurements have been obtained, the flat jacks are depressurized and removed from the slots. The damage caused to the fabric is then repaired using a material compatible with the existent fabric.

The stress in the masonry between the jacks according to RILEM is calculated according to EQ. 3:

$$f_m = K_e p \frac{\bar{A}_{slot}}{\bar{A}_{je}} \qquad \textit{EQ. 3}$$

Where:

- p = Pressure in the flat jacks.
- $\bar{A}_{slot}$ = Average area of the two slots.

- $\bar{A}_{je}$ = Average of the effective area of both slots obtained via calibration (RILEM, 2004a).
- K_e = Dimensionless geometrical efficiency constant obtained either from calibration or from literature. May be taken as 1 if data is not available.

On the other hand, as for the single flat jack test, ASTM uses EQ. 1 to calculate the stress in the masonry between the jacks. To calculate the tangent modulus, E_t, and the secant modulus (RILEM) or chord modulus (ASTM) at a point i, E_{si}, of the fabric the standards use EQ. 4 and EQ. 5, respectively:

$$E_t = \frac{\delta f_m}{\delta \varepsilon_m} \qquad \textit{EQ. 4}$$

Where:

- δf_m = Increment of stress.
- $\delta \varepsilon_m$ = Corresponding increment of strain.

$$E_{si} = \frac{f_{mi}}{\varepsilon_{mi}} \qquad \textit{EQ. 5}$$

Where:

- f_{mi} = Stress (cumulative) at a point i.
- ε_{mi} = Corresponding (cumulative) strain at a point i.

Stress/strain curves can be plotted for the data collected corresponding to the vertical control points as for the data corresponding to the horizontal control points. By comparing the values of vertical deformation against horizontal deformation at a specific value of pressure within the elastic range of the material, the material's Poisson´s ratio can be estimated. Finally, a logarithmic regression curve is fitted to the stress/strain dots recorded and it is extrapolated to a reference strain value, at which it is known the material would attain its peak strength, in order to compute the compressive strength of the fabric (Lombillo, 2010).

2.1.8 Structural analysis

The objective of a structural analysis consists of determining the response of a structure subjected to a series of loads. Such response is provided in the form of stresses, deformations, reactions and failure modes of the structure. Within the field of heritage conservation, the structural analysis contributes to the safety evaluation of the structure, the diagnosis of the causes of damage and decay, and to the validation of interventions. The information obtained through a numerical analysis should always be complemented and validated with the information obtained via other sources of information; namely, historical research, inspection, experimental tests, and monitoring.

Most modern approaches to structural analysis are based on the use of mathematical models and numerical simulations of a simplified, but realistic, model of the structure and the actions acting on it. The simplification of a model is based on conceptual and specific hypothesis. Conceptual simplifications take the form of the idealization of the physical problem, the identification of the phenomena of interest such as the load capacity of the structure, its displacements and failure modes, the definition of mathematical variables and the relations between them. The specific simplifications consist in the choice of material constitutive model, geometry and kinematics simplifications, and the representation of the actions acting on the structure.

A numerical modelling approach is presented in Figure 2. 7. On a first step, the information (inputs) collected during the geometrical survey, historical research, inspection, experimental tests and monitoring of the structure is used to provide the basic information necessary to create the model. The second stage of the modelling process consist of the calibration and validation of the model. Calibration is done by tuning the values of the input parameters in order to obtain a satisfactory response of the structure whereas that validation is performed by comparing the simulated structural behaviour with the empirical information obtained through the aforementioned activities. Once the model is deemed to be appropriately calibrated, it is used to reproduce the state and behaviour of the structure. If the model is not capable of reproducing the response of the structure with sufficient accuracy, a refining process should be implemented by going back to the building stage and revising the simplifications adopted. Once the model is capable of predicting the response of the structure accurately enough, it can be used to evaluate (in combination with the information collected from the historical, qualitative

and experimental approaches) the safety level of the structure and predict its behaviour under different actions (such as under seismic loads, for example).

Historical structures posse a series of structural analysis challenges linked to their complex characterisation. Old construction materials are not standardised and are usually characterised by very complex mechanical and strength phenomena. The geometry of historical buildings is often quite intricate including a combination of different dimensional elements such as beams, columns, walls, pillars, arches, vaults, domes, fillings and pendentives. Moreover, structural members are non-homogeneous, and their connections often involve problems of contact, friction and eccentric loading, which are difficult to characterise by using only MDT or NDT techniques. The various loads acting on the structure during its lifetime can be cyclic and repetitive, accumulating significant effects in the long term, depending on the behaviour of the materials. To capture the true condition of a historical structure, existing damage and alterations need to be taken into account. Finally, historic interventions, such as extensions, demolitions, repairs, etc., may influence the structural response and other phenomena, such as earthquakes, floods, freeze-and-taw cycles, etc., may have contributed to the existing damage state of the structure.

Structural analysis can be performed by using different methods: Limit analysis (Heyman, 1982, 1995), generalized matrix formulations (Lagomarsino *et al.*, 2013, Siano *et al.*, 2017), FEM (Zienkiewicz, 2013), Discrete Element Method (DEM) (Cundall and Strack, 1979), Discontinuity Layout Optimization (DLO) (Gilbert and Smith, 2007), Smooth Particle Hydrodynamics (SPH) (Lucy, 1977), among others. A thorough description of the application of these numerical tools applied to the conservation of cultural heritage is given by Lourenco (2002) and by Roca *et al.* (2010).

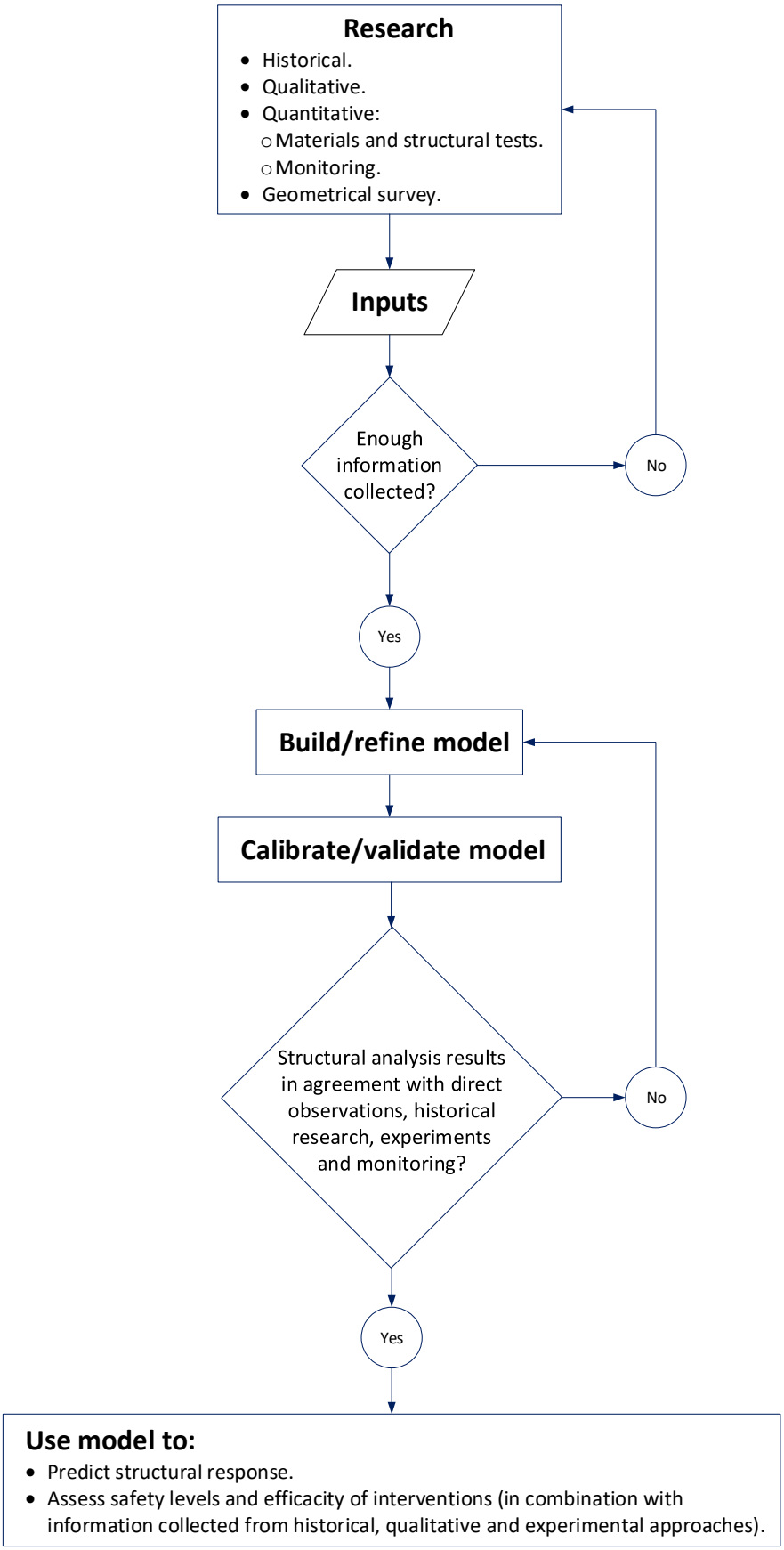

Figure 2. 7. Scientific approach to numerical modelling in conservation.

2.1.9 Conservation standards

Besides the conservation documents developed by ICOMOS, there are series of standards developed by different bodies for the conservation of cultural heritage. At an international level, the International Organization for Standardization (ISO) has published ISO 13822 Bases for Design of Structures – Assessment of Existing Structures (ISO, 2010) that recognises the paramount, and increasing, importance of the conservation of existing structures as economic and cultural assets.

At a regional level, the European Committee for Standardization (CEN) has developed and published EN 16853 on the conservation of cultural heritage (CEN, 2017). In this document, the conservation process is defined. Moreover, guidelines regarding decision making, planning and implementation of such process are also provided.

At a national level, a Guide to the Conservation of Historic Buildings, BS 7913, has been published by British Standards (2013) (British Standards are commonly accepted and applied in Ireland). A new national heritage plan was being developed at the moment this thesis was written to (DCHG, 2019):

- Revitalise and refresh the Government's commitment towards heritage conservation.
- Recognise the paramount role of heritage in the community, the economy and society.
- Create a coherent, comprehensive and inspiring framework of values, principles and strategic priorities to better guide and inform the heritage sector.
- Enshrine the shared responsibility of people, communities, businesses, and local and national Governments in the protection of heritage.
- Help to enjoy, understand and care for heritage.

Specialized standards in the conservation of earthen structures have unfortunately not been published yet in any country and only few guidance documents have been published recently. The standards available deal with the construction of new earthen buildings (NZS, 1998b, 1998a, 1998c, ASTM International, 2010) and specialized in the earthen construction techniques such as adobe, rammed earth and compressed earthen blocks (CEB). No earthen standard provides specialized guidance for cob structures (Cid

et al., 2011). The Cob Research Institute (CRI) based in Berkeley, California, USA, has as mission to "*make cob legally accessible to all who wish to build with it*". As the result of their work, a proposal (Cob Research Institute, 2019) to include specialized guidelines on the cob construction of new buildings as an appendix of the 2021 International Residential Code (IRC) was submitted, but unfortunately was rejected based on the lack of evidence on cob's fire resistance in accordance with ASTM. On the other hand, a document published by the Devon Earth Building Association (DEBA) proves how cob dwellings comply with the Building Regulations of the UK and how its use to build new buildings can perfectly be considered as suitable under such regulation (Stokes, 2008).

The Getty Conservation Institute has developed a series of guidelines and recommendations on the conservation of earthen buildings within the frame of its Seismic Retrofitting Project (SRP), which is part of its broader Earthen Architecture Initiative (EAI) (Tolles *et al.*, 2003, Cancino *et al.*, 2013, Lourenço *et al.*, 2018, Lourenço and Pereira, 2018, Torrealva *et al.*, 2018).

2.2 Earthen construction techniques

Since ancient times, people all over the world have used soil as their main building material. Earthen architecture has in a way become a symbolic expression of the human capacity to build, and to make the best use of the resources available in the local environment. Today, earthen architectural heritage includes a great diversity of building types, ranging from archaeological sites to living monuments and from groups of buildings to historic towns and some cultural landscapes (UNESCO, 2007).

2.2.1 Environmental, thermal, hygroscopic and construction characteristics

The use of earth, and other natural materials, for construction purposes can significantly contribute to the reduction of energy consumption and environmental impact. The performance of earth-based materials is positively associated with a high thermal capacity, low embodied energy, low emissions, high recyclability, fire resistance and indoor air humidity control.

Thermal capacity or, in other words, thermal mass is measured by the Volumetric Heat Capacity (VHC) of a material. Thermal mass is the ability of a material to absorb and store heat energy (Reardon, 2013). When thermal mass is appropriately used, it will help to moderate indoor temperatures in buildings which will result in higher comfort levels and reduced energy costs. The thermal lag obtained with high thermal mass materials will produce a "*warmer house at night in winters and a cooler house during the day in summer*" (Wilson, 1998). Table 2. 4 presents averaged thermal mass values of some typical materials used in the construction industry. Earthen-based materials (adobe, rammed earth, and compressed earth blocks) have similar thermal mass values as those of bricks or stone, and slightly lower to those obtained with conventional concrete. Values of cob's VHC are reported as 1153 kJ/m^3*K by Goodhew and Griffiths (2005) and between 720-2100 kJ/m^3*K by Moevus *et al.* (2012).

Table 2. 4. Thermal mass values of building materials (Baggs and Mortensen, 2006).

Material	Thermal mass, VHC (kJ/m^3*K)
Water	4186
Concrete	2060
Autoclaved Aerated Concrete	550
Brick	1360
Stone (sandstone)	1800
Adobe	1300
Rammed earth	1673
Compressed earth blocks	1740

Embodied energy refers to the amount of energy necessary to extract, refine, process, transport and fabricate a material or product (Circular Ecology, 2019). Table 2. 5 presents the energy consumption necessary to produce certain building materials. As can be seen, earth and straw, which are used in most earthen construction techniques, have a relatively low embodied energy in comparison to modern materials such as steel or cement. The values in Table 2. 5 do not take into account the embodied energy attached to material transport processes. As earthen buildings are constructed mostly where appropriate soil can be locally sourced their total embodied energy, in comparison with other modern construction materials, will not vary significantly. On the other hand, when soils are stabilized with the use of cement, lime or other manufactured materials, their energy consumption can increase considerably.

Table 2. 5. Embodied energy consumption of some building materials (Reddy and Jagadish, 2003, Keefe, 2012).

Material	Energy consumption (kWh/m^3)
Aluminium	178258
Steel	91583
Cement	2640
Lime	900
Fired brick (solid)	1140
Fired brick (perforated)	590
Chipboard	1100
Plasterboard	900
Natural sand/aggregates	45
Earth	5-10
Straw	4.5

In modern studies, the concept of embodied energy has been substituted by the concept of Embodied Carbon (EC), which is considered as a more useful indicator. EC is defined by the Inventory of Carbon and Energy (ICE) as the sum of fuel related to carbon emissions and process related carbon emissions (Jones, 2019). One way to estimate the amount of CO_2, which is a major contributor to greenhouse effects, emissions of building materials consists of taking into account their full life-cycle. The life-cycle of a structure can be divided into manufacturing, construction, operation and demolition stages. A simplified quantifying method that only considers the manufacturing stage is known as cradle-to-gate.

The sample values presented in Table 2. 6 were taken from the ICE and correspond to a cradle-to gate boundary (Jones, 2019). As can be seen, natural materials such as soil, general aggregates and sand are the ones with less emissions (besides from water), as almost no energy is necessary for their sourcing. Seo and Hwang (2001) determined that up to 87.5-96.9 % of the total CO_2 emissions come from the operation of buildings, thus placing more importance on energy efficiency during the life span use of the building than on the embodied energy of the materials. The selection of natural materials has as an additional advantage, as long as they are kept dry they are non-toxic and present no risk to health (Keefe, 2012).

Table 2. 6. EC of some building materials (Jones, 2019).

Material	Details	EC ($kgCO_2/kg$)
Soil	General (Rammed Soil)	0.024
Aggregates and sand	General UK, mixture of land won, marine, secondary and recycled, bulk, loose	0.00747
Aggregates and sand	From recycled resources, with heat treatment, bulk, loose	0.11877
Aggregates and sand	Expanded clay, bulk, loose	0.39321
Aluminium	Aluminium General, European Mix, Inc Imports	6.67
Aluminium	Aluminium General, Worldwide	13.1
Aluminium	Aluminium, China	14.6
Bitumen	Straight-run bitumen	0.191
Bitumen	Bitumen emulsion	0.222
Bricks	General (common brick)	0.21
Cement and mortar	Average CEM I, Ordinary Portland Cement (OPC)	0.912
Cement and mortar	CEM V/B - 36% GGBS and 36% cement replacement	0.284
Cement and mortar	Mortar (1:3 cement:sand mix)	0.200
Cement and mortar	Concrete admixtures – Hardening Accelerators	2.28
Clay	General simple baked clay products (inc. terracotta and bricks)	0.24
Clay	Tile	0.48
Concrete in-situ	20/25 MPa	0.112
Concrete precast	Concrete - Ordinary Portland Cement (OPC) concrete - CEM I based - with total cementitious content of 300 kg per m3 of concrete	0.148
Concrete blocks	Concrete block, medium density solid, average strength, per kg	0.0931
Concrete blocks	AAC concrete block	0.28
Glass	Glass, General, per kg	1.44
Lime	General	0.78
Water		0.00008

Soil is a material that can only be considered as renewable in geological time terms. Its potential as a renewable material arises from the fact that the material can be almost fully recyclable (Minke, 2000). Moreover, soil dug out from civil engineering works, which usually ends up in landfills, can be used on the construction of new buildings (Keefe, 2012) or to grow vegetation (Rael, 2009).

Healthy levels of air humidity are within 40 to 70 %. Lower levels will cause dry mucous membrane, which may lead to a resistance decrease to colds and related disease. On the other hand, higher levels of air humidity will propitiate the grow of fungus which, in large quantities, can cause several types of allergies (Minke, 2012). Air humidity control depends on material porosity and its capacity to absorb and release the humidity from the ambient air. Figure 2. 8 shows the absorption curves of different building materials. As loam materials (earthen materials) can absorb relatively big quantities of water with respect to, for example, cementitious materials (see Figure 2. 8), their superior indoor air humidity control performance can be proved.

The good absorption capacity of earthen materials could become a disadvantage since, as identified by several authors (see Figure 2. 19 and Figure 2. 20 in section 2.3.4), the compressive strength of earthen specimens reduces as the level of moisture increases. Constant high levels of moisture would also reduce fibres' durability, thus affecting the mechanical properties of fibre reinforced earthen structural elements (Saxton, 1995). Furthermore, repetitive drying/wetting cycles, with the consequently opening of cracks due to swelling and shrinkage of the structural elements' volume, may negatively impact on the durability of the material by facilitating rainwater erosion, which is one of the main causes of earthen buildings' decay (Maheri *et al.*, 2011). Other causes of decay are presented in Figure 2. 9. For a detailed discussion on decay and durability of earthen architecture the reader can consult the Practical Building Conservation series published by English Heritage (English Heritage, 2013).

Ley and Widgery (1997) estimate that a cob wall with 400 to 600 mm thickness will have a fire resistance of at least two hours. Therefore, satisfying building regulations for low rise residential building. Compressed Earth Blocks (CEB) (Buson *et al.*, 2012) and rammed earth (Dobson, 2000) have also been tested and proofed to comply with fire resistance building regulations. The problem of earthen construction does not come directly from the performance of the material against fire, but from the fact that in the case of a fire starting, water will be used to extinguish the flames. This will increase the

water content of the mixes, weakening the earthen material and perhaps lead to collapse of the structural elements.

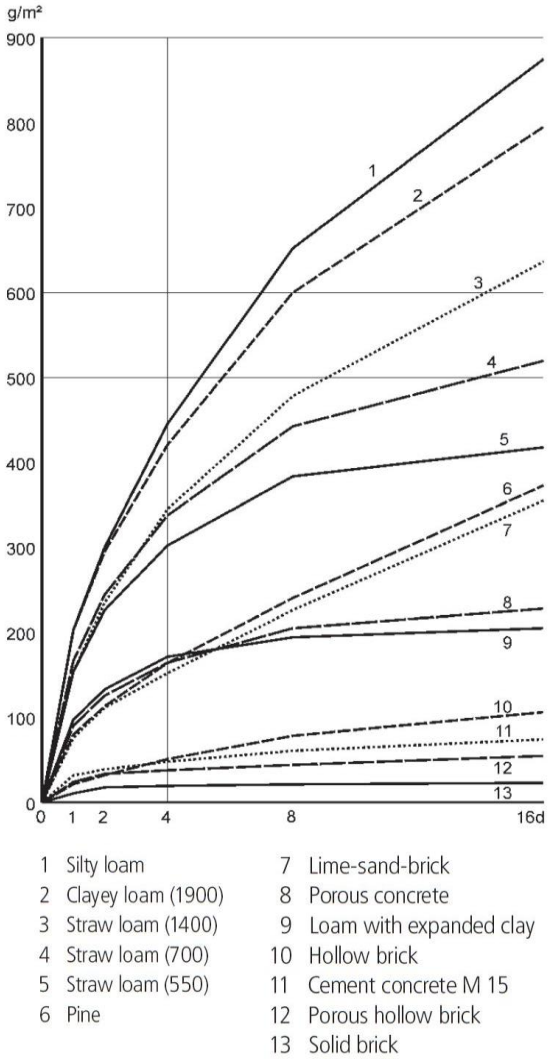

Figure 2. 8. Absorption curves of 11.5 cm thick interior walls with two sides exposed at a temperature of 21 °C after a sudden rise in humidity from 50 % to 80 % (Minke, 2012).

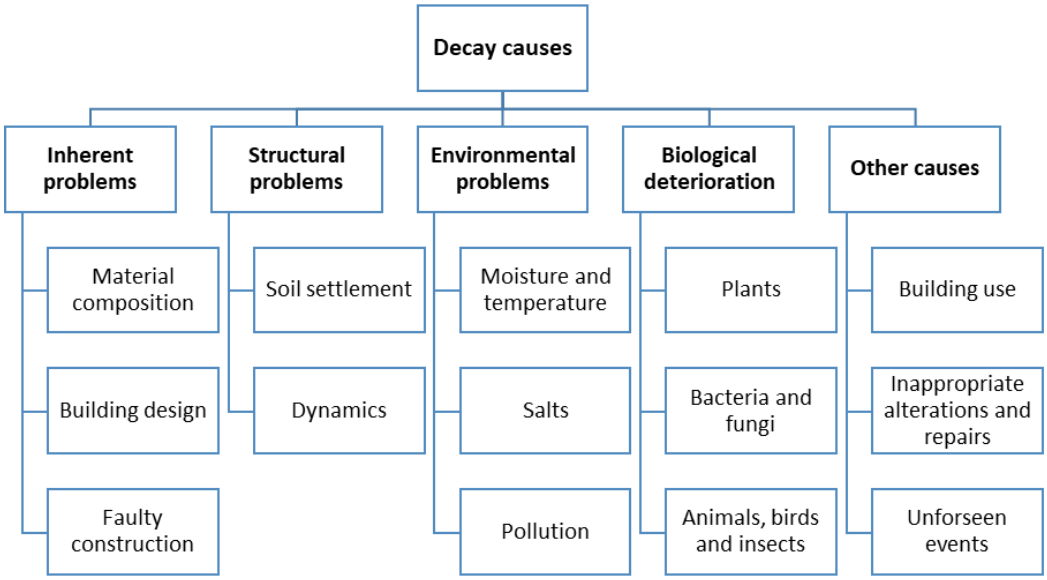

Figure 2. 9. Classification of decay causes on earthen buildings (English Heritage, 2013).

Finally, earthen construction techniques are considered as ideal for self-building projects. Even though they are labour intensive, these construction techniques only require simple and inexpensive tools, and can be performed under the supervision of a single experience builder (Keefe, 2012, Minke, 2012). Furthermore, the extra costs of earthen construction in comparison with industrialized systems usually comes from labour. This factor can actually be used as a trigger to incentivize local economies and improve equality in agreement with the UN SDGs (United Nations, 2018a).

The main disadvantages of earthen construction techniques are their relatively low strength in comparison with modern conventional materials such as concrete or steel, their vulnerability to water, the lack of material standardization, high U-values, considerable required maintenance and their relatively high labour intensity (Keefe, 2012, Minke, 2012).

2.2.2 Earthen construction techniques classification

The most common earthen construction classifications are based on:

- The type of method; dry or wet.
- The structural function; load bearing or non-load bearing.
- The type of element; monolithic, masonry or infill.

The classification shown in Figure 2. 10 is based on the type of element.

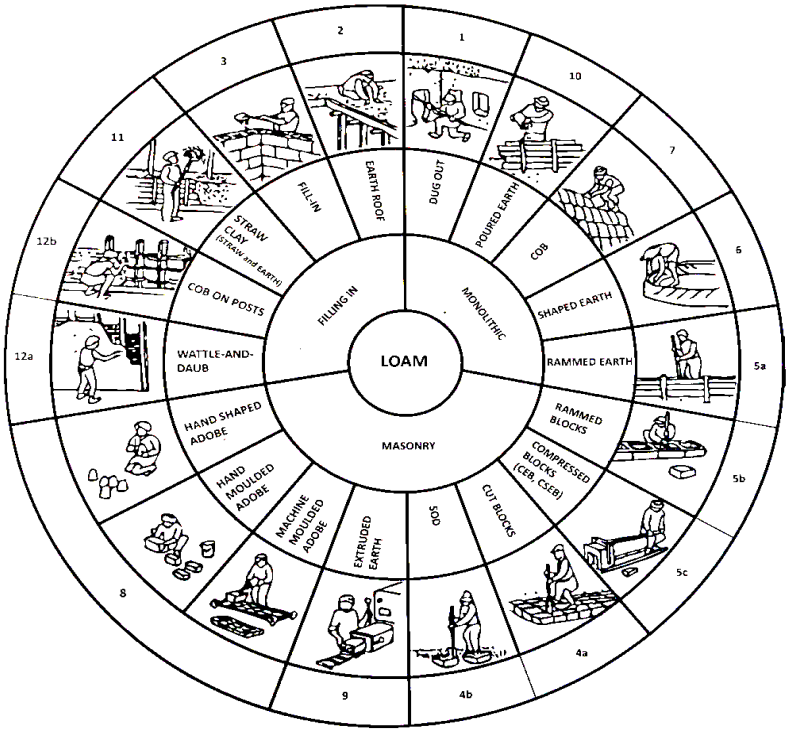

Figure 2. 10. Earthen construction techniques classification (Teixeira et al., 2018).

With filling in techniques earth usually does not play a structural function. The structure is composed usually of timber elements in the form of frames and lattices which are later filled with soil in either liquid (fill-in and straw clay) or plastic (cob on posts, wattle and daub) state. The addition of soil mass to the timber structure helps to improve its thermal performance. Moreover, in the case of earthen roofs, it helps to improve water quality by detaining, absorbing and filtering rainfall (Teixeira *et al.*, 2018).

The masonry techniques consists of an arrangement of pieces or blocks, which are obtained either by directly cutting dry pieces of soil (sods and cut blocks), by compressing humid soil into moulds (rammed earth blocks or CEB) or by working with soil in plastic or viscous state to mould blocks either by hand (hand shaped adobe or hand moulded adobe) or with a machine (machine moulded adobe or extruded earth). The pieces are assembled and glued together using clay mortars and the resulted walls are loadbearing (Teixeira *et al.*, 2018).

Different monolithic techniques implement the soil in different consistency states: humid for rammed earth construction, plastic for shaped earth and cob, liquid for poured earth and dry for soil dug out. Poured earth and rammed earth require the use of shuttering, whereas for cob and shaped earth the material is directly placed and this fact allows for great shape flexibility (Teixeira *et al.*, 2018).

2.3 Cob

2.3.1 Components

The loam necessary to build with cob is basically a mix of soil, fibres and water. Water should be clean and not contain hazardous substances that could threaten the health of the builders or the building's occupants. The amount of water will mainly determine the consistency of the mix and its strength (Keefe, 2012).

The natural fibres added to the loam play several roles. First of all, fibres are added for workability purposes. They facilitate the mixing (Watson and McCabe, 2011, Hamard *et al.*, 2016) and keep the wet soil together in clumps and allow for its placement without disaggregation (Keefe, 2012). Fibres also increase the tensile strength of the material and its ductility (Doat, 1979, Rizza and Böttger, 2013, Miccoli *et al.*, 2014). They allow the soil to suffer relatively high deformations without suddenly failing. Furthermore, the fibres, randomly distributed within the volume, will also distribute the tensile stresses caused by the shrinkage of the material, thus limiting and controlling the opening of cracks (Neves, 2003, Watson and McCabe, 2011, Keefe, 2012, Minke, 2012) (see Figure 2. 11).

Fibres proportions usually make up 25 kg per cubic meter (Doat, 1979) or between 1 % and 2 % by mass (Hamard *et al.*, 2016). The fibres have lengths of 15 to 40 cm. Percentages by volume of 1.0 to 1.5 are suggested as the optimal straw content by Akinkurolere *et al*. (2006) and by Saxton (1995). On the other hand, Miccoli *et al*. (2014) reported the use of straw in percentages of 2 to 3 % and with lengths of 30 to 50 cm. A relatively important variability in the characteristics of the fibres, as reported by these authors, can be observed being the length of the fibres between 15 to 50 cm and the percentages in the mix of between 1 to 3 % by volume, which may significantly affect the mechanical properties of the cob (see Laborel-Preneron *et al.* (2016)). The drying of the material is also accelerated by the fibres and inversely, they allow the material to increase its humidity absorption rate. The addition of fibres leads to a decrease in the density of the material, thus, improving its thermal insulation performance (Doat, 1979, Keefe, 2012). It has even been suggested that the addition of fibres improves resistance to erosion and frost damage (Historic England, 2015). A thorough review of the effects of plant aggregates and fibres in earth construction materials can be found in the review

paper of Laborel-Preneron *et al*. (2016). Nevertheless, these authors highlight the lack of studies on the contribution of fibres to the properties of traditional cob.

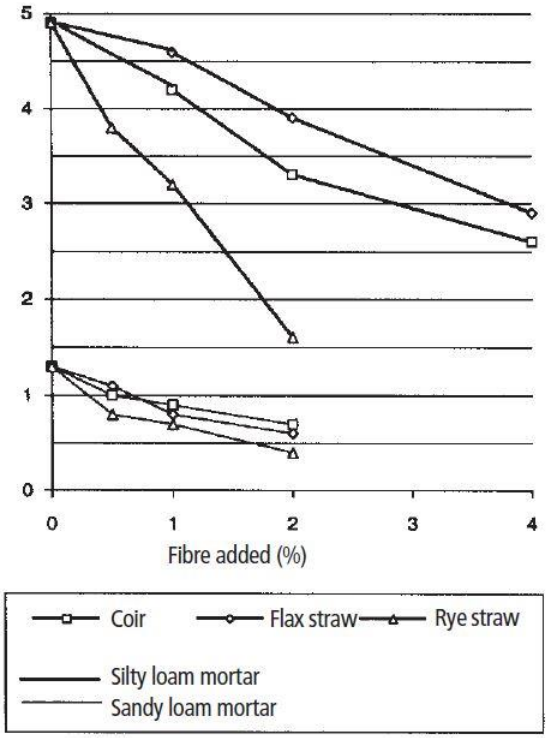

Figure 2. 11. Shrinkage ratio of loam mortars with addition of fibres (Minke, 2012).

The suitability of soil, the third component needed for making cob, can be assessed by taking into account the parameters presented in Figure 2. 12. Soil type can be classified according to its underlying geology, its mineralogy, its stratigraphy and its colour, which for aesthetic purposes may be of interest (Keefe, 2012).

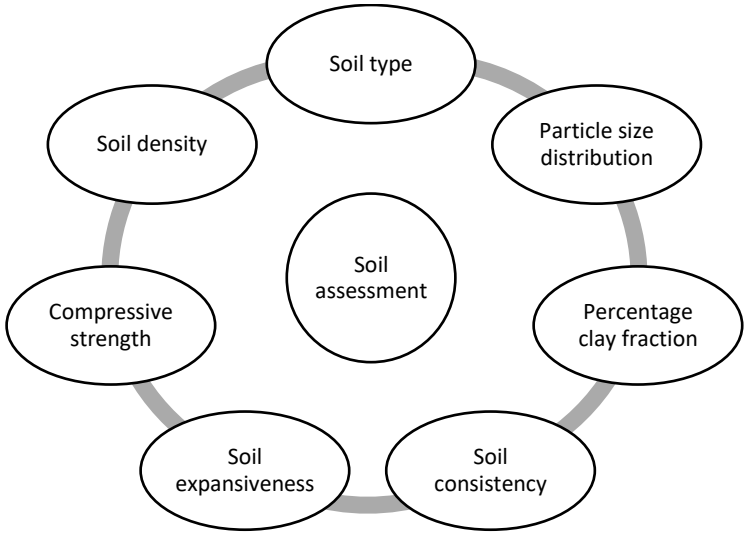

Figure 2. 12. Soil assessment parameters.

One of the most important aspects to take into account regarding the characteristics of the soil is its granulometric composition, also known as Particle Size Distribution (PSD). According to their size, soil particles may be classified as cobbles (greater than 63 mm), gravels (coarse between 63 mm and 20 mm, medium between 20 mm and 6.3 mm, fine between 6.3 mm and 2 mm), sand (coarse between 2.0 mm and 0.63 mm, medium between 0.63 mm and 0.2 mm, fine between 0.2 mm and 0.063 mm), silt (coarse between 0.063 mm and 0.02 mm, medium between 0.02 mm and 0.0063 mm, fine between 0.0063 and 0.002 mm) or clay (smaller than 0.002 mm) (British Standard, 2016a). Results obtained from samples of old cob houses in Devon, England, showed a material composition of about 33 % to 21 % clay and 1.6 % fibres (Doat, 1979). Keefe (2012) presents a PSD curve in which the upper and lower levels for suitable soil for the production of cob are indicated (see Figure 2. 13). Whereas Jaquin and Augrade (2012) present suitable PSD curves of soils suitable for different earthen construction techniques; namely, adobe, rammed earth and cob (see Figure 2. 14). By comparing Figure 2. 13 with Figure 2. 14 it can be seen that Keefe limits the maximum size of the particles to 20 mm whereas that Jaquin and Augrade allow the use of particles with a size of up to 50 mm (the presence of gravels has been detected in several cob vernacular buildings in Ireland see section 5.3.1). The clay content is limited by Keefe to values of 15 to 30 % whereas that Jaquin and Augrade´s PSD curve shows values of between 0 to 33 % (soils with a clay content of 0 % are not suitable for cob construction as reported for all other authors referenced in this thesis and according to the author own experience). Harries *et al.* (2000) suggest the use of soils with a clay content between 10 % and 25 %, silt content between 10 % and 20 %, and sand/gravel content of about 55 % to 70 %. Watson and McCabe (2011) propose similar ranges for silts and clays, whereas they recommend having about 25 % to 30 % of sand and 30 % to 40 % of gravel.

Once again, different authors recommend different soil PSD and clay contents as for the "*ideal*" soil to be used for cob construction. In fact, cob vernacular buildings were constructed using local materials, thus the broad variability on soil characteristics, and the "*most appropriate*" soil would correspond to that of the existent material, as interventions must implement compatible materials. Thus, it is advised to perform a research to define the index properties of the existent cob walls and source a soil with similar PSD and clay content for the intervention, criteria that in many cases would be satisfied by the local soil.

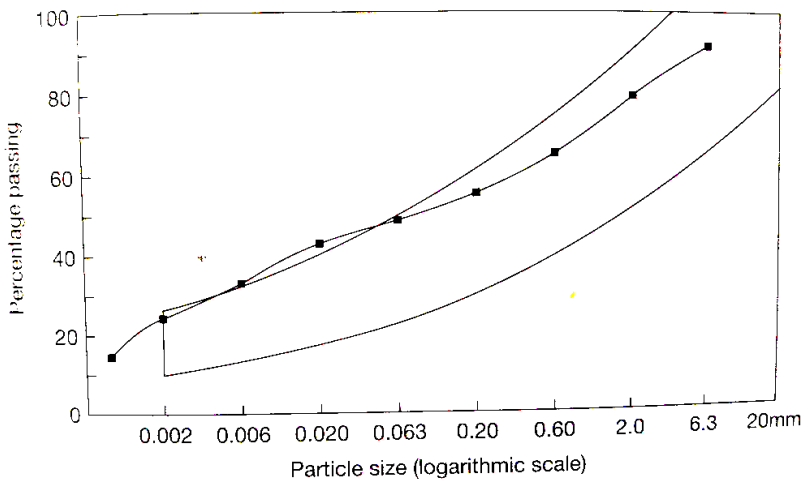

Figure 2. 13. Suitable PSD of soils for cob (Keefe, 2012) (continuous lines represent the recommended PSD soil envelope for a suitable soil for cob and dotted line represents the PSD of a Devon soil analysed by Keefe).

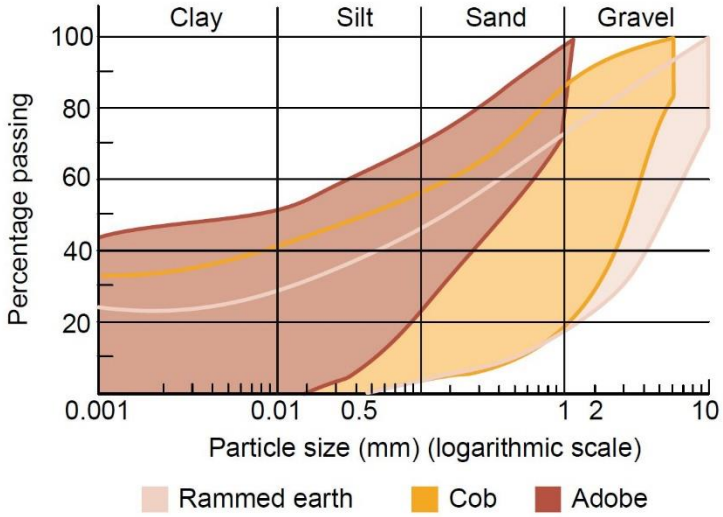

Figure 2. 14. Suitable PSD of soils for different earthen construction techniques (Jaquin and Augrade, 2012).

Clay content is of paramount importance for soil behaviour as clay will keep the coarser particles together in a cohesive and homogenous way (Keefe, 2012). Cohesive forces in a soil will develop due to water suction between clay particles (Jaquin and Augrade, 2012, English Heritage, 2013). Nevertheless, clay content must be limited to a certain percentage, usually no more than 30 %, as too much clay would cause an excess of expansion and contraction in the structure.

The consistency of a soil can be expressed in terms of its plasticity and its cohesion. Explained in simple terms, “Plasticity is the ability of a material to be moulded without fracturing, while cohesion is the ability to maintain that deformed shape” (Carter and Bentley, 2016). A soil mainly composed by sand and silts will be prone to erosion

and structural failure, therefore, quite unsuitable for building purposes (Keefe, 2012). Soil consistency depends, among other factors, on the water content of the mix. Based on this parameter, soils can be classified into four different stages of consistency: liquid, plastic, semi-solid and solid (Minke, 2012). The limits between the different stages are determined by the so called Atterberg limits (see Figure 2. 15).

A moisture content of zero percent can only be obtained after the soil has been dried in an oven. At this point soils are in a solid state and all its pores, or voids, are filled with air. The Equilibrium Moisture Content (EMC) is attained for a moisture content of about 3 to 4 % (Keefe, 2012). Soil's voids can be filled with water by increasing its moisture content without causing a change of its volume until the shrinkage limit is reached. After this point, the soil has a semi solid consistency and gradually starts to lose its cohesion. After the plastic limit is reached, the soil will acquire a plastic consistency and will start to deform irreversibly if external forces act upon it. If water content keeps increasing, the soil will reach its liquid limit and at this point it will start to deform under its own weight. The difference of moisture content between the liquid limit and the plastic limit of a soil is known as the plastic index. This parameter could be used as an indication of the shear failure type of a soil, which may be either sudden through rapid crack propagation, or progressive due to the plastic deformation of the structure (Keefe, 2012).

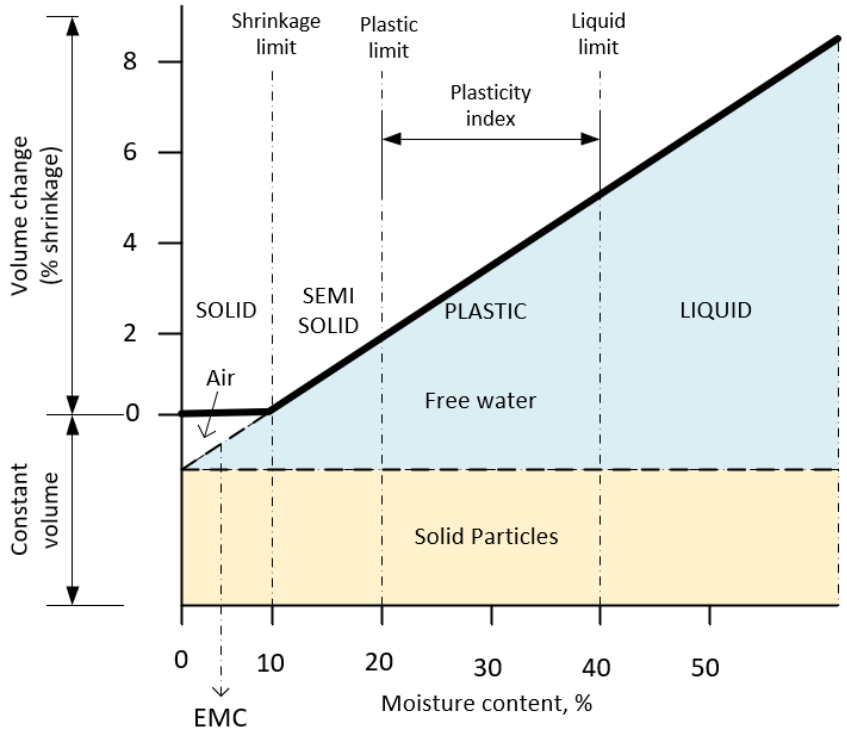

Figure 2. 15. Consistency of soils based on moisture content (Keefe, 2012).

Soil expansiveness, or swelling, plays an important role during the mixing, building and specially during the drying out process of cob. While mixing, it is important to keep the amount of water to a minimum necessary for adequate workability. This is done with the aim of reducing the amount of water that will evaporate when cob dries, thus, reducing the amount of volume shrinkage and the opening of cracks (Historic England, 2015). The amount of swelling/shrinkage of a soil will mainly depend on the clay content and type of clay. Montmorillonites will suffer bigger volumetric changes in comparison to kaolinites or illites (Minke, 2012). If cob is loaded before it dries completely, it will suffer consolidation deformation. For any given load, consolidation deformation is always bigger in a taller wall than a shorter one (Historic England, 2015).

The load bearing capacity of cob walls is mainly determined by the compressive strength of the soil used. The principal factors affecting the dry compressive strength of a soil are the grading of the particles, the size and mineralogy of the clay fraction, and the degree of soil compaction (Keefe, 2012). Soil strength comes from the friction forces between its particles (Jaquin and Augrade, 2012). Those forces depend on the macroscopic angle of friction, ϕ, which for sands and gravels can go up to 40°, but usually, for most soils, lies between 15° and 30° (Jaquin and Augrade, 2012). The shear strength of a soil, τ (see EQ. 6) also depends on the effective stress, σ', and cohesion, c. Thus:

$$\tau = \sigma' tan\phi' + c \qquad \textit{EQ. 6}$$

Where ϕ' represents the effective macroscopic angle of friction, which depends upon the interparticle sliding friction and a geometrical interference parameter. The effective stress depends on the total stress, σ, and the pore water pressure, u. Thus:

$$\sigma' = \sigma - u \qquad \textit{EQ. 7}$$

We can see from EQ. 7 that if pore water pressure increases, caused by an increase in the moisture content, the effective stress of the soil will decrease, consequently reducing its shear strength. This will lead to the failure of the material even if the applied loads are kept constant (Jaquin and Augrade, 2012). EQ. 6 and EQ. 7 are derived assuming full soil saturation and effective stress parameters. Nevertheless, cob is actually a manufactured unsaturated soil and its behaviour is not entirely well described with such assumptions. The field of unsaturated soil mechanics applies more complex theories and

allows to better describe the observed macroscopic unsaturated behaviour of soils by analysing them at particle level (Fredlund, 2006, Baker and Frydman, 2009, Jaquin and Augrade, 2012, Ng and Menzies, 2014).

Density varies according to the soil's particle type and size distribution, as well as according to the compaction degree (Keefe, 2012). Density is mainly used to compute the soil's porosity and thermal performance. Well compacted soils would be stronger than poorly compacted materials. Lose soil will be weaker and prone to deterioration (Historic England, 2015).

In order to determine the different characteristics of a soil, two approaches can usually be adopted: empirical tests and standardized tests (see Figure 2. 16). Empirical tests serve as a first approach to get to know the characteristics of a soil. They are subjected to interpretation; therefore their accuracy depends on the experience of the person performing them. Empirical tests are based on the senses and direct observation of the soil behaviour. Some empirical tests are described in the following references: (Avrami *et al.*, 2008) (Teixeira *et al.*, 2018) (Minke, 2012) (ASTM International, 2010) (NZS, 1998b) (Historic England, 2015). Standardized tests are formal tests that allow the accurate measurement and determination of a soil's index properties. The British Standards describe in detail the required classification tests applied on soils for civil engineering purposes (British Standard, 1990).

2.3.2 Loam preparation

Loam preparation requires relatively small industrialization in comparison with the preparation of modern construction materials such as concrete or steel. Nevertheless, the steps shown in Figure 2. 17 should be taken into account to obtain maximum benefit from it. Preferably the soil should be locally sourced or reused from other infrastructure projects in cases when otherwise it may end up disposed in a landfill. In cases where the soil's quality is poor, stabilization may be implemented.

Stabilization is achieved by modifying soil's grading or by mixing it with other substances such as cement, lime or bitumen. Grading is achieved by adding sand to extremely clayey soils and, on the other hand, by adding clay to low clay content soils (Keefe, 2012, Historic England, 2015). Chemical stabilization should only be implemented under extreme conditions such as flood prone or seismically active areas,

otherwise it should be avoided as this will increase the material embodied energy and highly limit its recyclability and natural capacity to return to the environment.

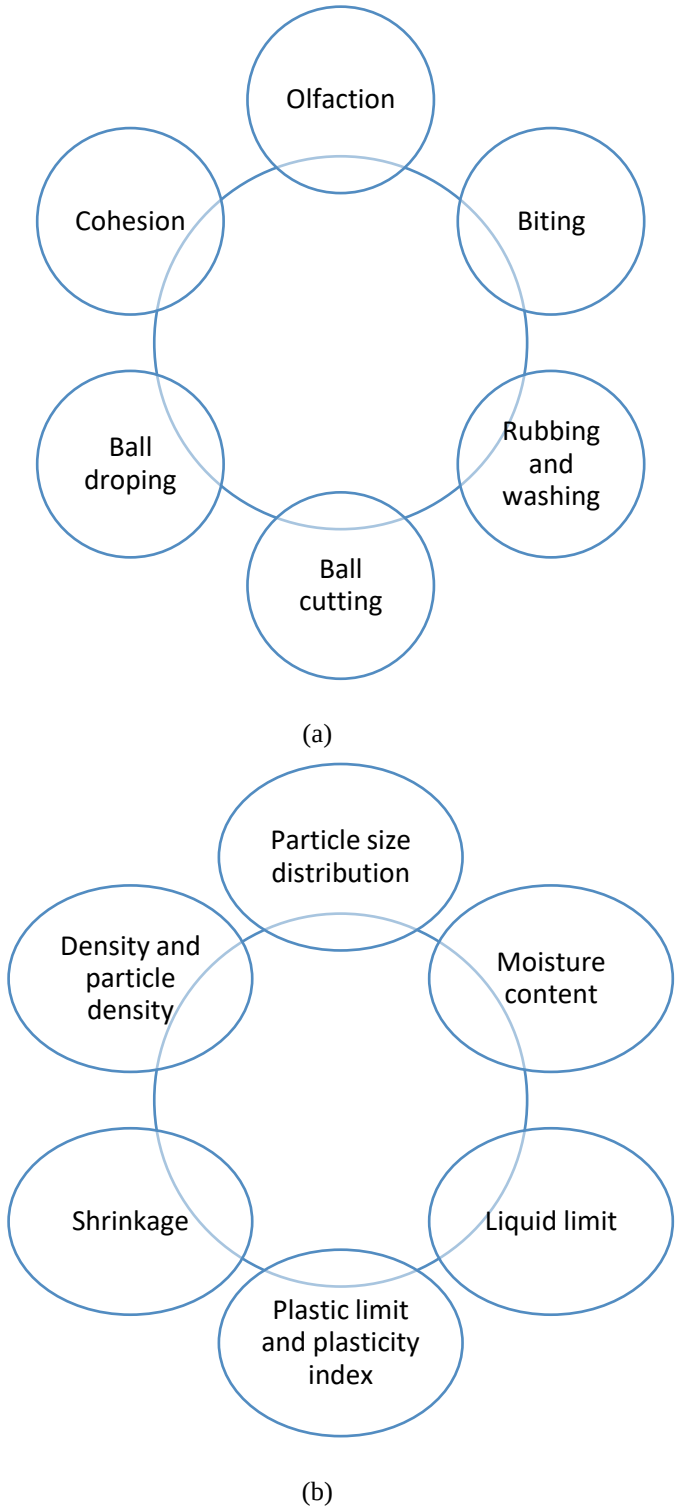

Figure 2. 16. Soil classification tests: (a) empirical and (b) standardized.

The soil in a construction site should be stored in an air-dry condition and in an area accessible by machinery, if machinery is planned to be used to handle the soil. The soil is finally sieved, to remove large particles and mixed by: adding water, kneading,

stirring and trampling until it reaches a viscous consistency (plastic consistency close to the liquid limit). At this point fibres are added and the whole mix is again kneaded, stirred and trampled until it reaches a plastic consistency (Danaher, 1957a).

Traditionally loam preparation was a slow and laborious process that sometimes was carried out by human or animal labour. Nowadays modern machinery can be used to increase the efficiency of the process. It is considered that the material is ready to be used when a sample of 45 by 30 cm would not bulge and at this point the construction of the walls could start (Macdonald and Doyle, 1997).

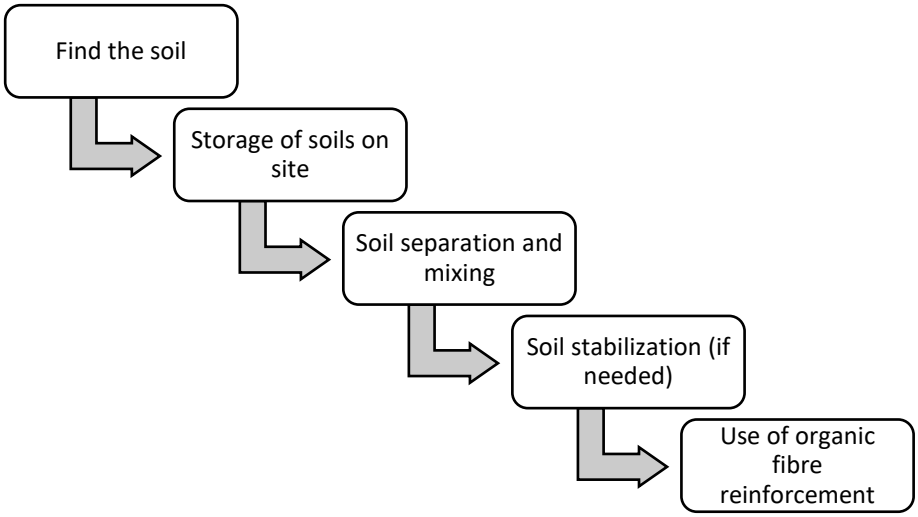

Figure 2. 17. Loam preparation process.

2.3.3 Construction process

The cob construction process starts on top of the foundation, which traditionally was built on stone masonry and nowadays is commonly built using reinforced concrete. The cob mix is directly placed on the foundation either by hand or with the use of a pitchfork or machinery, while its consistency is still plastic (see Figure 2. 18 (a)). Extra moulding work is done directly over the wall, either by hand/feet or using tools such as a pitchfork or a shovel, to fill all air voids. The material is also beaten on the wall sides to keep its verticality. The material will protrude from the lateral faces of the wall and its shape is going to be quite irregular.

Lifts of between 30 and 60 cm in height are built in this manner, one on top of the other. It is necessary to wait during a drying period of about 5 to 7 days before adding a new lift to the wall. Before proceeding with subsequent layers, the previous one is paired

using a sharpened shovel, a timber saw or any similar tool that will allow the removal of extra material from the wall's faces. After pairing, the wall shape will be more even and if it is planned to apply a render the wall should be prepare while the material is still easily deformable by creating small holes in its surface (see Figure 2. 18 (b)). Subsequent cob layers are added until the desired wall height is reached. As new lifts are added before previous ones are entirely dry, the whole wall dries in a similar time frame, thus no weak planes are created, and the final result is a monolithic element.

2.3.4 Material testing: cob's mechanical properties and structural behaviour

Cob walls are monolithic elements. Its cohesion is provided mainly by the clay cementing properties and the added organic fibres such as straw or heather (Miccoli *et al.*, 2014). Monolithic techniques have the advantage of not presenting weakness planes such as it is in the case of modular constructions (namely adobe or CEB). Table 2. 7 summarizes some of cob's mechanical properties as reported by different authors.

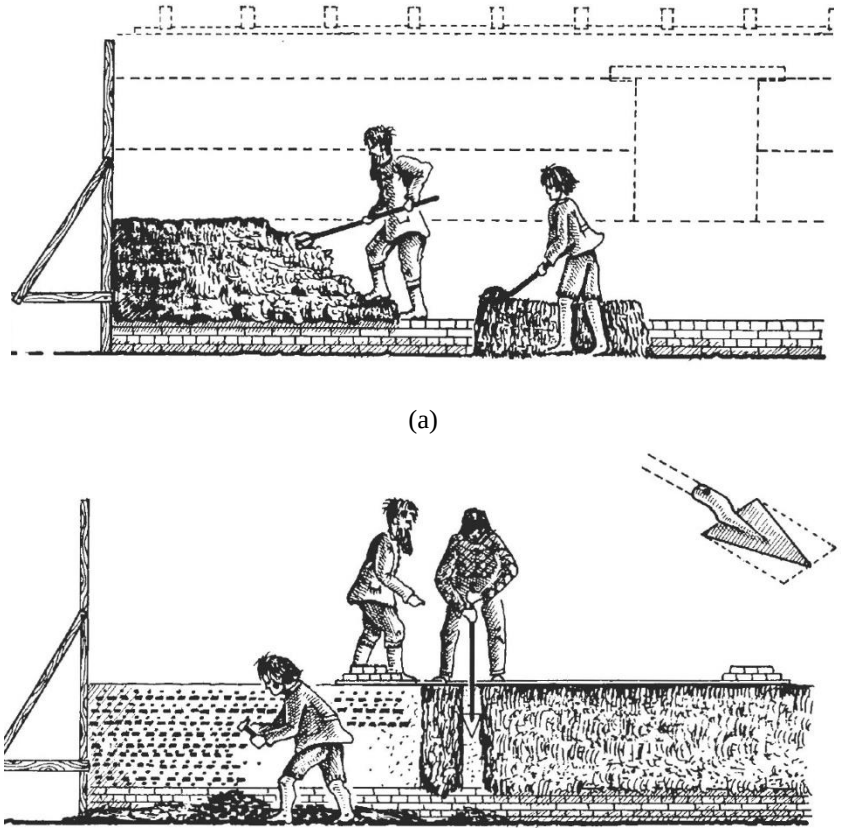

(a)

(b)

Figure 2. 18. Traditional cob construction process: (a) piling and (b) paring (Doat, 1979).

Table 2. 7. Cob's mechanical properties according to several authors.

Author/Property	Saxton (1995)	Minke (2000)	Ziegert (2003)	Akinkurolere *et al.* (2006)	Keefe (2012)	Miccoli *et al.* (Miccoli *et al.*, 2014, Miccoli *et al.*, 2017)	Quagliarini and Maracchini (2018)
Compressive strength f_c (MPa)	0.00 – 1.65	0.5 – 5.0	0.45 – 1.40	0.6 – 2.2	0.6 – 1.4	1.59	1.12 – 1.35
Tensile strength f_t (MPa)	NR*	0	NR*	NR*	NR*	(0.10-0.16) f_c	NR*
Tensile fracture energy (N/mm)	NR*	NR*	NR*	NR*	NR*	(0.3-0.8) f_t	NR*
Bending strength (MPa)	NR*	0	NR*	NR*	NR*	NR*	NR*
Shear strength (MPa)	NR*	NR*	NR*	NR*	NR*	0.5	NR*
Shear modulus (MPa)	NR*	NR*	NR*	NR*	NR*	420	NR*
Young's modulus (MPa)	NR*	600 – 850	170 – 335	NR*	NR*	651	16.90 – 23.73
Poisson´s ratio (-)	NR*	NR*	NR*	NR*	NR*	0.15	0.12 – 0.09
Density (kg/m^3)	NR*	1700 - 2200	1400 - 1700	NR*	NR*	1475	1860
Straw content (% by mass)	0 - 3	NR*	NR*	0 – 3	NR*	1.7	NR*
Grading	30 % gravel, 35 % sand, 35 % silt and clay	NR*	NR*	50 % coarse aggregate, 35 % fine aggregate, 15 % silt and clay	NR*	18 % gravel and sand, 61 % silt, 21 % clay	13.5 % sand, 50.5 % silt, 36 % clay
Clay mineralogy	NR	NR*	NR*	NR*	NR*	Kaolin, Illite and smectite-illite	NR*
Compaction	Eight layers using a 2.5 kg rammer	NR*	NR*	NR*	NR*	NR*	NR*

*NR = Non-reported.

Table 2. 7. Cob's mechanical properties according to several authors. (continuation).

Author/Property	Saxton (1995)	Minke (2000)	Ziegert (2003)	Akinkurolere et al. (2006)	Keefe (2012)	Miccoli et al. (Miccoli et al., 2014, Miccoli et al., 2017)	Quagliarini and Maracchini (2018)
Specimens	Cylinders 300 mm length by 150 mm diameter	NR*	NR*	NR*	Cylinders 300 mm length by 150 mm diameter	Wallettes with 420 mm length by 420 mm height by 115 mm thickness	Wallettes with 930 mm length by 456 mm height by 310 mm thickness
Experimental method	Unconfined compression tests at different moisture contents	NR*	NR*	Unconfined compression tests at different moisture contents	Unconfined compression tests at different moisture contents	Simple and diagonal compression tests	Compression tests under different load rates

*NR = Non-reported.

Keefe (2012) performed a series of cube and cylinder compressive tests to determine the compressive strength of cob. He found that compression cubes presented between 20 % to 25 % higher resistance in comparison to cylinders (ratios 1:1 vs ratios 2:1). This variation in percentage is also common when the compressive strength of concrete is obtained from specimens with similar ratios. According to Keefe cob's compressive strength varies according to grading, clay content and clay mineralogy and to the degree of compaction of the material. He concluded that cob walls may attain strengths between 0.6 MPa and 1.1 MPa and even possibly higher values if clay-rich soils are used (1.4 MPa). More importantly, Keefe found out that cob's Unconfined Compressive Strength (UCS) seems to variate linearly with respect to moisture content. Figure 2. 19 shows the UCS values found by Keefe when cob cylinders where tested at different moisture content. Similar negative linear variation trends were found by Akinkurolere *et al*. (2006) (see Figure 2. 20 (a)) and by Saxton (1995) (see Figure 2. 20 (b)) after determining the compressive strength of cob mixes at different levels of moisture content (and different levels of straw contents as well). Further details on the effect of moisture content on the compressive strength (and rigidity) of cob can be found in the PhD thesis of Matthew James Addisson Greer submitted to the School of Architecture at Plymouth University (Greer, 1996).

Moisture content is also important during manufacturing and operational conditions. During the manufacturing process the consistency of the mix should be plastic. The ideal moisture content should allow the mix to be deformed under mechanical pressure but at the same time, maintain the given form and do not deform under its own weight. At operational conditions the moisture content should be maintain as low as possible with two aims; to allow material absorbing moisture from the environment, thus regulating the indoor building conditions (see discussion in section 2.2.1), and secondly, to avoid an excessive weakening of the material, which may cause the failure of the structure under constant loads.

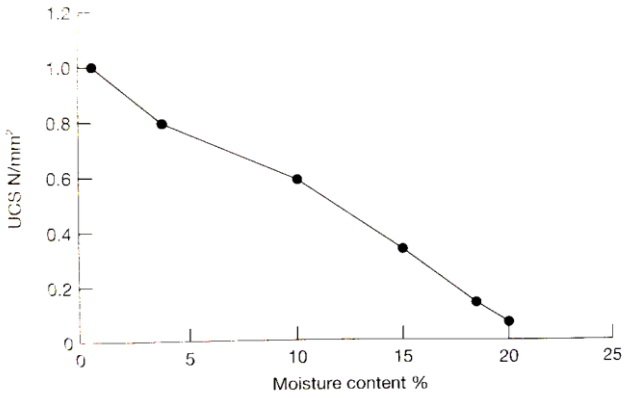

Figure 2. 19. Cob's unconfined compressive strength vs moisture content graph (Keefe, 2012).

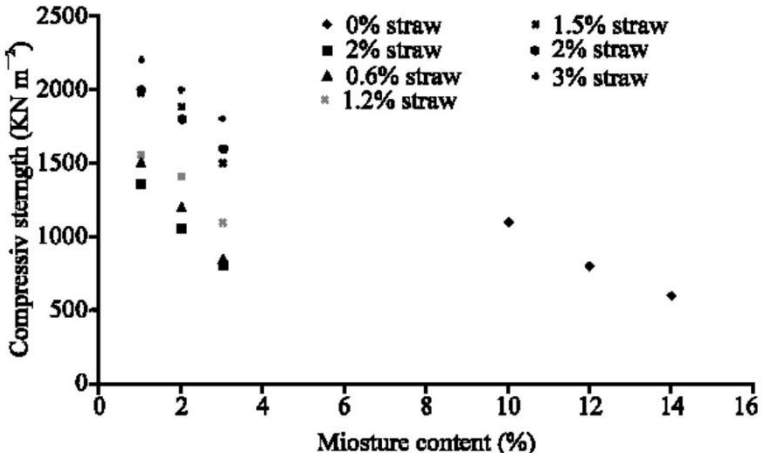

(a)

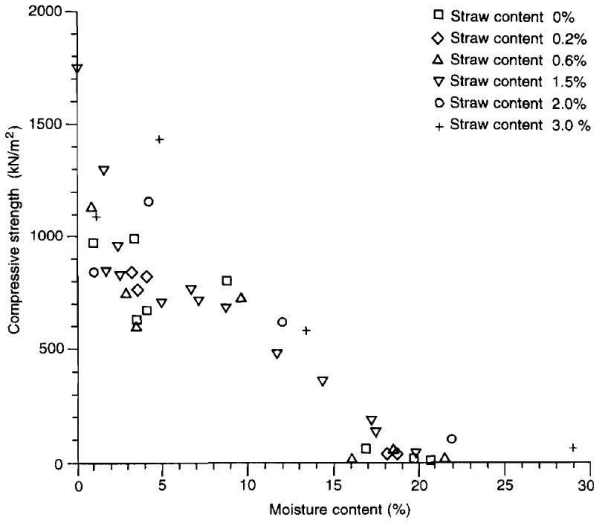

(b)

Figure 2. 20. Cob's compressive strength as a function of moisture and straw content according to (a) Akinkurolere et al. (2006) and (b) Saxton (1995).

Miccoli *et al.* determined experimentally the stress/strain curves of cob both under uniaxial compression (see Figure 2. 21 (a)) and under diagonal compression (see Figure

2. 21 (b)) (Miccoli *et al.*, 2017). They also reported the failure mechanism and the crack patterns of the tested wallets (see Figure 2. 22) (Miccoli *et al.*, 2014).

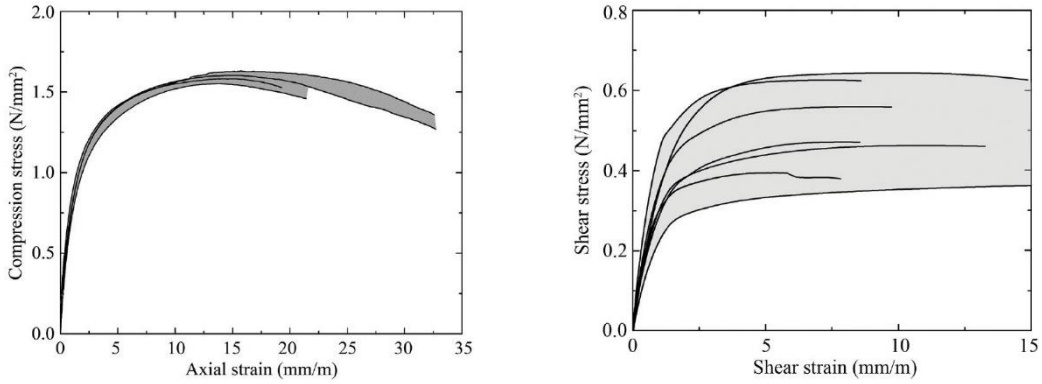

(a) (b)

Figure 2. 21. Cob's structural behaviour under: (a) simple compression and (b) diagonal compression (Miccoli et al., 2017).

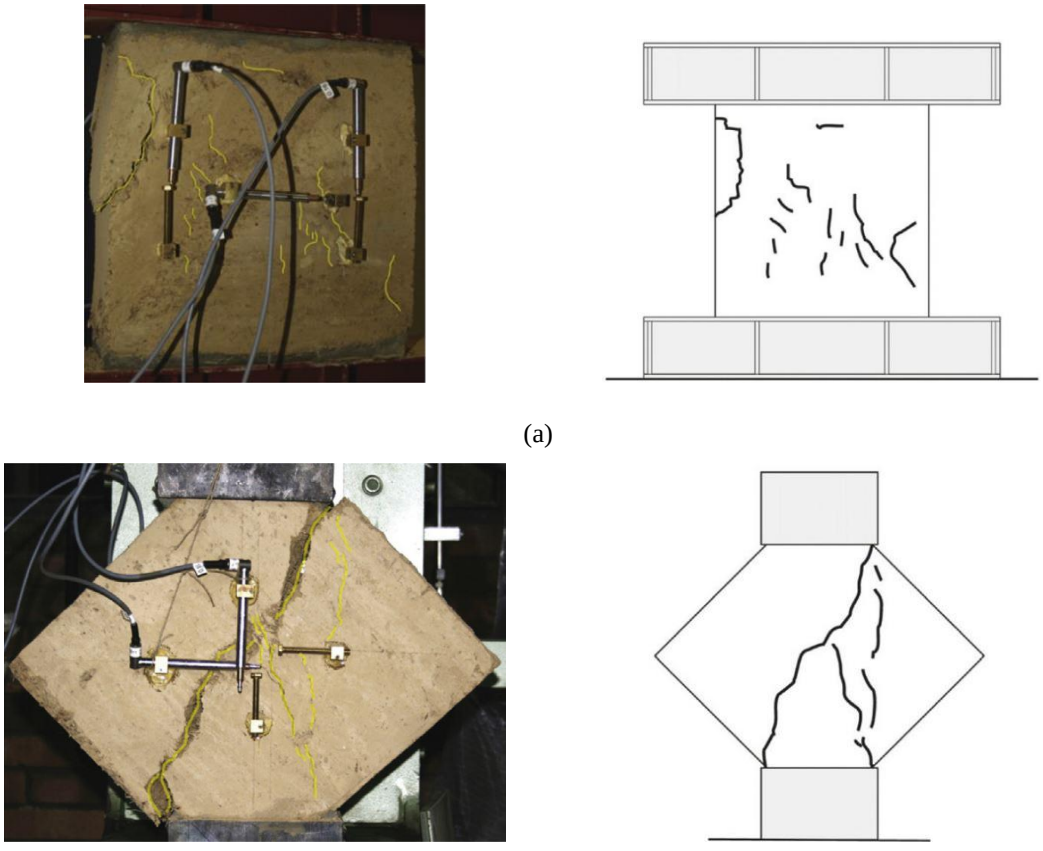

(a)

(b)

Figure 2. 22. Cob's failure modes under: (a) simple compression and (b) diagonal compression (Miccoli et al., 2014).

Despite the relatively low compressive strength of cob (mean compressive strength of adobe and rammed earth of 3.28 and 3.73 MPa respectively, as determined by

the experimental work of Miccoli *et al*. (2014)), this material presents a relatively good performance in terms of shear strength if compared with other earthen construction techniques. Moreover, cob appears to be quite ductile, since it presents a relatively long post-peak curve due to the fibres added to the mixture (Miccoli *et al.*, 2014).

Axial compression tests were also performed by Quagliarini and Maracchini (2018). Their tests were performed under force control (see Figure 2. 23). Load rate application (walls B, C and D attained failure after 15-20 min (about 0.77 MPa/min), whereas wall A failed after 50 min (about 0.025 MPa/min)), as well as water content influence, were explored. They reported an average compressive strength value, f_c, of 1.12 MPa, a Poisson's ratio, v, of 0.12 and a Young's modulus, E, of only 16.9 MPa, considerably smaller in comparison with values reported by other authors (see Table 2. 7), for walls B, C and D. The stress/strain curves obtained by Quagliarini and Maracchini for those walls are shown in Figure 2. 24. Quagliarini and Maracchini reported an increase of 20 % for the compressive strength and of 40 % for Young's modulus of wall A. Poisson's ratios seems to be not affected by the load rate according to them.

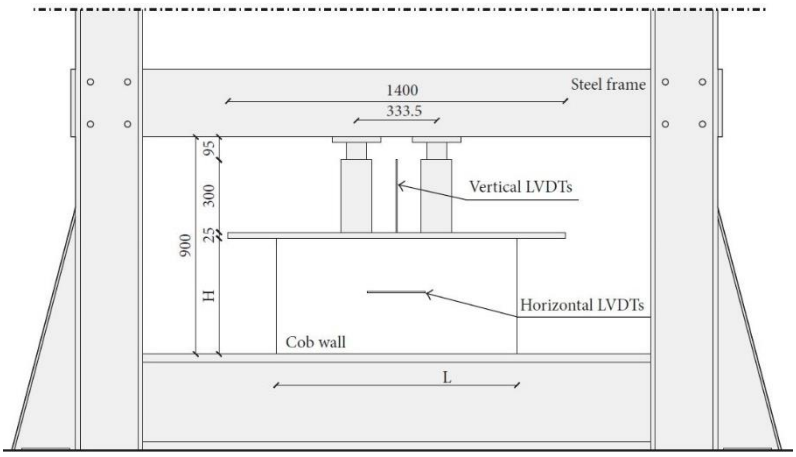

Figure 2. 23. Axial compression experimental setup of cob wallettes (measurements in mm) (Quagliarini and Maracchini, 2018).

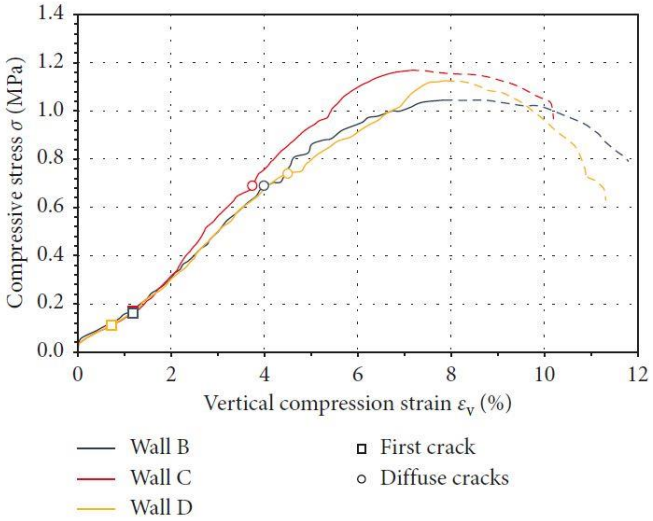

Figure 2. 24. Cob's structural behaviour under axial compression (Quagliarini and Maracchini, 2018).

McPadden and Pavia (2016) performed a study to identify cob's mechanical properties and the effect of different stabilization materials on its compressive strength. The materials used in that study were lime and cement in percentages of 5 and 15 % by weight. The stress/strain curves obtained by McPadden and Pavia are shown in Figure 2. 25. Cob's stabilisation is outside the scope of this thesis, as there is no evidence that vernacular cob walls had ever been chemically stabilized; readers can get more information about it in the reference (McPadden and Pavía, 2016).

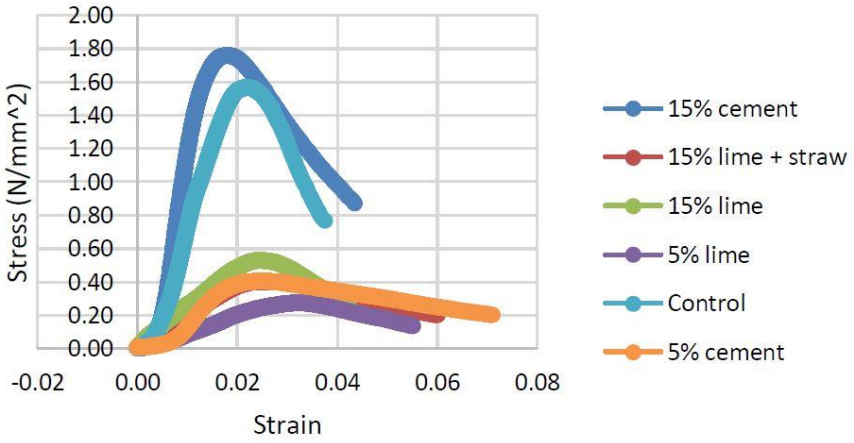

Figure 2. 25. Stress/strain curves of stabilized cob (McPadden and Pavía, 2016).

2.3.5 Cob numerical modelling

Numerical modelling of cob has been undertaken by Miccoli *et al*. using an FEM macro-modelling approach in the software Diana (DIANA, 2014). They assumed plane stress and that cob is a homogenous and continuous material. A Total Strain Rotating Crack

Model (TSRCM), constitutive model, which is based in a fracture energy smeared approach, was used with a multilinear definition of the stress/strain relationship for the compressive behaviour with an initial linear segment of 0.3 f_c and a post peak segment with a negative slope of 0.02 times the Young's modulus value (Figure 2. 26 (a)) and an exponential relationship for tensile behaviour (Figure 2. 26 (b)) (Miccoli *et al.*, 2019).

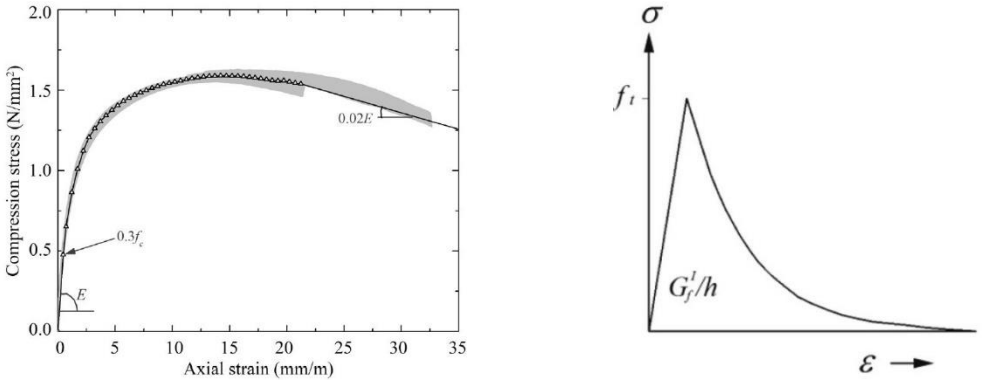

(a) (b)

Figure 2. 26. Cob's material constitutive model implemented by Miccoli et al. (a) Compression behaviour and (b) tensile behaviour (Miccoli et al., 2019).

Miccoli's *et al*. calibrated model was able to replicate the development of the shear stress/shear strain relationship (see Figure 2. 27). Deviations with respect to the experimental values obtained for the maximum shear stress and respective shear strain were reported within 10 %. They also reported the specimen damage in terms of maximum principal strains for four load levels (see Figure 2. 28), namely, $0.83f_s$, $0.92f_s$, $0.97f_s$ and $1.0f_s$, where f_s is the maximum shear stress. According to the authors the numerical model was not able to replicate the diagonal failure pattern observed in the experiments (see Figure 2. 22 (b)) due to the non-symmetric conditions in the samples and the testing setup.

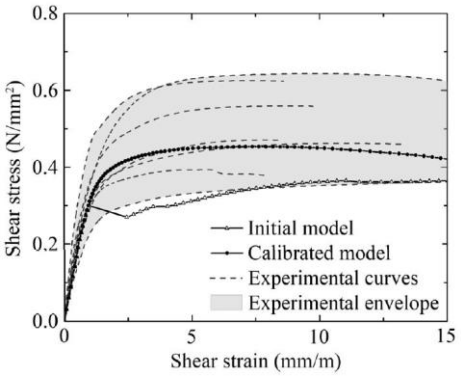

Figure 2. 27. Cob's structural response comparison between experimental and numerical results (Miccoli et al., 2019).

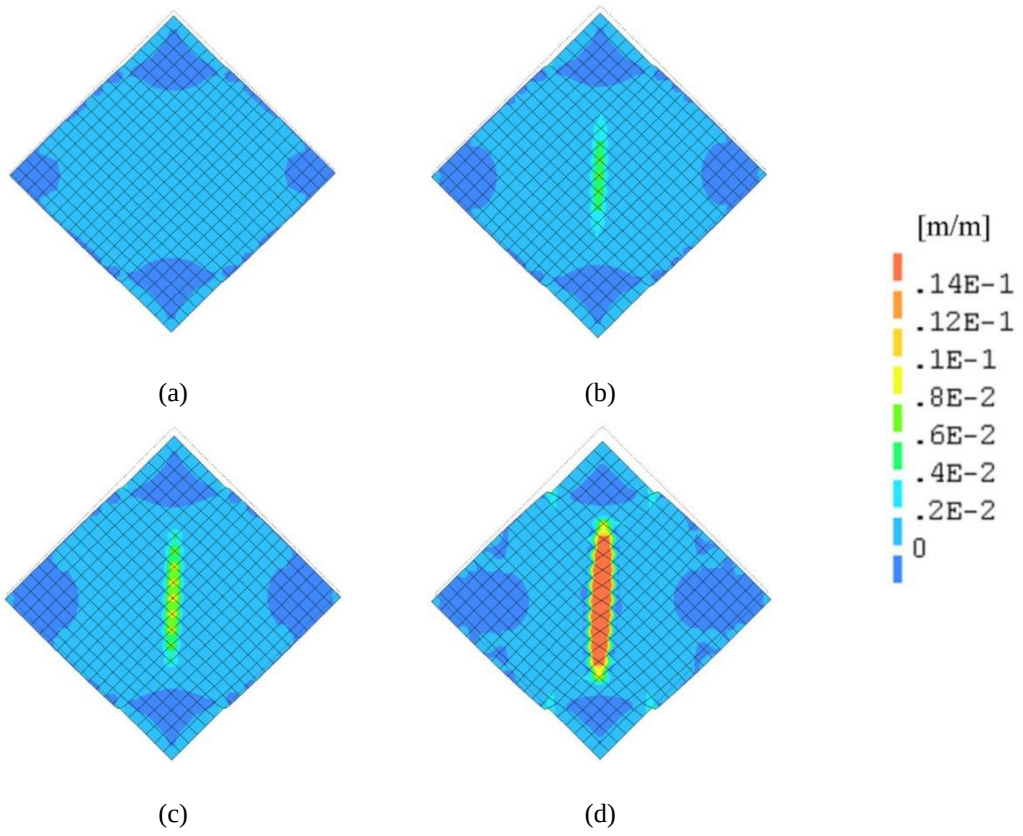

Figure 2. 28. Maximum principal strains reported by Miccoli et al. (2019) for load levels of (a) 0.83 fs, (b) 0.92fs, (c)0.97fs and (d) 1.0fs.

Quagliarini and Maracchini (2018) also performed numerical simulations of cob. They used the finite element software MIDAS FEA (MIDAS, 2006), and applied a smeared-crack macro modelling approach adopting a 2D plane stress simplification. The material constitutive models implemented by them are shown in Figure 2. 29. The stress/strain curve reported by these authors agrees with the experimental results until the peak strength of the material is reached (see Figure 2. 30). Unfortunately, no post-peak behaviour was reported, which is of great importance in terms of energy dissipation capacity of the material. The damage was reported in terms of principal stresses (see Figure 2. 31 (b)) and according to Quagliarini and Maracchini's interpretation the failure pattern reproduced matched the typical crack pattern observed on the compressive tests of the specimens (see Figure 2. 31 (a)).

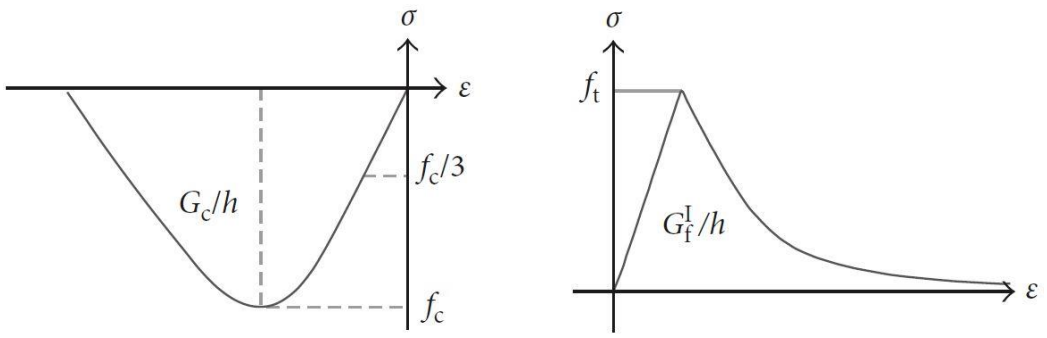

(a) (b)

Figure 2. 29. Cob's material constitutive model implemented by Quagliarini and Maracchini (2018). (a) Compression behaviour and (b) tensile behaviour.

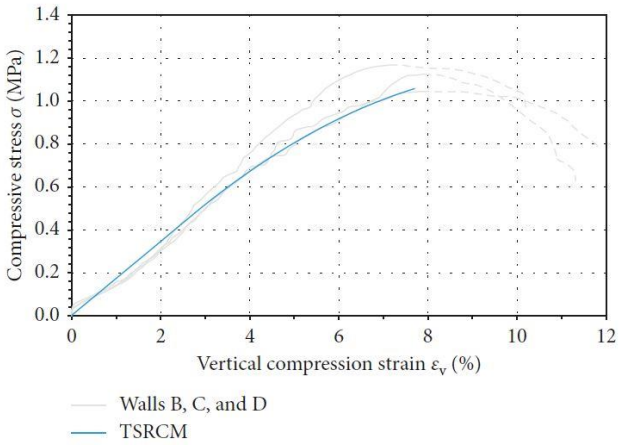

Figure 2. 30. Cob's structural response comparison between experimental and numerical results (Quagliarini and Maracchini, 2018).

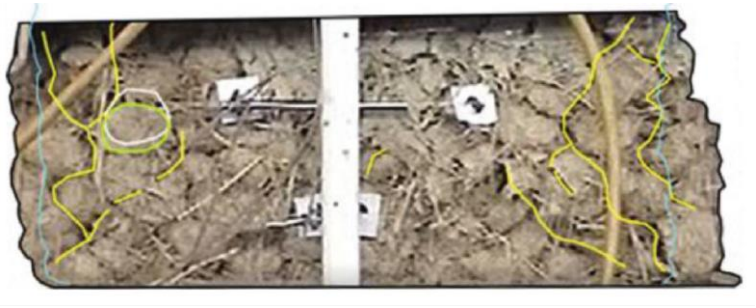

(a)

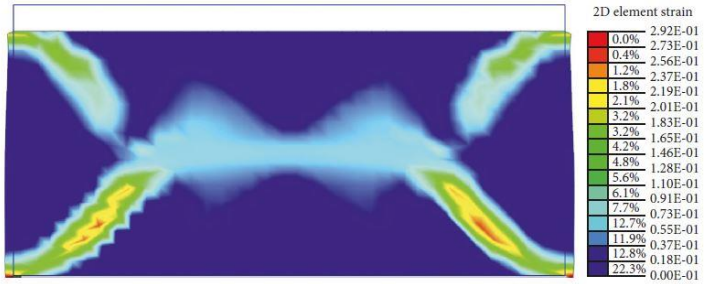

(b)

Figure 2. 31. Cob wallets failure modes: (a) experimental crack patterns and (b) principal tensile strains for ε_v of 8 % (Quagliarini and Maracchini, 2018).

2.3.6 Cob's dynamic behaviour

Research and publications concerned with cob's dynamic behaviour are scarce. A comparison between an unreinforced cob wall panel and a bamboo strips/steel meshing retrofitted cob panel has been performed by Rafi and Lodi (2017). They determined the changes in the dynamic properties of both walls, namely, equivalent viscous damping ratio, ζ, and fundamental frequency of vibration, f, by the means of Free Vibration Tests (FVT) after subjecting them to dynamic excitation in a shaking table. By comparing the dynamic response of both panels, they clearly observed the efficiency of the applied retrofitted design as it increased the in-plane shear capacity of the retrofitted cob wall in comparison with the non-retrofitted wall.

Rafi *et al*. (2018) tested further the retrofitting technique proposed by Rafi and Lodi (2017). They built a one-third model of a prototype building with typical characteristics of traditional cob buildings from Awaran, Pakistan reinforced with the system of bamboo strips/steel meshing. The model was subjected to different levels of a scaled acceleration time history record of the 1940 El Centro earthquake. For the different excitation levels, the damage in the scaled building, its dynamic characteristics, its acceleration responses and amplifications, its walls' in-plane and out-of-plane

accelerations, as well as its energy dissipation were recorded and analysed. They concluded that the observed structural damages suffered by the model corresponded to four performance levels, namely, operational level, immediate occupancy, life safety and collapse prevention, which were correlated with accepted damage limit states (Rafi *et al.*, 2018).

Another dynamic test was carried out in a cob building model by the Stanley Park Ecology Society in collaboration with the University of British Columbia (UBC) (Kutarna *et al.*, 2013). After subjecting the building model, of circular plan, to an acceleration equivalent to a 7.2 magnitude earthquake on the Richter scale, only minor cracks were observed. Significant damage was caused after applying an acceleration equivalent to a 9.0 magnitude earthquake on the Richter scale and even for such a high level of accelerations the cob walls did not collapsed completely.

No 3D dynamic FEM non-linear simulations of cob structures were found in the literature review. Furthermore, numerical simulations of reinforcement techniques to strengthen cob buildings are not available.

2.3.7 Cob's advantages and disadvantages

In comparison with other earthen construction techniques, cob has the following advantages (Doat, 1979):

- No formwork needed (in comparison with rammed earth).
- Relatively cheaper (not as cheap as turf though).
- Simple tools required.
- Excellent alternative for humid soils and weather conditions.
- Compatible with renders, highly sculptural and malleable.

On the other hand, cob presents the following disadvantages (Doat, 1979):

- The drying period could be relatively long.
- More prone to weather decay.
- Lower compressive strength.

In addition to what Doat mentioned, cob, which results in monolithic walls, has the advantage of not presenting localised weakness planes, like in the case of adobe, CEB, sods and other masonry techniques, between the units and mortar joints. On the other

hand, cob's compressive strength is relatively lower to the compressive strength of adobe or rammed earth walls as reported by Miccoli *et al*. (2014).

2.4 Vernacular architecture

Vernacular architecture, also understood as folk or popular architecture (Rapoport, 1969), represents the way in which communities throughout the world inhabiting a certain territory, characterised by specific environmental conditions and where different materials are locally available, create their own buildings. It can also be described as "*architecture without architects*" (Rudofsky, 1964), since it is a product of the socio-cultural aspects characterising each one of the different communities that create it. Vernacular architecture is the result of intergenerational refinement of building knowledge and construction technique know-how. Skills were traditionally transferred either from master to apprentice or from elder to younger and the different cultures' construction practices thrived for centuries (Piesik, 2017). Thus, it is a communal product which represents the world's cultural diversity.

Furthermore, vernacular architecture has been for a long time the engine of local economies satisfying those communities' demands for shelter with the use of local craftsmanship, as well as with the use of local and cheap materials. A state-of-the-art review of the economic benefits of vernacular materials applied in contemporary construction of housing is presented by Zami and Lee (2010).

As such, vernacular architecture embodies the intangible and material wealth of traditional knowledge. Vernacular architecture's values and the need of their preservation has been universally recognized (UNESCO, 2005). Moreover, vernacular architecture embodies the environmental, socio-cultural and socio-economic concepts that define sustainability (Correia *et al.*, 2014).

The study and understanding of vernacular architecture will not only help us to preserve its historical, cultural, and architectural values, it can also guide us through the achievement of a contemporary sustainable architecture. Examples of how vernacular materials, construction techniques and typologies may help contemporary buildings to be more sustainable are presented by numerous authors (Moquin, 1994, Oliver, 2007, Rael, 2009, Pacheco-Torgal and Jalali, 2012, Correia *et al.*, 2013, Correia *et al.*, 2014, Mileto *et al.*, 2014, Nash, 2016, Schroeder, 2016, Piesik, 2017). A full analysis of how vernacular

architecture knowledge can be applied for building seismic retrofitting is presented elsewhere (Correia *et al.*, 2015).

The European research project VERSUS (Correia *et al.*, 2014) identified a series of principles and strategies integrated in vernacular architecture that could be adopted and applied in new building projects to create a contemporary sustainable architecture. These principles are organized around the environmental, socio-cultural and socio-economic aspects that define sustainability itself.

Environmental sustainability is defined as:

> *"The capacity of the human intervention in decreasing or avoiding a building's adverse environmental impacts, reacting to every change in the environment understood as the set of conditions in which life is possible and regarding the whole biological quality" (Correia et al., 2014).*

Socio-cultural sustainability considers aspects such as social identity, community culture and social cohesiveness (Choi and Sirakaya, 2006). It is tightly linked to environmental sustainability since the deterioration of the environment and the consequently lack of natural resources leads to social inequalities, conflicts, social segregation and instability (Chiu, 2004).

Socio-economic principles of vernacular architecture deal with the efficient management of local resources; self-management economies; the impact of the economic factor on local development; the assessment of the economic value of vernacular architecture and with the impact of its conservation in economic terms (Correia *et al.*, 2014).

Figure 2. 32, Figure 2. 33 and Figure 2. 34 summarise the environmental, socio-cultural and socio-economic sustainability principles and the strategies, respectively, intrinsic of most types of vernacular architecture, necessary to achieve them. These diagrams were prepared by the author based on the information presented in the VERSUS project report (Correia *et al.*, 2014).

2.5 Summary

This chapter has presented the state of the art on the conservation of earthen vernacular buildings in Ireland. More specifically, it has been divided into three different headings; conservation approach, earthen construction techniques and vernacular architecture.

The current conservation philosophy, which is broadly accepted and applied by conservators, is based on the different Charters, guidelines and recommendations issued by ICOMOS. To perform an adequate conservation of the architectural heritage, in accordance with this philosophy, an iterative process must be followed. The process is divided into four stages; research, diagnosis, intervention and control. Three different approaches are defined and advised to be applied during the research stage in order to obtain a full understanding of the structure under study. Those approaches are: historic, qualitative and quantitative. During the quantitative approach material and numerical tests, structural analysis and monitoring investigation are performed. The type of tests available for the investigation of historical buildings are divided based on their level of invasibility into: NDT, MDT and DT. A gap on the application of MDT techniques to cob buildings has been identified. This is addressed in the current thesis by presenting the experimental campaign performed in the laboratory facilities of TCD for the validation of the application of the flat jack test to cob walls to determine in-situ the local levels of stresses and mechanical properties of cob walls.

Furthermore, the experimental was also used to involve a great number of people and disseminate knowledge about the conservation of earthen vernacular building. Academics, technical staff, researchers, as well as undergraduate students and the general public participated in the different activities developed during this PhD related to the conservation of earthen vernacular buildings and the use of natural materials for sustainable construction purposes.

Few authors have attempted to reproduce the characteristic non-linear behaviour of cob by implementing numerical methods. Miccoli *et al.* (2019) used a simplified plane stress and FEM macro-modelling approach to calibrate a TSRCM based on the experimental results Miccoli *et al.* (2014) presented of a diagonal compression test. Quagliarini and Maracchini (2018) also performed a calibration of a plane-stress smeared-crack macro model to replicate the stress/strain curve and failure mode they observed after subjecting a series of cob wallettes to simple compression tests. The lack

of full 3D simulations and validation of calibrated models to reproduce the structural response of cob walls is one of the gaps this thesis aims to fill by presenting a series of, both 2D and 3D, cob walls simulations. The calibration of the numerical models presented in this thesis was based on the experimental results reported by Miccoli *et al*. (2014) after subjecting a series of cob wallettes to simple compression tests whereas that their validation was performed by trying to reproduce the experimental diagonal compression test results reported by the same authors.

It has been identified that vernacular architecture is the result of intergenerational refinement of building knowledge and construction technique know-how. In that sense, it is agreed that there is much to be learn from historic buildings. Thus, in this thesis existent cob buildings in Ireland are analysed by a parametric analysis to provide guidance for practitioners on the analysis of existent cob vernacular buildings and for the design of new sustainable and resilient ones.

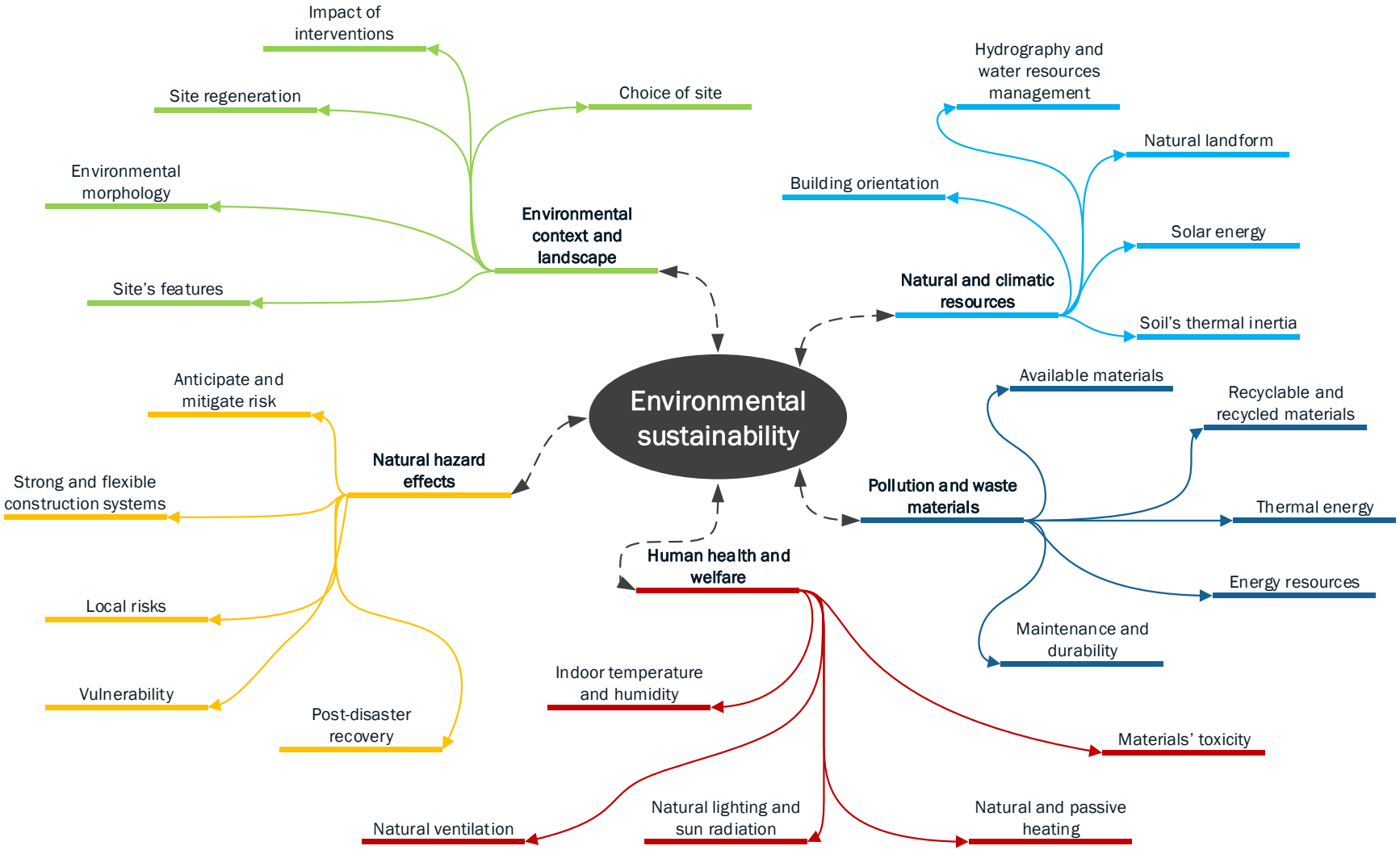

Figure 2. 32. Environmental sustainability principles and strategies.

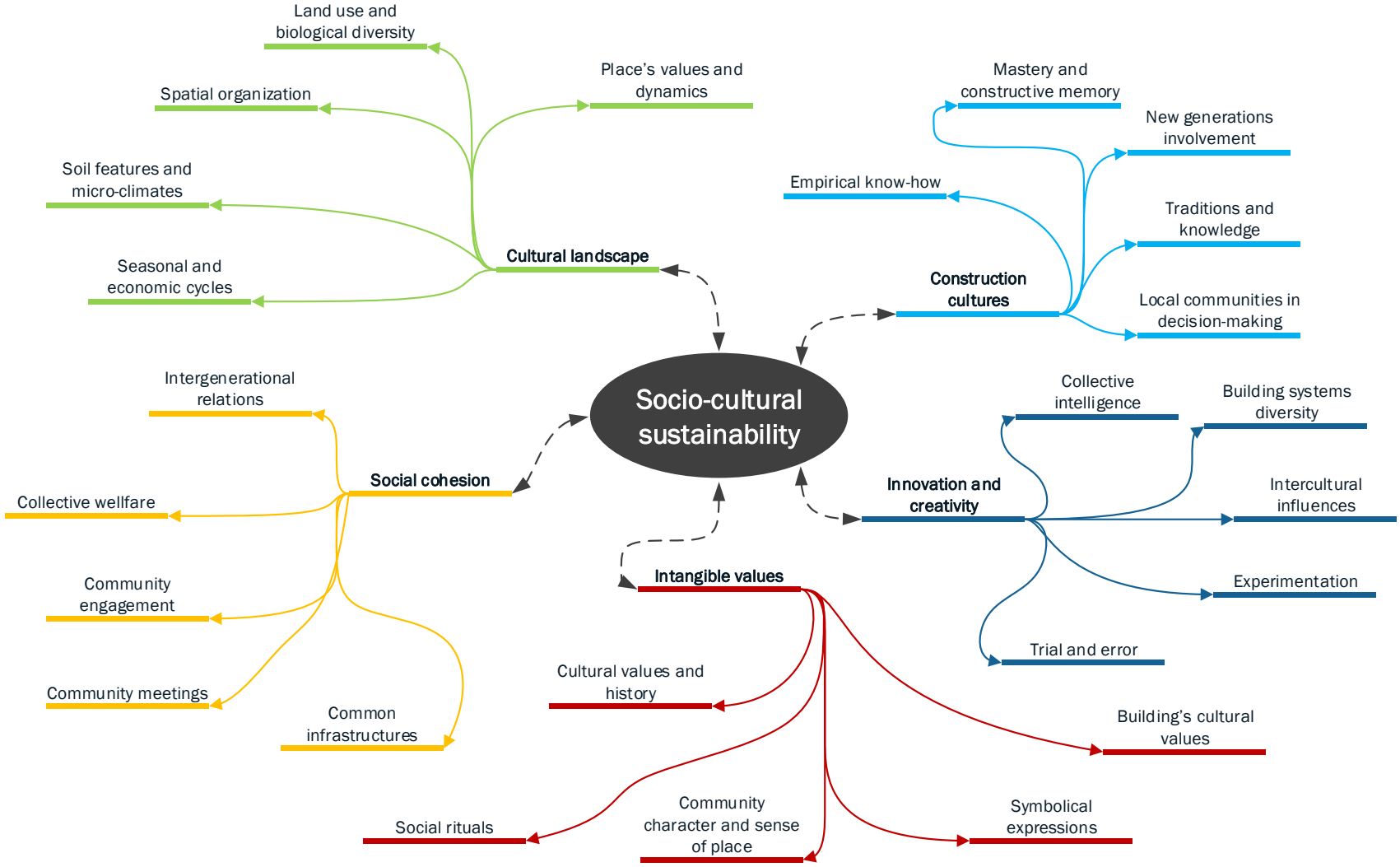

Figure 2. 33. Socio-cultural sustainability principles and strategies.

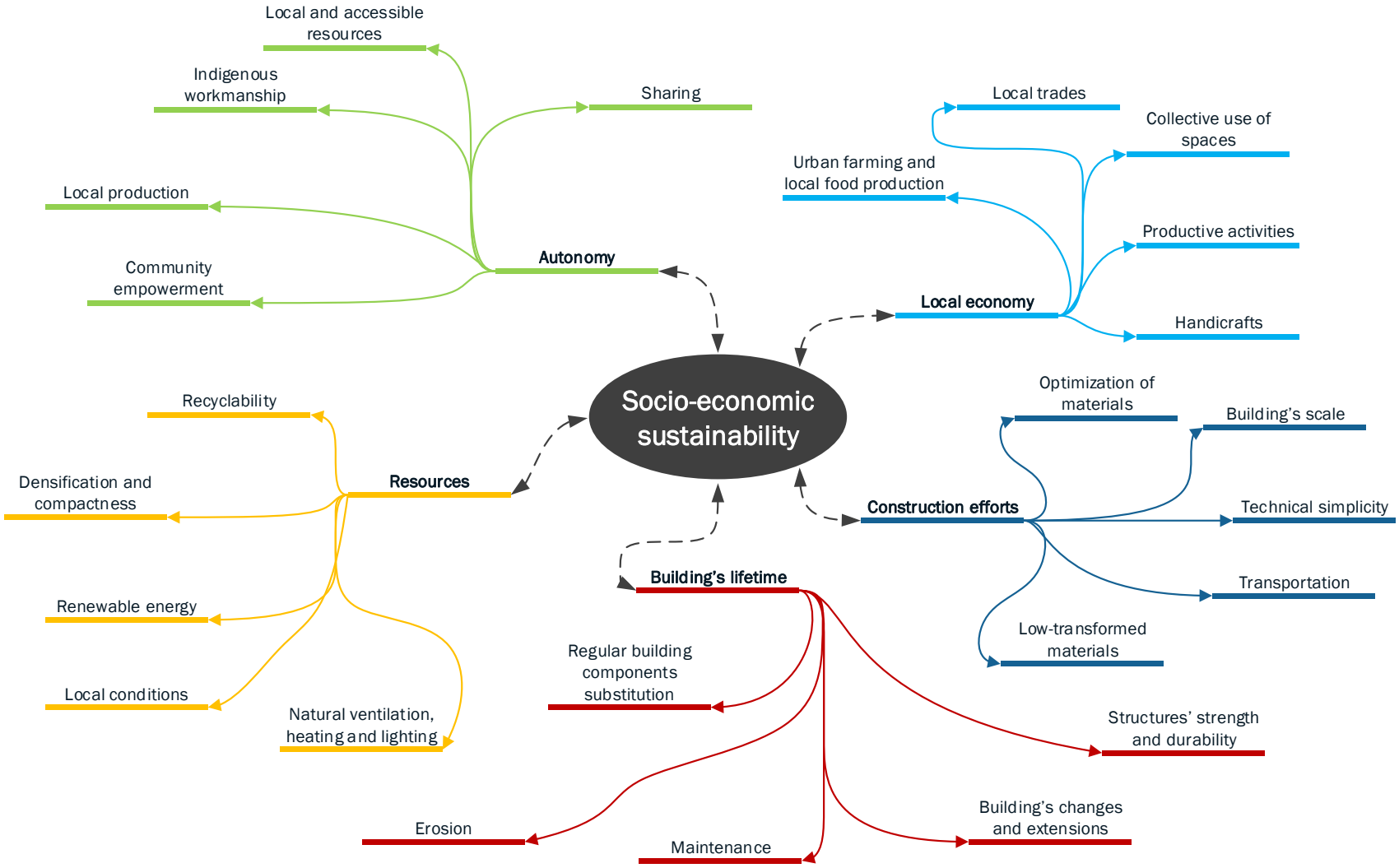

Figure 2. 34. Socio-economic sustainability principles and strategies.

Chapter 3: Earthen vernacular buildings in Ireland

This chapter contains the results of a thorough literature review on the surviving earthen vernacular buildings in Ireland. Historical context as well as social, cultural and economic aspects influencing their development and leading to their current situation are described. Based on this information, the essential qualifying factors that define the authenticity of the surviving earthen vernacular buildings in Ireland are identified.

3.1 Historical context

3.1.1 General figures

The Republic of Ireland is a country with a population of 4.804 million[1], a surface area of 69,797[2] km^2 and a population density of 69.7[3] habitants per km^2. The territory of the country is divided into four provinces (Munster, Leinster, Ulster and Connaught) and 26 counties. 63 % of the population of Ireland lives in cities, whereas 37 % lives in rural areas (United Nations, 2019b).

Ireland's CO_2 emissions are estimated at 34.1 million tons per annum corresponding to 7.3 tons per person per annum (United Nations, 2019b). In accordance with the Paris Agreement (United Nations, 2015a), Ireland has committed to reduce its CO_2 emissions by 20 % by 2020 and by 80-95 % by 2050 (SEAI, 2016).

On average, Ireland is visited every year by 8 million people (15-year average), almost twice as many people living in the country. The number of tourists in 2018 surpassed 10 million (United Nations, 2019b), a figure initially planned to be achieved by 2025. The tourist activity is an important contributor to the economy of the country. According to the Department of Transport, Tourism and Sport's (DTTS) overall goals it

[1] Projected estimate (medium fertility variant).
[2] 2015
[3] Projected estimate (medium fertility variant).

is expected that the revenue contributed by tourism by 2025 reaches 5 billion euros (DTTS, 2015).

Ireland and the United Kingdom (UK) are considered to be located in "*very low seismicity*" and in "*low seismicity*" regions in the context of Eurocode 8 (CEN, 2004). A seismic intensity map on the European Macroseismic Scale (EMS) is available showing that Ireland's territory is located within the 3rd to 5th level of the scale (see Figure 3. 1 (a)). Unfortunately, no onshore seismic zonation map is currently available with information about Peak Ground Acceleration (PGA) necessary to define seismic loads on buildings. On the other hand, an offshore seismic hazard map has been developed through a British-Norwegian collaboration and is presented in Figure 3. 1 (b) (Solomos *et al.*, 2008).

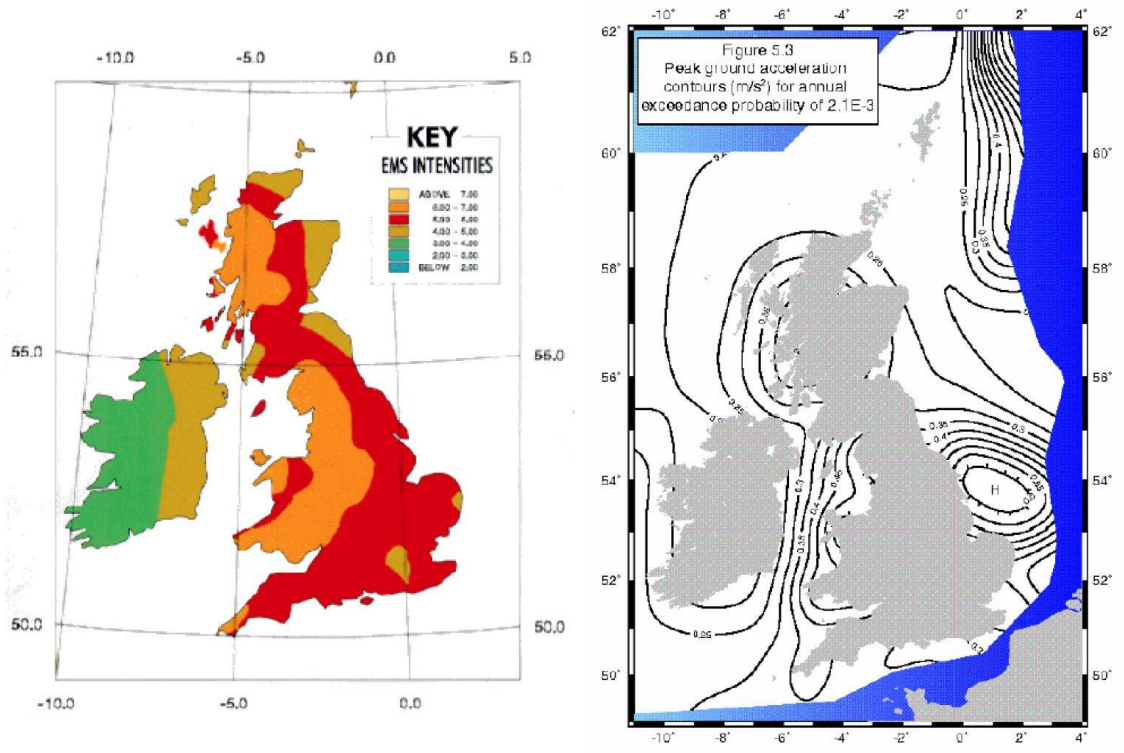

(a) (b)

Figure 3. 1. (a) Ireland's map of seismic intensity on EMS scale, (b) Ireland's offshore seismic hazard map (Solomos et al., 2008).

No active volcanoes exist in the island. It is said that the last eruption in Ireland happened 200 million years ago. Some extinct volcanoes have been identified in County Galway (Loch Na Fooey), County Offaly (Croghan Hill) and County Dublin (Lambay Island) (Geological Survey Ireland, 2019).

Ireland's weather can be classified as temperate according to the Köppen-Geiger climate classification. More specifically the weather in Ireland is Cfb (C: temperate, f: fully humid, b: warm summer) (Köppen *et al.*, 2011). The average annual mean temperature in Ireland varies from 3 to 12 °C depending on the area (see Figure 3. 2 (a)) and the average annual rainfall can go from only 600 mm in some eastern regions to over 3600 mm at some locations on the western cost of the country (see Figure 3. 2 (b)). These figures were obtained as the 30 years averages from 1981 to 2010 (Walsh, 2012).

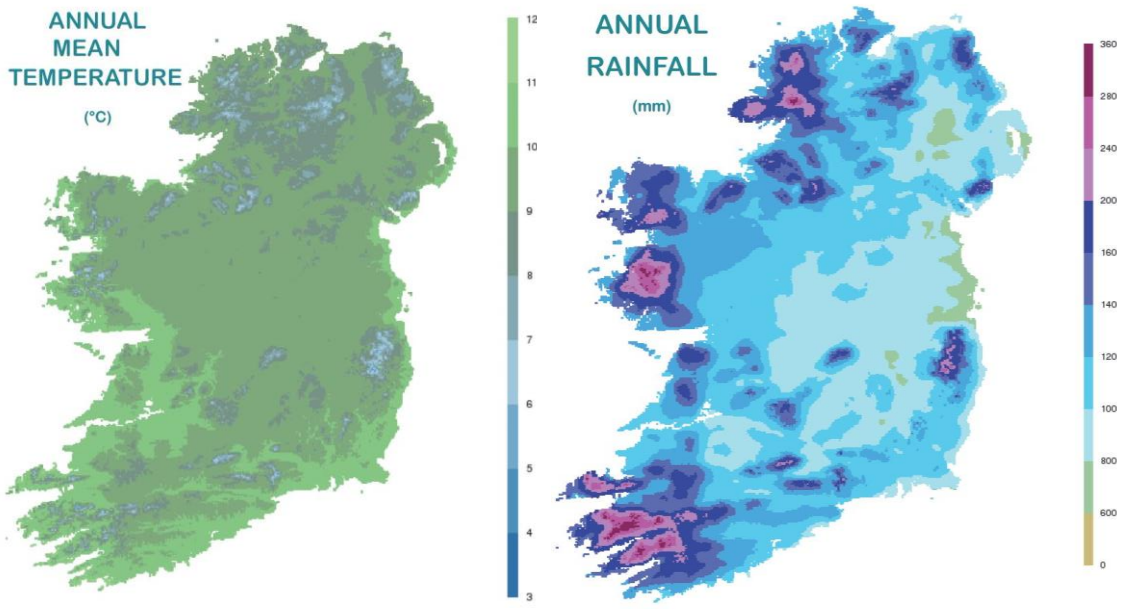

(a) (b)

Figure 3. 2. (a) Ireland's 30 years average annual mean temperatures, (b) Ireland's 30 years average annual rainfall (Walsh, 2012).

Glacial clay soil in Ireland can be found in extensive deposits (ICOMOS UK Earth Structures Committee, 2000). Clayey soil suitable for earthen construction is available and easily accessible in most areas of Ireland with the exception of the Wicklow Mountains, the south-west peninsula of counties Cork and Kerry, the western most territories of Galway and Mayo, and Donegal County, where bedrock is found at surface level.

Ireland can be considered to be a privileged country, as it is very rarely if ever affected by extreme events such as earthquakes, volcanic eruptions, cyclones, tsunamis, etc. On the other hand, Irish weather has earned its reputation as a wet country where it rains a lot (in some parts of the country up to 255 days of rain and an annual average rainfall of 3000 mm (Walsh, 2012)). Water, humidity and moisture are not propitious factors for the development and maintenance in good condition of earthen buildings.

Regardless of such meteorological circumstances, the inventiveness of the Irish and the broadly abundant presence of adequate soil has favoured the development of earthen construction techniques. In Ireland, soil has been used for building purposes for more than 5000 years. The earthen built heritage of Ireland has partly contributed to attract large number of tourists to the country that contribute to improving its economy. Moreover, a revival of the traditional earthen construction techniques may help to achieve the environmental targets agreed in the Paris Agreement for 2030 and 2050 (United Nations, 2015a).

3.1.2 From 4000 BC to the 12th century

According to Oram (ICOMOS UK Earth Structures Committee, 2000), earthen constructions in Ireland can be classified within three broad categories: (i) field monuments, (ii) housing and other buildings, and (iii) engineering and industrial construction.

At Bru na Boinne, one of the two UNESCO sites in Ireland (UNESCO WHC, 2019), earth was used in a horizontal layered structure of gravel and soil to provide the sacred Neolithic mounds with their characteristic shape. Other important earthen sites include Cashel, Dun Ailinne, the hill of Uisneach and the complexes of Tara and Rathcroghan, all of which are included on the UNESCO World Heritage Sites Tentative List. Earthen constructions of lesser scale such as grave monuments and burial mounds, ritual and defensive earthworks, ecclesiastical and settlement enclosures, and ancient land divisions are part of the different ringforts, hillforts and royal sites from the bronze and iron ages scattered through the whole country (ICOMOS UK Earth Structures Committee, 2000).

Archaeological evidence of the earliest housing in Ireland has shown that the construction technique used was a kind of primitive timber post and frame system. According to Gailey (1984), earth has been used in Ireland for the construction of dwellings since the 5th or 8th centuries. He based this statement in the discovery of archaeological remains of what is known as "*roundhouses*". Roundhouses used to have a structure based on wattle and daub walls covered by a conical timber thatched roof. A Mesolithic site has been discovered in Mount Sandel, Derry (Northen Ireland) where the postholes of some round plan houses, approximately 6 m long, have been excavated

(Aalen, 1978). A modern reconstruction of such vernacular architecture can be found at the Irish National Park, Wexford (house shown in Figure 3. 3).

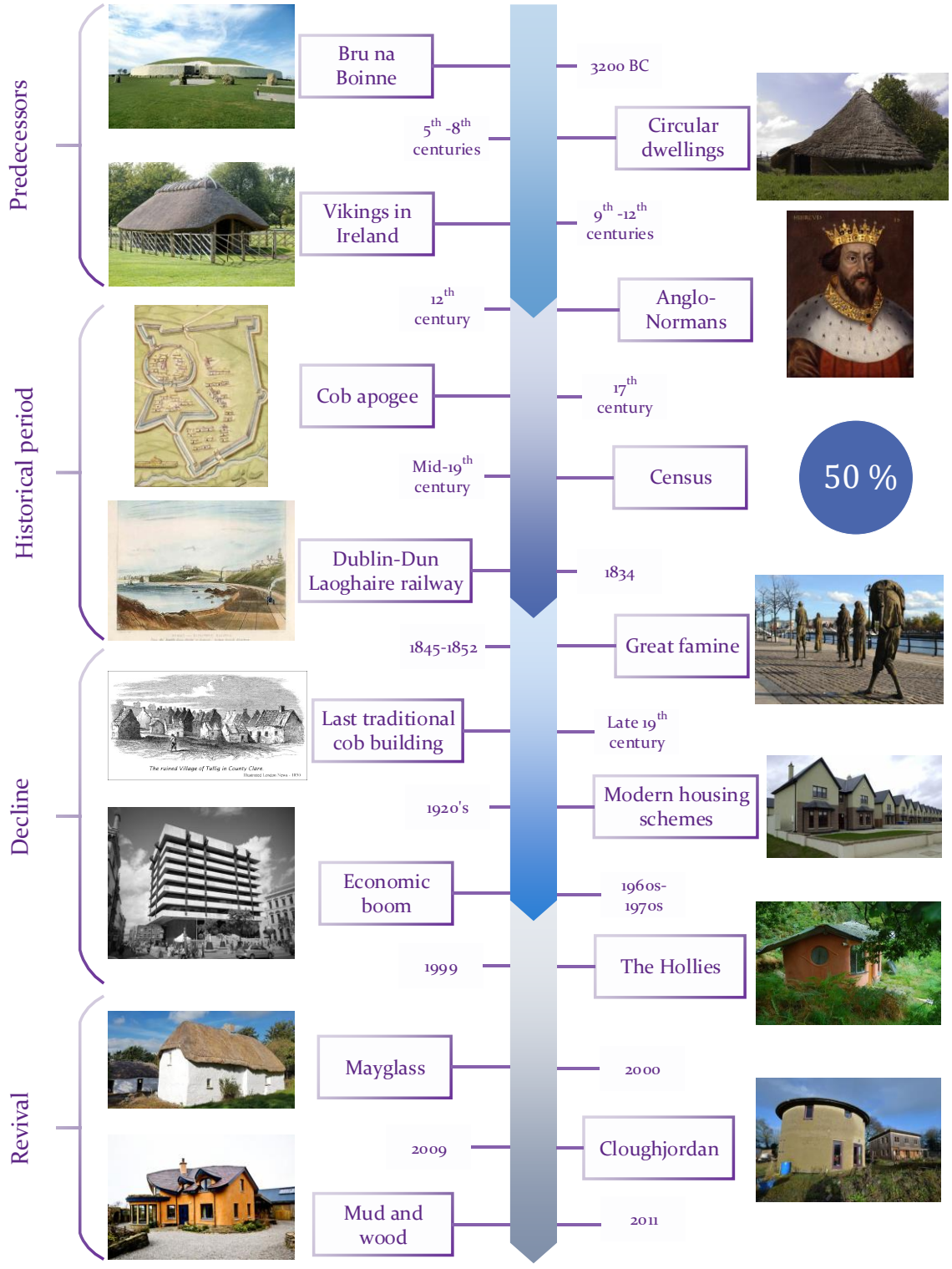

Figure 3. 3. Timeline of earthen buildings in Ireland.

MacDonald and Doyle (1997) also report the presence of wattle and daub buildings during the 9th and 12th centuries, period also known and characterised by the

presence of Vikings in Ireland. For such constructions, earth was used as an infill material and structures were built using the construction system known as wattle and daub. Those buildings were located inside defensive walls in order to facilitate their protection during conflicts. A modern reconstruction of a Viking house can be appreciated at the Botanical Gardens, Dublin (house shown in Figure 3. 3).

Another popular earthen construction technique in Ireland during this period was the one known as sods or turf tradition. This construction technique was similar to the one found in Scotland and Iceland, a tradition that is still alive nowadays in those countries and is also part of Iceland UNESCO World Heritage Sites Tentative List (Wilkinson, 2009). In Ireland, sods were used mainly by families of the lowest economic scale or as temporary shelters. Unfortunately, none of those buildings have survived and the construction tradition seems to have completely disappeared.

3.1.3 From the 12th century to the late 19th century

The cob construction technique, which is the main subject of study of this thesis, was introduced in Ireland after the 12th century when the Anglo-Norman invasions were undertaken under the rule of King Henry (Macdonald and Doyle, 1997). The technique reached its zenith during the 17th century when it displaced other popular earthen construction techniques, such as wattle and daub and sods, for the construction of dwellings both in rural and in urban contexts (Danaher, 1957a). In the middle of the 19th century, a census revealed that up to 50 % of the rural population in Ireland was living in cob walled houses. In other words, a rough estimate[4] of 1.5 million Irish people were living in a cob dwelling during this period (Macdonald and Doyle, 1997).

Cob was so commonly used mainly because the basic components could be locally sourced and transportation costs were unnecessary or low. Furthermore, the tools required were similar to those used for agriculture; thus, most of the population had access to them. Furthermore, the necessary construction knowledge and skills were passed from generation to generation.

[4] Assuming 50 % of the total population, 6,528,799 CSO. (2019). "*Population at Each Census 1841 to 2016 (Number) by Sex, County and Census Year.*" Retrieved 06/08/2019, 2019, from https://www.cso.ie/px/pxeirestat/Statire/SelectVarVal/saveselections.asp., being rural.

3.1.4 Cob's decline and revival

The construction of vernacular cob buildings in Ireland started to decline due to several economic and social factors. It began with the construction of the first railway in Ireland, which linked the city of Dublin with the port of Dun Laoghaire. This line opened in 1834 (Cox and Donald, 2013) and was followed by the construction of thousands of miles of railway tracks that, along with the existent navigable canals throughout the country, facilitated the transportation of construction materials and reduced their cost (Pfeiffer and Shaffrey, 1990). Thus, the population in the island was no longer constrained to the use of local materials for the construction of their dwellings, as the transportation of all sorts of materials was facilitated by the development of the civil engineering infrastructure in the country.

Another event that influenced the tradition of cob buildings in Ireland, and the history of the whole country as well, was the great famine. During this period, 1845 to 1852, a quarter of the population died or emigrated. Many cob buildings became uninhabited, either because of the death of their occupants, due to illness or starvation, or because they emigrated, thus falling into decay. Those that continued to be occupied were no longer properly maintained, as the low income of most families during this period would be allocated to satisfy their basic needs, and started to become derelict (Danaher, 1970, Shaffrey and Shaffrey, 1985).

Evictions were also very significant during those hard famine and post-famine years. Landlords were trying to get rid of their tenants to reduce their taxation burden. Once the families were evicted from their homes, the buildings' roofs were dismantled, and others completely demolished (see Figure 3. 4 (a)). A project lead by Ciaran Reilly aims to document the evidence of such evictions during the great famine. In Figure 3. 4 (b), a map is shown with all the eviction events that have been documented so far (July 2019). From the years of the great famine, earthen vernacular buildings were associated with poverty, squalor and starvation, harsh evictions, and a sub-standard way of life and hence their popularity decreased drastically (Shaffrey and Shaffrey, 1985). According to Pfeiffer and Shaffrey (1990), the last historical cob vernacular building was built in Ireland during the last years of the 19th century.

(a)

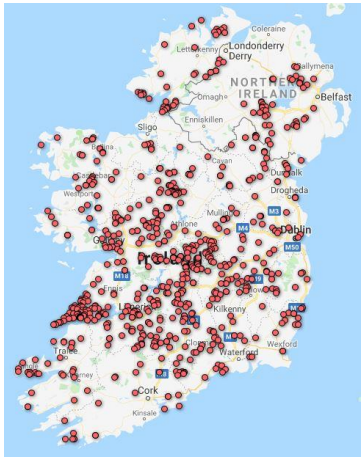

(b)

Figure 3. 4. (a) Eviction and demolition of an Irish cottage (Maggie, 2014) and (b) map of evictions in Ireland (Reilly, 2017).

Even though efforts were made to try to build again using cob after the famine years, they were unsuccessful. For example, during the Second World War, a period known in Ireland as the Emergency, the architect Frank Gibney sent a proposal to the Industrial Research Council to encourage the use of soil for building purposes (Macdonald and Doyle, 1997). He highlighted the material's superiority, with respect to those standardized thin-walled cottages being built at the time, in economic, hygienic and aesthetic terms. His proposal was rejected due to the prejudice against the vernacular building tradition. The plans of one of the proposed clay cottages by Gibney are shown in Figure 3. 5 (O'Riordan, 2014). Thus, cob buildings continued disappearing and falling into dereliction as they were regarded as being of inferior quality and had attached to themselves the horrible association of the years of scarcity and in the 20th century the spectre of the tuberculosis.

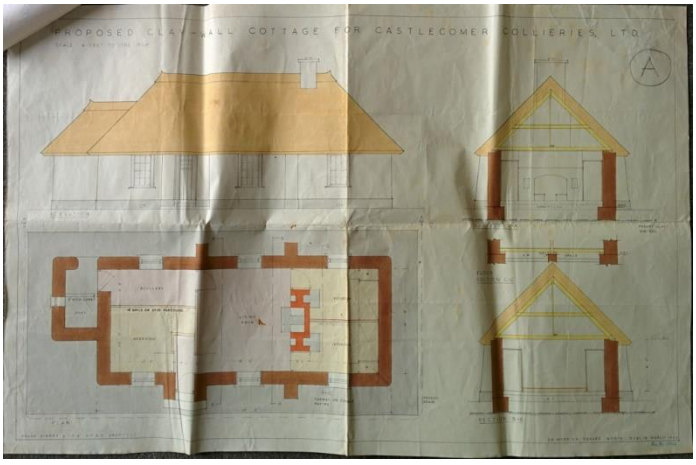

Figure 3. 5. Gibney's clay cottage proposal (O'Riordan, 2014).

After the 1920s another factor that contributed to the further neglect of the vernacular tradition in Ireland was the establishment of modern housing schemes and the development of new purpose-built state villages. The new constructions followed repetitive designs based on pattern books and were mostly built using masonry bricks or concrete. During this period, many vernacular cabins were also modernised and lost their vernacular character. Others were demolished and replaced completely with modern typologies (Danaher, 1970).

Finally, the economic boom of the 1960s and 1970s arrived. During this period, modern materials, such as reinforced concrete and structural steel, were broadly used for building purposes. In Figure 3. 3 we can see the Central Bank of Ireland's building. Located in Dame Street, Dublin, it was built during the 1970s and clearly testifies to the Irish economic boom and the replacement of traditional construction materials with modern ones. During the second half of the 20th century, industrialised materials and novel features replaced traditional ones. Earthen vernacular houses kept being completely demolished and rebuilt in different typologies. The decline of the earthen construction tradition in Ireland was accelerated during the economic boom period because vernacular buildings were considered to be ancient looking, reeked of poverty and not impressive for visitors, among other negative adjectives attached to them (Shaffrey and Shaffrey, 1985).

Luckily some traditional buildings have survived and at the end of the 20th century earthen vernacular buildings received renewed interest both from the general population and authorities. Factors that foster this revival are concerned with the association of the earthen vernacular building tradition to cosiness, easiness to heat, and the distinctive, and pleasant aesthetic character of the traditional cob buildings (Shaffrey and Shaffrey, 1985).

The Hollies, a center for training in practical sustainability located in Cork, has been working and teaching about natural building techniques since 1999. It is known as "*the prime place for the revival of cob building in Ireland*" (The Hollies, 2019).

One of the most important cases of conservation in Ireland corresponds to the intervention performed between 1998 and 2001 on a vernacular cob cottage in Mayglass, County Wexford. The Mayglass project was performed based on the importance attached to the authenticity of the farmstead complex. Evidence found in the wall oven of the house allowed researchers to date the construction of the cob buildings from the 17th century

and it had remained unchanged since then (Reeners, 2003). Other restoration projects of cob buildings in Wexford include St. Awaries Cottage, John Barry House at Ballysampson, The Dunes at Ballinesker, Kilmuckridege House and Ballyedmond House.

Two modern cob houses have been built in the eco-village of Cloughjordan, County Tipperary. This eco-village was officially launched in autumn 1999 (Winston, 2012) when construction started on a 67 acre site. At the present day (July 2019), more than 50 low energy buildings have been built using different sustainability approaches (Cloughjordan Ecovillage, 2019).

Another centre in Ireland for training on sustainable, natural building and design is Mud and Wood (Ritchie and Butler, 2019). Founded in 2011 by Colin Ritchie and Feile Butler, they specialize in cob construction and provide consultation to self-builders interested in using this material to build their own dwelling. Ritchie and Butler live in a cob house built by themselves (house shown in Figure 3. 3).

Even though a cob revival in Ireland is currently well under way, the consequences of a gap of almost 100 years in the cob vernacular tradition in the country cannot be ignored. During the 20th century some of the knowledge and know-how has unfortunately been lost. New cob buildings and conservation projects of cob buildings performed nowadays are of an experimental nature and important efforts are required to re-learn this vernacular construction technique.

3.2 Social and cultural aspects

Even though geographical and climatic conditions, as well as availability of local materials, may have a certain influence on regional architectural styles, these factors are not enough to explain the huge variety of shapes and styles found in different regions. According to Aalen (1978), in Ireland socio-cultural factors are the main determinants of the vernacular style. Other important factors to take into account when trying to describe a specific vernacular building tradition are: the historical experience of the society, its organization at community and family level, as well as the economic and technological level of that society.

Several authors discuss two different perceptions of cob buildings by society; a positive one and a negative one. On the one hand, the positive aspects are related to a romantic picture of the Irish countryside populated with cosy welcoming cob walled and thatched cottages with white walls and colourful roofs. In his book recording his visit to Ireland, Young Hutton (1892) said:

"And if the Irish cabins continue like what I have hitherto seen, I shall not hesitate to pronounce their inhabitants as well off as most English cottagers. They are built of mud walls 18 inches or two feet thick, and well thatched, which are far warmer than the thin clay walls in England".

Shaffrey and Shaffrey (1985) also confer cob buildings with positive aesthetic qualities such as an intimate scale of the buildings with the landscape that surrounds them, a variety of shapes and an informality of the layout. They described such buildings in the following way:

"...farm buildings and country houses fitting snugly and comfortably into the landscape as if they were also natural rather than artificial structures".

Danaher considered that vernacular dwellings had well balanced forms and pleasant proportions between walls and roof and that the lesser features such as chimneys, porches, doors and windows were well placed. Moreover he said that the texture of local materials gave them a high degree of environmental harmony (Danaher and Irish Tourist Board, 1975). Although simple and modest, vernacular houses melted perfectly with their surroundings by being built with local and ecological materials and their aesthetic characteristics are of great value in harmonizing quite nicely with the Irish countryside landscape.

The image of communities living in harmony with the landscape was reinforced by artists such as Paul Henry, William Evans and George Petrie. Elements of Irish rural life were reproduce in the works of these painters suggesting modest ways of living and using the environment in a respectful way. See for example Figure 3. 6 which is titled "*A Connemara Village*", created in 1930-1933 by Paul Henry (1930). This painting was part of the exhibition at the National Gallery of Ireland called "*Shaping Ireland: Landscapes in Irish Art*" (Maguire, 2019) and clearly depicts the harmony of the cultural landscape achieved between vernacular buildings and their setting.

Figure 3. 6. "A Connemara Village" by Paul Henry (1930).

On the other hand, there is the negative conception of earthen buildings which, according to Shaffrey and Shaffrey, are associated with nineteenth century poverty, squalor and starvation, harsh evictions, and a sub-standard way of life (Shaffrey and Shaffrey, 1985). They were sometimes also associated with cottiers and landless labourers. Danaher reported (1957a):

"In the heart of the best walled towns, cities and boroughs, there stand many poor cottages of straw, chaff and clay to the eyesore of the whole town".

It is worth noting that such negative ideas about earth buildings were more related to the poorer and older cottages built using either sods or wattle and daub techniques and not necessarily to cob buildings since the use of cob was applied for both labourers and landlords to build their dwellings (Gailey, 1984).

Furthermore, this dualist conception, positive and negative, of traditional dwellings is not only a function of different historical periods or different locations. The social composition of the families inhabiting the houses and their economic resources greatly influenced the conditions of the dwellings. As noted by Nicholson after visiting some cottages in Dublin in 1844, just one year before the great famine:

> *"... and if I found nothing to imitate, I always found something to admire. The first we entered was cleanly; the dishes tastefully arranged upon a white cupboard, and a family of young girls in cleanly garb. And had I visited no other, I might have written a romantic tale on the bright pots and buckets of the Irish peasantry.*

They were employed in a sail-cloth factory. The next we saw was a pitiful reverse. A slender, discouraged looking man was sitting on a stool in one corner; a sickly-looking mother, with four ragged children, in another; all waiting the boiling of a pot of potatoes, which certainly fell short of the three pounds and a half allowed to each man in the poorhouse" (Nicholson, 1847).

Some interesting social and folklore aspects of the Irish vernacular buildings are described by Gailey and agree with other authors as well. They point out that buildings were built by a "*meitheal*", men, women and children participated in communal construction of a vernacular building while alternating working with singing and dancing to the rhythm of one or two fiddlers. Thus, construction techniques were inherited from generation to generation and shared among most members of the society.

The choice of the construction site was influenced by a folklore superstition related to fairy paths; the site would have been marked by flat stones at the corners and left overnight, if the flat stones were still in place the next morning then the construction could continue, otherwise the site would be moved as the "*fairies*" would have dropped the stones in the night as the selected site was placed in the middle of their crossing paths. Another folklore tradition, influenced by superstition, consisted in placing empty horse skulls under the hearth of the house to get good luck, or as argued by Gailey, to improve the acoustics of the room (Gailey, 1984).

Nowadays, most of the remaining cob cottages are inhabited by "*refugees from the town*", people with urban rather than rural occupations migrating to the countryside to avoid the stress and the high real-estate prices that come with living in a city (Shaffrey and Shaffrey, 1985, Pfeiffer and Shaffrey, 1990).

3.3 Economic aspects

Economic factors had a great influence in the development and characteristics of vernacular buildings in Ireland. Even though good construction materials were available almost everywhere around the island, only the wealthy members of higher classes could afford the payment of the professional skills of a master or the required tools needed to use more durable and stronger materials such as stone. Transportation of materials was

also an issue up until the second half of the ninetieth century, therefore most of the rural population was constrained to the use of local materials to build their dwellings (Gailey, 1984).

As Ireland had always been a farming country, even during the industrial revolution period, up until the 20th century, the lifestyle and life quality as well as the characteristics and size of the buildings, were always influenced by the quality and features of the land. Whereas stone was mainly used for the construction of important buildings and most landlords' residencies, the vernacular was mostly limited to the lower socio-economic segment of the population as earthen construction skills were shared among most members of the rural communities (Gailey, 1984).

Despite those facts, cob was used in some regions by both upper and lower classes as reported by Danaher (1970). In fact, most of the remaining cob buildings still inhabited today appertained to middle or upper-class families and if they have survived up to now is because their owners could afford constant maintenance and repairs. Unfortunately, most of the earth cabins owned by the lower classes are in ruins or have completely disappeared since they were built using a lower material quality such as sods or wattle and even if they were built with cob, as were those of the landlords, the lack of maintenance has caused their disappearance.

House construction costs from the 1770s for different counties of Ireland made from different construction materials are presented in Table 3. 1. These values were reported for Arthur Young in his book of his tour of Ireland (Hutton, 1892). Macdonald and Doyle also reported several figures compiled from different sources (see Table 3. 2). Some of these numbers come from official reports or archives and some of them were mere speculations, but one thing is clear based on the data presented by both authors, the price of a stone house was about three to four times higher than one constructed using an earthen technique.

Sometimes sod, which is an inferior technique, was selected over cob because even though both materials were widely available, cob required very heavy labour to be tempered. The average dimensions of a common tenant's house in the 17th century were perhaps 12.2 m long by 6.1 m wide, single storey and thatched (Gailey, 1984), whereas that the landlords' houses were bigger, sometimes multi-storeys and incorporated elements of other materials such as stone or brick.

Table 3. 1. House construction costs from the 1770s in Ireland based on the location and material as reported by Hutton (1892).

County	Material	Cost
Fermanagh	Sod	£2
Fermanagh	Stone	£15
Donegal	Cob	£3
Donegal	Stone	£40
Roscommon	Cob	£5 5s
Roscommon	Stone	£15
Cavan	Cob	£4
Cavan	Stone	£17

Table 3. 2. House construction costs in the 18th century based on the location and material as reported by Macdonald and Doyle (1997).

County	Material	Cost
Fermanagh	Sods	£2
Roscommon	Cob	£5 5s
Roscommon	Stone	£15

Another factor that influenced the construction of new houses or the modification of existing ones was the implementation of window and hearth taxes in Ireland. Thus, houses were limited to a single hearth and some existing windows were sealed in order to reduce the economic burden that taxation would impose on poor families (Gailey, 1984).

3.4 Typology

Traditional vernacular cottages in Ireland were usually occupier-built (Gailey, 1984). Thus, these constructions present smooth variations in shape and size as the traditional countryside occupant; farmer, artisan, carpenter, blacksmith, weaver, fisher, etc., aimed to adapt his home to his own necessities and to the requirements of his profession. Nevertheless, the typology study of surviving earthen vernacular buildings has allowed researchers to identify certain regionally shared characteristics.

3.4.1 Farm layout

Even though cob was used both in rural and urban contexts, almost all urban buildings have been either destroyed, replaced or modified to the point where it is no longer possible to recognize their original features. Fortunately, many examples of cob rural buildings have survived and important characteristics have been identified by using farms as case studies. In a farm, traditionally the dwelling was the first building to be built. As the economic condition of the family improved over time, extensions to the original building

and other buildings were added for several farming purposes (Shaffrey and Shaffrey, 1985), thus creating several patterns.

Aalen *et al*. (1997) have identified the farm patterns presented in Figure 3. 7. The legend of this figure presents a distinction between the main dwelling, farm outbuildings or sheds, and walls delimiting a courtyard type space. Pattern A corresponds to an irregular farm plan. Patterns B and C present a long house plan and a parallel or "*street*" plan respectively. Pattern B is characteristic of the north and west of Ireland, whereas Pattern C is characteristic of the south west of the country. These two patterns evolved from the traditional byre dwelling where human and livestock used to share the same building. Pattern D, known as "*half courtyard*", presents buildings in two sides of the courtyard. Patterns E, F and G present buildings in three sides of the courtyard. Pattern G is an improved version of patterns E and F. It can also be noticed that the entrance to the main dwelling in pattern G does not face the courtyard, thus marking a clearer division between habitation and work spaces. Similar farm layout patterns are reported by O'Reilly and Murray (2005) and by Shaffrey and Shaffrey (1985).

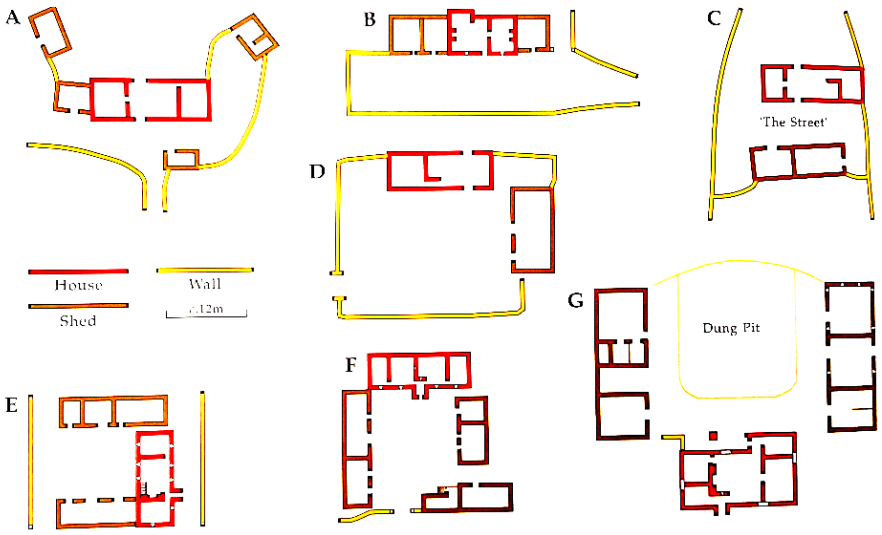

Figure 3. 7. Traditional Irish farmyard patterns.

Traditional Irish farmyard patterns distributions are presented in Figure 3. 8. From this figure it can be observed that no clear geographical distribution exists as different farmyard patterns overlap in several regions of the country (Aalen *et al.*, 1997). Traditionally, countryside settlements were characterised by single farmsteads standing on their own land at some distance from the nearest neighbour (Danaher, 1970). Farmyards and their constituent buildings varied in size and layout according to the economy and prosperity of the farms (Danaher and Irish Tourist Board, 1975). Thus,

farms were traditionally grouped by their size into four different categories: small (up to 20 acres), medium (20 to 40 acres), classic substantial (40 to 100 acres) and large (100 or more acres) (Shaffrey and Shaffrey, 1985).

Figure 3. 8. Traditional Irish farmyard pattern distributions: (a) scattered buildings, (b) long-house extension, (c) buildings long two sides of rectangular yard and (d) buildings along three sides of rectangular yard (Aalen et al., 1997).

3.4.2 Dwelling layout

Although geographical and climatic conditions, as well as availability of local materials, may have had a certain influence on the regional architectural styles, these factors on their own do not justify the huge variety of shapes and styles found along the different regions of the country. Thus, the factors affecting the evolution of the different

dwelling typologies in Ireland can be classified in three different groups: environment, tradition and external contact (Danaher and Irish Tourist Board, 1975). According to Aalen (1978), socio-cultural factors are the main determinants of the vernacular style of a particular place. Other important factors to take into account when trying to describe a specific vernacular building tradition are: the historical experience of the society, its organization at community and family level, as well as the economic and technological level of that society.

Geographically, geologically and climatically speaking, a rough division can be established between north-western and south-eastern Ireland. In Figure 3. 2 (b) it can be seen that the north-western regions are the ones that receive greater levels of rainfall. In the north and west coast of Ireland the wind is stronger in comparison to their south-eastern counterparts. Clayey soils are broadly available in the central, south, east and north-west of the country; thus, it was used for building purposes, whereas that stone was the most used material in the western and north-western regions. Moreover, the geographic and geologic characteristics of Ireland have also conditioned the traditional economic activities of the population. Agriculture has thrived almost everywhere in Ireland except in the western and northern regions, where rock is at surface level. In these regions, pasturage and livestock have played a more important role in the historical development of vernacular buildings.

From a socio-cultural point of view, a division between south-eastern and north-western Ireland can be identified as well. According to Danaher (1975), people in south-eastern Ireland are more open to change and to adopt new features as this region has always had more contact with the rest of Europe due to its geographical proximity. On the other hand, north-western Irish have been traditionally more resistant to change and their buildings more prone to conserve older attributes and characteristics.

A questionnaire circulated by Danaher between 1945 and 1956 revealed important information regarding regional differences of the dwelling vernacular tradition in Ireland (Danaher, 1957b). The information obtained from this survey showed that a feature known as bed-outshot, recess or alcove was present in many north-western dwellings (see Figure 3. 9 (a)). This small sleeping space was usually built with the same material and construction technique of the rest of walls in the house. The presence of a dwelling typology known as byre-dwelling was also identified in the north-western regions of the island (see Figure 3. 9 (b)). In a byre dwelling both humans and livestock were housed in

the same building space. This fact has probably influenced on the presence of another characteristic feature of the north-western Irish dwellings: the opposite entrance doors. The opposite entrance doors as described by Danaher (1970) and Aalen (1978) may have been necessary to enhance the circulation of livestock in and out of the dwelling. Another characteristic feature of north-western, as well as western and south-western, dwellings located nearby the coast is the roped thatch (see Figure 3. 9 (c)). In those regions thatch was held in position by a network of ropes which lay on the thatch and was fastened to pegs or weights along the edges of the roof to prevent the strong winds lifting the roof and destroying it.

Whereas the roofs on the north-western regions of Ireland were traditionally gabled, those in the south-eastern regions were hipped (see Figure 3. 9 (d)). Another feature characteristic of eastern dwellings is the jamb wall (see Figure 3. 9 (e)). A jamb wall is a short wall that projects from the hearth wall and supports the mantel beam of the chimney. Finally, the questionnaires showed the regions where clay was traditionally used as a construction material (see Figure 3. 9 (f)). These regions correspond with the distribution of cob buildings in Ireland reported by Aalen *et al*. (1997) and more recently by O'Reilly (Terra Incognita, 2011).

The typical layout of a western vernacular house consist on a central kitchen flanked with one room at each end (three-room house) (Aalen, 1966). According to some ethnologists this typology has evolved from previous byre-dwellings (Danachair, 1964). In contrast to the western typology, no evidence have been found that shows that dwellings were shared between livestock and humans in eastern Ireland (Aalen, 1978). Eastern houses, characterized by their central hearth, two-room plans and hipped roofs, evolved most likely from the primitive wattle and daub round dwellings.

Regardless of the inter-regional difference of the vernacular architecture, traditional buildings in Ireland shared certain characteristics such as the fact that most of them were rectangular in plan. Besides, they used to be longer than wide as timber for dwelling construction purposes became a scarce material after the depletion of Irish forests caused by the diverse industrialization activities of the 16th and 17th centuries (Forest Service, 2008). In addition, roofs were usually built from salvaged timber and it was complicated to cover spans of more than a few meters. Moreover, houses were only one room wide and rooms were directly connected. Lime washing of buildings' walls was also a well spread element of the vernacular tradition in Ireland. Most vernacular

dwellings originally had only 1 or 1 ½ stories and sometimes extended to 2 stories but most building extensions were done by adding rooms adjacently to the longitudinal axes of the original house. Finally, cob loadbearing walls were traditionally built over stone plinths to protect them from raising damp and rain splashing, while roofs were built with important overhanging, approximately 40 to 50 cm, to protect the walls from direct rain (Danaher, 1970, Danaher and Irish Tourist Board, 1975, Aalen, 1978, Gailey, 1984, Shaffrey and Shaffrey, 1985, Pfeiffer and Shaffrey, 1990).

In addition to the variations in the typology of vernacular buildings in Ireland between different regions, inter-regional differences have also been identified. Inter-regional variations were mainly driven by economic factors which greatly influenced the size and characteristics of the dwellings (Danaher, 1970, Aalen, 1978). According to Pfeiffer and Shaffrey (1990), land quality dictated to a large degree the life-style and the dwelling characteristics of the people. Macdonald and Doyle (1997) identified 4 different dwelling categories according to size: Gentleman's residence being the largest one, larger farmhouse, smaller farmhouse and one-room houses. Gailey reports that in a census carried out in 1841, 40 % of the rural dwellings had from 3 to 4 rooms and up to 37 % of the rural houses in the country had only 1 room (Gailey, 1984). Different traditional sizes and layouts of vernacular Irish buildings are shown in Figure 3. 10 (ICOMOS UK Earth Structures Committee, 2000).

Wall thickness of a traditional Irish earthen vernacular building typically varies from 0.40 m up to 0.90 m. The height of the walls normally goes from 1.80 m to 3.00 m. Wall lengths can go from 3.00 m up to 4.50 m in the short span direction of the building whereas that along its length buildings can reach a total distance of up to 19.00 m (Hutton, 1892, Danaher, 1957b, Gailey, 1984, Pfeiffer and Shaffrey, 1990, Keefe, 1993, Reeners, 2003).

Finally, an overall picture of what could be defined as a traditional Irish vernacular dwelling can be established taking into account the definition of the typical Irish house given by Danaher (1970), as it mostly agrees with descriptions provided by other authors referenced earlier:

> *"We can therefore conclude that this type of house, the long, rectangular, one-storey, solid building, with its steep thatched roof and white or colour-washed walls, is the typical Irish farmhouse".*

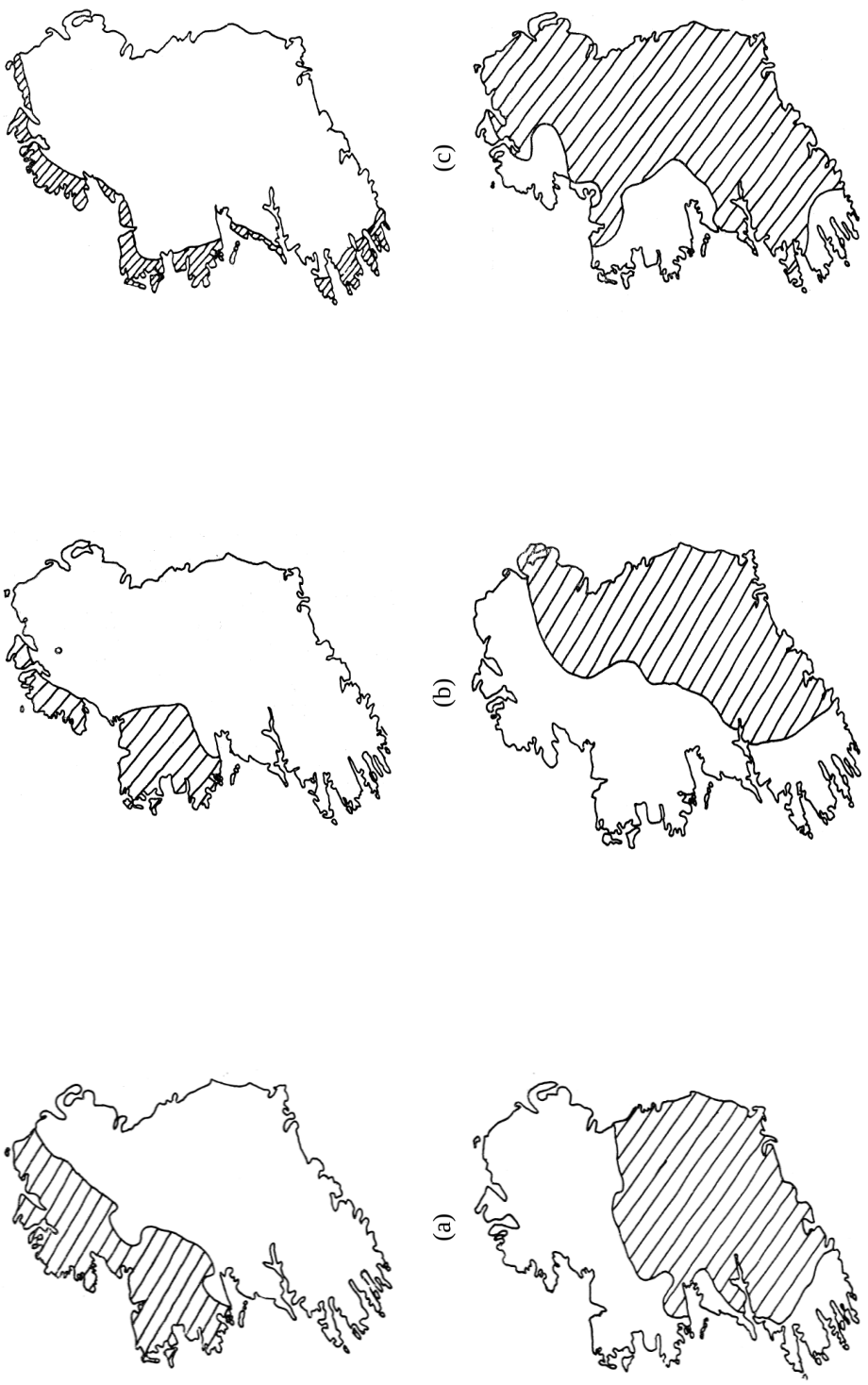

Figure 3. 9. Irish dwelling typologies' distribution: (a) Bed outshot, (b) Byre dwellings, (c) Roped thatch, (d) Hip roof, (e) Jamb wall and (f) Clay used for building (Danaher, 1957b).

3.5 Authenticity

In order to better understand the values attached to Irish earthen vernacular heritage, it is necessary to define its authenticity. Heritage authenticity varies from culture to culture and no fixed criteria exists to define it. As every culture deserves to be respected, it is indispensable that every cultural heritage is assessed in consideration of the cultural context to which it belongs (ICOMOS, 1994). Thus, the capacity to understand and define each culture's heritage values is based on the understanding of the information provided by several sources. Authenticity values were presented in Figure 2. 1, Chapter 2.

Regarding the form and design of the buildings forming part of the Irish earthen vernacular heritage, most traditional buildings are rectangular in plan, have a single story and are one room wide with either hipped or gabled roofs. The material used for the construction of the monolithic loadbearing walls was a mix of soil, water and straw applied according to the so-called cob construction technique. The walls were built over a stone plinth foundation in order to protect them from raising damp. Earthen vernacular buildings were traditionally roofed with reeds or straw thatching. This roofing system would typically provide protection to the walls from direct rain thanks to the overhanging of the material at the building's eaves. Finally, cob walls were lime washed to provide extra resistance against rain and erosion. The technique used to build the walls is internationally known as cob and in Ireland such buildings are usually described as mud wall buildings.

The main use of vernacular earthen buildings in Ireland was assigned for accommodation of the population and for agricultural and animal husbandry purposes. They formed part of a farmstead layout and farms were traditionally scattered through the landscape in an isolated pattern. Buildings were traditionally constructed by a "*meitheal"*, people, family and neighbours, would gather to help the builder construct his dwelling, while listening to traditional music and sharing the construction know-how and knowledge with younger generations. The selection of the construction place was determined by a folklore tradition related to fairy paths and skulls would be buried to provide the dwellers with good luck.

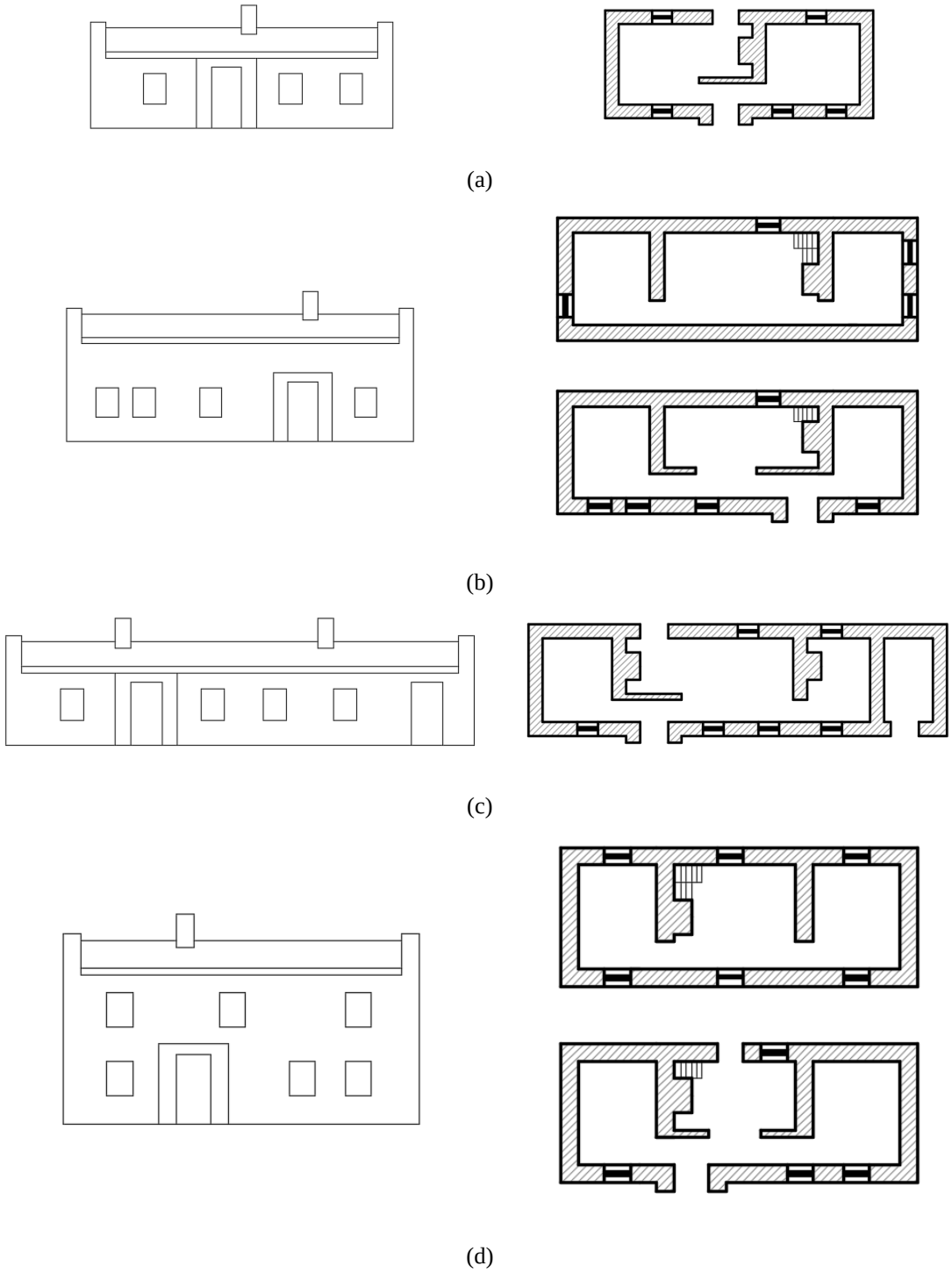

Figure 3. 10. Traditional sizes and layouts of vernacular Irish buildings (elevation and plans): (a) one story two room house, (b) one and a half stories house, (c) three room house with diary, (d) two story house and (e) gentleman's house (ICOMOS UK Earth Structures Committee, 2000).

A dualist perception exists with respect to the remaining vernacular earthen buildings in Ireland. Part of the population associate them with negative concepts such as poverty, evictions, squalor and starvation, whereas that other part of the population confers these buildings with positive attributes such as cosiness, beauty, comfort and cultural value. Moreover, the remaining Irish cob buildings possess economic,

environmental and sustainable values. They contribute to the housing stock of the country, were built with recyclable materials and are deemed to provide comfort to their inhabitants. A summary of the characteristic authenticity values of Irish earthen vernacular buildings is shown in Figure 3. 11.

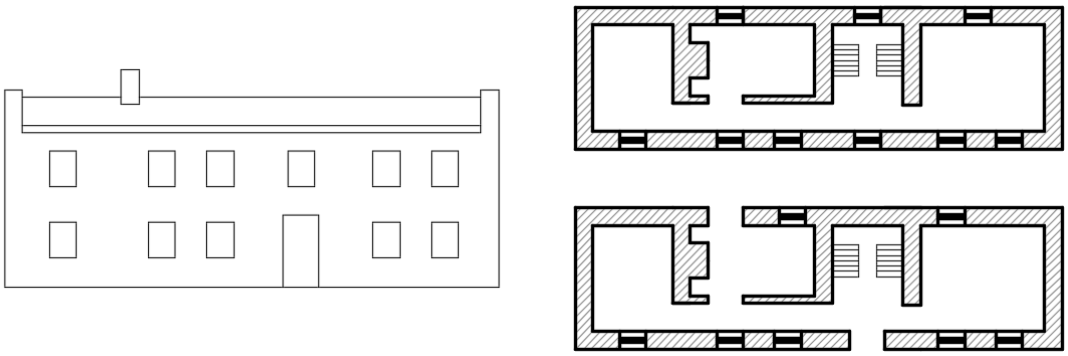

(e)

Figure 3. 10. Traditional sizes and layouts of vernacular Irish buildings (elevation and plans): (a) one story two room house, (b) one and a half stories house, (c) three room house with diary, (d) two story house and (e) gentleman's house (ICOMOS UK Earth Structures Committee, 2000). (Continuation)

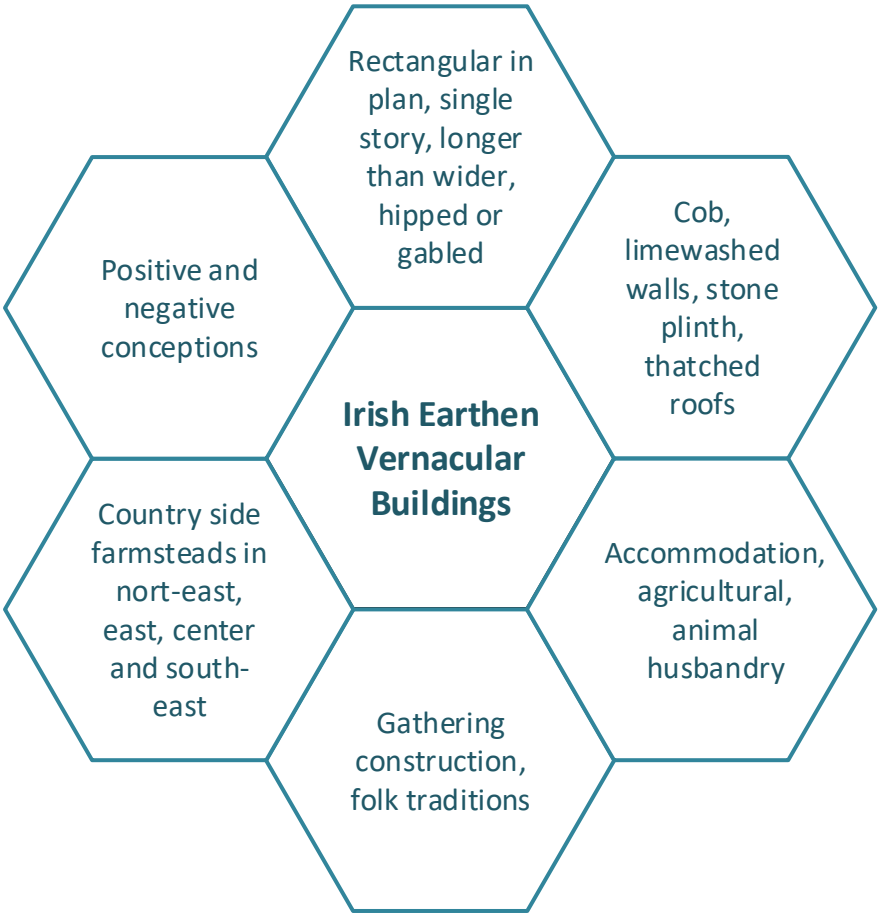

Figure 3. 11. Authenticity qualifying factors of Irish earthen vernacular buildings.

3.6 Summary

The predecessors of cob in Ireland date back to the stone age in the form of the sacred mounts characteristic of sites like Bru na Boinne. Other earthen construction techniques used in Ireland correspond to the wattle and daub and sods (also known as turf), typically used by the inhabitants of the Island to build their dwellings during the 5th to the 12th century.

Cob was brought to Ireland during the 12th century and reached its apogee at the 17th century. This technique was used in both rural and urban environments as well as by lower and upper socio-economic classes. It is roughly estimated that by the mid-19th century, a total of 1.5 million people was living in a cob building in Ireland.

Cob's decline was due to several social, economic and technical factors. The decline period of cob started by the construction of civil infrastructure in the Island, which facilitated the transportation of construction materials and reduced their costs. It was aggravated during the years of the great famine when many cob buildings lost their occupants and fell into decay and dereliction. Other factors such as the development of modern housing schemes and the improvement of the economy, contributed to the further neglect of the earthen vernacular tradition in Ireland during the 20th century.

The 21st century on the other hand, has seen a revival period for the cob construction technique in Ireland. Fostered by conservation projects of emblematic remaining vernacular buildings as well as by new construction projects, the re-learning of the technique and its know-how sharing by several groups of environmentally friendly enthusiastic builders have aided to this new period of interest for cob.

The qualifying factors that best describe the remining earthen vernacular buildings in Ireland can be group in accordance with the Nara document of Authenticity (ICOMOS, 1994). Such buildings are typically characterised by a rectangular, longer than wider plan. They are usually single storied, have hipped or gabled thatched roofs, are composed of loadbearing cob walls built in top of stone plinths, and served as accommodation for their inhabitants or for agricultural and husbandry purposed. Normally built during a community gathering, earthen vernacular buildings in Ireland are surrounded by folk traditions and are associated with intangible values.

Chapter 4: Numerical modelling of cob's non-linear monotonic structural behaviour

This chapter contains one of the new contributions of this thesis to the state of knowledge. Results obtained by simulating cob's non-linear monotonic behaviour using two well-known finite element commercial packages are presented. Furthermore, the results of a mesh size sensitivity analysis performed following a mesh refinement approach are discussed. Pros and cons of the different available constitutive material models explored are identified and discussed.

4.1 Introduction

Regardless of the great research done by several authors (Minke, 2000, Ziegert, 2003, Keefe, 2012, Miccoli *et al.*, 2014, McPadden and Pavía, 2016, Miccoli *et al.*, 2017, Quagliarini and Maracchini, 2018, Miccoli *et al.*, 2019) cob's structural behaviour is not yet fully understood, nor have material constitutive models been specifically developed to simulate cob's structural response. Moreover, standards are not available for the design of new cob buildings or for the conservation of existent ones. After an extensive review of 55 documents related with the normalization and standardization of earthen construction techniques around the world, it was identified by Cid *et al*. (2011) that none of them specialised in providing guidance for cob.

FEM (Zienkiewicz, 2013) is one of the most important simulation tools in engineering nowadays (Wu and Gu, 2011). Therefore, in this chapter the assessment of the suitability of several material constitutive models available in ANSYS (*ANSYS Inc.*, 2017) and in ABAQUS (Dassault Systemes, 2013) to reproduce the structural monotonic behaviour of cob is presented. The simulations are based on the experimental campaign and the numerical simulations (plane stress modelling of the diagonal compression test) performed previously by Miccoli *et al*. (Miccoli *et al.*, 2014, Miccoli *et al.*, 2017, Miccoli *et al.*, 2019) as the results reported by those authors are among of the best studies

performed to determine cob's mechanical properties and understand its structural behaviour that are available in the published literature. The novelty of the work presented in this chapter arises from the simulation of both simple compression and diagonal compression tests using simplified plane stress and full 3D models.

The purpose of a non-linear model is to identify the peak strength of a structure and reproduce more accurately its pre-peak and post-peak behaviour. By doing so, a better safety evaluation of existent buildings can be performed, thus avoiding the implementation of over conservative intervention measures that may cause the loss of their authenticity. Non-linear models also hold the promise of potentially describing the behaviour of cob structures under the action of earthquakes or other extreme loading events. Hence, the importance of finding a numerical constitutive material to describe cob's non-linear structural response.

Furthermore, an alternative simulation tool known as DLO (Gilbert and Smith, 2007) has been explored to try to simulate cob's structural behaviour. This method started to be developed in 2007, and has been further developed since, at the University of Sheffield by Matthew Gilbert and Colin Smith and is presented as a promising alternative to other analysis methods such as FEM. The results obtained with the DLO method using the software LimitState GEO (GEO, 2017) are presented in Appendix A and compared with FEM.

4.2 Methodology

Two well-known FEM programs were used to simulate the simple and diagonal compressive tests performed on cob wallettes by Miccoli *et al.* (2014). Stress/strain curves for cob, adobe and rammed earth were determined experimentally both under simple compression and under diagonal compression by those authors (see Figure 2. 21). The failure mechanisms and the crack patterns of the tested wallettes (see Figure 2. 22) were also reported by them. Miccoli *et al.* also performed pull-off tests to determine cob's tensile strength (Miccoli *et al.*, 2019).

The simulated wallettes have side dimensions of 420 by 420 mm with a thickness of 115 mm (see Figure 4. 1, these are the same dimensions of the physical test pieces). The boundary conditions adopted in the models consisted on fixing the bottom plates' translational degrees of freedom to replicate the support of the wallette and applying a

monotonic vertical displacement on the top plates to simulate the application of the compressive load. The displacement values were increased until the point where the finite elements failed, and the damage extended through the wallettes. The failure types of the different material constitutive models studied are discussed in more detail in sections 4.2.1 and 4.2.2. Self-weight of plates and wallettes was neglected which was also done in the simulations reported by Miccoli *et al*. (2019) as it was considered that its contribution to the damage of the wallettes was negligible in comparison to the effect of the external loads. The values of the mechanical properties determined experimentally by the referenced authors (see Table 4. 1) were adopted in the numerical simulations of this paper. Other necessary material parameters were calibrated for each one of the different material constitutive models studied. The calibration process was performed with the simulation of the single compression test and the models obtained used to simulate the diagonal compression test contrary to Miccoli's *et al.* calibration, which was performed with the diagonal compression test simulation. Materials' parameters calibration in ANSYS was done using the design exploration module available in the software (ANSYS Inc., 2013a), whereas the calibration for ABAQUS models was performed using the statistical software Minitab (Minitab, 2013).

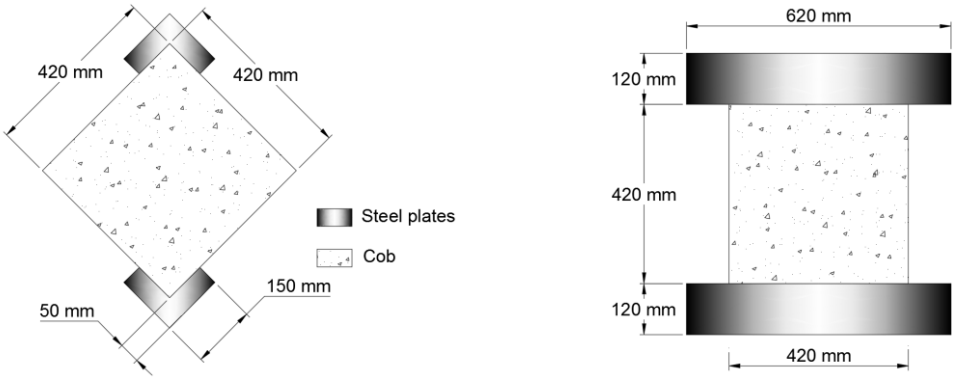

(a) (b)

Figure 4. 1. Dimensions used for (a) diagonal compression and (b) simple compression simulations.

Miccoli *et al*. (2019) also performed numerical simulations to describe cob's structural behaviour. Their simulations consisted of 2D plane stress models. They implemented a macro-modelling approach with a TSRCM constitutive model and a multilinear definition of the stress/strain relationship for the compressive behaviour with an initial linear segment of 0.3 times the compressive strength of cob, f_c, and a post peak segment with negative slope. An exponential relationship was employed for the tensile post-peak behaviour (see Figure 2. 26). The software they used was DIANA (DIANA,

2014). In the constitutive model used by Miccoli *et al*. the ultimate crack strain, ε_{ult}, is a function of the element area, A. Thus, they assumed that the model was mesh-size independent, and their report does not include a mesh sensitivity analysis. Their simulations did not deal with the 3D geometry of the models nor did they report the capabilities of the calibrated model to reproduce the behaviour of cob under the simple compression test condition.

Table 4. 1. Cob's mechanical properties (Miccoli et al., 2014, Miccoli et al., 2017).

Property	Value
Compressive strength f_c (MPa)	1.59
Tensile strength f_t (MPa) [a]	(0.10-0.16) f_c
Tensile fracture energy (N/mm) [a]	(0.3-0.8) f_t
Shear strength (MPa)	0.5
Shear modulus (MPa)	420
Modulus of elasticity (MPa)	1021
Poisson´s ratio (-)	0.14
Density (kg/m3)	1475

[a] Ranges of recommended values proposed for numerical analysis purposes (Miccoli *et al.,* 2017).

Miccoli *et al.*'s experimental tests were simulated in this thesis using ANSYS and ABAQUS. Both programs were selected as none of them had been used before to simulate cob's structural behaviour. Three different material constitutive models were studied in ANSYS: Multilinear Isotropic Hardening (MISO), Concrete (CONCR) and Damage Initiation/Damage Evolution (DMGI/DMGE). The material constitutive models studied in ABAQUS were the Concrete Damaged Plasticity (CDP) and Concrete Smeared Cracking (CSC) models.

All the constitutive material models tested in this thesis were subjected to a mesh size analysis. For the mesh sensitivity analysis, a mesh refinement method was selected. The maximum element sizes studied were 50, 30 and 10 mm. Finally, the element type for each one of the simulations performed is indicated in Table 4. 2.

Table 4. 2. Finite elements used for the simulations.

Material	Geometry	Finite element (# of nodes)
MISO	2D	PLANE183 (8)
	3D	SOLID186 (20)
CONCR	3D	SOLID65 (8)
DMGI/DMGE	2D	PLANE183 (8)
CDP	2D	CPS8R (8)
	3D	C3D20R (20)
CSC	2D	CPS8R (8)
	3D	C3D20R (20)

PLANE183 is a higher order 2D, 8-node structural solid with two degrees of freedom per node, namely, translation in the nodal x direction (UX) and nodal y direction

(UY). This element can be used to model plane stress, plane strain, generalized plane strain and axisymmetric situations. This element is also adequate to modelling irregular meshes as it can degenerate into a 6-node triangular element. More details in the description of PLANE183 can be found in the software documentation (ANSYS Inc., 2013d, 2013b).

SOLID186 is a higher order 3D, 20-node structural solid with three degrees of freedom per node, namely, translation in the nodal x direction (UX), nodal y direction (UY) and nodal z direction (UZ). It is available in two forms: homogenous structural solid and layered structural solid, the first one being the form used to create the models presented in this chapter. This element can degenerate into tetrahedral, pyramid or prism elements which make it well suited to modelling irregular meshes. More details in the description of SOLID186 can be found in the software documentation (ANSYS Inc., 2013d, 2013b).

SOLID65 is a legacy 3D, 8-node reinforced concrete structural solid with three degrees of freedom per node, namely, translation in the nodal x direction (UX), nodal y direction (UY) and nodal z direction (UZ). It is capable of reproducing cracking in tension and crushing in compression. It is suitable for modelling geological materials and reinforced composites. More details in the description of SOLID65 can be found in the software documentation (ANSYS Inc., 2013d, 2013b).

CPS8R is an 8-node, biquadratic plane stress, quadrilateral, reduced integration element with active degrees of freedom 1 and 2. C3D20R is a 20-node quadratic brick, reduced integration element with active degrees of freedom 1, 2 and 3. More details in the description of these elements can be found in the software documentation (Dassault Systemes, 2014).

4.2.1 ANSYS constitutive models

MISO

MISO is a rate-independent plasticity model characterized by a Von Mises yield criterion (ANSYS Inc., 2013c), an associative flow rule, and an isotropic hardening in which the yield surface remains centred about its initial centreline and expands in size as the plastic strains develop (ANSYS Inc., 2013d). The stress/strain multilinear behaviour and the

initial and subsequent yield surfaces for isotropic hardening plasticity are shown in Figure 4. 2. This constitutive material model can be used with both plane and solid finite elements. MISO does not support the definition of negative slopes for the stress/strain relationship. A post-peak horizontal curve was defined with constant stress equivalent to the compressive strength of cob. The multilinear stress/plastic strain curve used to define the 2D and 3D MISO models is shown in Figure 4. 3.

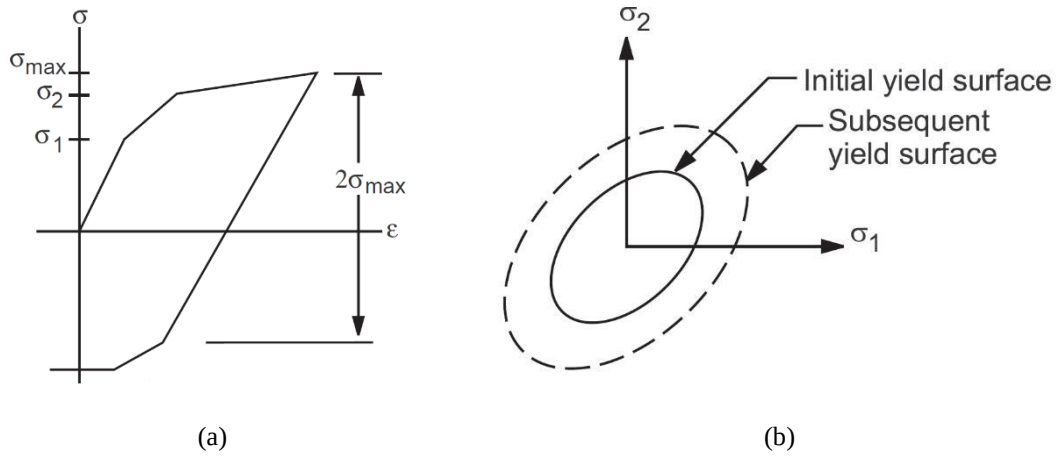

Figure 4. 2. (a) Stress/strain multilinear isotropic behaviour. (b) Initial and subsequent yield surfaces for isotropic hardening plasticity (ANSYS Inc., 2013d).

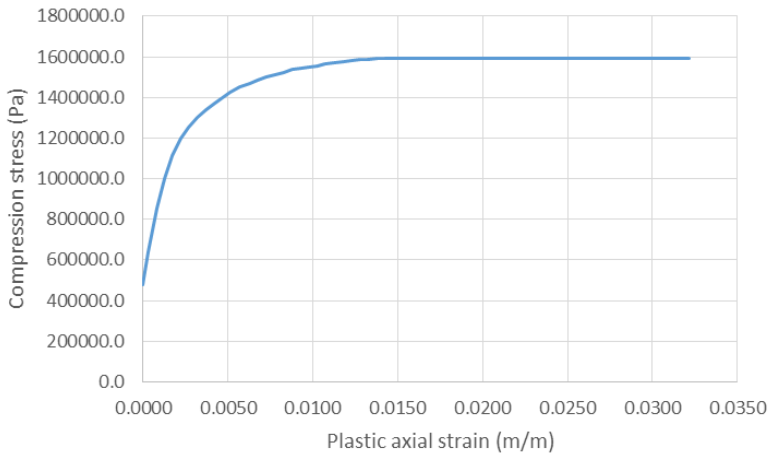

Figure 4. 3. Compression stress/plastic strain curve to define the 2D & 3D MISO models (based on the one reported by Miccoli et al. (2017).

CONCR

CONCR is a material constitutive model that can only be applied in combination with the legacy element SOLID65 (ANSYS Inc., 2013c). CONCR is capable of predicting brittle materials' failure. The criterion for failure due to a multiaxial stress state is expressed in EQ. 8 (ANSYS Inc., 2013d):

$$\frac{F}{f_c} - S \geq 0 \qquad \textit{EQ. 8}$$

Where:

- F = Function of principal stress state (σ_{xp}, σ_{yp}, σ_{zp}).
- S = Failure surface expressed in terms of principal stresses and five input parameters:
  - f_c = Compressive strength (taken from Table 4. 1).
  - f_t = Tensile strength (taken from Table 4. 1).
  - f_{cb} = Ultimate biaxial compressive strength.
  - f_1 = Ultimate compressive strength for a state of biaxial compression superimposed on hydrostatic stress state.
  - f_2 = Ultimate compressive strength for a state of uniaxial compression superimposed on hydrostatic stress state.

Both the F and S, expressed in terms of principal stresses denoted as: $\sigma_1 = max(\sigma_x, \sigma_y, \sigma_z)$, $\sigma_3 = min(\sigma_x, \sigma_y, \sigma_z)$ and $\sigma_3 \leq \sigma_2 \leq \sigma_1$, are categorized into four domains:

1. $\sigma_3 \leq \sigma_2 \leq \sigma_1 \leq 0$ (Compression-compression-compression).
2. $\sigma_3 \leq \sigma_2 \leq 0 \leq \sigma_1$ (Tensile-compression-compression).
3. $\sigma_3 \leq 0 \leq \sigma_2 \leq \sigma_1$ (Tensile-tensile-compression).
4. $0 \leq \sigma_3 \leq \sigma_2 \leq \sigma_1$ (Tensile- tensile- tensile).

Thus, four F functions denoted as F_1, F_2, F_3 and F_4, and four S functions denoted as S_1, S_2, S_3 and S_4 describe the failure surface for each domain. Detailed description of these functions can be found in the software documentation (ANSYS Inc., 2013d).

The presence of a crack at an integration point is represented through modification of the stress/strain relations by introducing a plane of weakness in a direction normal to the crack face. Also, a shear transfer coefficient, β_t, is introduced to represent the shear strength reduction for those subsequent loads which induce sliding (shear) across the crack face. If the crack closes, then all compressive stresses normal to the crack plane are transmitted across the crack and only a shear transfer coefficient for a closed crack, β_c, is introduced (ANSYS Inc., 2013d). If the material at an integration point fails in uniaxial,

biaxial, or triaxial compression, the material is assumed to crush at that point. In SOLID65, crushing is defined as the complete deterioration of the structural integrity of the material (ANSYS Inc., 2013d). To obtain a more detailed description of CONCR see the provided reference (William and Warnke, 1974).

β_t, β_c and T_c, the multiplier that accounts for the amount of tensile stress relaxation (see Figure 4. 4), were calibrated using the design exploration module available in ANSYS. A response surface optimization approach was followed. The type of Design of Experiment (DOE) used corresponded to a face-centred Central Composite Design (CCD). A CCD is a tool that allows to study the influence that the input parameters have in the response of the model. The standard response surface was created using full second order polynomials. Finally, the optimization was performed with a screening method of 1000 samples to obtain a target response from the simple compression wallette simulation as similar as possible to the one reported in the referenced experimental campaign. The final values adopted for the calibrated parameters of the CONCR model are summarized in Table 4. 3.

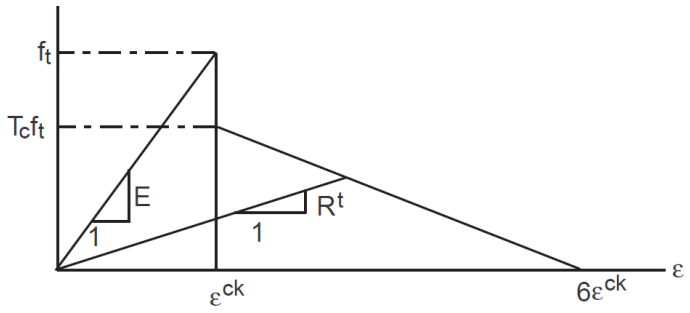

Figure 4. 4. CONCR model for cracked condition (ANSYS Inc., 2013d).

Table 4. 3. CONCR model parameter's values adopted after calibration.

Parameter (Units)	Definition	Value
f_{cb} (MPa)	Ultimate biaxial compressive strength.	$1.20fc$
f_1 (MPa)	Ultimate compressive strength for a state of biaxial compression superimposed on hydrostatic stress state.	$1.45fc$
f_2 (MPa)	Ultimate compressive strength for a state of uniaxial compression superimposed on hydrostatic stress state.	$1.725fc$
β_t (-)	Shear transfer coefficient.	0.25
β_c (-)	Shear transfer coefficient for closed cracks.	0.90
T_c (-)	Tensile stress relaxation multiplier.	0.80

DMGI/DMGE

DMGI determines the onset of material damage under loading. It needs to be used in combination with DMGE, which defines the way in which the material degrades once the damage has started (ANSYS Inc., 2013c). A Hashin criteria was adopted to determine the DMGI material model using a continuum damage mechanics method (not supported by any 3D finite element). This physical failure criteria accounts for four damage modes, namely, fibre tension (rupture), fibre compression (kinking), matrix tension (cracking), and matrix compression (crushing) (ANSYS Inc., 2013d).

In the continuum damage mechanics method, damage variables increase gradually based on the amount of energy dissipated for the various damage modes. To achieve an objective response, the dissipated energy for each damage mode is regularised according to EQ. 9 (ANSYS Inc., 2013d):

$$g_v = \frac{G_c}{L_e} \qquad \textit{EQ. 9}$$

Where:

- g_v = Energy dissipated per unit volume.
- L_e = Characteristic length of the element calculated from the element area, A_{elem}, as equal to:

$$L_e = \begin{cases} 1.12\sqrt{A_{elem}}, & for\ a\ square\ element \\ 1.52\sqrt{A_{elem}}, & for\ a\ triangular\ element \end{cases} \qquad \textit{EQ. 10}$$

- G_c = Fracture energy in compression, which for a specific damage mode is given by:

$$G_c = \int_0^{U_e^f} \sigma_e dU_e \qquad \textit{EQ. 11}$$

Where:

- σ_e = Equivalent stress.
- U_e = Equivalent displacement.

- U_e^f = Ultimate equivalent displacement, where total material stiffness is lost for the specific mode.

The idea behind using a regularised energy dissipation parameter to describe material damage was originally proposed by Hilleborg *et al*. (1976). The main advantage of using this approach is that displacements in the damaged zone can be expressed independently of the specimen size.

Viscous damping coefficients, η, are also specified respectively for all four damage modes. For a specific damage mode, the damage evolution is regularised as shown in EQ. 12 (ANSYS Inc., 2013d):

$$d'_{t+\Delta t} = \frac{\eta}{\eta + \Delta t} d'_t + \frac{\Delta t}{\eta + \Delta t} d_{t+\Delta t} \qquad \textit{EQ. 12}$$

Where:

- $d'_{t+\Delta t}$ = Regularised damage variable at current time.
- d'_t = Regularised damage variable at the end of the last sub step.
- $d_{t+\Delta t}$ = Non-regularised current damage variable.

Hashin's fibre and matrix failure criterion, ξ_4 and ξ_5, are described according to EQ. 13 and EQ. 14, respectively (ANSYS Inc., 2013d).

$$\xi_4 = \begin{cases} \left(\frac{\sigma_x}{\sigma_{xt}^f}\right)^2 + \frac{\sigma_{xy}^2 + \sigma_{xz}^2}{\left(\sigma_{xy}^f\right)^2}, & if\ \sigma_x > 0 \\ \left(\frac{\sigma_x}{\sigma_{xc}^f}\right)^2, & if\ \sigma_x \leq 0 \end{cases} \qquad \textit{EQ. 13}$$

$$\xi_5 = \begin{cases} \left(\frac{\sigma_y + \sigma_z}{\sigma_{yt}^f}\right)^2 + \frac{\sigma_{yz}^2 - \sigma_y\sigma_z}{\left(\sigma_{yz}^f\right)^2} + \frac{\sigma_{xy}^2 + \sigma_{xz}^2}{\left(\sigma_{xy}^f\right)^2} & if\ \sigma_y + \sigma_z > 0 \\ \frac{1}{\sigma_{yc}^f}\left(\left(\frac{\sigma_{yc}^f}{2\sigma_{yz}^f}\right)^2 - 1\right)(\sigma_y + \sigma_z) + \left(\frac{\sigma_y + \sigma_z}{2\sigma_{yz}^f}\right)^2 + \frac{\sigma_{yz}^2 - \sigma_y\sigma_z}{\left(\sigma_{yz}^f\right)^2} + \frac{\sigma_{xy}^2 + \sigma_{xz}^2}{\left(\sigma_{xy}^f\right)^2} & if\ \sigma_y + \sigma_z \leq 0 \end{cases} \qquad \textit{EQ. 14}$$

Where:

- $\sigma_x, \sigma_y \; and \; \sigma_z$ = Normal stresses.
- $\sigma_{xt}^f, \sigma_{yt}^f$ = Failure stress in tension for the x and y directions.
- $\sigma_{xc}^f, \sigma_{yc}^f$ = Failure stress in compression for the x and y directions.
- $\sigma_{xy}, \sigma_{xz} \; and \; \sigma_{yz}$ = Shear stresses.
- $\sigma_{xy}^f, \sigma_{yz}^f$ = Failure shear stresses in the xy and yz directions.

Orthotropic elasticity parameters, Young's modulus, Poisson's ratio and Shear modulus, were defined according to the values presented in Table 4. 1, assuming the same value for all directions (x, y and z). Similarly, orthotropic stress limits, tensile, compressive and shear, were assumed to have the same values in all directions. Finally, the dissipated energy and viscous damping coefficients values used for the simulations after calibration correspond to those presented in Table 4. 4.

The values of the non-participating modes ($C1$ and $C3$) were set at a relatively high value to avoid their interference in the study of the typical cob damage modes, namely, cracking and crushing ($C5$ and $C7$) as advised by other authors (Barbero and Shahbazi, 2017). The values of the correspondent viscous damping coefficient for tensile and compressive fibre damage ($C2$ and $C4$) were randomly assigned as they were not affecting the material's response. Whereas those for tensile and compressive matrix damage ($C5$, $C6$, $C7$ and $C8$) were calibrated by a trial and error approach to obtain the reported peak strength in the simple compressive test.

Further description of the ANSYS material constitutive models can be consulted on the software documentation (ANSYS Inc., 2013c, 2013d, 2013b).

Table 4. 4. Dissipated energy and viscous coefficient values for the DMGE/DMGI models adopted after calibration.

Material constant	Meaning	Value
$C1$	Energy dissipated per unit area from tensile fibre damage (N/m).	1.0×10^{10}
$C2$	Viscous damping coefficient for tensile fibre damage.	0.001
$C3$	Energy dissipated per unit area from compressive fibre damage (N/m).	1.0×10^{10}
$C4$	Viscous damping coefficient for compressive fibre damage.	0.001
$C5$	Energy dissipated per unit area from tensile matrix damage (N/m).	1.035×10^{5}
$C6$	Viscous damping coefficient for tensile matrix damage.	0.37
$C7$	Energy dissipated per unit area from compressive matrix damage (N/m).	7.950×10^{5}
$C8$	Viscous damping coefficient for compressive matrix damage.	0.37

4.2.2 ABAQUS constitutive models

CDP

The CDP constitutive model is suitable for reproducing the material's response to monotonic, cyclic and dynamic loading (Dassault Systemes, 2014). This thesis is concerned only with the monotonic behaviour of cob, nevertheless, the CDP material represents an interesting option for future works in which the simulation of cob's dynamic behaviour could be studied.

The material's density and elastic properties, namely Young's modulus and Poisson's ratio, were defined according to the values reported by Miccoli *et al*. and shown in Table 4. 1. The inelastic behaviour of the material is controlled by a combination of concepts in isotropic damaged elasticity, isotropic tensile and compressive plasticity (Dassault Systemes, 2014). The parameters controlling this behaviour are the dilation angle, ψ, eccentricity, ϵ, the ratio σ_{b0}/σ_{c0} which represents the relationship between initial equibiaxial compressive yield stress to the initial uniaxial compressive yield stress, the ratio of the second invariant on the tensile meridian to that on the compressive meridian, K, and finally a viscosity parameter which helps to achieve convergence by regularising the constitutive equations. To obtain realistic damage patterns, the viscosity parameter has to be limited to a maximum value of 0.001 according to Szczecina and Winnicki (2015).

The stress/strain relationship reported by Miccoli *et al*. (2017) (see Figure 2. 26 (a)) was transformed into a yield stress/inelastic strain relationship and used to define the compressive behaviour of cob (see Figure 4. 5 (a)). Inelastic strains, $\tilde{\varepsilon}_c^{in}$, the difference between total strains and elastic strains, were computed using Eq. (8).

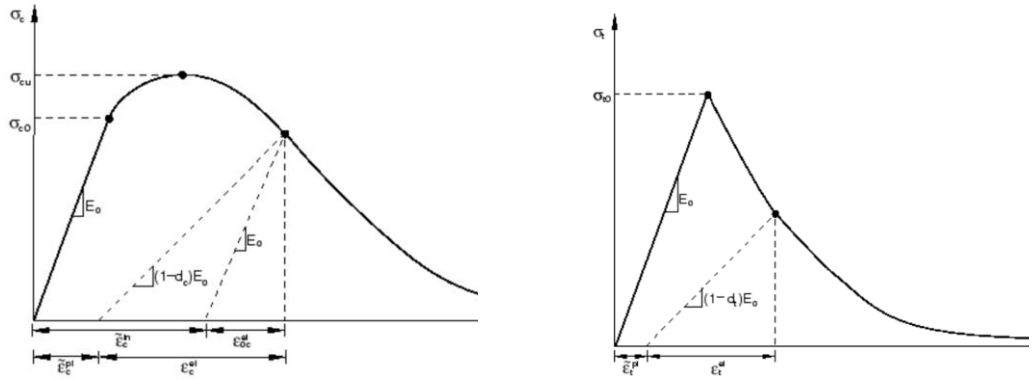

(a) (b)

Figure 4. 5. (a) Compressive and (b) tensile behaviour expressed in terms of inelastic strains (Dassault Systemes, 2014).

$$\tilde{\varepsilon}_c^{in} = \varepsilon_c - \varepsilon_{0c}^{el} \qquad EQ.\ 15$$

Where:

- ε_c = Total strain.
- ε_{0c}^{el} = Elastic strain corresponding to the undamaged material.

Finally, the tensile behaviour of cob was defined in terms of tensile yield stress and fracture energy (see Figure 4. 5 (b)). Miccoli *et al*. (2017) suggest using values for the tensile strength between 0.10 and 0.16 times the compressive strength and values for the fracture energy equivalent to 0.30 to 0.80 times the value of the tensile strength.

As no information was found in the literature regarding the application of the CDP model for the numerical modelling of cob, the input parameters shown in Table 4. 5 were calibrated to match the value of the compressive strength of cob reported in Miccoli *et al*. (2014). The calibration was performed on the simple compression test plane stress simulation model for a maximum element size of 50 mm. It was decided to use the plane stress model because the numerical simulation reported by Miccoli *et al*. (2019), on which this study is based and whose experimental setup is close to plane stress conditions, also used the plane stress assumption. Furthermore, the use of the 50 mm element size allowed the performance of large number of simulations in a relatively fast manner.

The statistical software Minitab was used to carry out the DOE based on a face-centred CCD approach. Once the responses were obtained for the different factors' combination the response surface was created using a full quadratic analysis approach. Finally, the target value was obtained by using the response optimizer module. As only

one goal was specified (i.e. match compressive strength to that obtained by Miccoli *et al*. (2019)) both weight and importance parameters were set to a value equal to one.

Table 4. 5. CDP model parameters' values adopted after calibration.

Parameter (units)	Definition	Value
ψ (degrees)	Dilation angle.	29.707
σ_{b0}/σ_{c0} (-)	Relationship between initial equibiaxial compressive yield stresses to the initial uniaxial compressive yield stresses.	1.009
K (-)	Ratio of the second invariant on the tensile meridian to that on the compressive meridian.	0.996
f_t (MPa)	Tensile strength.	0.160
${G_f}^I$ (N/mm)	Fracture energy in tension.	0.049
Viscosity (-)	Regularizing parameter.	9.04 x 10^{-8}

CSC

The CSC, based on a smeared crack concept, was selected due to the fact that the numerical simulations reported by Miccoli *et al*. (Miccoli *et al.*, 2019) also implemented a constitutive model based on a similar approach. Moreover, the software documentation specifies that the CSC model is suitable for reproducing monotonic behaviour (but limited to a low level of confining pressure) (Dassault Systemes, 2014).

The most important feature of the CSC model is its capacity to detect cracks. Crack detection is achieved by the means of an isotropic hardening yield surface, also known as crack detection surface, which is a linear relationship between the equivalent pressure stress, p, and the Mises equivalent deviatoric stress, q (see Figure 4. 6).

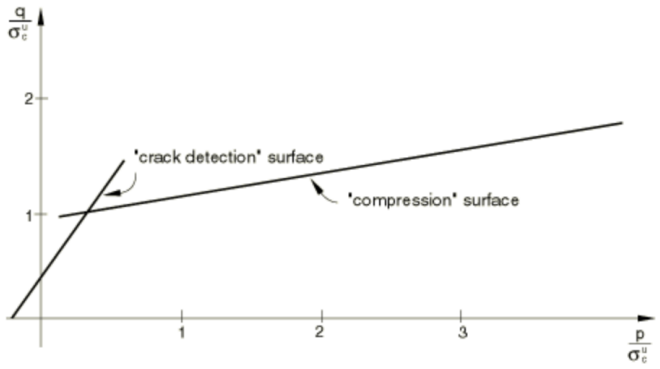

Figure 4. 6. CSC crack detection surface (Dassault Systemes, 2014).

The compression behaviour of the material was defined using a compressive stress/plastic strain relationship (see Figure 4. 3). The tabular values were once again

obtained from the stress/strain relationship reported by Miccoli *et al*. (2017) and total strains, ε_c, were transformed into plastic strains, ε_{pl}, with EQ. 16.

$$\varepsilon_{pl} = \varepsilon_c - \varepsilon_y \qquad \textit{EQ. 16}$$

Where:

- ε_y = Yield strain.

Full shear retention was considered as after an initial set of trial and error simulations it was realized that neither the multiplying factor, ρ_{CSC}, nor the user defined parameter ε^{max} affected the response under the assumed conditions of the simulation. The strain softening behaviour of the material was defined by means of a fracture energy cracking criterion in which the brittle behaviour was characterised with a stress/displacement response (Hillerborg *et al.*, 1976). EQ. 17 was used to define the value of the characteristic crack length, u_0; in other words, the displacement value at which the stresses will be zero after the material cracks (see Figure 4. 7).

$$\mathrm{u}_0 = \frac{2G_f}{\sigma_t^u} \qquad \textit{EQ. 17}$$

Where:

- σ_t^u = Failure stress.
- G_f = Fracture energy per unit area.

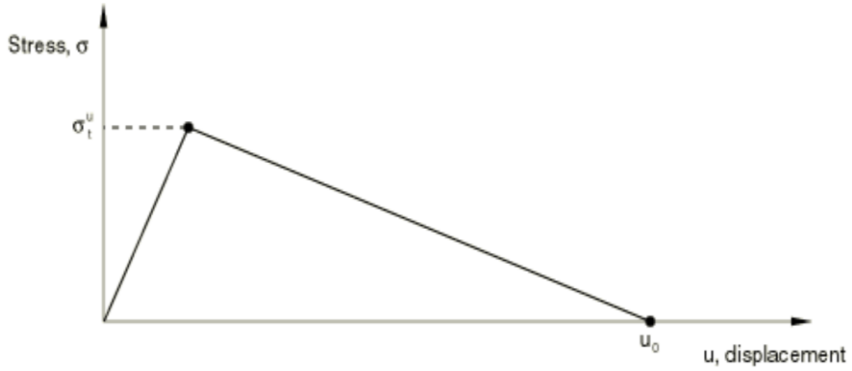

Figure 4. 7. CSC fracture energy cracking model (Dassault Systemes, 2014).

To complete the definition of the CSC model four failure ratios need to be specified as well. As no information was found in the literature regarding the application of the CSC model for the numerical modelling of cob, the input parameters shown in

Table 4. 6 were calibrated to match the value of the compressive strength of cob reported in Miccoli *et al*. (2014). The calibration of the CSC model was performed using a method similar to the one described for the CDP model. The final values adopted in the simulations for the definition of the CSC model are shown in Table 4. 6.

Further description of these ABAQUS material constitutive models can be consulted in the software documentation (Dassault Systemes, 2014).

Table 4. 6. CSC model parameters' values adopted after calibration.

Parameter (units)	Definition	Value
u_0 (m)	Characteristic crack length	0.0016
Failure ratio 1 (-)	The ratio of the ultimate biaxial compressive stress to the ultimate uniaxial compressive stress.	1.00
Failure ratio 2 (-)	The absolute value of the ratio of the uniaxial tensile stress at failure to the ultimate uniaxial compressive stress.	0.16
Failure ratio 3 (-)	The ratio of the magnitude of a principal component of plastic strain at ultimate stress in biaxial compression to the plastic strain at ultimate stress in uniaxial compression.	1.00
Failure ratio 4 (-)	The ratio of the tensile principal stress at cracking, in plane stress, when the other principal stress is at the ultimate compressive value, to the tensile cracking stress under uniaxial tension.	0.25

4.3 Results and discussion

The results obtained from the simulations are presented in the form of stress/strain graphs and maximum principal stress plots. The values plotted for the stress/strain graphs were obtained as the maximum values developed in the cob wallettes for the different simulations, thus the location at which those parameters where taken varies according to the constitutive material model (see appendix E for the detailed strain location of the different models). The upper and lower limits of the stress/strain graphs represent the experimental envelope reported by Miccoli *et al*. (2017). Besides, crack and crushing plots are shown for the CONCR models. Finally, a table is presented to show the discrepancy of the results using as reference the values obtained for the peak strengths for all the material constitutive models studied.

4.3.1 Results of simple compression tests' simulations

MISO

Plane stress and 3D simple compression stress/strain curves using MISO are shown in Figure 4. 8 and Figure 4. 9, respectively. The plane stress model reproduced the pre-peak behaviour of cob quite accurately. Unfortunately, as this plasticity model is not capable of reproducing post-peak softening, it was not able to follow the loss of strength of the material after the peak strength was attained. Regarding the mesh sensitivity, the same behaviour path was reproduced for the three element sizes. The discrepancy values computed between the peak strengths obtained and the reference value are smaller than 10 % for the three mesh sizes implemented, as can be seen in Table 4. 7.

The 3D MISO model results were not as accurate as the results obtained from the plane stress simulations. It presented a similar stiffness, but the plastic strains started to develop at a higher stress. The plots produced from the 3D MISO simulations did not fit with the experimental ones. This may be explained by the fact that the stress/strain multilinear curve used, which was calibrated with a plane stress simulation, neglects Poisson's effects. The extra compressive strength may have been caused by the Poisson´s ratio effect in the orthogonal directions of the wall plane that provided some confining to the material. Therefore, the compression stress/plastic strain curve used to define the 3D MISO models turned out to be inadequate. Table 4. 7 presents the discrepancy values for the peak strengths obtained for the 3D MISO model which were above 20 and 30 % with respect to the reference value for the different mesh sizes implemented.

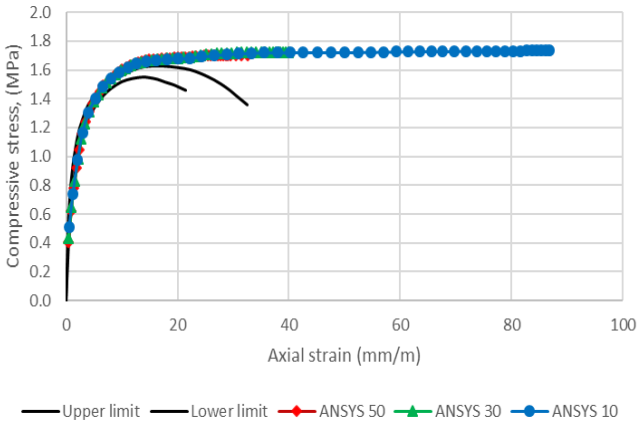

Figure 4. 8. Plane stress simple compression stress/strain curves using MISO.

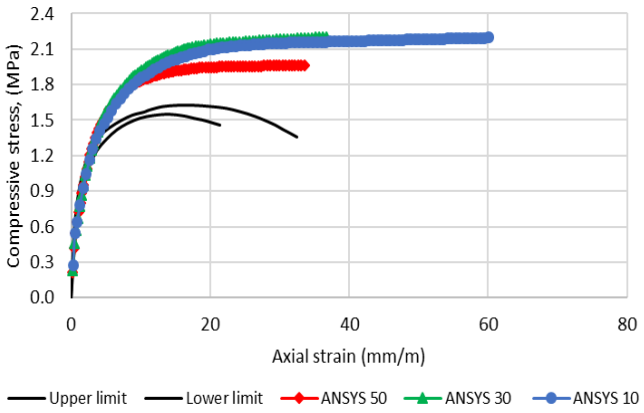

Figure 4. 9. 3D simple compression stress/strain curves using MISO.

MISO models do not provide the location of cracks or crushing within the material directly nor their extension. As an indication for such failure modes the maximum principal strains, shown in Figure 4. 10, can be interpreted (only the plots obtained for the 10 mm models are presented for the sake of brevity, but similar patterns were found for the 30 and 50 mm models see Appendix E). It is not possible to make a straight-forward comparison between Figure 4. 10 (a) and Figure 4. 10 (b) with Figure 4. 10 (c), which is the failure mode reported by Miccoli *et al*. (2014).

Interpreting the failure mode of a cob wall is a complicated task. The specimens' faces may be quite irregular if they were built following traditional construction techniques, they may have apparent cracks in the surface, caused by shrinkage, even before any load is applied, pieces of straw may protrude from the surface those hidden structural cracks, etc. Furthermore, the referenced authors only reported the failure pattern of one of their tested wallettes even though in total four wallettes were tested in simple compression. Therefore, the failure pattern shown in Figure 4. 10 (c), which seems to give a random failure pattern, does not tell us much about the general failure pattern of cob under compression. The relatively short cracks in the centre of the wallette reported by Miccoli *et al*. may have been just caused by shrinkage during the drying of the wallette, whereas the big crack located at the upper-left corner of the wallette may have been influenced by a poor quality construction as it seems like a clod of cob detached from the main volume.

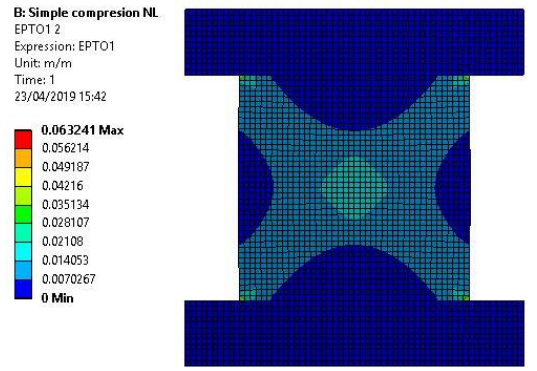

(a)

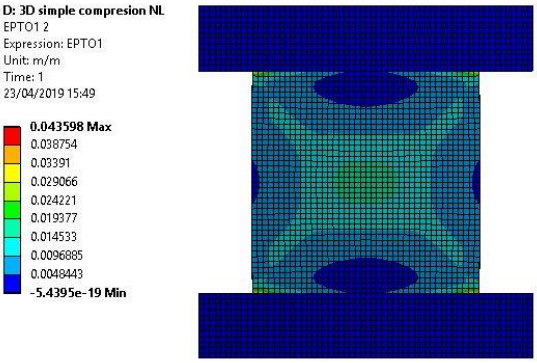

(b)

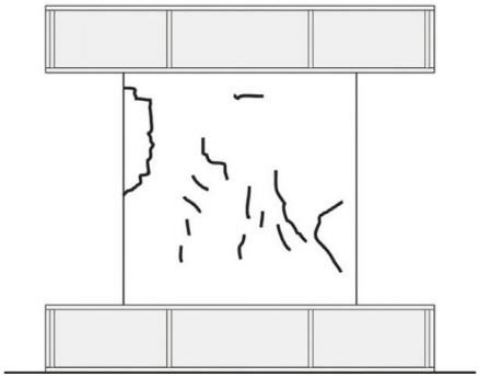

(c)

Figure 4. 10. Maximum principal strains for the simple compression MISO models (a) plane stress, (b) 3D and (c) crack pattern reported in (Miccoli et al., 2014)(repeated).

However, it can be seen in Figure 4. 10 (a) and Figure 4. 10 (b) that both, plane stress and 3D models, show a symmetric "*x*" pattern of the strains which is typical of simple compression tests of brittle materials.

CONCR

The stress/strain curves obtained with the CONCR model for the simple compression simulation are shown in Figure 4. 11. These curves display a slightly stiffer pre-peak behaviour in comparison with the experimental response of cob. Nonetheless, the overall behaviour turned out to be quite accurate. Regarding the mesh sensitivity results, discrepancy values for the peak strengths were computed within 10 % of the reference value for the three mesh sizes implemented (see Table 4. 7).

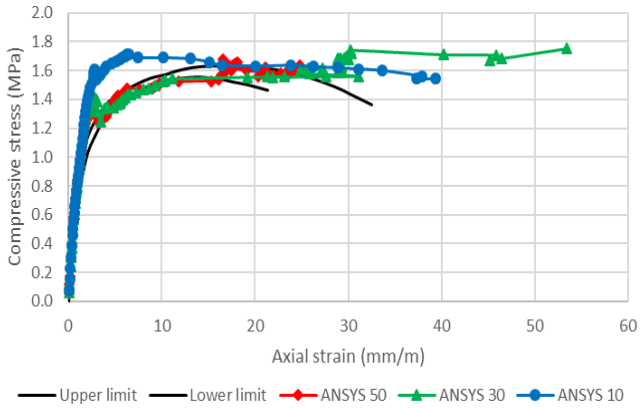

Figure 4. 11. 3D simple compression stress/strain curves using CONCR.

The CONCR material model, in combination with the finite element SOLID65, has the capability to represent cracks and/or crushing explicitly in a graphical way. Figure 4. 12 shows those plots at three different stages of the simulation, namely, at sub steps 40, 50 and 100 (last sub step). The damage is shown at the integration points of the element. An octahedron represents crushing while a circle represents cracking. Furthermore, a red, green or blue circle would represent the first, second or third crack, respectively (each integration point can show a crack per every principal direction, thus a maximum of three cracks per integration point could be observed). It can be appreciated how the failure starts at the corners of the wallette (Figure 4. 12 (a)), propagates to the centre forming the typical cone shape failure pattern of compression tests (Figure 4. 12 (b)) and finally reaches the total damage of the material (Figure 4. 12 (c)). It is not possible to make a straight forward comparison between these figures and Figure 4. 12 (d), which shows the failure mode reported by Miccoli *et al*. (2014), as the experimental failure seems to give a random pattern. However, it can be seen that the crack pattern reproduced by the CONCR model forms a typical "*x*", or double cone characteristic of simple

compressive tests. This pattern is considered as a satisfactory failure pattern in simple compression tests in accordance with BS EN 12390 Part 3 (British Standard, 2009b).

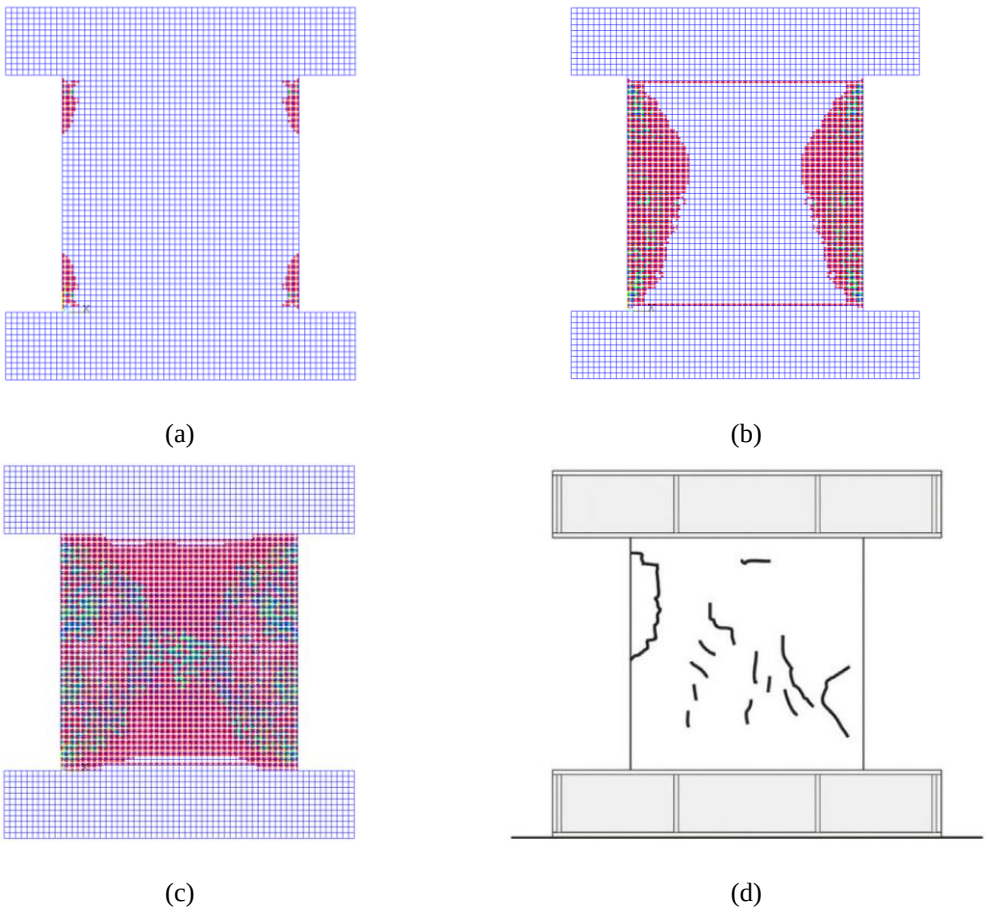

Figure 4. 12. Crack and crushing development for a simple compression test using CONCR; (a) at sub step 40, (b) at sub step 50, (c) at sub step 100 and (d) crack pattern reported in (Miccoli et al., 2014)(repeated).

DMGI/DMGE

The stress/strain curves and the maximum principal strain plots for the DMGI/DMGE simple compression models are presented in Figure 4. 13 and Figure 4. 14, respectively. Even though input parameters were calibrated to provide an accurate strength value for the simple compression test (see Figure 4. 13 and the mesh sensitivity values for the discrepancy of the peak strengths presented in Table 4. 7), neither the pre-peak nor the post-peak behaviour of cob was captured properly. DMGE/DMGI material showed a stiffer pre-peak behaviour and, after reaching the peak strength, a sudden loss of strength. Thus, depicting a fully brittle material behaviour rather than the progressive loss of capacity and ductile post-peak behaviour characteristic of cob.

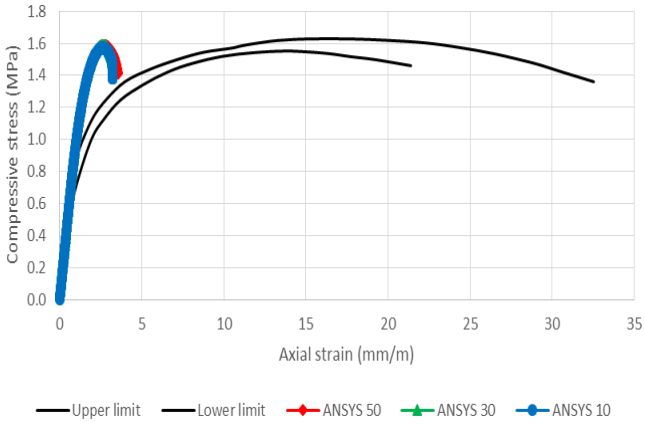

Figure 4. 13. Plane stress stress/strain curves using DMGE/DMGI for the simple compression model.

As can be seen in Figure 4. 14 (a), the simple compression maximum principal strains do not correspond with the expected "*x*" pattern considered as satisfactory. Strains accumulate at the interface between the steel plates and the top and bottom of the cob wallette instead.

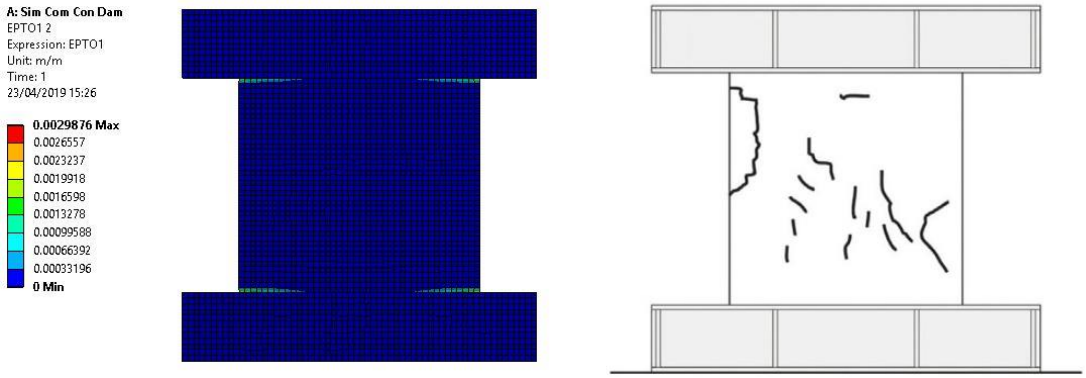

(a) (b)

Figure 4. 14. Maximum principal strains using DMGE/DMGI for the simple compression model.

The input parameters of the DMGE/DMGI models were calibrated to obtain the same peak strength as the reference for the simple compression test. Although the discrepancy values are quite small (within 1 %), neither pre-peak/post-peak behaviour nor the distribution of the maximum principal strains corresponded to the results obtained from the experimental campaign. Therefore, it was deemed that the DMGE/DMGI material model was the least suitable constitutive material model for reproducing cob´s structural response under simple compression among the set of different ANSYS material models explored.

CDP

Plane stress and 3D simple compression stress/strain curves obtained for the simple compression simulations using CDP are shown in Figure 4. 15 and Figure 4. 16, respectively. The plane stress model reproduced quite accurately the pre-peak behaviour and the slight loss of post-peak capacity characteristic of cob. Regarding the mesh sensitivity, the same behaviour path was reproduced for the three element sizes. The discrepancy values computed between the peak strengths obtained and the reference value are between 10 % and 15 % for the three mesh sizes implemented, as can be seen in Table 4. 7.

The 3D CDP model results were not as accurate as the results obtained from the plane stress model. Similarly, as happened with the MISO model of ANSYS, the CDP model presented a similar stiffness but the plastic strains started to develop at a higher stress. The plots produced did not fit with the experimental ones. As 3D models include the Poisson´s ratio effect in the directions orthogonal to the plane of the wall, the stress/strain multilinear curve used, which was calibrated with a plane stress simulation that neglects such effect, turned out to be inadequate. Table 4. 7 presents the discrepancy values for the peak strengths obtained for the 3D CDP model of between 59 % and 87 % with respect to the reference value for the different mesh sizes implemented.

CDP models do not provide directly the appearance of cracks or crushing within the material. As an indication for such failure modes the maximum principal strains, which are shown in Figure 4. 17, can be interpreted (only the plots obtained for the 10 mm models are presented for the sake of brevity, but similar patterns were found for the 30 and 50 mm models). The plane stress model shows a symmetric "*x*" pattern of strains, which is typical in simple compression tests. However, the strains appear to be concentrated at the corners of the wallette and this could only indicate the place where the cracks could appear first, but it does not depict their actual location and extent when the failure of the material is reached. This concentration is even more evident for the 3D model.

Special attention should be paid to the 10 mm 3D CDP model results as they were obtained by implementing symmetric boundary conditions and modelling only one eight of the problem. These simplifications were necessary in order to reduce the size of the model and the simulation's running time.

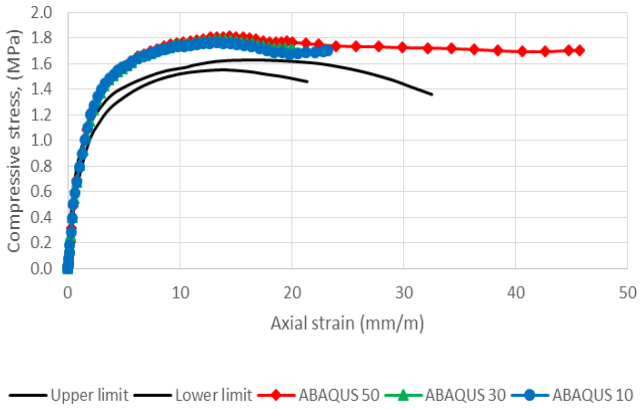

Figure 4. 15. Plane stress stress/strain curves using CDP for simple compression simulations.

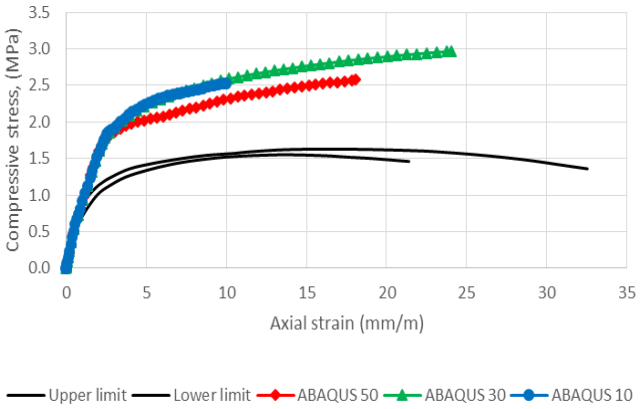

Figure 4. 16. 3D stress/strain curves using CDP for simple compression simulations.

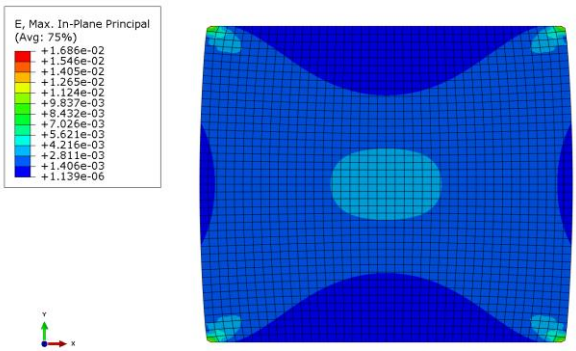

(a)

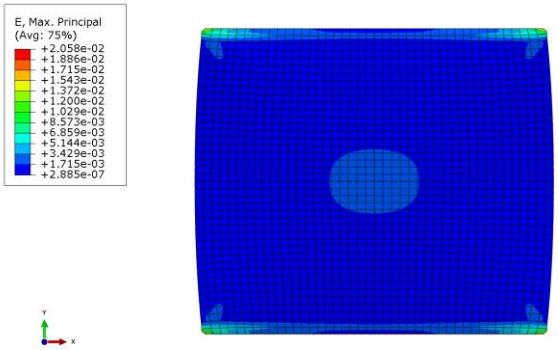

(b)

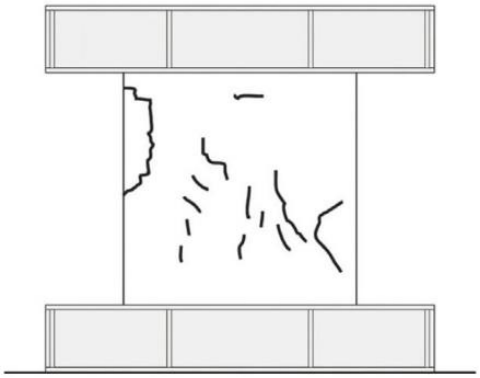

(c)

Figure 4. 17. Maximum principal strains for the simple compression CDP models (a) plane stress, (b) 3D and (c) crack pattern reported in (Miccoli et al., 2014)(repeated).

CSC

Plane stress and 3D simple compression stress/strain curves using CSC are shown in Figure 4. 18 and Figure 4. 19, respectively. The plane stress model reproduced quite accurately the behaviour of cob as the stress/strain curves capture the post-peak fall-off in stress, but overestimated slightly its peak compressive strength. Regarding the mesh sensitivity, the same behaviour path was reproduced for the three element sizes. The

discrepancy values computed between the peak strengths obtained and the reference value are the same for the three different element sizes implemented, 15 %, as can be seen in Table 4. 7.

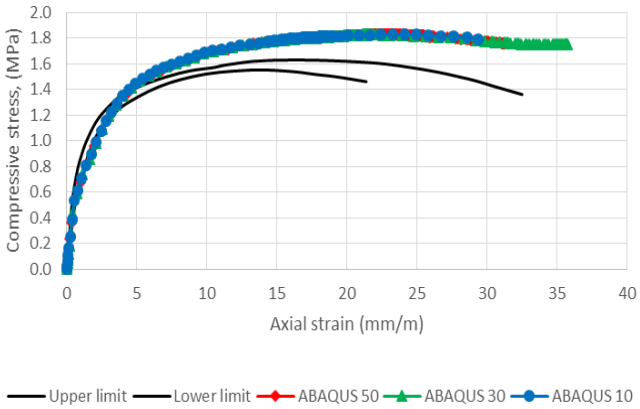

Figure 4. 18. Plane stress stress/strain curves using CSC for simple compression simulations.

The 3D CSC model results were unsatisfactory. The model presented an initial pre-peak behaviour in accordance with the reference until the elastic limits of the material, but it did not capture the post-peak softening and large strain values characteristics of cob. Table 4. 7 presents the discrepancy values for the peak strengths obtained for the 3D CSC model, between 1 % and 50 %, but those values are misleading as it can be observed in Figure 4. 19 that the model did not capture the expected behaviour.

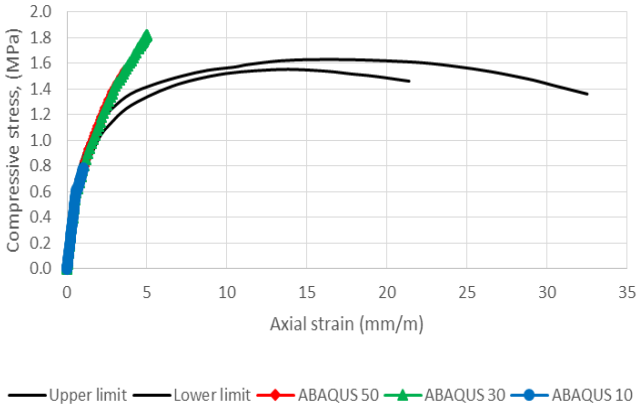

Figure 4. 19. 3D stress/strain curves using CSC for simple compression simulations.

The maximum principal strains distribution for the plane stress CSC model (see Figure 4. 20 (a)) were in good agreement with the expected "*x*" pattern characteristic of simple compression tests. On the other hand, the strains were concentrated near to the corners for the 3D model (see Figure 4. 20 (b)) and the behaviour observed in the experimental tests was not reproduced by the model. Special attention should be paid to

the 10 mm 3D CSC model results as they were obtained by availing of symmetric boundary conditions and modelling only one eight of the problem. These modifications were necessary to reduce the size of the model and the simulation time.

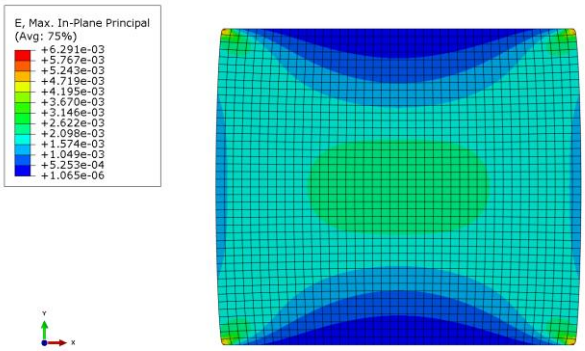

(a)

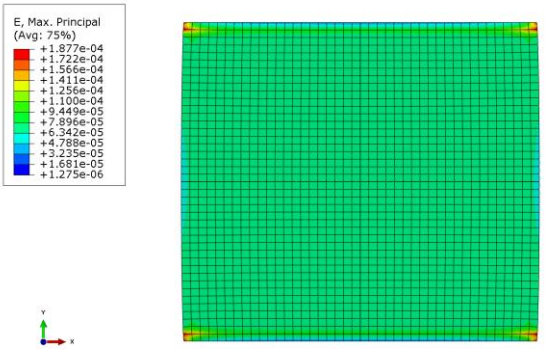

(b)

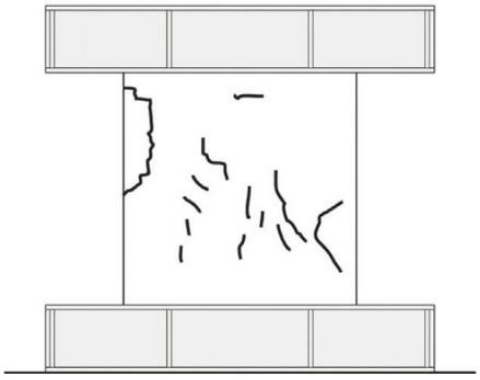

(c)

Figure 4. 20. Maximum principal strains for the simple compression CSC models (a) plane stress, (b) 3D and (c) crack pattern reported in (Miccoli et al., 2014)(repeated).

Discrepancy percentages obtained between experimental reference value reported by Miccoli *et al*. (2014) and the values obtained from both ANSYS and ABAQUS simulations of the peak strength of the material for the simple compression case are

summarized in Table 4. 7 for all material constitutive models and mesh sizes studied. Discrepancy percentages were computed using EQ. 18.

$$Discrepancy = \frac{Peak\ strength - Peak\ strength\ reference}{Peak\ strength\ reference} * 100 \qquad EQ.\ 18$$

The mean compressive peak strength reported by Miccoli *et al*. was 1.59 MPa. They also reported a Standard Deviation (SD) of 0.292 MPa and a Coefficient of Variation (COV) of 2 %. Assuming that the four wallettes tested by them represented the total population and with a confidence level of 95 % a CI would give the values (1.56, 1.62). Besides from the DMGI/DMGE models, which were deemed to be non-suitable to reproduce cob's structural behaviour, none of the other material constitutive models explored was capable to reproduce peak strength values within such interval.

Table 4. 7. Mesh sensitivity in terms of peak strengths for the simple compression simulations.

Model	Mesh size (mm)	Peak strength (MPa)	Discrepancy (%)[a]
2D MISO	50	1.70	7.2
	30	1.72	8.3
	10	1.74	9.1
3D MISO	50	1.97	23.6
	30	2.20	38.4
	10	2.20	38.1
CONCR	50	1.68	5.7
	30	1.75	10.2
	10	1.71	7.8
DMGI/DMGE	50	1.59	-0.2
	30	1.59	-0.2
	10	1.57	-1.1
2D CDP	50	1.82	14.5
	30	1.78	11.9
	10	1.76	10.7
3D CDP	50	2.58	62.3
	30	2.97	86.8
	10	2.53	59.1
2D CSC	50	1.83	15.1
	30	1.83	15.1
	10	1.83	15.1
3D CSC	50	1.56	-1.9
	30	1.82	14.5
	10	0.78	-50.9

[a] Experimental peak strength reference value of 1.59 MPa.

4.3.2 Results of diagonal compression tests' simulations

MISO

The stress/strain curves from the diagonal compression simulations are shown in Figure 4. 21 and Figure 4. 22 for the plane stress and 3D models, respectively. Wider scattering was reported by Miccoli *et al*. (2014) for the shear response of the cob wallets as can be seen from the upper and lower limit curves. All plane stress MISO models fit within such limits. Unfortunately, the discrepancy values for the peak strengths are slightly high, between 13 and 22 %, as can be seen in Table 4. 8.

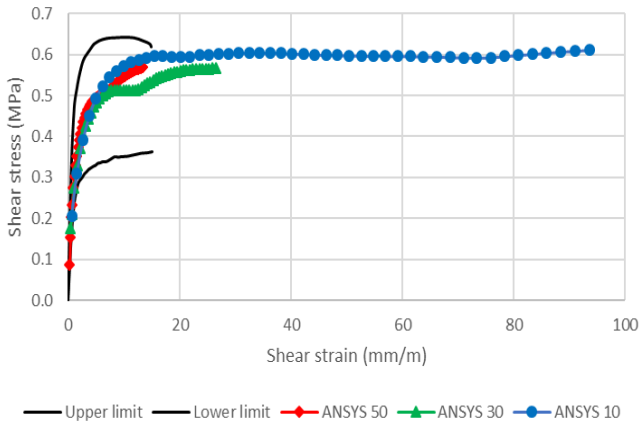

Figure 4. 21. Plane stress diagonal compression stress/strain curves using MISO.

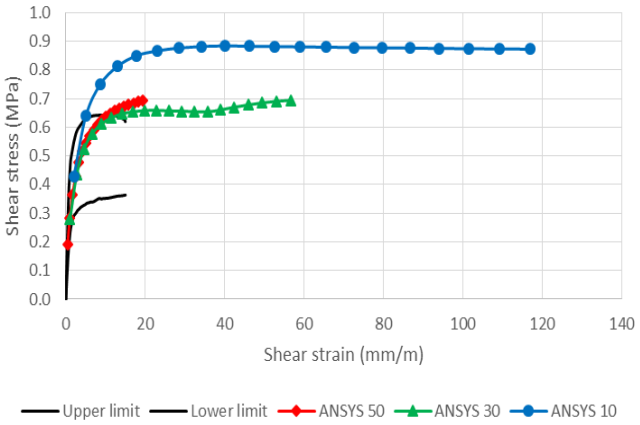

Figure 4. 22. 3D diagonal compression stress/strain curves using MISO.

On the other hand, 3D MISO stress/strain curves did not fit within the experimental reference range. These results are similar as those reported for the 3D MISO simple compression curves. The development of plastic strains at relatively higher values of stress that can be observed may be explained by the Poisson´s ratio effect in the

orthogonal directions of the wall plane for the 3D models. Moreover, an important difference between the finer mesh (10 mm) and the coarser ones (30 and 50 mm) can be seen. Discrepancy values for the peak strengths are within 39 and 41 % for the 30 and 50 mm models, whereas for the 10 mm model this value increases up to 76 % as shown in Table 4. 8.

Figure 4. 23 (a) and Figure 4. 23 (b) show the maximum principal strains from the diagonal compression simulations, whereas Figure 4. 23 (c) presents the experimental failure pattern observed during the diagonal compression test. According to Miccoli *et al*. (2019) the diagonal orientation of the main crack was caused by lack of symmetry in the specimens and testing setup.

Due to the geometry of the models, singularity points appear at the contact between the sharped edges of the steel plates with the cob wallettes. These principal strains distributions do not match with the failure pattern observed during the experimental campaigns and place doubts regarding the validity of the results obtained as the stress concentration at the elements in contact with the steel plates may invalidate the stress/strain curves obtained.

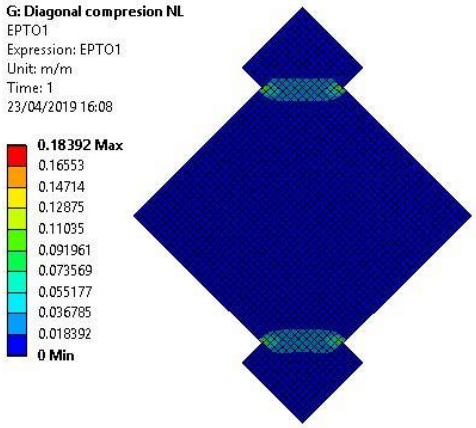

(a)

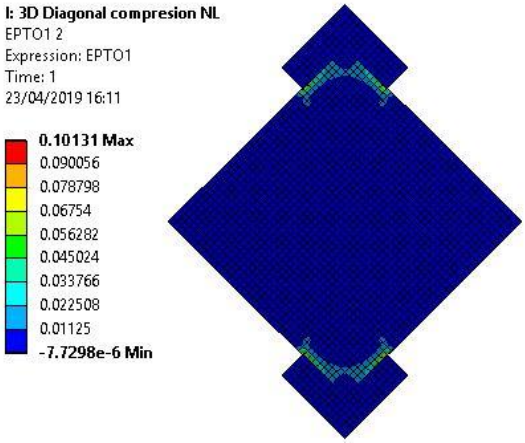

(b)

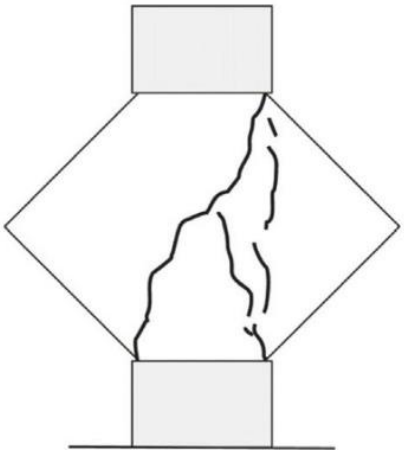

(c)

Figure 4. 23. Maximum principal strains for the diagonal compression MISO models (a) plane stress, (b) 3D and (c) crack pattern reported in (Miccoli et al., 2014)(repeated).

CONCR

The simulation of the diagonal compression test with CONCR presented a more evident mesh size sensitivity with respect to the simple compression simulation as can be seen in Figure 4. 24. None of the three models was capable of reproducing the post-peak ductile behaviour of cob reported in the experimental campaign. Moreover, the models with 30 and 50 mm mesh size gave discrepancy values regarding the peak strengths, around 47 %. On the other hand, the 10 mm model gave a very accurate peak strength value (see Table 4. 8). Even though it presented a relatively brittle post peak behaviour, the values for the final strains are similar to those reported by Miccoli *et al*. (2014).

Regarding the failure pattern of the CONCR model for diagonal compression, Figure 4. 25 presents the development of crack and crushing at different steps of the simulation. Cracks initially appear at the centre of the wallette (Figure 4. 25 (a)), then propagate diagonally in both directions (Figure 4. 25 (b)), until they reach the faces of the wallette (Figure 4. 25 (c)), forming the typical "x" pattern expected from a compression test. Among the three different ANSYS material models studied, the CONCR model represents the most accurate way of reproducing cob's non-linear monotonic behaviour.

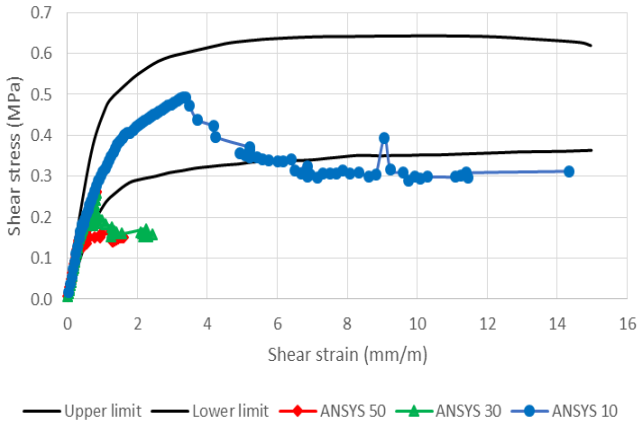

Figure 4. 24. 3D diagonal compression stress/strain curves using CONCR.

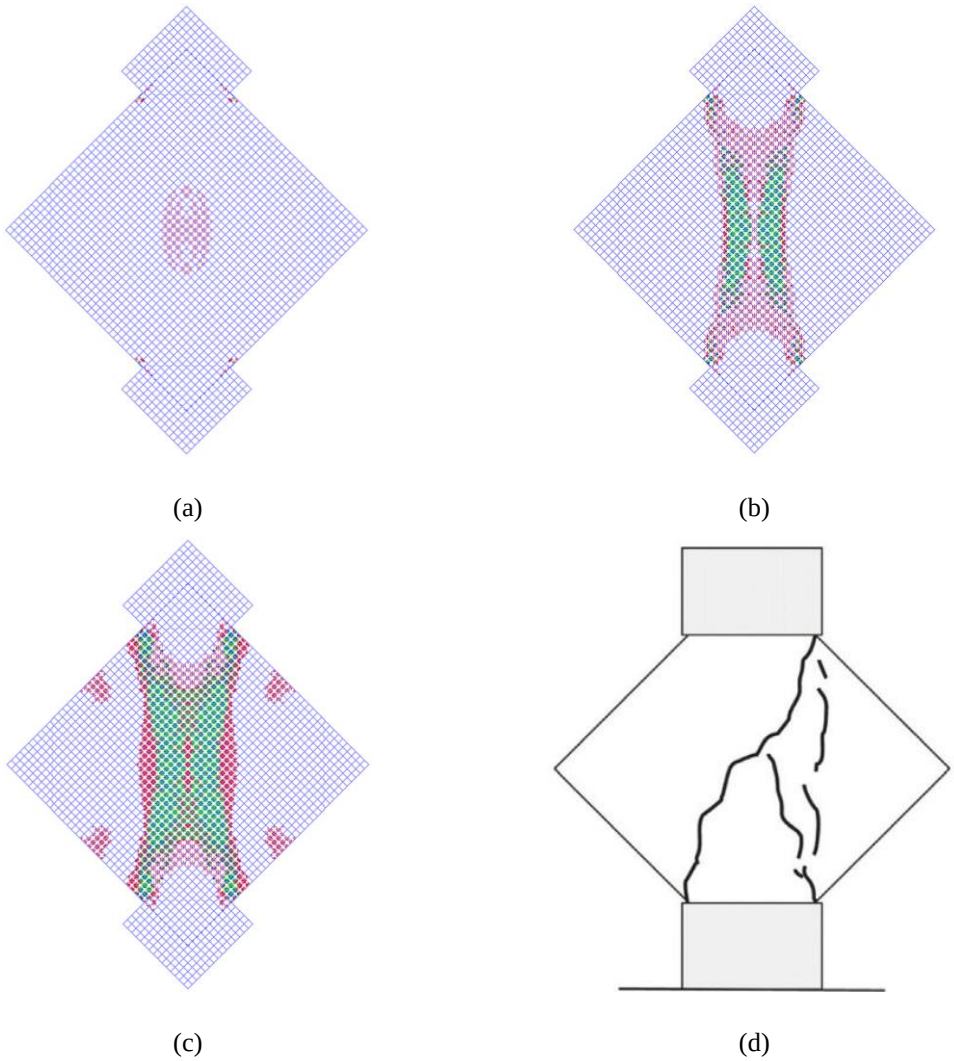

Figure 4. 25. Crack and crushing development for a diagonal compression test using CONCR; (a) at sub step 50, (b) at sub step 70, (c) at sub step 100 and (d) crack pattern reported in (Miccoli et al., 2014)(repeated).

DMGI/DMGE

The stress/strain curves and the maximum principal strain plots for the diagonal compression DMGE/DMGI models are presented in Figure 4. 26 and Figure 4. 27, respectively. The shear responses from the simulations were far from replicating the cob performance reported by Miccoli *et al*. (2017). Neither the pre-peak nor the post-peak behaviour of cob was captured properly with this model. Furthermore, the discrepancy values for the peak strengths of the diagonal test are the highest ones among all the sets of simulations as reported in Table 4. 8 (ranging from 48 % up to the 86 %).

As can be seen in Figure 4. 27, the diagonal compression maximum principal strains do not correspond with the expected "*x*" pattern considered as satisfactory. Strains

accumulate at the singularity points between the sharpened edges of the steel plates in contact with the faces of the cob wallettes and propagate vertically towards the centre of the wallette.

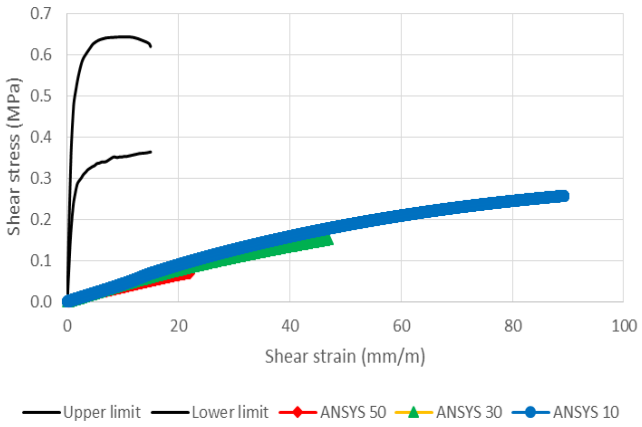

Figure 4. 26. Plane stress stress/strain curves using DMGE/DMGI for the diagonal compression simulations.

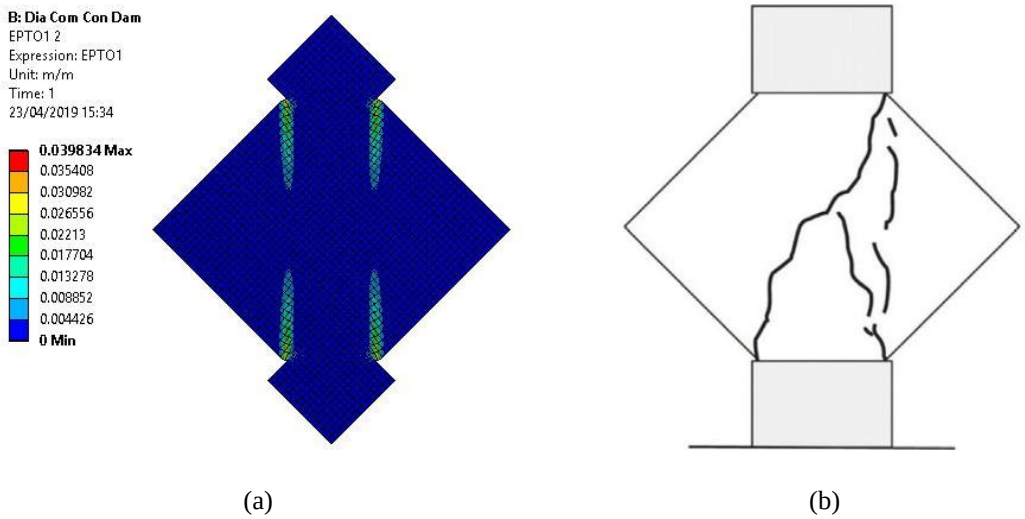

(a) (b)

Figure 4. 27. Maximum principal strains using DMGE/DMGI for the diagonal compression model.

As neither pre-peak/post-peak behaviour nor the distribution of the maximum principal strains corresponded to the results obtained from the experimental campaign, the DMGE/DMGI material model turned out to be the least suitable one for reproducing cob´s structural response among the set of ANSYS different material models explored.

CDP

The obtained stress/strain curves from the diagonal compression simulations using the CDP model are shown in Figure 4. 28 and Figure 4. 29 for the plane stress and 3D models,

respectively. All plane stress CDP models fit within such limits. The discrepancy values for the peak strengths are all smaller than 10 %, as can be seen in Table 4. 8. Unfortunately, the model was not able to reproduce the large values of post-peak strains characteristic of cob.

On the other hand, the three 3D CDP models captured the large values of strain observed on the experiment stress/strain curves. Nevertheless, they presented a more significant variation due to the mesh size. The three element size models show a similar behaviour in their elastic region, but after the yielding point the coarser mesh's models developed a stiffer response and attained a higher shear stress peak value with respect to the 10 mm element size model. Discrepancy values for the peak strengths are within 30 % and 60 % for the 30 and 50 mm models, respectively, whereas that for the 10 mm model the peak strength almost matches the reference value, with only 2 % discrepancy (see Table 4. 8).

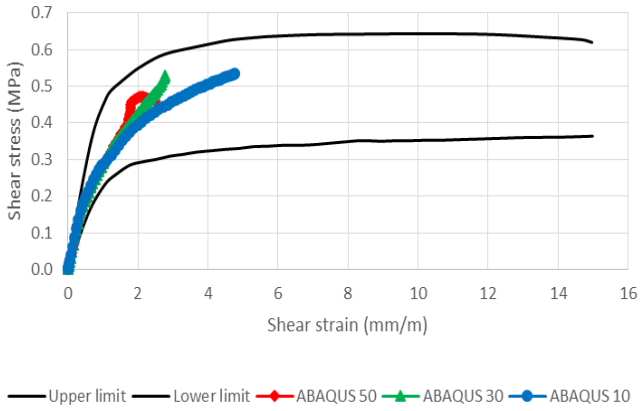

Figure 4. 28. Plane stress stress/strain curves using CDP for diagonal compression simulations.

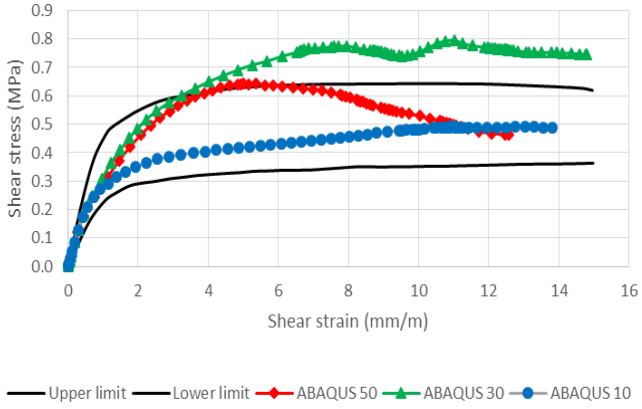

Figure 4. 29. 3D stress/strain curves using CDP for diagonal compression simulations.

Figure 4. 30 shows the maximum principal strains from the diagonal compression simulations. Due to the geometry of the models, singularity points appear at the edge of the interface between the steel plates and the cob wallettes. Nevertheless, the distribution of the strains matches at certain level the one found during the experimental campaign. "*Cracks*" initiate at the centre of the wallette and propagate diagonally until reaching the wallette edges forming the expected typical "*x*" pattern. The 10 mm 3D CDP model results were obtained by availing of the use of symmetry conditions, thus modelling only one eight of the problem.

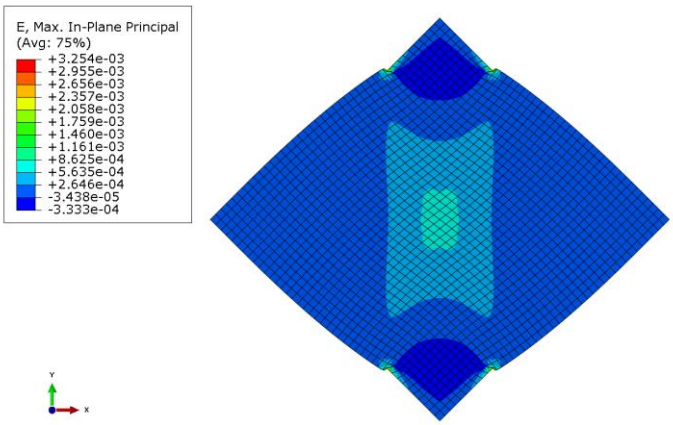

(a)

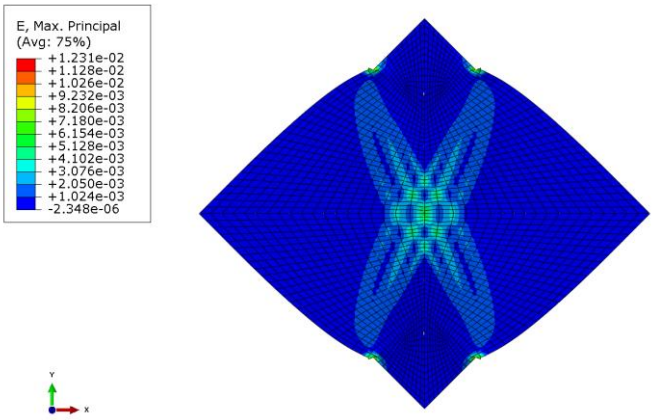

(b)

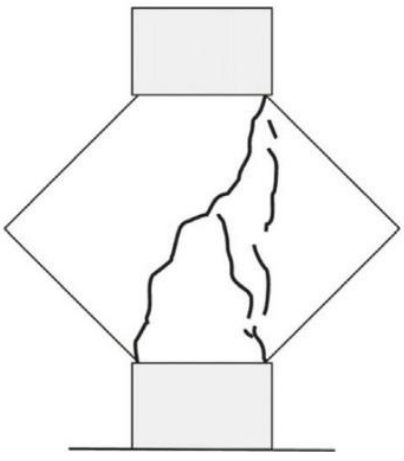

(c)

Figure 4. 30. Maximum principal strains for the diagonal compression CDP models (a) plane stress, (b) 3D and (c) crack pattern reported in (Miccoli et al., 2014)(repeated).

CSC

The obtained stress/strain curves from the diagonal compression simulations are shown in Figure 4. 31 and Figure 4. 32 for the plane stress and 3D models, respectively. All plane stress CSC models fit within the reference limits, unfortunately, the discrepancy values for the peak strengths are slightly high, between 8 % and 20 %, as can be seen in Table 4. 8. Even though the 3D CSC stress/strain curves also fit within the reference range, this model was not capable of capturing the characteristic post-peak large strain values of cob. Moreover, an important difference between the finer mesh (10 mm) and the coarser ones (30 and 50 mm) can be seen. Discrepancy values for the peak strengths correspond to 14 % and 16 % for the 30 and 50 mm, models, respectively whereas the corresponding value for the 10 mm model was only 4 % (see Table 4. 8).

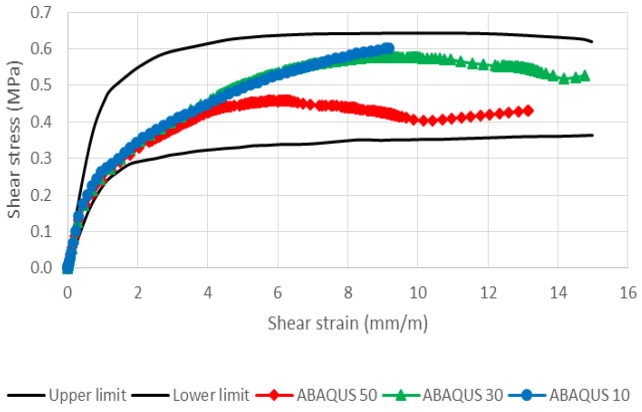

Figure 4. 31. Plane stress stress/strain curves using CSC for diagonal compression simulations.

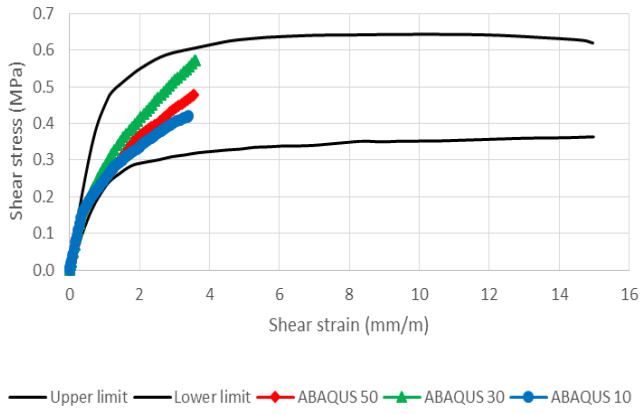

Figure 4. 32. 3D stress/strain curves using CSC for diagonal compression simulations.

Figure 4. 33 shows the maximum principal strains from the diagonal compression simulations. Due to the geometry of the models, singularity points appear at the boundaries of the contact region between the steel plates and the cob wallettes. These

principal strains distributions do not match the failure pattern observed during the experimental campaigns. Once again, the 10 mm 3D CDP model results were obtained by modelling only one eight of the problem.

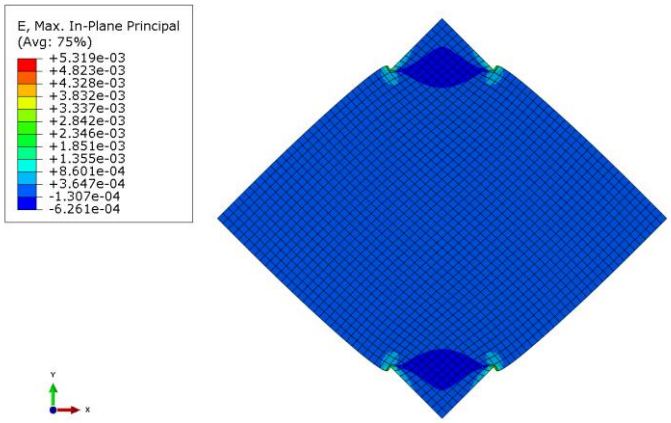

(a)

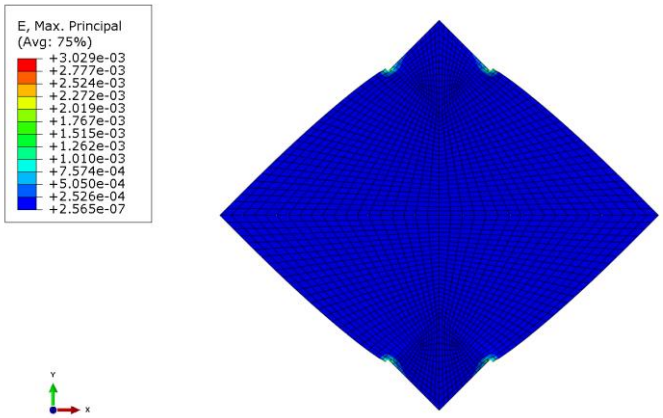

(b)

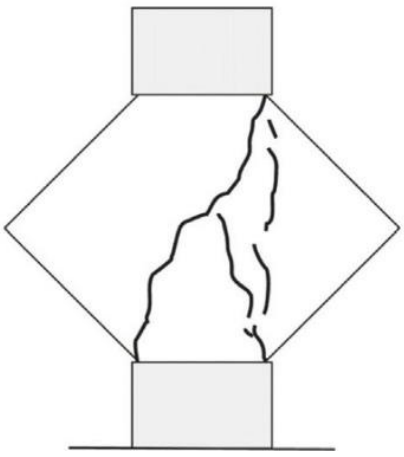

(c)

Figure 4. 33. Maximum principal strains for the diagonal compression CSC models (a) plane stress, (b) 3D and (c) crack pattern reported in (Miccoli et al., 2014)(repeated).

Discrepancy percentages obtained between the experimental reference value, reported by Miccoli *et al*. (2014), and the simulation values obtained with ANSYS and ABAQUS of the shear peak strength for the diagonal compression case are summarised in Table 4. 8 for all material constitutive models studied. Discrepancy percentages were computed using EQ. 18.

The mean shear peak strength reported by Miccoli *et al*. was 0.50 MPa. They also reported a SD of 0.1045 MPa and a COV of 20.89 %. Assuming that the four wallettes tested by them represented the total population and with a confidence level of 95 % a CI would give the values (0.43, 0.57). Several material constitutive models explored were capable to reproduce peak strength values within such interval.

Table 4. 8. Mesh sensitivity in terms of peak strengths for the diagonal compression simulations.

Model	Mesh size (mm)	Peak strength (MPa)	Discrepancy (%)[a]
2D MISO	50	0.57	13.7
	30	0.57	13.3
	10	0.61	22.2
3D MISO	50	0.71	41.3
	30	0.70	39.1
	10	0.88	76.5
CONCR	50	0.26	-47.4
	30	0.26	-47.6
	10	0.49	-1.7
DMGI/DMGE	50	0.07	-86.1
	30	0.15	-69.6
	10	0.26	-48.7
2D CDP	50	0.47	-8.0
	30	0.53	6.0
	10	0.53	-8.0
3D CDP	50	0.65	30.0
	30	0.80	60.0
	10	0.49	-2.0
2D CSC	50	0.46	-8.0
	30	0.58	16.0
	10	0.60	20.0
3D CSC	50	0.48	-4.0
	30	0.57	14.0
	10	0.42	-16.0

[a] Experimental peak strength reference value of 0.50 MPa.

4.4 Conclusions

The suitability of three constitutive material models available in ANSYS (MISO, CONCR and DMGE/DMGI) and two constitutive models available in ABAQUS (CDP and CSC) to replicate the non-linear monotonic structural behaviour of cob was assessed.

The simulations' models were based on previous experimental campaigns performed by Miccoli *et al*. (2014) and the results of the simulations were compared against those experimental results.

MISO was the simpler material constitutive model studied. The values of the material's Young's modulus, Poisson's ratio, density, and compressive stress/ strain relationship were used as reported by the referenced authors. It was not necessary to perform any calibration as the material is completely defined with those parameters. Unfortunately, Miccoli *et al*. calibrated their stress/strain curve assuming a plane stress behaviour of the cob wallettes and it turn out to be inadequate for the 3D simulations. 3D models, not only for the MISO but also for the CDP and CSC for which the stress/strain curve was used, gave higher values of peak strength in comparison to the reference value reported by Miccoli *et al*. from the experimental testing of the cob wallettes. A plane stress simplified model usually gives accurate enough results when the thickness of the element is relatively small to its other two dimensions. In the case of the cob wallettes tested by Miccoli *et al*. the T_{wall}/L_{wall} (thickness/length) and T_{wall}/H_{wall} (thickness/height) ratios gave values of 0.27. Based on the results observed in the MISO models, as well as in the CDP and CSC models, it can be concluded that this ratio is not small enough to adopt a plane stress simplification. The thickness of the wallettes provided enough confinement to the material out of its plane as to create a significant difference between the plane stress and the 3D models. Furthermore, the MISO constitutive model does not have the capability of defining a post-peak loss of strength. Therefore, the MISO models were not capable of reproducing the port-peak loss of strength observed from the experimental campaign. Moreover, the MISO model is not suitable for reproducing the behaviour of materials with different compressive/tensile strengths (cob's tensile strength is between a tenth and a sixteenth of its compressive strength). For all these reasons, the MISO material constitutive model is considered to be inadequate to reproduce cob's structural behaviour.

The model that best represented the behaviour of cob in ANSYS was the 3D CONCR with a 10 mm mesh size. The discrepancy values for both simple and diagonal compression peak strengths are smaller than 10 %. Moreover, the cracks obtained in the model are in good agreement with the typical failure pattern presented in these types of experimental tests. Nevertheless, caution should be exercised while interpreting results when CONCR is used to model cob structural behaviour under different conditions from

those studied in this paper as it was noticed that the model is sensitive to the mesh size that is implemented. Furthermore, the CONCR model is one of the more complex models studied in this thesis, as it requires the use of snippets in Workbench and the calibration of several parameters for its definition which may limit its application to advanced users of the software. Moreover, this material constitutive model can only be used in combination with the element SOLID65 which is a legacy element. Currently the software documentation advises the use of the current-technology SOLID185 element and the SOLID65 may no longer be able in future versions of the software.

The DMGI/DMGE models with a Hashin failure criteria and continuum damage mechanics approach adopted did not reproduced accurately enough the cob's structural behaviour. Nevertheless, this material constitutive model can be defined in different terms, i.e. using a maximum stress or maximum strain criteria along with a continuum damage mechanics or with a material property degradation approach, and those approaches may provide better results. The DMGI/DMGE would have to be further studied in future works before providing a definitive recommendation for its use to model cob structural behaviour.

The model that best represented the behaviour of cob in ABAQUS was the 2D CDP with a 10 mm mesh size. The discrepancy values for both simple and diagonal compression peak strengths are smaller than 10 %. Besides, the maximum strain plots obtained in the model are in good agreement with the typical failure pattern presented in these types of experimental tests. Moreover, the CDP material constitutive model is of special interest as according to the software documentation this model is suitable for reproducing the cyclic and dynamic behaviour of the material and this capability could be further explored in future research. The CSC model on the other hand, presented quite limited capabilities in comparison with the CDP model. Based on a comparison of the results obtained with both material constitutive models, the use of CDP would be advised over the use of CSC to model cob walls in ABAQUS.

General conclusions regarding the mesh size sensitivity (h-refinement) are complicated to drawn as different material constitutive models developed different trends. The MISO stress/strain curves obtained show that a finer mesh would provide larger strain values. This may have been caused by the presence of stress concentrations between the contacts of the cob wallette with the steel plates. The plasticity of the material would affect the four corners in a small element whereas that for larger elements it would be

averaged and slightly reduced as some corners in the element may not have reached the plasticity point. The mesh sensitivity was negligible for the simulation of the simple compression test using the CONCR constitutive model, whereas for the simulation of the diagonal compression test an important difference, between coarser and the 10 mm mesh model, was observed in the shear stress/shear strain curves obtained. Similarly, the DMGI/DMGE models did not show significant difference for the simple compression simulations, whereas for the diagonal compression simulations the finest mesh presented larger strain values in comparison to the coarser ones. The participation of the shear induced stresses in the material would influence the failure of the material, which concentrated in a smaller element, and cause the lager values of strain observed. Regarding the ABAQUS models, the symmetric simplification adopted, to reduce the size of the 3D models, may have caused that the 10 mm models present smaller strain values than the coarser ones for the cases of CDP and CSC simple compression and CSC diagonal compression. Nevertheless, since CDP diagonal compression do not present this phenomenon the actual cause may be found elsewhere. Further analysis of this and the mesh sensitivity results of the plane stress ABAQUS models is required.

The results obtained with the simulations presented in this chapter were not completely satisfactory. The structural behaviour of cob was not perfectly reproduced by any of the tested models; thus, further work is required either to keep exploring the available materials in the two programs or to develop an exclusive material constitutive model capable of reproducing cob's structural behaviour. In addition, from the element size influence and the values of the parameters calibrated to define the material constitutive models presented on this thesis, other aspects which can significantly affect the simulation results (i.e. solver parameters, element type (p-refinement), convergence) should be considered on future studies.

A material constitutive model capable of reproducing the non-linear behaviour of cob subjected to different load scenarios would improve the quality of the quantitative research of cob heritage structures. An accurate description of cob's structural behaviour would contribute to perform better safety evaluations, diagnosis of causes of damage and decay, and validation of interventions in historical cob buildings. Furthermore, once the information provided by the structural analysis of the structure is properly reconciled with the information obtained from the qualitative and historic research approaches, the design of over invasive interventions that may endanger the historic fabric could be avoided.

A better description of cob’s structural behaviour could also improve the design of new cob buildings and the development of cob building standards. That topic would not be further discussed since it is outside the scope of this thesis.

Chapter 5: Experimental validation of the use of flat jack tests in cob walls

This chapter presents another important contribution of the thesis. Here the experimental campaign carried out on the use of the flat jack tests in cob walls is described. The characteristics of the raw materials used are reported, the construction process of the cob wallettes is described, the consolidation and flat jack tests procedures explained and, finally, the data obtained, and the results analysis are presented and discussed.

The development of this experimental campaign is intimately linked to the non-linear simulations presented in chapter 4 of this thesis. As highlighted in section 4.2, in order to describe any of the constitutive models tested, the basic mechanical properties of the material are required; namely, compressive strength, Young's modulus and Poisson's ratio. The non-linear simulations performed in the previous chapter were based on the experimental campaign performed by Miccoli *et al*. (2014), but as cob is a natural non-standardized material, it would be expected to find a great variability for the values of those mechanical properties from region to region, and of course, from country to country (notice the variability of the values presented in Table 2. 7 for example). The application of the MDT technique to cob walls, validated during this experimental campaign, is presented as a viable, respectful and efficient quantitative option for conservators working on the study of remaining cob vernacular buildings.

5.1 Introduction

The experimental campaign described in this chapter was performed based on the hypothesis that it was possible to determine the levels of stress and the mechanical properties of existent cob walls by implementing the flat jack test. In conservation practice the information obtained from the flat jack test is used to assist in the structural safety evaluation of existent structures.

The objectives of the experimental campaign were:

- To reproduce representative wall specimens of cob vernacular buildings in the laboratory.
- To carry out both, simple and double, flat jack tests to determine the levels of compressive stress at a location in the wall and cob's mechanical properties, namely, Young's modulus, Poison's ratio and compressive strength.
- To assess the performance of the test and its suitability for the assessment of historical cob buildings.

The experimental campaign started to be planned in the spring of 2018 and was concluded in the summer of 2019. The necessary technical knowledge to implement the flat jack test technique was acquired thanks to a research collaboration carried out at the University of Cantabria (UC) in Santader, Spain, during the months of June and July 2018. The expertise and know-how shared by the Professor Ignacio Lombillo proved to be invaluable for the successful performance of the flat jack tests.

The traditional cob construction technique was learned during the participation at the International BASEhabitat Summer School organized by the University of Linz, Austria. Becky Little and Francois Streiff, two experienced earthen builders and researchers, taught the traditional skills used in France, UK and Ireland to build vernacular cob walls and these skills were used to build the wallettes at the laboratory of CSEE in TCD. The different stages of the experimental campaign are shown in the timeline of Figure 5. 1.

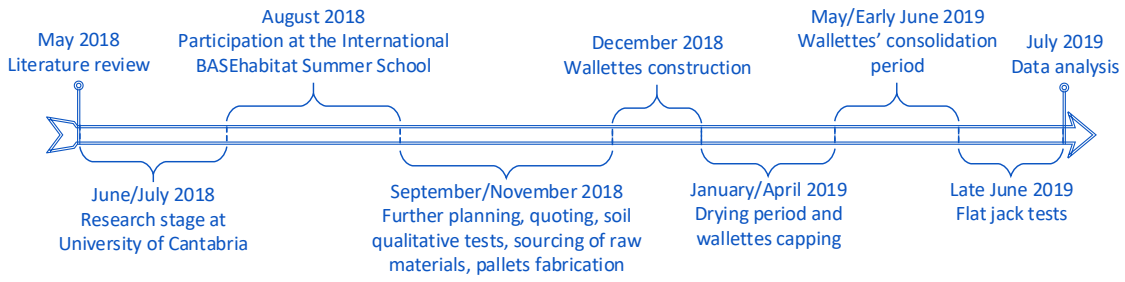

Figure 5. 1. Experimental campaign's timeline.

5.2 Methodology

A schematic of the methodology process carried out to achieve the objectives of the experimental campaign is presented in Figure 5. 2. Each one of the steps is explained into more detail throughout the sections of this chapter.

5.3 Materials

The basic raw materials needed to build a cob wall are: straw, water and soil. It was intended to build the wallettes of this experimental campaign in a sustainable way and try to reproduce the characteristics of a historical cob wall as closely as possible. Thus, materials were sourced locally and traditional construction methods were used. The selection of the raw materials was based on recommendations provided by several authors (Doat, 1979, Keefe, 1993, Jaquin and Augrade, 2012, Keefe, 2012, Minke, 2012, Miccoli *et al.*, 2014, Hamard *et al.*, 2016, Teixeira *et al.*, 2018). Those recommendations are mainly concern with the water quality, the type and the length of the straw, the clay content and the PSD of the soil.

The water used was clean and potable. It came directly from the tap in the laboratory of CSEE at TCD.

Both the straw and the soil were sourced from within the County Dublin and County Kildare areas. The straw used was wheat straw. It was bought from a farmer whose farm is located at Athy, County Kildare. Two bales of 2.5 m by 1.5 m by 1 m dimensions were bought for a total cost of € 100 but only a small quantity was used (roughly 1/10 of a bale). The remaining straw was returned to the farmer (the mixing proportions used are specified in section 5.5).

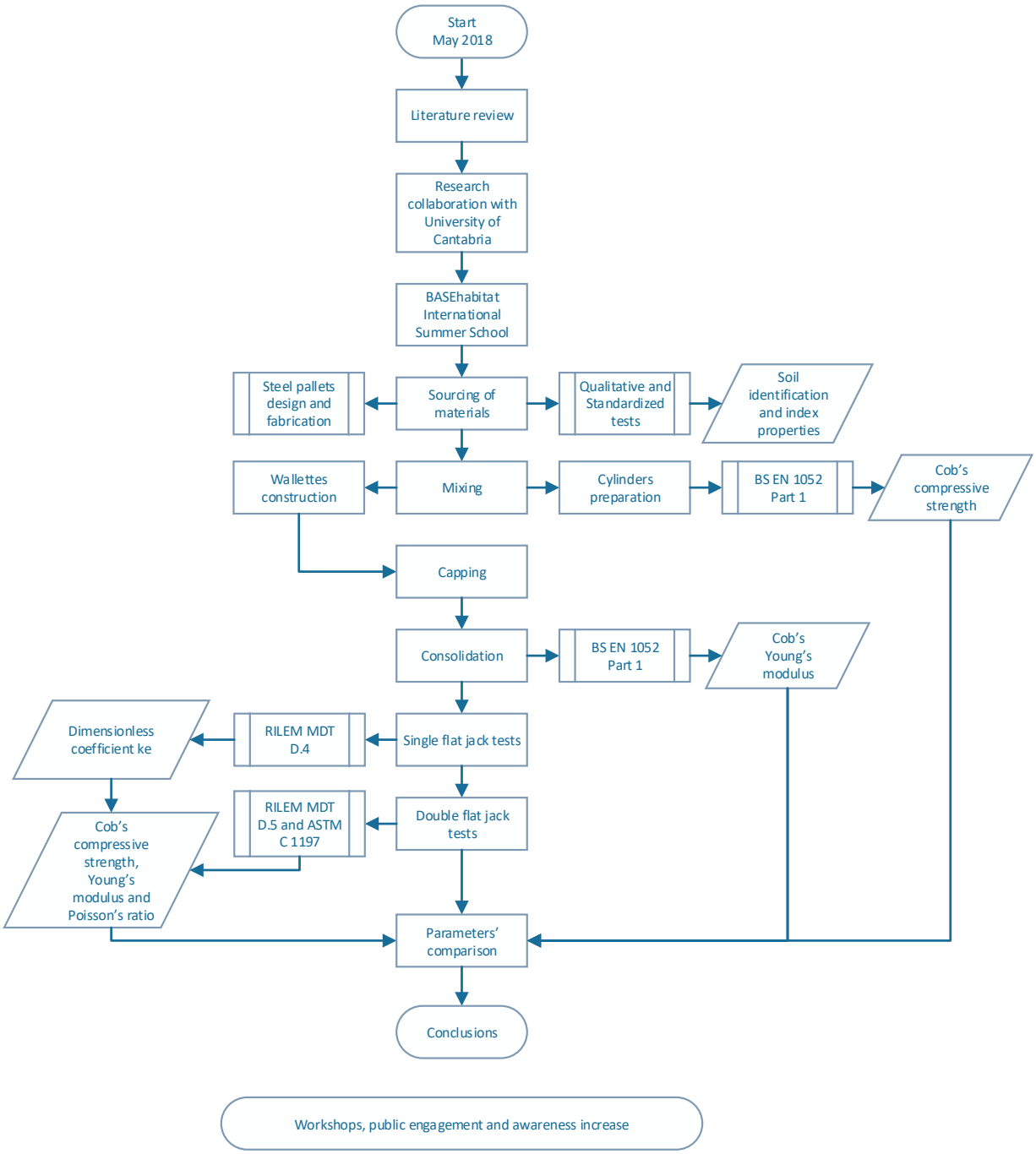

Figure 5. 2. Experimental campaign methodology.

The soil was bought from a local soil supplier, Landscape Depot, located in Tallaght, County Dublin. Before placing the soil order a series of qualitative tests were undertaken to assess its suitability for the project (details of those tests are provided in section 5.3.1). Once its suitability was stablished, four 1 m^3 bags of "*clay topsoil*" (as named by the soil supplier on its website) sieved through a 1 cm sieve were ordered. This amount of soil proved to be insufficient for the completion of the wallettes and two extra

1 m^3 bags were bought of the same soil at a later stage of the construction process. Figure 5. 3 shows the soil and the straw bought for the construction of the cob wallettes.

(a) (b)

Figure 5. 3. Soil (a) and wheat straw (b) locally sourced for the construction of the cob wallettes.

5.3.1 Soil qualitative tests

Qualitative soil tests have been traditionally used by vernacular builders, who had no access to complex equipment and laboratory facilities, to assess the suitability of the material for earthen construction purposes. These testes are highly related to the human senses and provide basic information about the constitution of the soil and of its behaviour. The advantages of qualitative tests are their simplicity, easiness, low-cost and their relatively fast data obtainment. On the other hand, the interpretation of qualitative tests is subjective and is dependent on the experience and personal judgement of the test performer. Qualitative tests were performed on a sample of soil collected directly from the soil supplier yard.

- **Visual**

First of all the soil was visually inspected. This quick qualitative test detects the presence of big soil particles (gravels) (Doat, 1979), relatively big pieces of organic material and garbage. The colour of the soil may also give an indication of its mineralogical composition and organic content. Water, organic matter, iron and, to a lesser extent, manganese are the main soil pigmenting component (Hillel and Hatfield, 2005).

The sample of soil used in this experimental campaign had a dark brown colour and seemed to be in a wet state. After carefully examining the soil, traces of organic material were detected. They seemed to correspond to small grass roots. Those organic particles were not considered to be a problem as they represented a tiny portion of the

whole volume. Lumps of particles were observed as well. This indicated the presence of clay which was necessary and desirable, as the soil was to be used to build cob wallettes. Particles bigger than 1 cm diameter were observed as well, which was not adequate for cob purposes according to the PSD graphs recommended by Keefe (2012) and Jaquin and Augrade (2012). This problem was easily solved by asking the soil supplier to sieve the soil through a 10 mm sieve. The soil sample is shown in Figure 5. 4 (a).

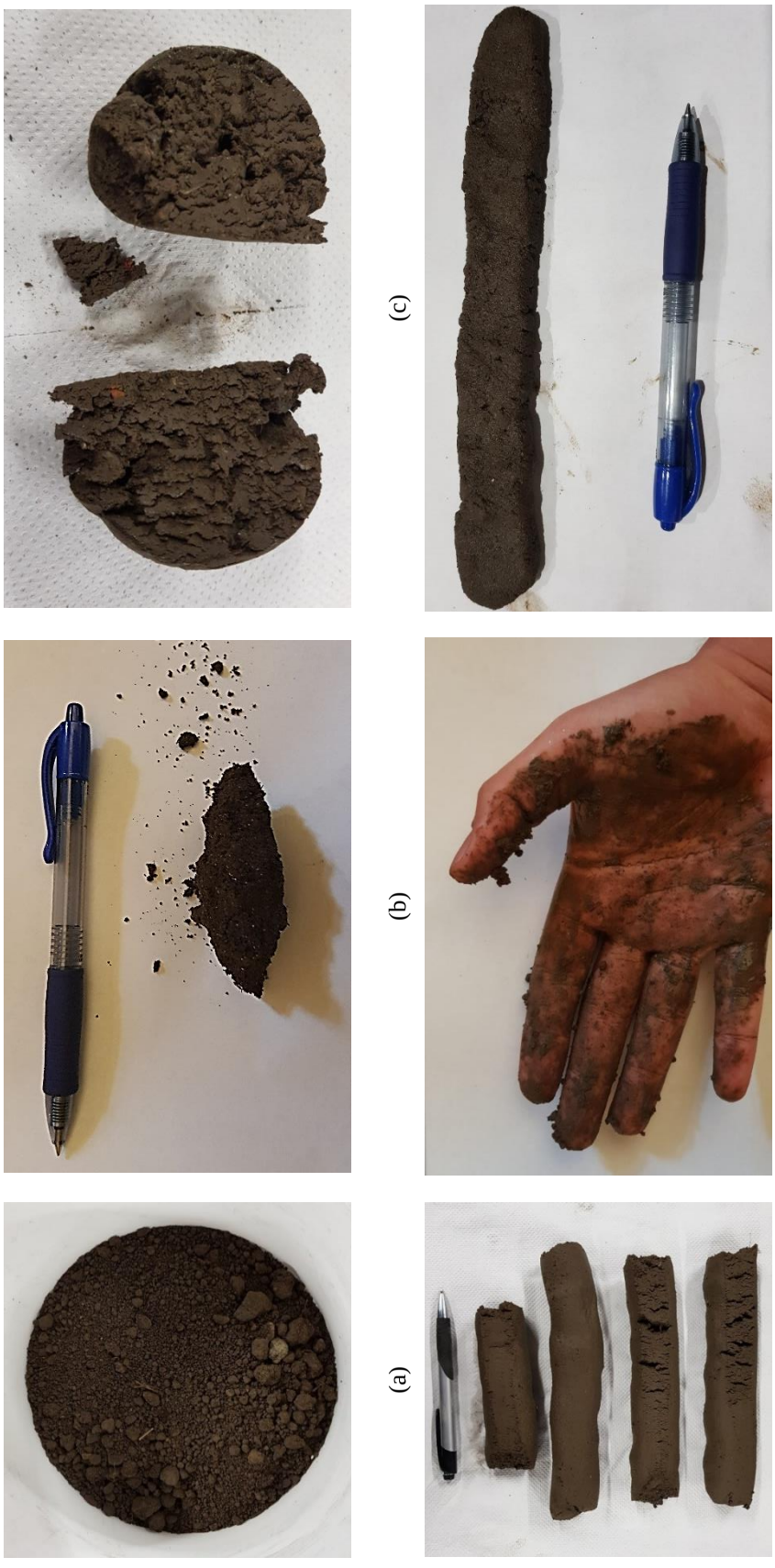

Figure 5. 4. Soil qualitative tests part 1; (a) visual test: detection of organic material and gravels, (b) touch test: lumped soil after pressing with the hand, (c) cutting test: two ball halves after cutting, (d) cigar test: segments of roughly 15 cm length, (e)

It is worth mentioning that particles bigger than 1 cm have been observed in several historical buildings visited by the author during the field trip along County Wexford of the Clayfest Conference organized by Earthen Buildings of the United Kingdom and Ireland (EBUKI) in 2018 (see Figure 5. 5 (a)) and in another cob vernacular building visited in 2019 located in the outskirts of Kildare Town in County Kildare (see Figure 5. 5 (b)). Therefore, the use of a sieved soil may not exactly reproduce representative traditional Irish vernacular cob walls. Nevertheless, it was decided to follow the experts' recommendations as this will facilitate the preparation of the loam and will ensure the removal of dangerous objects from the soil (such as broken glass) thus ensuring good health and safety practices.

(a) (b)

Figure 5. 5. Remaining vernacular cob walls in (a) County Wexford and (b) County Kildare showing the presence of gravels in the mix.

- **Smelling**

Pure soil has a neutral smell. On the other hand, a mouldy smell may indicate the presence of abundant organic material (Teixeira *et al.*, 2018). The soil sample had a neutral smell. No mouldy or rotten smell was detected. Thus, it was deemed that the amount of organic material present in the soil was negligible and that the soil may be adequate for cob building purposes.

- **Sound**

Attention has to be paid to the sound produced while the soil is rubbed between the fingers. An unpleasant crunchy sound characterizes sandy soils whereas that a smooth sound indicates the presence of clay (Teixeira *et al.*, 2018). A slight crunchy sound was detected when the soil sample was rubbed between the fingers. This indicated the presence of sand but in a suitable proportion.

- **Touch**

To perform this test the soil has to be handled in its present state (without adding water the day the test is performed). If the soil is smooth to squash and sticks to your hand when it is saturated that indicates the presence of clay (Teixeira *et al.*, 2018). The soil sample was relatively smooth but, since it was only in a wet state, it did not stick to the hand (later when more water was added to the soil it did stuck to the hand see the washing test description). On the other hand, when the soil was pressed within the palm of the hand it lumped and conserved the given shape which indicated a moderate amount of clay present in the soil (see Figure 5. 4 (b)). The soil seemed to be satisfactory for its use in the construction of the cob wallettes.

- **Ball cutting**

The ball cutting tests consist on creating a ball with the soil in a humid state and then the ball is cut in half with the help of a sharp knife. Gravels are pick-handed and removed prior to the formation of the ball. Using a knife, cut the ball in half. If the cut surface is mat that indicates the presence of silt. If on the other hand it is shinny that indicates the presence of clay. If there is sand in the mix the surface would be rough (Teixeira *et al.*, 2018).

The result of this test is shown in Figure 5. 4 (c). As can be seen that the cut surface was not smoot, which indicates the presence of sand. A mat surface was identified which may indicate the presence of silt instead of a shiny surface which would have indicated a sufficient clay content. The interpretation of this test's result is in disagreement with other qualitative. Nevertheless, as previously stated, qualitative tests are subjected to the experience and subjectivity of the operator. Evidence found with other tests, i.e. the washing, cigar, ribbon, ball pressing and ball dropping tests, actually confirmed the presence of clay in the sample of soil studied. Furthermore, the soil was used and the construction of the cob wallettes successfully achieved.

- **Cigar**

Once particles bigger than 5 mm are eliminating, a sample of soil is brought into a plastic state. With this material a cigar of roughly 3 cm in diameter is prepared with a length of approximately 50 to 60 cm. The cigar is gently pushed off the edge of a table which will cause the cigar to break into segments. The broken segments are recovered and measured. Segments with a length smaller than 5 cm indicate that the material is a sandy soil whereas

that segments longer than 20 cm indicate a clayey loam (Teixeira *et al.*, 2018). It is considered that a suitable soil for cob construction purposes will present segments of length between 10 and 20 cm.

The length of the segments obtained from the cigar test were close to 15 cm. This indicated the presence of an acceptable content of clay. The results of this tests are shown in Figure 5. 4 (d).

- **Washing**

A humid sample of soil is moulded in the hand. If the soil does not stick to the skin it indicates the presence of a sandy soil. If the soil sticks to your hand but it is easily washed away it indicates the presence of silts. Finally, if it sticks to the hand and it is necessary to rub hard to get rid of it that gives a strong indication of the presence of clay in the sample (Teixeira *et al.*, 2018).

The soil sample tested showed signs of clay content on it. After it was handled in a humid consistency for several seconds it stuck to the hand and it was necessary to rub while washing in order to get it off from the skin (see Figure 5. 4 (e)). This result confirmed the presence of a suitable amount of clay in the soil to be used for cob building purposes.

- **Ribbon**

The ribbon test is used to estimate the plasticity and cohesion of the soil (ASTM International, 2010). A soil sample in a wet state is worked out by hand as to give it a ribbon shape of approximately 2 cm thickness by 15 to 20 cm in length. Half of the ribbon should hang from the hand without breaking in order to consider the soil suitable for earthen construction purposes.

The wet sample of soil allowed the preparation of a ribbon as indicated in the standard. The length of the ribbon hanging from the hand was slightly larger than the recommended size (see Figure 5. 4 (f)). Therefore, this test result indicated that the tested soil was suitable to be used to build the cob wallettes.

- **Ball pressing**

Several balls of roughly 2 cm diameter are rolled out from the soil sample in a wet state. The balls are left to dry for several days in a place protected from the direct sunlight. When the balls are completely dry, dry state estimated after the ball colour turns

completely into a lighter tone, they are pressed between the thumb and the forefinger. Balls made out of a suitable soil for construction purposes should be hard enough not to break with the applied pressure (ASTM International, 2010).

Five balls were prepared with the soil sample tested. None of them broke when subjected to finger pressure after a drying period of 3 days (see Figure 5. 6 (a)).

- **Ball dropping**

The soil sample should be in a wet state. Several balls of about 4 cm diameter are prepared and dropped from a height of approximately 1.5 m. The ball breaking pattern, if it occurs, is observed. If the balls break completely in an explosive pattern that gives an indication that the soil sample contains too much sand for earthen construction purposes. If the balls only get a few cracks and flatten then the soil has too much clay and it would be necessary to add sand to the mix if the soil is intended to be used for cob construction purposes. A satisfactory tests would present a break pattern into 3 to 4 relatively big pieces, which would indicate that the soil may have just enough clay to be suitable for earthen construction purposes (Teixeira *et al.*, 2018).

The results obtained from this test were satisfactory as can be observed from the pictures presented in Figure 5. 6 (b). The three balls tested broke into several big lumps indicating the presence of a clayey soil.

- **Carazas**

The Carazas test is used to study the combination of three different manufacturing processes; pouring, pressing and ramming, with five different soil consistencies; dry, wet, plastic, viscous and liquid. Cubic moulds with 20 by 20 cm dimensions where prepared using all parameter combinations. Furthermore, a second Carazas test was performed to study the effect of adding fibres (wheat straw) to the soil under the different manufacturing and hydric state parameters' combinations. The different parameters when taken in combination give an indication of the soil's suitability for the different building techniques available (cob, adobe, rammed earth, etc.) (Amaco, 2014).

The results obtained from the Carazas test are presented in Figure 5. 7, where the two grids, soil in the top and soil + straw in the bottom, present the different parameter combinations. Detailed views of every manufacturing/hygric state combination are presented from Figure 5. 8 to Figure 5. 17. The fibres provided the mix with more stability and allowed the material to keep its shape by holding the soil particles together. More

importantly, it can be observed from Figure 5. 15 and Figure 5. 16 that the best soil consistency to apply the cob construction technique corresponded to a state between plastic and viscous consistencies as the cubes produced in such states with the pressing manufacturing process were the ones that better kept the mould shape.

- **Others**

Other qualitative tests that are sometimes used and are available in the literature are: the simplified sedimentation test, which gives an indication of the soil particle size distribution (Teixeira *et al.*, 2018); the chewing test, which allows to assess the presence of sand, silt or clay in a soil; the seepage test to estimate the amount of fine particles (Doat, 1979); the disc test, which gives indication of the amount of shrinkage and the dry resistance of the soil (Teixeira *et al.*, 2018); the Habert test used to explore the rheology of the soil (Amaco, 2014); and finally, the Emerson test, which is a quick clay identification test (Doat, 1979). None of these tests were performed in the soil sample tested as it was deemed that sufficient information had been obtained from the rest of qualitative tests presented in this section.

(a)

(b)

Figure 5. 6. Soil qualitative tests part 2; (a) ball pressing test: five ball samples and finger pressure applied after drying, and (b) ball dropping test: balls broke into several relatively big pieces indicating an adequate amount of clay for earthen construction

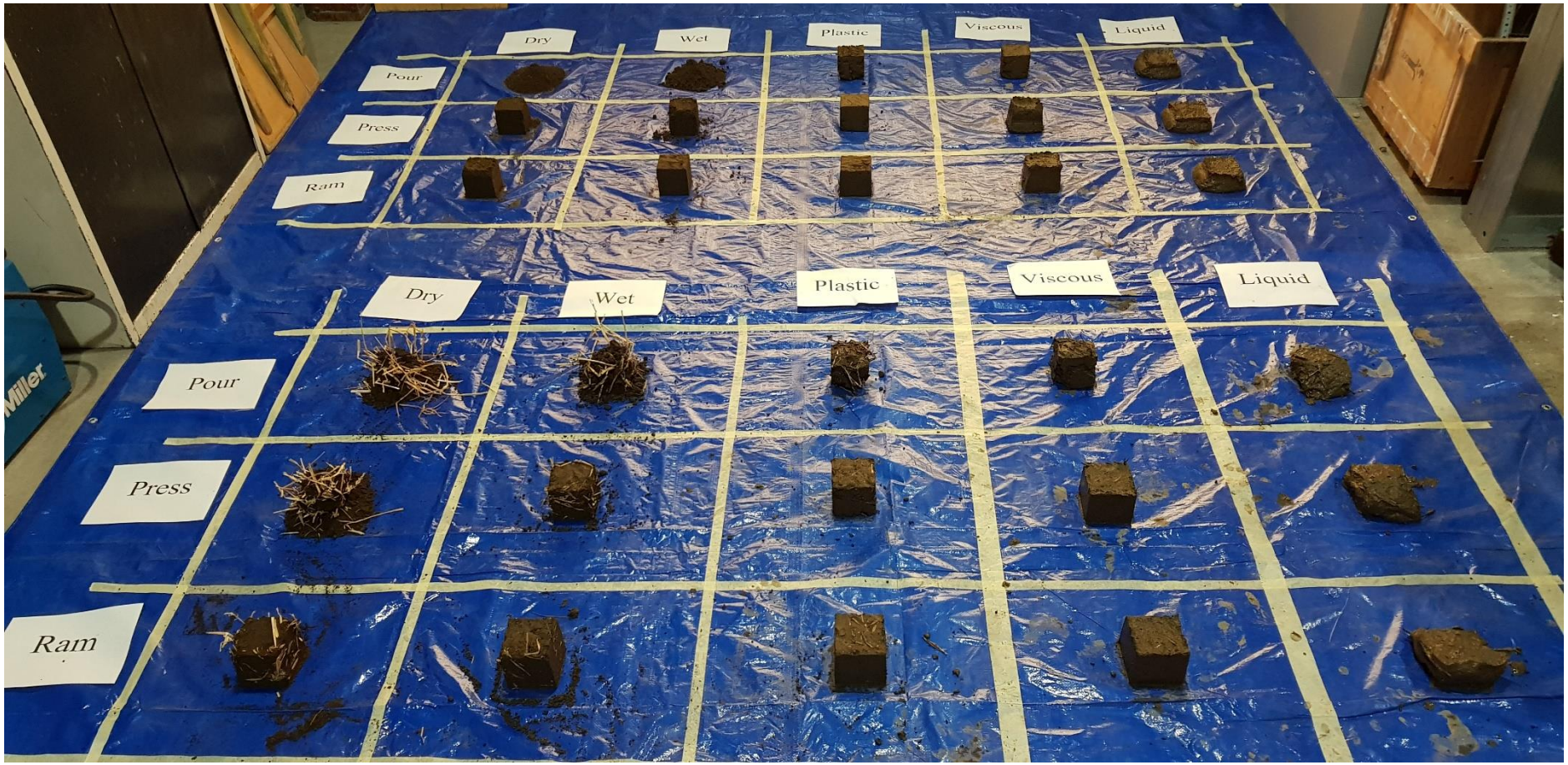

Figure 5. 7. Carazas test overall results.

(a) (b) (c)

Figure 5. 8. Carazas test dry consistency soil: pour (a), press (b) and ram (c).

(a) (b) (c)

Figure 5. 9. Carazas test wet consistency soil: pour (a), press (b) and ram (c).

(a) (b) (c)

Figure 5. 10. Carazas test plastic consistency soil: pour (a), press (b) and ram (c).

(a) (b) (c)

Figure 5. 11. Carazas test viscous consistency soil: pour (a), press (b) and ram (c).

(a) (b) (c)

Figure 5. 12. Carazas test liquid consistency soil: pour (a), press (b) and ram (c).

(a) (b) (c)

Figure 5. 13. Carazas test dry consistency soil + straw: pour (a), press (b) and ram (c).

(a) (b) (c)

Figure 5. 14. Carazas test wet consistency soil + straw: pour (a), press (b) and ram (c).

(a) (b) (c)

Figure 5. 15. Carazas test plastic consistency soil + straw: pour (a), press (b) and ram (c).

(a) (b) (c)

Figure 5. 16. Carazas test viscous consistency soil + straw: pour (a), press (b) and ram (c).

(a) (b) (c)

Figure 5. 17. Carazas test liquid consistency soil + straw: pour (a), press (b) and ram (c).

5.3.2 Soil standardized tests

To classify and determine the basic properties of a soil engineers use a series of standardized tests. The standards followed in this experimental campaign were the BS 1377: Methods of test for soils for civil engineering purposes Part 1: General requirements and sample preparation (British Standard, 2016a), Part 2: Classification tests (British Standard, 1990) and Part 3: Chemical and electrochemical tests (British Standard, 2018a). Based on the data obtained from this standardized tests, the soil was identified and classified in accordance with BS EN ISO 14688 Geotechnical investigation and testing – Identification and classification of soil Part 1: Identification and description (British Standard, 2018b) and Part 2: Principles for a classification (British Standard, 2018c), respectively. Standardized tests were performed on a sample of soil obtained from the 1 m^3 bags delivered by the soil supplier.

In accordance with BS EN ISO 14688 Part 1 (British Standard, 2018b) the soil used in this experimental campaign is identified as an anthropogenic reconstituted soil without reworked natural materials. It was sieved by a 1 cm sieve. Nevertheless, anthropogenic constituents, namely, small pieces of broken glass, were identified while working with the soil. The soil was free of chemical waste and any other dangerous or hazardous substances. No signs of underground heat or combustion were found neither.

- **Loss on ignition**

As few pieces of organic material was identified during the qualitative visual test it was decided to perform a loss on ignition test in accordance with BS 1377 Part 3 (British Standard, 2018a) to estimate the actual organic content in the soil. The loss on ignition test only provides reliable results if applied to peat, organic sand and materials that do not contain minerals that decompose or dehydrate at the test temperature such as clay minerals, calcium carbonate and gypsum.

As no mineralogical test was performed to identify the type of constituent clay minerals of the soil used in this experimental campaign it was not possible to determine whether the test would be reliable or not. In any case, the test was performed and the data obtained is presented in Table 5. 1. An average loss on ignition percentage of 6.55 was found. As its organic content was found to be between 6 to 20 % of its dry mass the soil can be classified as medium-organic in accordance with BS EN ISO 14688 Part 2 (British Standard, 2018c).

Table 5. 1. Lost on ignition tests' data and results.

Sample I.D:	1	2
Mass of Initial Sample m_1 (g):	69.02	69.02
Mass of soil passing 2 mm sieve m_2 (g):	69.02	69.02
Fraction finer than 2 mm (%):	100.0	100.0
Mass of crucible m_c (g):	17.2521	17.0585
Mass of crucible and dry soil m_3 (g):	32.1699	33.5009
Mass of crucible and soil after ignition m_4 (g):	31.1922	32.4218
Loss on ignition as % of soil passing 2 mm (%):	6.55	6.56
Percentage of soil remaining after ignition (%):	93.4	93.4
Average loss on ignition (%):	6.55	

- **Moisture content**

Moisture content, w, is known as the amount of water, expressed as a proportion by mass of the dry solid particles. Moisture content is required as a guide to classification of natural soils and as a control criterion in recompacted soils. Moreover, it is measured on samples used for most field and laboratory tests. The oven drying method is the definitive procedure used in standard laboratory practice. The determination of the moisture content of the soil used to build cob wallettes was carried out in accordance with BS 1377 Part 2 (British Standard, 1990).

The data collected from the tests is presented in Table 5. 2. An average water content of 22 % was determined.

Table 5. 2. Moisture content tests' data.

Sample no.	Tin no.	Tin + wet mass (g)	Tin + dry mass (g)	Tin only mass (g)	Mass of moisture (g)	Dry mass (g)	Water content (%)
Al. 1	S1	1925.3	1716.7	774.3	208.6	942.4	22.1
Al. 2	S2	1511.5	1376.3	759.7	135.2	616.6	21.9

- **Liquid limit, plastic limit, plasticity index, liquidity index and consistency index**

The liquid limit, w_L, is the empirically established moisture content at which a soil passes from the liquid state to the plastic state and the plastic limit, w_P, is the empirically established moisture content at which a soil becomes too dry to be plastic (British Standard, 1990). Both limits provide a means to classify the soil under study. The plasticity index, I_P, of a soil is computed as the numerical difference between its liquid

limit and its plastic limit. Furthermore, the liquidity index, I_L, and the consistency index, I_C, are measures of the consistency of the soil in the remoulded state (British Standard, 2018d).

According to BS 1377 Part 2 from the two types of test available, cone penetrometer and Gasagrande, the former is more satisfactory as it is essentially a static test depending on soil shear strength. The cone penetrometer method is also easier to perform and gives more reproducible results. Thus, the liquid limit of the soil was determined in accordance with BS 1377-2:1990 cone penetrometer method (British Standard, 1990). The plastic limit of the soil was determined in accordance with BS 1377-2:1990 and it was used together with the liquid limit to determine the plasticity index (British Standard, 1990). Figure 5. 18 shows the liquid limit graph and the data obtained from both liquid limit and plastic limit tests is presented in Table 5. 3.

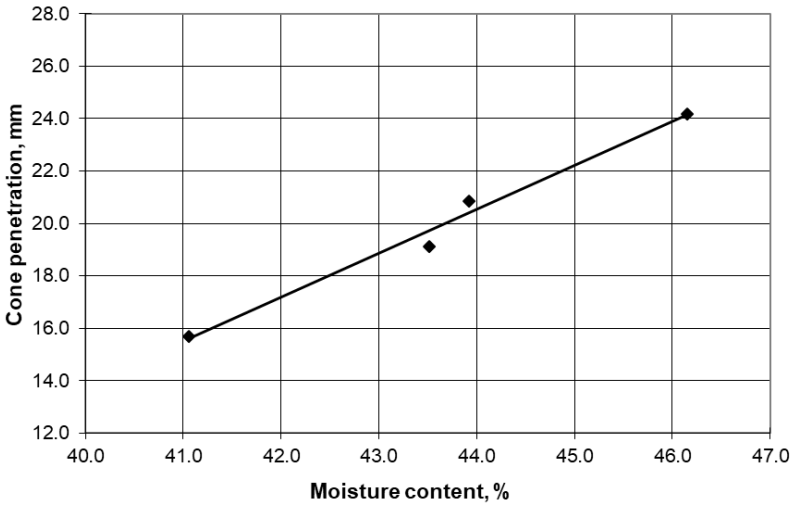

Figure 5. 18. Liquid limit graph.

Table 5. 3. Liquid and plasticity limits tests' data.

	w_{L1}	w_{L2}	w_{L3}	w_{L4}	w_{P1}	w_{P2}
Penetration (mm)	19.2	23.9	21.5	15.9		
Penetration (mm)	18.9	24.7	20.6	15.5		
Penetration (mm)	19.3	23.9	20.5			
Average penetration (mm)	19.1	24.2	20.9	15.7		
Container No.	8	7	9	10	2	4
Mass of tin + wet soil (g)	51.91	53.7	55.19	59.51	33.89	34.33
Mass of tin + dry soil (g)	42.92	43.68	45.12	48.61	31.34	31.66
Mass of tin only (g)	22.26	21.97	22.19	22.06	22.23	22.35
Mass of moisture (g)	8.99	10.02	10.07	10.9	2.55	2.67
Dry weight (g)	20.66	21.71	22.93	26.55	9.11	9.31
Moisture content (%)	43.5	46.2	43.9	41.1	28.0	28.7

The liquid limit is determined as the moisture content correspondent to a cone penetration of 20 mm. It is expressed to the nearest whole number. Thus, from Figure 5. 18 the liquid limit of the soil corresponded to 44 % with a material percentage retained in the 425 μm sieve of 30.6 %. The plasticity limit was determined to be 28 %. Thus, the plasticity index computed as the difference between liquid and plastic limit was equal to 15 %. Finally, the liquidity index and the consistency index were calculated using EQ. 19 and EQ. 20 respectively.

$$I_L = \frac{w - w_P}{w_L - w_P} = -0.4 \qquad \textit{EQ. 19}$$

$$I_c = 1 - I_L = 1.4 \qquad \textit{EQ. 20}$$

In accordance with BS EN ISO 14688 Part 2 (British Standard, 2018c) and based on the plasticity chart shown in Figure 5. 19, the soil used to build the cob wallettes of this experimental campaign can be classified as CIM (Medium Clay). Furthermore, the soil can also be classified as a very stiff clay as its consistency index was greater than one (British Standard, 2018c).

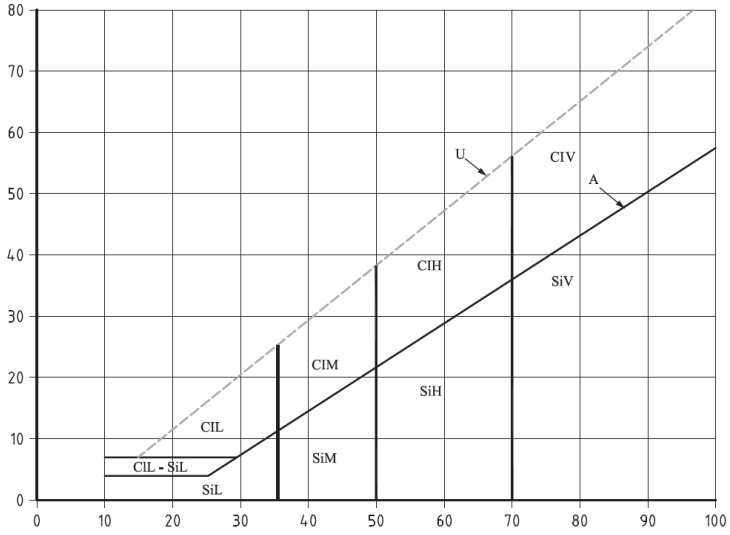

Figure 5. 19. Plasticity chart: w_L values on horizontal axis and w_P values on vertical axis (British Standard, 2018c).

- **Shrinkage characteristics**

To determine the shrinkage characteristics of the soil the linear shrinkage method was applied in accordance with BS 1377 Part 2 (British Standard, 1990). The shrinkage limit is the moisture content below which a clay ceases to shrink. The percentage of linear shrinkage provides a way of quantifying the amount of linear shrinkage likely to be

experienced by clays. The data collected from the tests is presented in Table 5. 4. The average linear shrinkage percentage was found to be 9 %.

Table 5. 4. Linear shrinkage test data.

Sample No:	A	B
Initial length (mm):	140.3	139.2
Oven-dry length (mm):	127.4	126.5
Linear shrinkage (%):	9.19	9.12

- **Density**

The bulk density of a soil, ρ, (expressed in Mg/m^3), is the mass per unit volume of the soil deposit including any water it contains. The dry density, ρ_d, is the mass of dry soil contained in a unit volume. Weight density (unit weight), denoted by γ, is used when calculating the force exerted by a mass of soil, and derived from the mass density using EQ. 21 (in kN/m3):

$$\gamma = g\rho \qquad \textit{EQ. 21}$$

Where g is the acceleration due to gravity (in m/s^2). The density of the soil was determined in accordance with BS 1377 Part 2 (British Standard, 1990). The soil was compacted in a 1.0 litre mould using the Proctor drop hammer with a mass of 2.5 kg and a drop height of 300 mm. The bulk density was determined to be of 1.91 Mg/m3. With a water content of 22.3 % and a dry density of 1.56 Mg/m3.

- **Particle density**

The particle density is also known as the specific gravity of a soil, ρ_s, (also expressed in Mg/m^3). According to BS 1377 Part 2 (British Standard, 1990) the small pycnometer method is the definitive test for soils consisting of clay, silt and sand particles thus that was the method used to determine the particle density of the soil used in this experimental campaign. The method gives only an average particle density for the range sizes of the soil.

The data collected during the tests is presented in Table 5. 5. The water temperature was 20 °C. Therefore, a correction factor of 0.9982 was used. The average particle density was found to be of 2.57 Mg/m^3:

Table 5. 5. Small pycnometer test data.

Pycnometer No:	6	7
Mass of bottle + soil + water (g):	82.036	79.594
Mass of bottle + soil (g):	36.147	34.548
Mass of bottle full of water (g):	75.548	73.295
Mass of bottle (g):	25.541	24.247
Mass of soil (g):	10.606	10.300
Mass of water in full bottle (g):	50.007	49.048
Mass of water used (g):	45.889	45.046
Volume of soil particles (ml):	4.12	4.00
Particle density (Mg/m^3):	2.57	2.57

- **PSD**

To determine the PSD of the soil it is divided into two portions; the coarse and the fine particle fractions. The wet sieving method, considered to be the definitive method applicable to essentially cohesionless soils, was used for the coarse fraction. To determine the size distribution of fine particles the hydrometer method was selected. Combined sieving and sedimentation procedures enabled the plot of a continuous PSD curve of the soil from the size of the coarsest particles down to the clay size particles. These tests were carried out in accordance with BS 1377 Part 2 (British Standard, 1990).

The soil sample total dry mass used for the tests was 411.8 g. From this amount, after wet sieving 296.9 g were retained in the 63 mm sieve and 114.9 g passed through it. The PSD of the retained fraction is presented in Table 5. 6 whereas that the PSD of the hydrometer test is presented in Table 5. 7. Finally, the combined PSD graph is shown in Figure 5. 20.

From Table 5. 6, Table 5. 7 and Figure 5. 20 the D_{60}, D_{30}, D_{10} and D_{50} (the median of the grading curve) of the soil were identified as 0.4250, 0.0630, 0.0018 and 0.3000 respectively. Then using EQ. 22 and EQ. 23 the coefficient of curvature, C_C, and the uniformity coefficient, C_U, of the soil were computed as 5.2 and 236 respectively. Thus, based on its PSD and the values computed of its coefficients, the soil was classified as a well graded soil in accordance with BS EN ISO 14688 Part 2 (British Standard, 2018c). Furthermore, in Figure 5. 21, it can be seen that the PSD of the soil perfectly fits within the upper and lower limits recommended by Keefe (2012) and Jaquing and Augrade (2012).

Table 5. 6. Wet sieve PSD data.

Sieve size (mm)	Weight retained (g)	% Retained	% Passing
10.0	0.00	0.0	100.0
6.3	20.91	5.1	94.9
5.0	16.07	3.9	91.0
3.35	22.55	5.5	85.5
2.00	25.61	6.2	79.3
1.18	24.63	6.0	73.3
0.600	32.88	8.0	65.4
0.425	22.34	5.4	59.9
0.300	30.96	7.5	52.4
0.212	32.17	7.8	44.6
0.150	24.16	5.9	38.7
0.063	44.57	10.8	27.9
Passing 0.063	114.9	27.9	

Table 5. 7. Hydrometer PSD data.

Particle diameter D (mm)	% Finer than D K (%)	Fine/Sed corrected % passing (%)	Corrected % passing (%)
0.0661	51.8	49.5	27.9
0.0466	49.2	47.0	26.5
0.0232	46.6	44.6	25.1
0.0149	41.5	39.6	22.3
0.0130	38.9	37.1	20.9
0.0083	36.3	34.7	19.5
0.0059	33.7	32.2	18.1
0.0041	28.5	27.2	15.3
0.0036	27.2	26.0	14.7
0.0018	18.1	17.3	9.8
0.0015	18.1	17.3	9.8

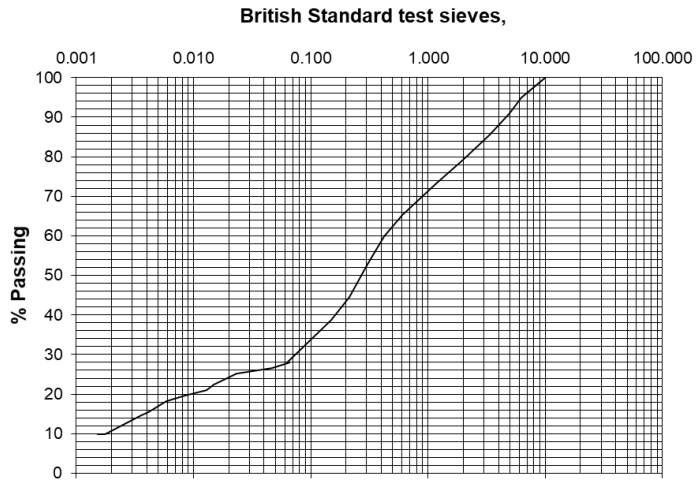

Figure 5. 20. Combined PSD graph.

$$C_C = \frac{D_{30}^2}{D_{10} D_{30}} \qquad \textit{EQ. 22}$$

$$C_U = \frac{D_{60}}{D_{10}} \qquad \textit{EQ. 23}$$

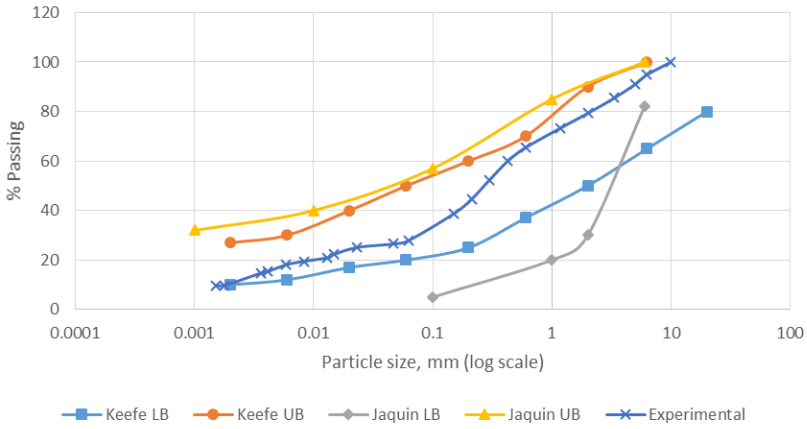

Figure 5. 21. PSD comparison.

As summary, it can be concluded that the soil used was effectively suited for cob construction purpose. Regardless of the soil's relatively high organic content (which was probably the cause why new grass grew from the top of the wallettes after construction, see discussion of section 5.6), its index properties, PSD and relatively low shrinkage percentage, were adequate according to other author's recommendations. Moreover, its suitability was reaffirmed during the mixing of the components and the construction of the wallettes (see sections 5.5 and 5.6, respectively).

5.4 Steel pallets design and fabrication

The cob wallettes were built on top of steel pallets to facilitate their transportation around the laboratory. Moreover, a top cap was also fabricated with the idea of connecting it with the bottom pallet through threated steel bars and applying low compression force during transportation of the wallettes. This was done in order to avoid damaging the wallette due to vibrations that might have led to tensile stresses and therefore the opening of cracks. The steel bottom pallets and top cap were designed using a Universal Beam (UB) 533x210x82 section (this section was selected to accommodate the dimensions of the cob wallettes and of the pallet jack used in the laboratory). The bottom pallets were perforated at four locations of their flanges to allow the pallet jack to go beneath them. On the other hand, four C-channel section segments were welded to the web of the top cap to act as points of attachment and provide symmetric points of attachment for the crane's chains, thus allowing the lifting of the wallettes. Finally, four pieces of hollow steel tube were welded to both bottom and top UB flanges to provide the points of connection of the threaded bars. Detailed drawings of the bottom steel pallets and top steel cap are provided in Figure 5. 22 and Figure 5. 23 respectively.

A 3D linear elastic FEM analysis was performed in ABAQUS to verify the suitability of the selected UB section in terms of stresses. The properties of the steel (S275) are presented in Table 5. 8 and the dimensions of the UB 533x210x82 section in Table 5. 9. A factored load of 16 tons was assumed to be applied in a central section of 0.4 m^2, which represented the area that would be occupied by the cob wallette, perpendicular to the web of the UB section. This load was adopted as a rough estimation of the force that would be needed to cause the yielding of the cob wall , which had a 0.4 m^2 cross section and an assumed compressive strength of 1.56 MPa ($f_y = 0.3f_c$). This value of load was not to be exceeded at any time during the experimental campaign, thus, its assumption would gave us enough margin of safety. Regarding the boundary conditions adopted the bottom edge of the flange was considered as simply supported whereas that a double symmetric boundary condition was used along the neutral axes of the UB section to reduce the model's size.

Table 5. 8. S275 Mechanical properties.

Property	Value

Self-weight (kg/m^3)	7850
Young´s modulus (N/m^2)	210x10^9
Poisson´s ratio (-)	0.3
Yield strength (N/m^2)	275x10^6

Table 5. 9. UB 533x210x82 section dimensions.

Dimension	Value (mm)	Sketch
D	528.3	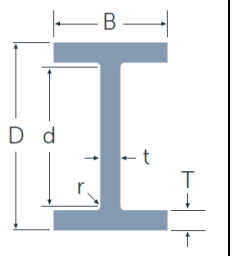
B	208.8	
t	9.6	
T	13.2	
r	12.7	

The steel pallet's vertical displacements and Von Mises stresses are shown in Figure 5. 24 and Figure 5. 25 respectively. As the maximum stresses developed due to the factored load applied to the UB section did not exceed the yield strength of the material and the vertical displacement at the centre of the UB section's web was relatively small (maximum displacement of only 0.7 mm as shown in Figure 5. 24) is was considered that the proposed section was adequate to support the cob wallettes. The experiment's success confirmed that the section was adequate.

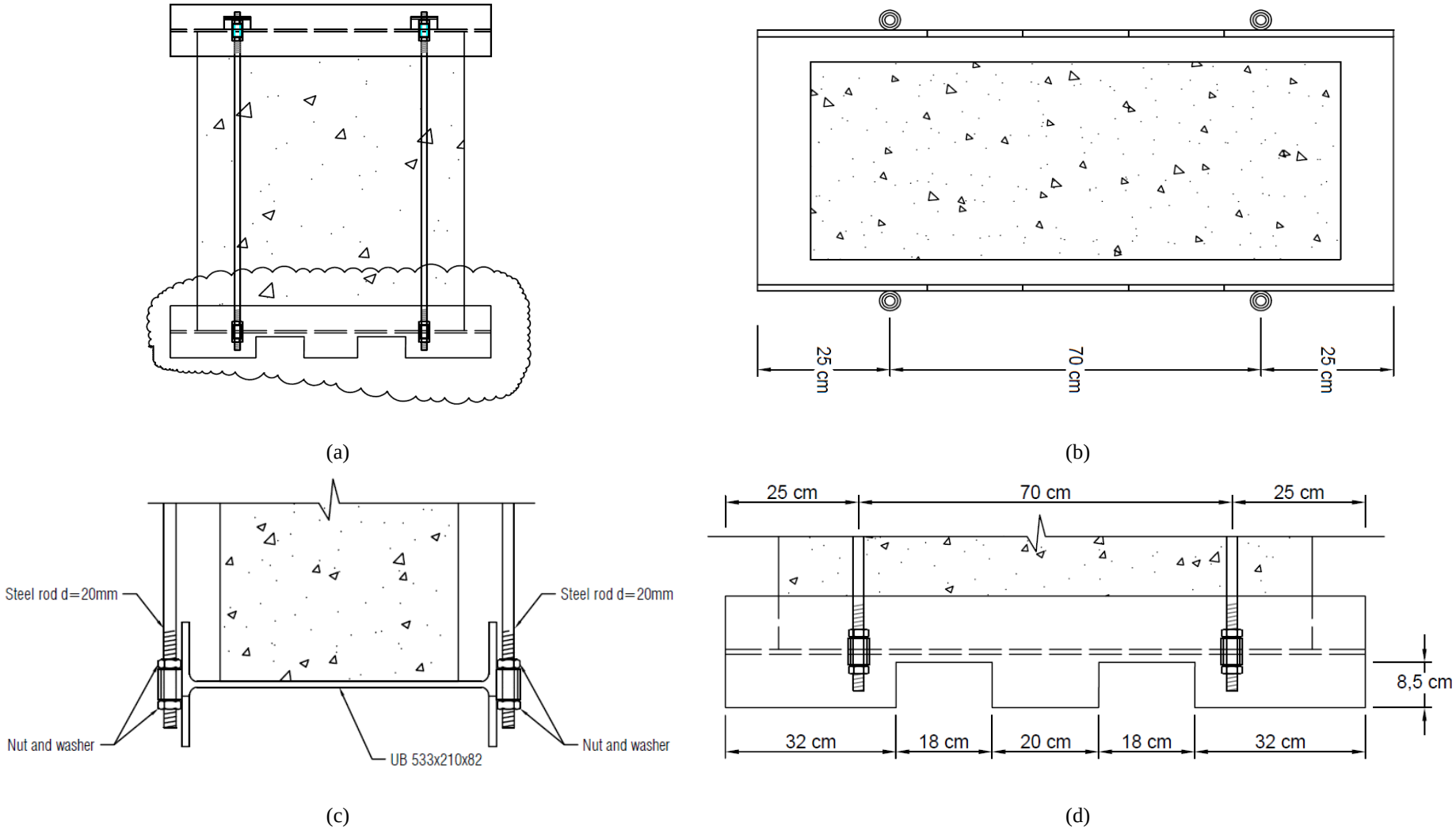

Figure 5. 22. Bottom pallet (a) general sketch, (b) top view, (c) side view and (d) front view.

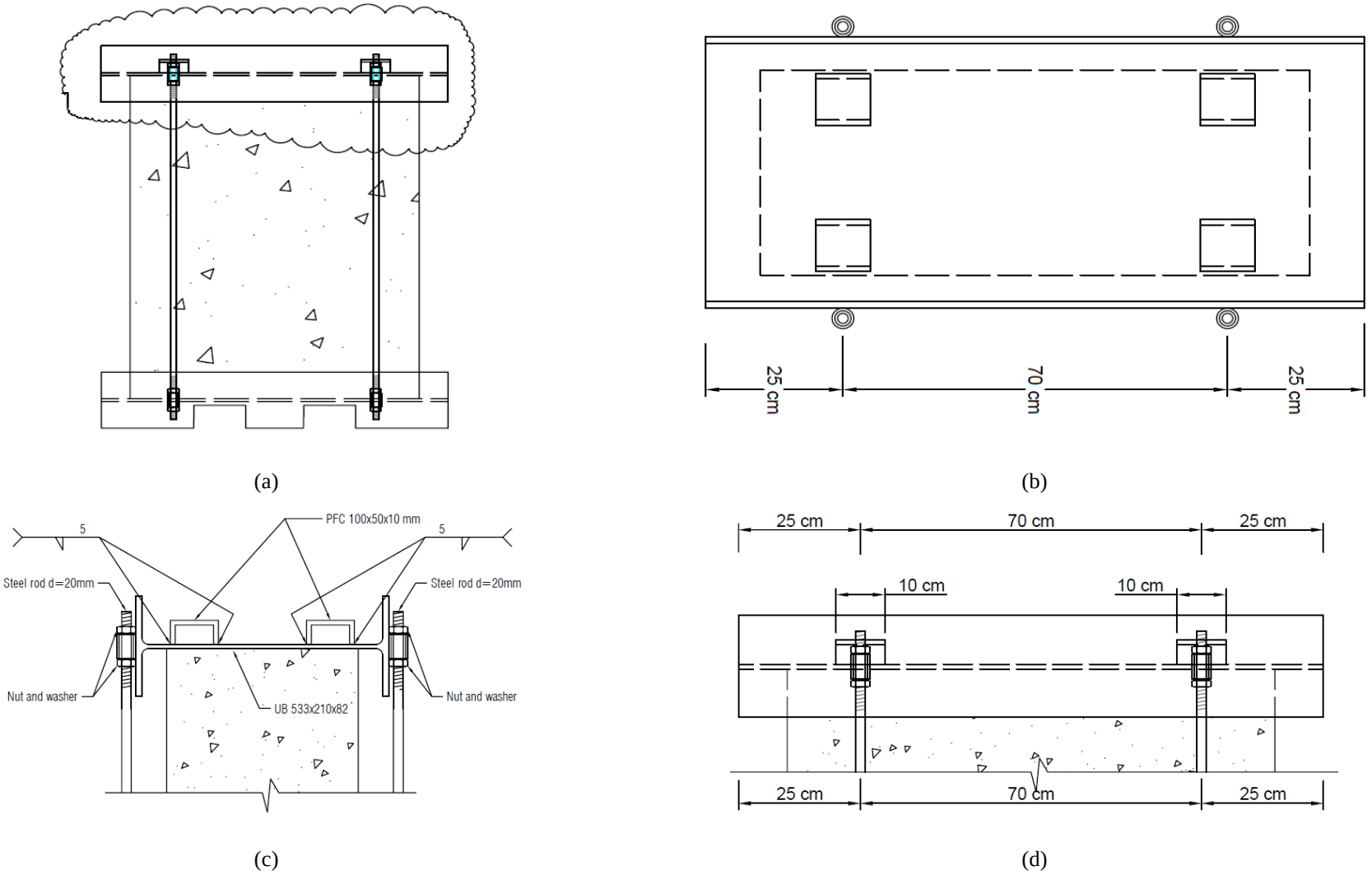

Figure 5. 23. Top cap (a) general sketch, (b) top view, (c) side view and (d) front view.

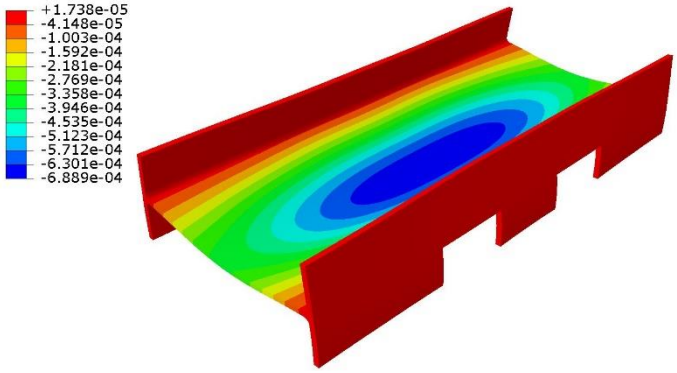

Figure 5. 24. Steel pallet's vertical displacements, m.

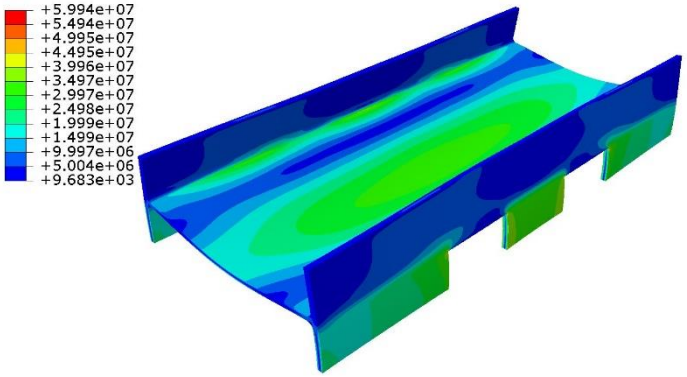

Figure 5. 25. Steel pallet's Von Misses stresses, Pa.

5.5 Cob mixing

The components' mixing proportions were based on recommendations given by several authors (Macdonald and Doyle, 1997, Watson and McCabe, 2011, Hamard *et al.*, 2016, Teixeira *et al.*, 2018) and adopted to the physical constrains of the laboratory of CSEE in TCD. The available space for mixing was approximately 5 m by 5 m. The dimensions of the tarpaulin were roughly 2 m by 3 m and it was realized that a mix of approximately 100 kg could be handled by a single person. Therefore, mixes of 80 kg of soil with 1.2 kg of straw and 12 kg of water were adopted. Each one of the mixes provided enough material to build a layer of approximately 10 cm thickness. Thus, in average, 10 mixes were necessary to build each one of the wallettes with approximate dimensions of 100 cm length by 100 cm height by 40 cm thickness.

The first step was to place the soil on top of the plastic tarpaulin (see Figure 5. 26 (a)). Then the soil was spread leaving a sort of crater at the centre (see Figure 5. 26 (b)). Water was poured inside the hole (see Figure 5. 26 (c)) and the soil was mixed with the

feet tamping on top of it and by using the tarpauling to roll it sideways until it was brought to a viscous consistency (see Figure 5. 26 (d)). After this, straw was added loosely all over the spread viscous mix (see Figure 5. 26 (e)) and tamped by foot until it was lost within the soil. Then, the tarpaulin was used to roll the loam (see Figure 5. 26 (f)) and more tamping was done. Rolling and tamping was repeated several times until a homogeneous consistency was obtained.

The whole mixing process took around 30 minutes per mix when a single person was performing the task. This time was reduced to approximately 20 to 25 min when two people performed the task. When bigger groups of people participated in the task the amount of material was increased to 100 kg and 120 kg of soil and applying respectively increments to the amount of straw and water used in order to keep the proportions constant with respect to the original ratios.

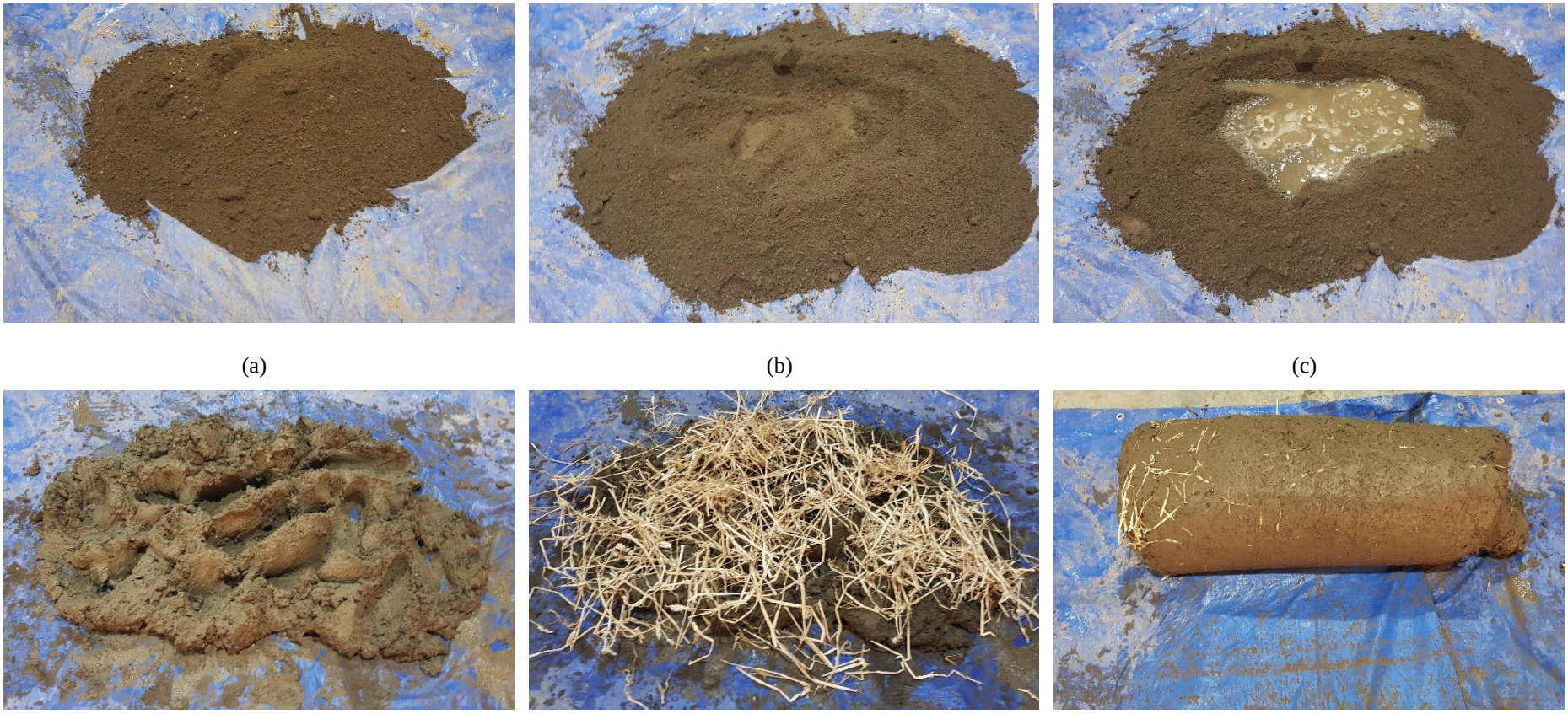

(a) (b) (c)

(d) (e) (f)

Figure 5. 26. Cob mixing process: (a) soil poured in top of the tarpaulin, (b) a hole is made in the middle of the soil, (c) water is poured in the created hole, (d) the water/soil combination is mixed until it is brought to a viscous consistency, (e) straw is added while the loam is constantly mixed and (f) the tarpaulin is used to role the mix and allow a thorough mixing of all the components, the final mix is considered to be ready when it acquires a plastic consistency and all components are well mixed.

5.6 Wallettes construction

The number of wallettes needed to obtain statistically significant results from the flat jack tests was estimated based on the values reported by Miccoli *et al*. (2014) regarding the mean (1.59 MPa) and SD (0.03) of cob's compressive strength. Adopting a confidence level of 95 % (significance level $\alpha = 0.05$) for a two-sided Confidence Interval (CI) (it was not known whether the test would over or under estimate the compressive strength of cob) whose margins of error (0.06) corresponded to two standard deviations a minimum sample of size of four was needed. This number was obtained using the statistical software Minitab (Minitab, 2013). Nevertheless, due to the great level of variability present when working with natural materials in a non-standardized way and since no previous experience with the technique nor the material was available, it was decided to build six cob wallettes to allow for mistakes in the execution of the test caused by human error and/or any other unforeseen problems.

The construction process took place between the 6th and the 20th of December 2018. The dimensions of the wallettes were of 100 cm length, 100 cm height and 40 cm thickness. They were built in three lifts, 30 cm, 30 cm and 40 cm height respectively. All dimensions varied by +/- 2 cm due to the inherent variability traditional construction process adopted.

Once the loam was ready it was divided into balls of approximately 20 to 30 cm in diameter (see Figure 5. 27 (a)). The balls were thrown to the steel pallet to build the first 10 cm layer of the first 30 cm lift of each one of the wallettes (see Figure 5. 27 (b) and (c))). Balls were thrown being careful to assure overlapping with previous balls and moulded with the fingers to try to fill all voids (see Figure 5. 27 (d)). The lifts were built a couple of cm bigger than the marked area of 0.4 by 1.0 m on the steel pallets with the aim of avoiding having any holes or cavities at the faces after the pairing of the surfaces. Once the bottom lifts achieved the desired height their top surface was marked with the fingers in order to create holes that would improve the interlocking with upper lifts (see Figure 5. 27 (e)).

The pairing of each one of the wallettes' lifts was done four or five days after their construction (see Figure 5. 27 (f)) and before adding the next lift on top of them. A timber saw was used to remove the extra material protruding from the faces and a bubble level

was used as guidance to achieve verticality (as accurate as realistically allowed by the traditional technique implemented) of the wallettes' faces. After the first lift was paired (see Figure 5. 28 (a)) the second lift was added ensuring that extra material would protrude over the sawn faces. Furthermore, the top surface of the second lift was also finger-marked to ease the interlocking of the last lift (see Figure 5. 28 (b)). Again, after a short drying period (4 or 5 days) the second lift was paired using the timber saw and the bubble level (see Figure 5. 28 (c)). Next, the last lift was added (see Figure 5. 28 (d)) and subsequently paired. Figure 5. 28 (e) shows the six finished wallettes on top of their bottom steel pallets that were stored indoors for a drying period of 4 months under uncontrolled environmental conditions.

A problem was faced while pairing upper lifts. It was noticed that since the bubble level was used to guide the cutting, the upper layers ended up being thicker than the original dimensions of the wallette. This could be due to two different factors. The first one was related to human error. If the first layer was not paired properly, in other words, if the first lift was smaller or bigger than the original dimensions (1.0 by 0.4 m) the error was carried to the upper lifts as the bottom lift was used as reference. This error could give either bigger or smaller sections. The second error had to do with the fact that upper layers that were built on top of the bottom lift induced vertical shortening and transversal bulging. Thus, as the bottom lift was used as reference to cut the upper lifts, the section became bigger than intended. This effect was almost negligible for the second lifts as the sections obtained had an error of +/- 1 cm. On the other hand, the bulging effect on the first lift, as the weight of the second lift has been added, was more obvious while cutting the third lift, and the obtained error were of +/- 2 cm.

Another problem appeared while finishing the corners. These parts of the wallettes were especially weak and, while pairing the faces, small pieces of material popped out of the wall. Even when the material at the corners stayed in place it was obvious that this part of the wallettes was not as solid as the middle or centre parts.

A curious phenomenon was observed after a few days after the building completion of the wallettes. A kind of whitish moss appeared in the surfaces of wallettes and new grass started to grow from their top (see Figure 5. 28 (f)). Both organisms disappeared after a period of few weeks as the wallettes got progressively drier.

(a) (b) (c)

(d) (e) (f)

Figure 5. 27. Wallettes' construction process part 1: (a) the cob mix is divided into balls, (b) and (c) balls are thrown in top of the steel pallet to create a roughly 10 cm thickness layer, (c) more layers are added in top of the first one until the lift height is reached, (e) top surface of the lift is finger-marked to improve interlocking with upper lifts and (f) the lift is paired with a timber saw to create a "straight" surface.

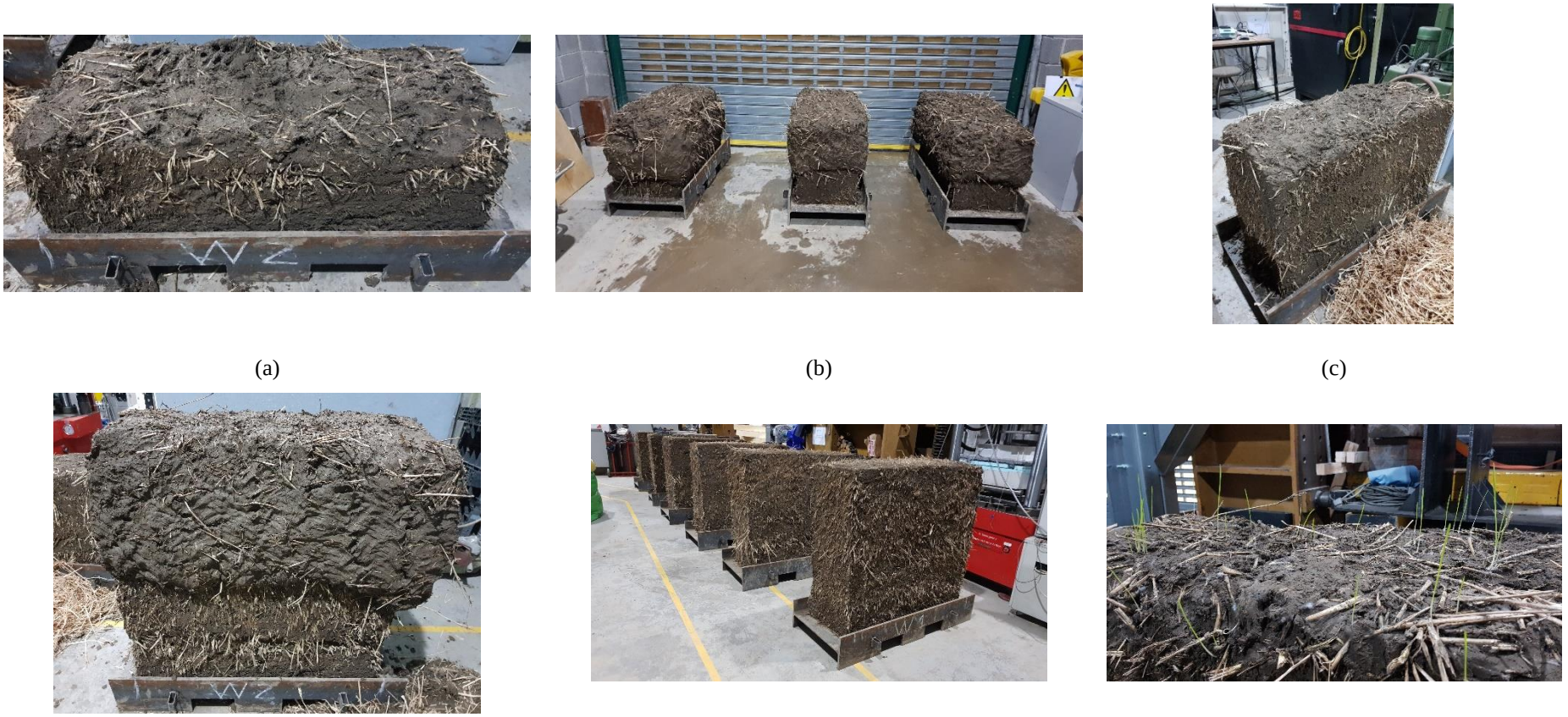

(a) (b) (c)

(d) (e) (f)

Figure 5. 28. Wallettes' construction process part 2: (a) the first lift was paired, (b) second lift was added, (c) second lift was paired, (d) third lift was added and subsequently paired, (e) six finished wallettes built in top of the steel pallets stored indoors for drying and (f) appearance of moss and new grass growth after a few days from the construction completion date.

5.7 Wallettes capping

To ensure a horizontal top surface and consequently an even distribution of the compressive load the wallettes were capped with a layer of cement mortar. Timber formwork was clamped to the wallettes and levelled with the help of a bubble level (see Figure 5. 29 (a)). The cement mortar was placed on top of the wallette (see Figure 5. 29 (b)) and levelled with a straight piece of timber (see Figure 5. 29 (c)). The finished surface was completely flat (see Figure 5. 29 (d)) and cured for several days with the application of a wet hessian cloth (see Figure 5. 29 (e)). Finally, the formwork was removed after the curing period. Figure 5. 29 (f) shows the capping of one of the wallettes after the formwork removal.

Two cubes were prepared with a sample of the mortar in order to determine the mechanical properties of the mortar. The cubes were prepared and cured in accordance with BS EN 12390 Part 2 (British Standard, 2009a) and tested in accordance with BS EN 12390 Part 3 (British Standard, 2009b). The compressive strengths of the two cubes were 34.7 MPa and 32.8 MPa. The average compressive strength of the cubes was of 33.75 MPa with a SD of 1.344 MPa and a COV of 3.98 %.

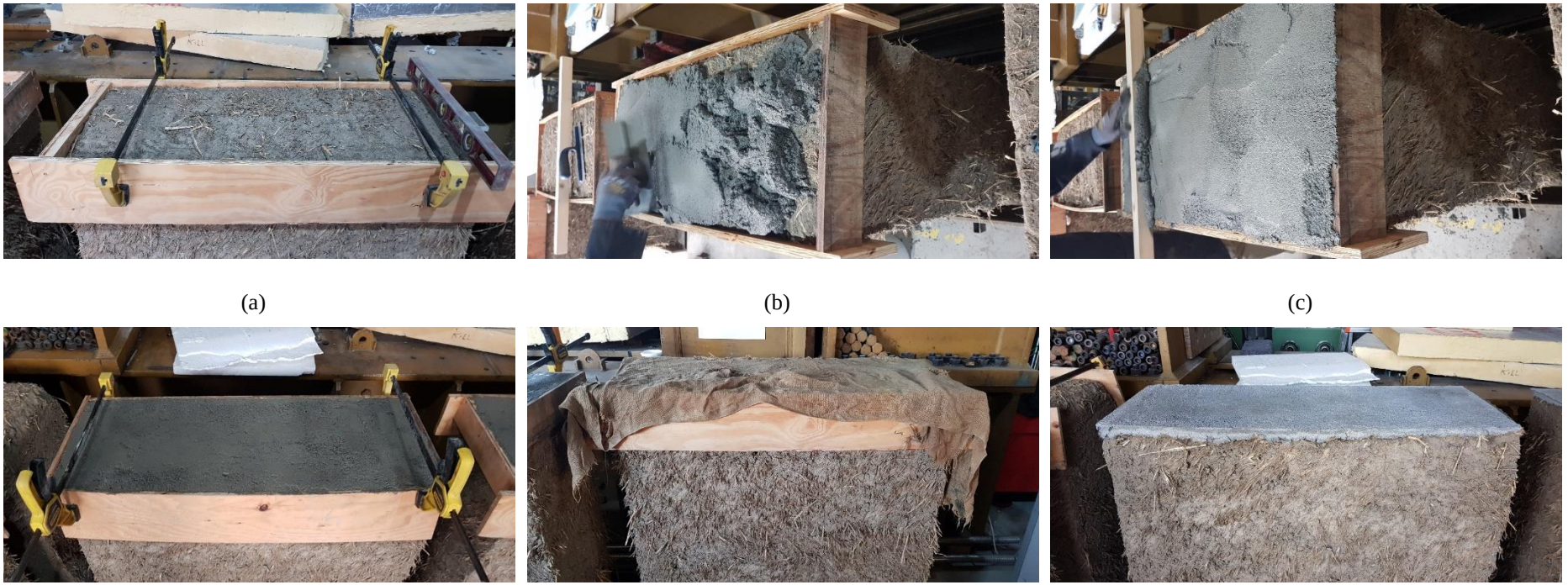

(a) (b) (c)

(d) (e) (f)

Figure 5. 29. Wallettes' capping process: (a) formwork levelling, (b) cement mortar placing, (c) cement mortar levelling, (d) surface finishing, (e) cap cutting and (f) removal of formwork.

5.8 Cob cylinders

Six cylinders were prepared, using randomly sampled material from the cob wallettes' mixes, with two objectives; to monitor the drying of the material and to perform compressive tests on them to estimate cob's compressive strength. This data would give a point of reference to establish the consolidation and test loads to be applied to the wallettes. The cylinders were prepared using 15 cm diameter by 30 cm length steel moulds. The mould was filled with six or seven layers of cob. Every layer was tamped by hand, pressing with the fingers to try to fill all the voids. This preparation procedure is similar to the one implemented by Pullen and Scholz (2011). The cylinders preparation dates are presented in Table 5. 10.

Table 5. 10. Cob cylinder's preparation dates.

Cylinder	Date
1	07/12/2018
2	11/12/2018
3	12/12/2018
4	13/12/2018
5	14/12/2018
6	17/12/2018

The six cylinders that were prepared, (see Figure 5. 30 (a)) were kept under similar conditions to the cob wallettes (uncontrolled environment protected from rain and wind). The density of the cylinders was monitored for a period of eight weeks, from the last week of December 2018 until the second week of February 2019, by which time it was observed that the density was maintained roughly constant. It was observed that cylinders dried at a much quicker pace than the wallettes due to their relatively bigger free surface/volume ratio. Therefore, it was not possible to use the cylinders' density as an estimation of the correspondent drying of the wallettes.

As the cylinders dried, they suffered shrinkage and their dimensions changed. Therefore, cylinders' diameters (see Figure 5. 30 (b)) and lengths (see Figure 5. 30 (c)) were measured weekly to calculate their volumes. After this drying period under uncontrolled environmental conditions, the cylinders were subjected to a period of 24 hours of drying in an oven at 60° C. This was undertaken to estimate their dry density (see Figure 5. 30 (d)).

The monitored density of the cylinders is presented in Figure 5. 31. A quadratic regression line with a coefficient of determination, R^2, of 0.9767 was fitted to the density data. Unfortunately, the equation was not suitable to be used to predict the cob wallettes' drying due to their different free surface/volume ratios.

The data collected from the cylinders after the 24 hours period in the oven at 60° C is presented in Table 5. 11. The average dry density was computed to be 1341.79 kg/m^3 which is slightly lower that the density of the cylinders after eight weeks under uncontrolled environmental conditions.

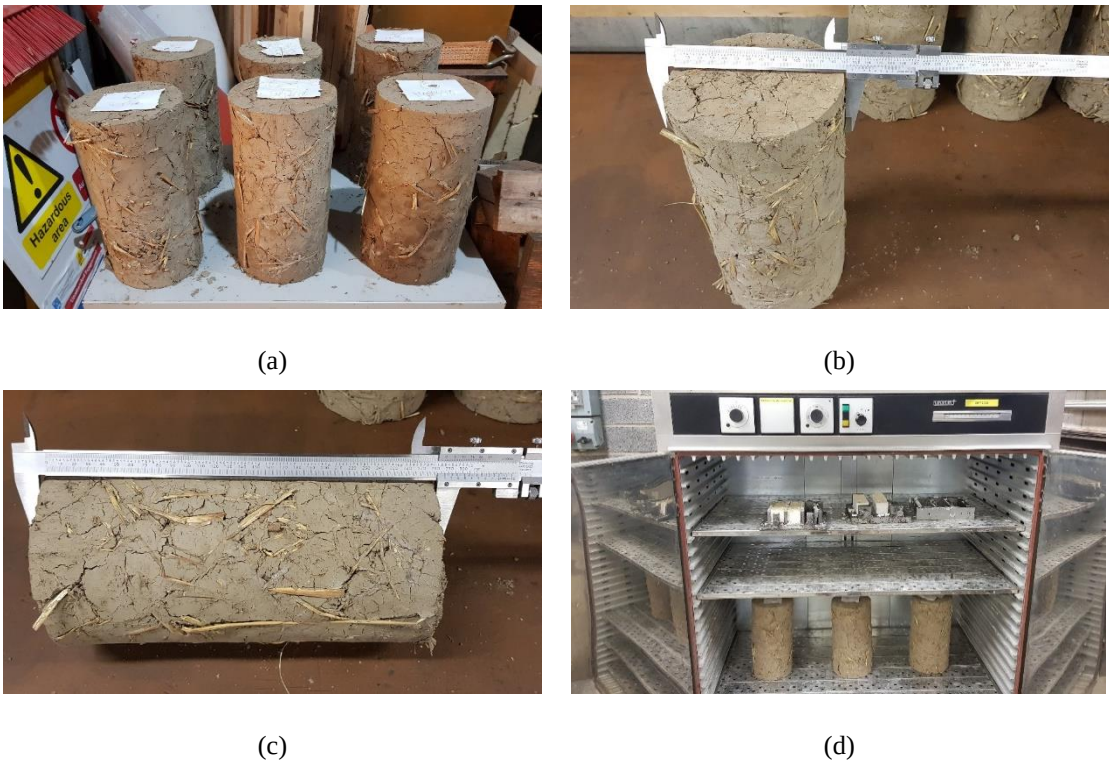

Figure 5. 30. (a) Cylinders' storage in the laboratory, (b) measurement of cylinders' diameter, (c) measurements of cylinders length and (d) oven drying of cylinders.

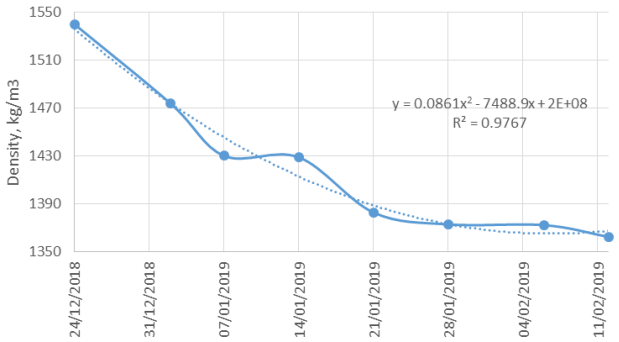

Figure 5. 31. Monitored cylinder's average densities.

Table 5. 11. Dry density of cob cylinders.

Date	Cylinder	Weight (kg)	Diameter (cm)	Height (cm)	Density (kg/m3)	Average Density (kg/m3)
After 24 h in oven at 60 °C	1	6.36	14.8	28.2	1310.98	1341.79
	2	6.27	14.6	27.6	1356.95	
	3	6.04	14.8	28.1	1249.45	
	4	6.47	14.5	28.6	1369.97	
	5	6.52	14.6	28.1	1385.94	
	6	6.48	14.6	28.1	1377.44	

The cob cylinders' top and bottom faces were levelled with the use of Neoprene 60 shore disks of 13 mm thickness placed inside loading stainless-steel plates. The testing machine used was a model Awick 1474 Universal T. M., equipped with a PID actuator control system, which allowed the compressive tests to be carried out under either force control or displacement control. Cylinders 1, 2 and 3 were loaded at a 100 N/s rate until a loss of 50 % force was detected. On average the compressive test of every cylinder took 3 minutes. Cylinders 3, 4 and 5 were loaded under displacement control to try to better capture the post-peak behaviour of the stress/strain curve. Thus, a displacement rate of 15 mm/min was applied for 3 minutes to the last three cob cylinders.

The data collected from the cob cylinder's compressive tests is presented in Table 5. 12. The testing set-up is shown in Figure 5. 32, along with an image of one of the cylinders after the test had finished where the damage to the cylinder can be observed. Figure 5. 33 (a) and Figure 5. 33 (b) present the cob cylinder's stress/strain and the stress/strain envelope curves respectively, whereas the failure modes of each one of the cob cylinders can be observed in Figure 5. 34. The Young's modulus of the material was estimated as the slope of the stress/strain curve's linear segment. The linear elastic segment was considered between the levels of stress correspondent to 0.05 and 0.30 of the maximum stress.

(a) (b)

Figure 5. 32.Cob cylinders (a) setup and (b) failure after test.

The average cob cylinders' compressive strength was 0.697 MPa with a SD of 0.083 and a COV of 11.91 %. The compressive strength value obtained was very similar to that reported by Pullen and Scholz (2011) of 102 psi (0.703 MPa). As the cob cylinders tested in this experimental campaign were prepared using a similar cob mix it is not surprising that the COV value was only half of that reported by these authors (22 %).

No obvious visual differences were observed between stress/strain curves of the load controlled and displacement controlled tests. Furthermore, after a mean comparison t-test of the two groups was performed with a confidence level of 95 % and a null hypothesis $H_0: \mu_1 - \mu_2 = 0$, a P-Value of 0.763 was found for the compressive strength means and a P-Value of 0.661 for the Young's modulus means (both 95 % CI included 0) which led to the acceptance of the null hypotheses. This proved that there was not a statistically significant difference between the means of the compressive strength nor the means of the Young's modulus of the two groups.

A linear curve segment can be identified just after a small seating segment and an average stress of 0.20 MPa. This value corresponded to roughly 30 % of the determined compressive strength of the cob cylinders. Similar elastic range percentage values were reported by Miccoli *et al*. (2017). After this value of stress, the curves followed a non-linear stress/strain relationship until reaching their peak strength and consequently a reduction of the stress was observed. The drop of stress in the curves followed more

closely a typical concrete failure (brittle failure) rather than the gradual loss of capacity reported by Miccoli *et al.* (2014) after their compressive tests on cob wallettes. A logical explanation for this different post-peak behaviour may be the relation between fibre length and specimen size. Straw fibres can be idealized as the steel rebar in reinforced concrete (Pullen and Scholz, 2011), they provide cob with its tensile strength. If the fibres are relatively long in comparison with the size of the element, as it is the case of the cylinders tested, there would not be enough material to develop a good bond between fibres and soil particles, consequently the contribution of the fibres to the tensile strength of the cob, and to its ductility, would be relatively small in comparison to the tensile strength provided by fully bonded fibres in larger cob specimens.

The Young's modulus of the cob cylinders was estimated as the slope of the stress/strain curve segment between 5 and 30 % of their correspondent compressive strength. The upper limit selected was the elastic limit value reported by Miccoli *et al*. (2017) and was confirmed visually from Figure 5. 33 whereas that the lower limit was selected only on the basis of visual estimation where the seating effect seemed to have disappeared (a value of 5 % of the peak strength was also used, as the low limit value of the stress/strain curves, to estimate the Young's modulus values reported by them). The average Young's modulus was computed as 22.10 MPa with a SD of 5.38 MPa and a COV of 24.35 %. This value is considerably lower in comparison with the values reported by Miccoli *et al.* (2014) as well as other authors (Minke, 2000, Ziegert, 2003). Nevertheless, it should be considered that different mixes as well as different methods to estimate the material Young's modulus were implemented by those authors and in this thesis (see Table 2. 7).

The strains presented in Figure 5. 33 are the total strains of the tested specimens (obtained by taking into account the relative displacement between loading plates). Even though it has been established that the friction forces developed between the cylinders' top/bottom faces and the loading plates affect the mechanical response of the specimens (Aubert *et al.*, 2016, Laborel-Preneron *et al.*, 2016), two main factors prevented the measurement of strains at the middle third of the specimens. The first one was related to the problem of finding an adequate substance that would glue the strain gauges to the cob cylinders' walls. The substance had to be strong enough to ensure a perfect attachment of the strain gauge to the cylinders' walls and at the same time flexible enough to directly transfer the deformation of the specimen to the measuring device. This problem was also

faced by Lombillo (2010) for the testing of rammed earth cylinders during his experimental campaign and was even more drastic in the case of cob cylinders due to their uneven and dusty faces' nature. This problem may be solved in future tests by implementing a displacement measuring contactless system, i.e., photogrammetric analysis (Miccoli *et al.*, 2014) or optical extensometers (Vinceslas *et al.*, 2018), which may allow to obtain a better estimate of the strains at the middle third of the cylinders. The value used as reference in this experimental campaign for cob's Young's modulus was the one estimated from the consolidation process of the wallettes (see section 5.10). The second factor that prevented the gluing of strain gauges was the fact that when cob deformed, pieces of straw would pop out (see Figure 5. 32 (b)), consequently leading to the detachment or even damage of the strain gauges.

The Young's modulus values estimated from the cob cylinders compression tests reported in this thesis are not completely accurate. Since the stress state at the top and bottom faces of the cylinders is different to the stress state at the middle third of the specimen, this is caused by the lateral displacements constraint provided by the steel plates in contact with the cob cylinder, the maximum strains, and consequently the failure of the specimens, occur at their middle third. The fact that the strains were computed by dividing the relative displacement between the steel plates divided by the total length of the cylinder results in an over estimation of the material's Young's modulus value. Furthermore, no transversal strains were measured and it was not possible to estimate Poisson's ratio of the cob cylinders.

A new laboratory procedure has been developed by Vinceslas *et al*. (2018) in which they deal with the problematic previously described in this section. They have studied the standardization of the specimen's preparation by applying a Proctor protocol, which may reduce the variability of the material mechanical properties associated to a non-standardized method of preparation. On the other hand, a standardized preparation may not be representative of traditional construction methods implemented by vernacular builders and the results obtained with the method proposed by those authors may not be useful for the study of historical cob buildings. Cob's Young's Modulus was estimated by these authors after a three-loading cycle during which deformations were measured using extensometers in the middle third of the specimens. The use of extensometers may provide an accurate measurement of the middle-third deformations and consequently a better estimate of Young's modulus could be calculated. Attention should be paid to the

measuring range capacity of the device to be sure it does not get damaged, as cob would certainly develop relatively large deformations, in comparison to concrete cylinders for example, before reaching its peak strength. Vinceslas *et al*. results were published in parallel to the development of this experimental campaign and it was not possible to adopt their recommendations.

Table 5. 12. Cylinders compressive tests summary results.

Cylinder	Average diameter (cm)	Average length (cm)	Area (m2)	Maximum load (N)	Compressive strength (MPa)	Young's modulus (MPa)
1*	14.73	28.03	0.0170	9992.30	0.586	18.71
2*	14.65	27.67	0.0169	12782.91	0.758	27.26
3*	14.70	28.00	0.0170	13284.59	0.783	15.36
4**	14.50	28.50	0.0165	10243.75	0.620	18.25
5**	14.62	28.23	0.0168	11236.57	0.670	24.57
6**	14.52	28.07	0.0166	12635.15	0.763	28.46
Mean	14.62	28.08	0.0168	11696.00	0.697	22.10
SD	0.095	0.275	0.0002	1401.00	0.083	5.38
COV (%)	0.65	0.98	1.30	11.98	11.91	24.35

*Load control. **Displacement control

The visual evaluation of the failure pattern of the cylinders was quite challenging since, as it can be seen in Figure 5. 34, no clear pattern could be identified. When the piston of the machine initially got in contact with the top steel plate a small jump was observed which indicated the seating of the steel plates and neoprene disks (the initial points of the stress/strain curve, up to approximately 5 % of the peak strength, discussed previously corresponded to this initial contact and seating of the experimental setup). After this seating movement no change was visually detected in the cylinders and the stress/strain curves presented a linear variation. After reaching a stress value of roughly 0.20 MPa the stress/strain curves developed a non-linear segment and it was possible to observe a small vertical movement of the piston and the top steel plate in the testing machine. Small cracks appeared at during this period of the test and some straw fibres detached from the surface and cause the crumbling of some soil particles. After the material reached its peak stress the stress/strain curves developed a softening segment and the identification of the cracks in the specimens was visually clear. The load controlled tests were stopped when a drop of the force of 50 % was detected whereas that the displacement control tests were stopped after 3 minutes. After lifting the piston, the specimens were removed from the loading machine and the loading plates were removed from the cylinders' top and bottom faces to inspect them in more detail. As can be seen

in Figure 5. 34, the top third of the six cylinders was pretty much detached from the bottom two thirds of the specimens. This is considered to be a satisfactory failure pattern in accordance with BS EN 12390 Part 3 (British Standard, 2009b).

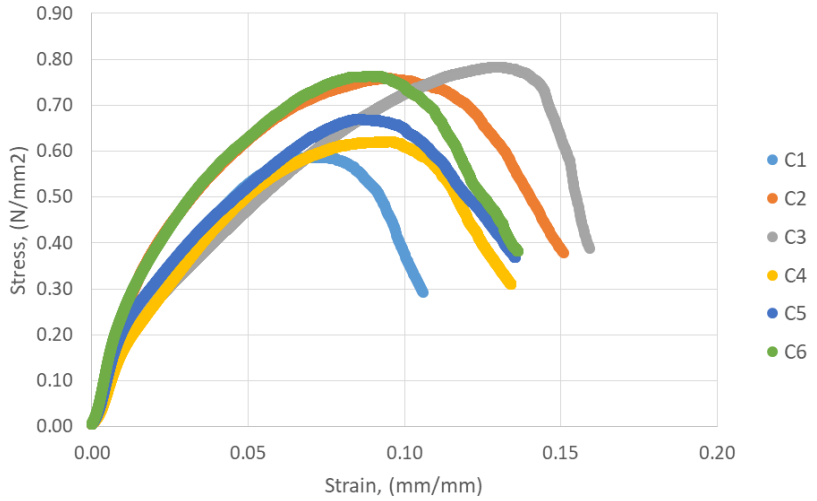

(a)

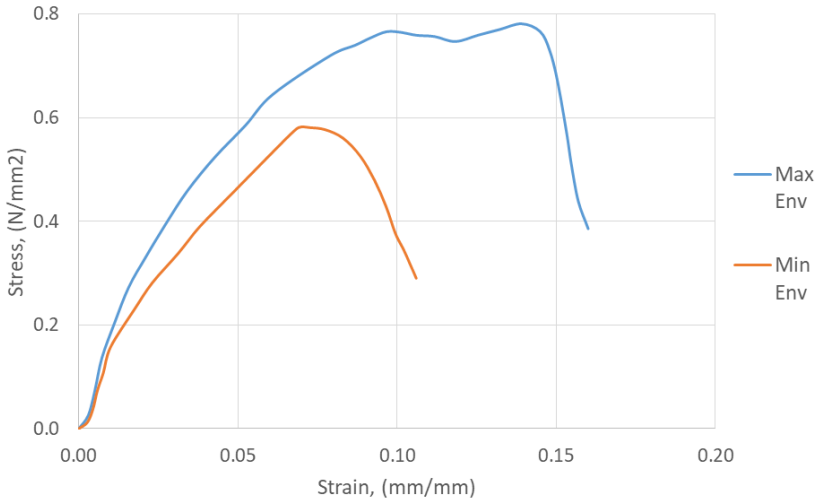

(b)

Figure 5. 33. (a) Cob cylinders' stress/strain curves and (b) stress/strain envelope curves.

Figure 5. 34. Compression failure modes of: (a) cylinder 1, (b) cylinder 2, (c) cylinder 3, (d) cylinder 4, (e) cylinder 5 and (f) cylinder 6.

5.9 Wallettes weighting and transportation

Two methods were used to transport the wallettes around the laboratory. The first one consisted in the use of a pallets jack which was introduced bellow the opening made in the flanges of the steel bottom pallets (see Figure 5. 35 (a)). The second transportation method consisted in hanging the wallettes from the roof crane, which has a capacity of 10 tones, either by passing the chains through the pieces of steel C channel welded to the web of the top steel cap or by strapping the wallets from the openings of the steel bottom pallet (see Figure 5. 35 (b)). Whatever method was used, a small pre-compression force was always applied to the wallettes by tightening the nuts by one or two revolutions to avoid having any tensile stresses caused by the movement or vibrations that might have caused weakening or damage of the specimens.

The hanging method was also used to weigh the wallettes (the weight of the rest of metallic components was later removed from the read value). The wallettes were measured and weighed after being consolidated in order to calculate their density and estimate their moisture content. A dynamometer PIAB NOW 1301 with a maximum capacity of 3000 daN and an accuracy of 20 daN was used to measure the weight of the wallettes (see Figure 5. 35 (c)).

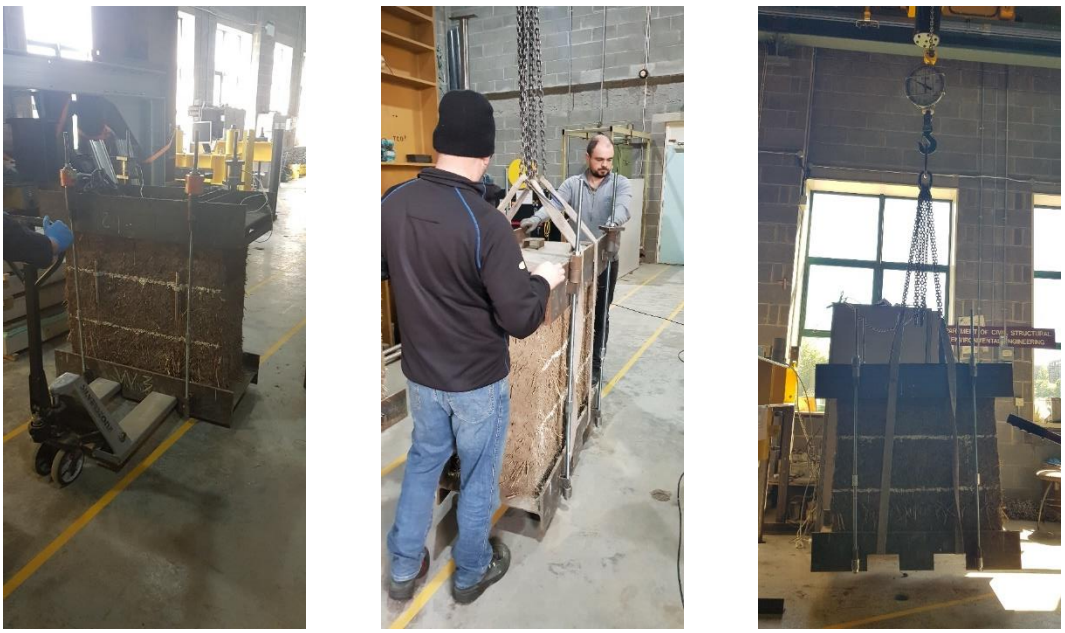

(a) (b) (c)

Figure 5. 35. Wallettes' transportation: (a) using the pallets jack and (b) using the roof crane. (c) Wallettes' weighing using the roof crane and a dynamometer.

5.10 Wallettes consolidation

The ratio σ'_p/σ'_{v0} is known as the Over Consolidation Ratio (OCR) where σ'_p represents the pre-consolidation pressure and σ'_{v0} is the effective overburden pressure. Soils that have never been subjected to effective vertical stresses higher than the present effective overburden pressure and that display values of $OCR = 1$ are called normally consolidated. On the other hand, Soils that have been subjected to effective pressures in excess of the present effective overburden are called "*pre-compressed*" or "*over consolidated*" (Terzaghi *et al.*, 1996).

The need to perform laboratory flat jack tests on "*over consolidated*" earthen wallettes, instead of on normally consolidated earthen wallettes, was identified by previous research (Lombillo, 2010). After not being able to recover the initial distance between control points on a single flat jack test done in a rammed earth wall under a constant load, Lombillo realized that the rammed earth wallette must have been undergoing consolidation. Lombillo decided to stop the test, as it was obvious that the increment of pressure in the flat jack would not be able to recover the initial distance between control points, and he maintained the pressure in the flat jack constant for a period of five days. During this time he monitored the distances between control points. Regardless of maintaining the pressure and external loads constant he observed an increase of the deformation. To solve this problem, he subjected the rammed earth wallette to a quasi-constant load bigger than the load at which the flat jack test would be performed and monitored the deformation of four vertical control points installed in the wallette. When the deformation of the control points stabilized (after a period of about five days) he reduced the load to the value of the test and proceeded to perform the flat jack test, this time obtaining a satisfactory result. The in-situ application of the flat jack test on historical walls does not present this problematic as the walls have naturally been consolidated over a long period of time due to the over imposed loads of roofs, floors and occupancy loads. Therefore, in order to obtain cob walls in the laboratory representative of existent cob walls it is necessary to undertake a process of consolidation.

After a four-months drying period the pre-consolidation of the wallettes began. The pre-consolidation load applied to the wallettes was fixed taking as reference the mechanical properties obtained from the cob cylinders tested in this experimental campaign. It was decided not to exceed the apparent yield point of cob which

corresponded approximately to 30 % of the computed average compressive strength of the cylinders. Therefore, the wallettes were subjected to a consolidation force of 84 kN +/- 1 kN.

The loading set-up consisted in 4 treaded bars fixed at the bottom and top steel pallets which were tensioned by tightening the nuts at the top. The tightening of the nuts was performed manually, in increments of approximately 2 kN per bar, and the initial loading process, going from 0 up to 85 kN took approximately 15 to 20 min for each wallette. The tension forces thus applied caused the shortening of the bars, deformation that subsequently translated into a compressive force applied to the cob wallettes. Therefore, loads were applied slightly eccentrically but in a symmetric way as the points of anchorage of the bars are located at the external faces of the steel pallets flanges. A load cell was installed between each point of support at the top steel pallet and the nut to measure the load transferred for each one of the bars to the wallette (see Figure 5. 36 (a)). The total load transferred to the wallette was calculated as the sum of the four bars' forces.

Four Linear Variable Differential Transformers (LVDT) were attached to the wallettes' faces, two in the front and two in the back, to measure the deformation caused by the compressive forces. The LVDT's were pinned through the material using stainless-steel pins of roughly 5 to 6 cm length by 2 mm diameter. The points of support were held in place at an initial distance of roughly 30 cm at the middle third of the specimens (see Figure 5. 36 (b)). This arrangement is in accordance with BS EN 1052 Part 1 (British Standard, 1999).

The full consolidation set-up is shown in Figure 5. 36 (c). The instrumentation was zeroed after all components were set in place. The effect of the steel cap and other devices' weight on the values recorded by the LVDT's was therefore eliminated and the obtained displacement values were only caused by the increment of the force in the bars.

After the load of 84 kN +/- 1 kN was imposed to the wallettes it was kept quasi-constant for a period of five days and displacements increments were monitored. The load in the bars was reapplied during the first hours of consolidation after registering approximately a drop of 1 kN per bar. The loads were not reapplied during the nights, therefore the over-night drop of the load was higher, up to 2 or 3 kN per bar. The subsequent 4 days of the consolidation process the loads were reapplied at interval of two hours. After this consolidation period the loads were completely removed manually by

untightening the nuts in decrements of roughly 2 kN per bar. A second load cycle was applied in a similar manner to the first one and loads and displacements were recorded.

(a) (b) (c)

Figure 5. 36. (a) Load cell between nut and point of support. (b) LVDT pinned to the wallette's face and (c) full consolidation set-up view.

5.10.1 Consolidation of W1

After proceeding with the first load cycle of W1 (the first wallette) a considerable bending deformation was observed in both the bottom steel pallet and the top steel cap (see Figure 5. 37). This deformation was caused by the eccentric application of the loads and the low stiffness of the UB web's section (the design of the steel pallets presented in section 5.4 only considered the application of the load in the centre area of the UB web). Initially it was thought that this deformation would explain the non-linearity of the force/displacement and stress/strain graphs obtained for W1 (see detail results on Appendix B) as the forces applied to the wallette were not supposed to cause the yielding of the material.

5.10.2 Consolidation of the other wallettes

After noticing such significant deformation on the pallets, which were originally designed only to resist centrically applied loads, it was decided to reinforce them transversally to increase the stiffness of their web. Such reinforcement can be seen in Figure 5. 38 (a) for the top steel cap and in Figure 5. 38 (b) for the bottom steel pallet. This intervention

reduced considerably the deformation of the pallets and improved greatly the transfer of the loads. The rest of the wallettes, W2, W3, W4, W5 and W6, were consolidated with this improved design and the possible effects of the bending deformation of the UB sections was practically eliminated.

Figure 5. 37. Bending deformation on bottom steel pallet and top steel cap.

(a)

(b)

Figure 5. 38. Transversal reinforcement of (a) top steel cap and (b) bottom steel pallet.

5.10.3 Consolidation results summary

Detailed results obtained during the cob wallettes' consolidation process are presented in Appendix B. The force/displacement and stress/strain curves obtained after the first load cycle are shown in Figure 5. 39 (a) and Figure 5. 39 (b), respectively. Figure 5. 40 presents the consolidation curves. Finally, force/displacement and stress/strain curves obtained after the second load cycle are shown in Figure 5. 41 (a) and Figure 5. 41 (b), respectively.

As it can be seen in Figure 5. 39 all wallettes presented a non-linear force/displacement relationship. This indicates that the cause of the non-linearity was not the bending deformation of the steel bottom pallet and steel top cap as was initially thought after the consolidation of W1 was performed. Nor was the load level the cause of the non-linearity of the curve as it never exceeded a maximum value of 85 kN, which induced a compressive stress of only 0.21 MPa in an idealized cross section of 0.4 m^2 (this value represented only 30 % of the compressive strength obtained from the cob cylinders' compressive strength tests performed in this experimental campaign).

The "*full*" consolidation of a soil is only achieved after a relatively long period of time, hundreds or thousands of years even. For practical reasons though it was accepted that for this experimental campaign the level of consolidation would be such that further deformations caused during the time period of the performance of the flat jack test would be negligible (i.e., displacement increment due to cob consolidation less than 1 %). To achieve this the load used for consolidation (roughly 84 kN) would be bigger than the load at which the flat jack test would be performed (approximately 50 kN). As can be seen in Figure 5. 40 the increase in average displacement between the fifth and sixth days of consolidation (roughly between 6000 and 7000 min) for all wallettes was practically null in comparison with the average displacement recorded during the first hours of the consolidation process (from minute 0 up to roughly 300 min displacement increments of up to 80 %, see Appendix B).

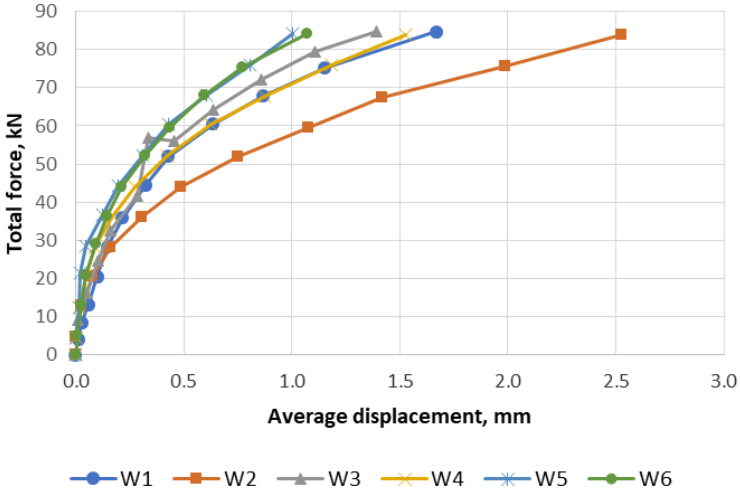

(a)

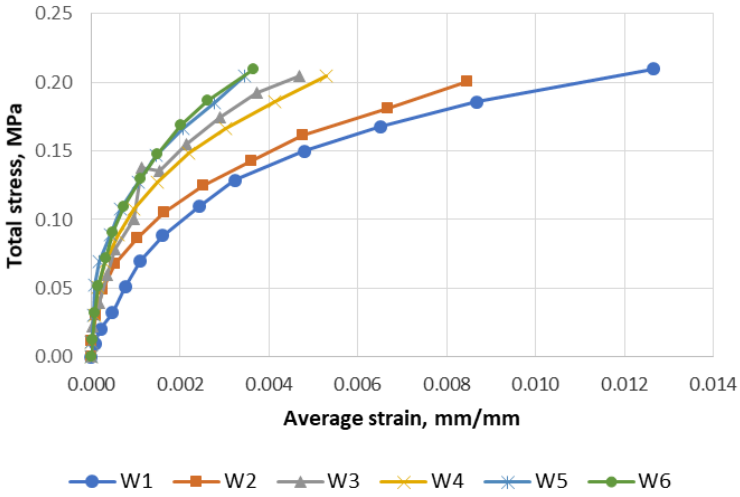

(b)

Figure 5. 39. First load cycle's (a) force/displacement and (b) stress/strain curves.

It is worth mentioning that the loads were only controlled within normal laboratory working hours, namely, from 9:00 to 17:00 h. In the first day of consolidation loads started to be applied to the wallettes around 10:00 to 11:00 h. Initially, as the consolidation was very considerable, the bars would shorten at a quite fast rate consequently losing the force that had been applied to them by tightening the nuts. Therefore, re-tightening of the nuts was done every 5 min, for a couple of times, every 10 min for a couple of times, every 15 min, then every 30 min and finally every 60 min until 17:00 h. As the load did not dropped significantly during the following days of the consolidation process the nuts were re-tightened at periods of 120 min. This is the reason why Figure 5. 40 presents such gaps between recorded groups of points, which indicate

the number of consolidation days. Loads were not controlled overnight and this caused the wallettes to be subjected to a lower consolidation load during overnight periods. Nevertheless, it was also observed that the overnight drop in force also reduced as the consolidation days passed, which indicated a reduction of the consolidation rate in the wallettes.

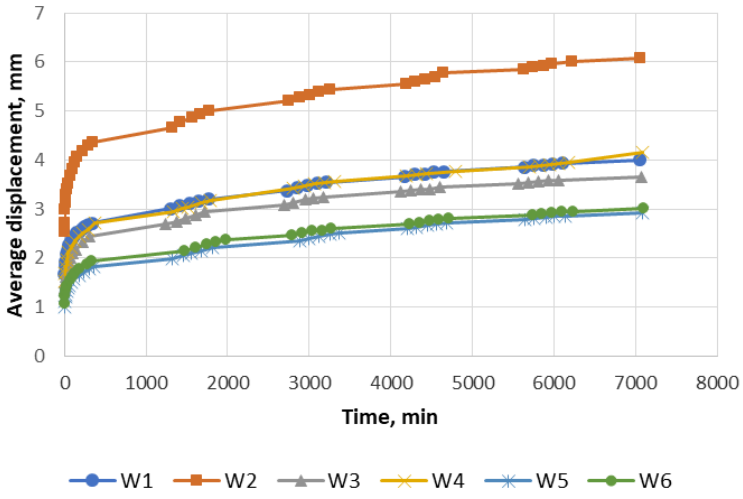

Figure 5. 40. Consolidation time/displacement curves.

After the consolidation period, the load was completely removed and a second load cycle was induced in the wallettes (except for W1). As it can be seen in Figure 5. 41 the load/displacement and the stress/strain shape of the curves drastically changed in comparison with the first load cycle. For the second load cycle a practical linear relationship was observed for both load/displacement and the stress/strain curves. This second load cycle can be seen as what is known for soil's consolidation as a "*recompression range*". As the load applied to the wallette in the second cycle did not exceeded that of the first cycle, the soil structure accommodated the stresses induced without suffering significant interparticle displacements. In order words, as the soil was "*pre-compressed*" and the stresses did not go beyond the elastic range of the material, the response of the cob wallettes exhibited an elastic behaviour. A more detailed explanation on the compressibility of soils and the theory of consolidation can be found in Terzaghi (1996).

These results confirm the importance of performing mechanical characterization tests on laboratory "*over consolidated*" earthen wallettes as initially identified by previous research (Lombillo, 2010). Pre consolidation of the wallettes is even more critical if the duration of the tests take more than 3 to 5 min as the influence of the soil

consolidation phenomena may influence to a great extend the values recorded of deformations, as can be seen by comparing the load/displacement curves of the first and second lad cycles presented in Figure 5. 39 (a) and Figure 5. 41 (a), respectively.

From the slopes of the stress/strain curves obtained during the second load cycle, the Young's modulus of the wallettes was estimated to be of 143 MPa (see Table 5. 13). This value is much higher in comparison with the one obtained from the cob cylinder's tests, but similar to values reported by other authors (Minke, 2000, Ziegert, 2003, Miccoli *et al.*, 2014). The higher value of the wallettes is due to the confining effect provided by their larger dimensions, i.e. their aspect ratio, in comparison with those of the cylinders, and also due to the soil being pre-compressed, which was not done for the cylinders.

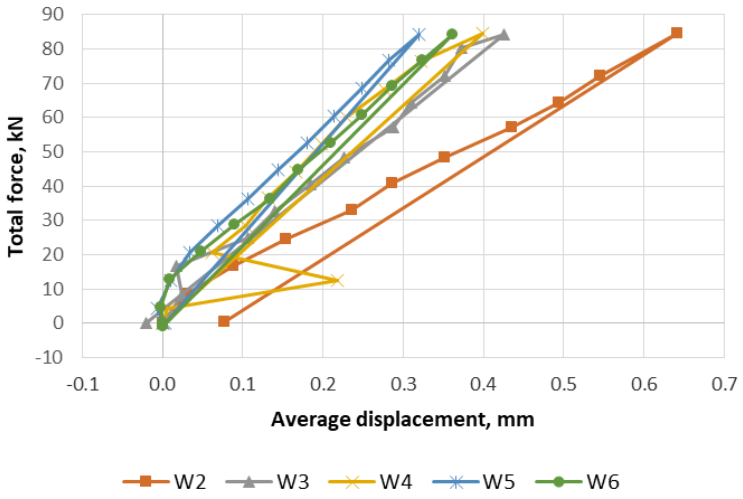

(a)

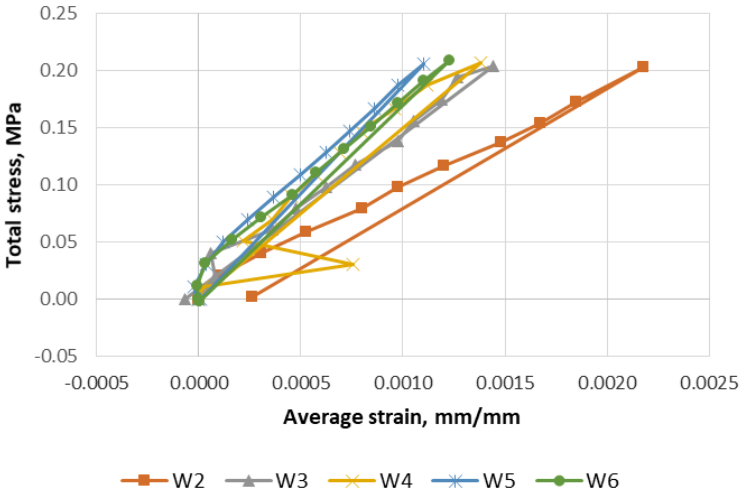

(b)

Figure 5. 41. Second load cycle's (a) force/displacement and (b) stress/strain curves.

Table 5. 13. Wallettes' Young's modulus.

Wallette	Young's modulus (MPa)
W2	92.05
W3	135.89
W4	148.45
W5	162.41
W6	177.70
Mean	143.3
SD	32.6
COV	22.77

5.11 Single flat jack tests

An description of the flat jack test method applied to masonry walls was provided in section 2.1.7 based on the recommendations given in ASTM (ASTM International, 2009, 2014) and RILEM (RILEM, 2004a, 2004b) standards. The objective of the single flat jack test is to determine the level of stress to which a wall is subjected at a specific location. In this section the equipment used to perform the flat jack tests is described, the modifications of the standard methodology for flat jack tests implemented for its application in cob walls are presented and, finally, a summary of the results obtained is presented and discussed.

The slot cutting equipment consisted in a ring saw model Husqvarna K3600 with a blade diameter of 370 mm (and a thickness of 6 mm) which allows for a maximum cut depth of 270 mm (see Figure 5. 42 (a)). A bubble level was glued to the ring saw to serve as a guidance to the operator and ensure a horizontal cut. The ring saw operates hydraulically. The Power plant used to operate the ring saw was a model Husqvarna Power Pack PP518 (see Figure 5. 42 (b)). An industrial vacuum was used to clean the slot created with the ring saw before measuring the depth of the cut and inserting the flat jack into it (see Figure 5. 42).

(a) (b) (c)

Figure 5. 42. (a) Ring saw, (b) hydraulic power plant and (c) industrial vacuum.

A template was fabricated with a piece of timber (see Figure 5. 43) to indicate the location where the cut would be performed in the wallette and serve as visual assistance to the operator of the ring saw. Due to the nature of the cob wallettes' surfaces (very dusty and irregular) the use of an adhesive to fix the control points proved to be infeasible. Therefore, it was decided to implement an alternative approach. It was decided to solder the stainless-steel control points to a 2 mm diameter rod of copper and sharpen its tip to create a kind of nail (see Figure 5. 43). As cob is a relatively soft material this allowed us to fix the control points relatively accurately and without causing much damage to the material. The length of the rod proved to be an important factor to take into account, if the rod was too short it would not be stable and the measurements could be completely invalidated. On the other hand, if the rod was too long it may rotate due to the non-uniform pressure transferred from the flat jacks to the material, as sketched in Figure 5. 44, thus altering the measurements as well. After some trial and error attempts it was decided to use rod lengths of 4 cm as it seemed that this was the minimum length necessary to obtain a solid anchorage of the control point to the cob substrate.

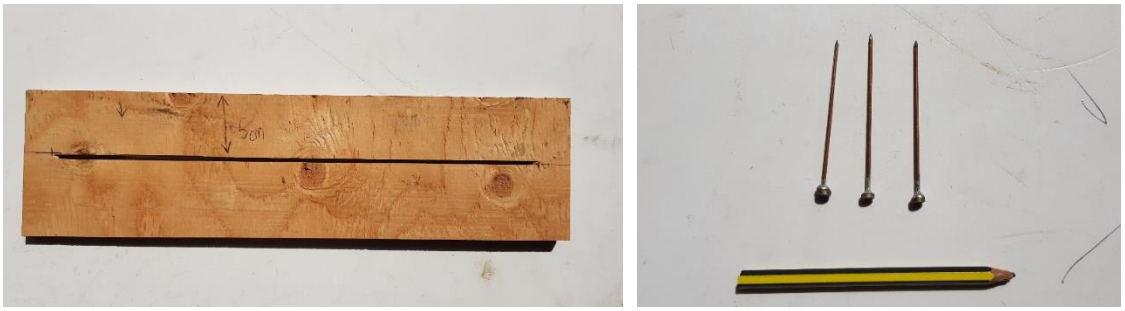

(a) (b)

Figure 5. 43. (a) Cut template and (b) control points.

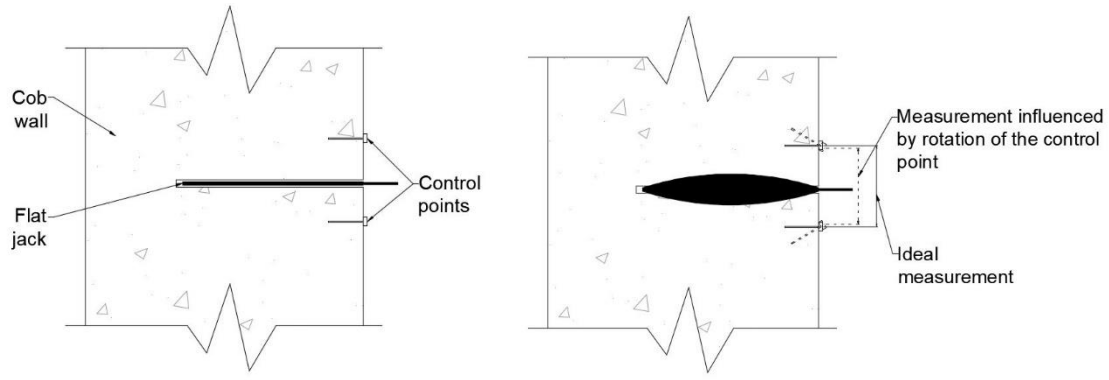

(a) (b)

Figure 5. 44. Sketch of nailed control points (a) before applying pressure in the flat jack and (b) after pressure is applied and the flat jack deforms.

The control points were fixed, approximately, according to the distances shown in the sketch of Figure 5. 45 (a). Figure 5. 45 (b) shows the location of the cut and the 4 pairs of vertical control points fixed to the cob wallette.

The strain measuring equipment used was a digital "*Vernier*" callipers with a precision of 0.01 mm with a digital display (see Figure 5. 46 (a)). The flat jacks used were eccentric flat jacks model SISGEO 0L103352600 (see Figure 5. 46 (b)) with the dimensions shown in Figure 5. 46 (c) and a thickness of 4 mm. A new flat jack was used for every single flat jack test carried out on the cob wallettes, thus the calibration coefficient, $K_m = 0.9155$, provided by the manufacturer was used for all calculations.

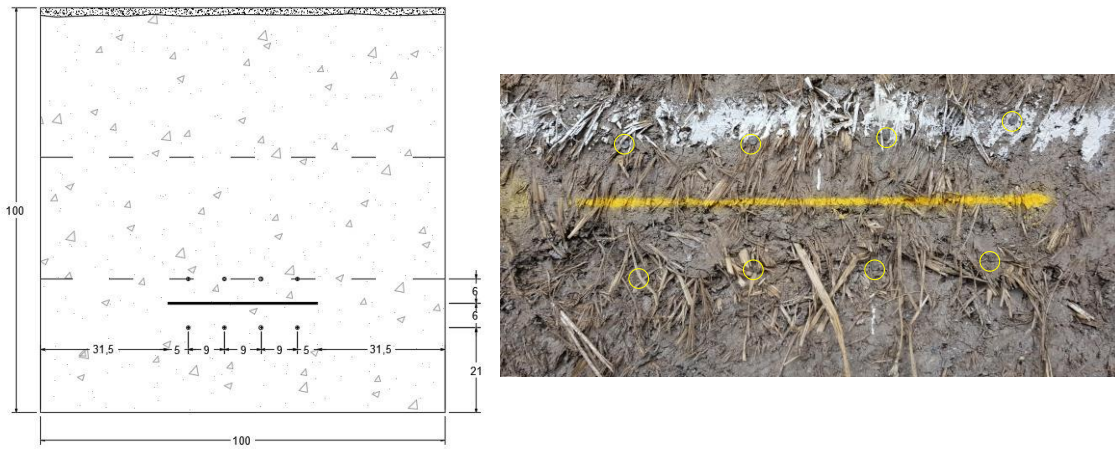

(a) (b)

Figure 5. 45. (a) Sketch of control points' location (values in cm) and (b) close up picture of installed control points in cob wallette.

(a) (b) (c)

Figure 5. 46. (a) "Vernier" callipers, (b) semi-circular flat jack and (c) flat jack's dimensions.

When the flat jack test is performed in masonry walls the slot is usually cut in a horizontal mortar joint, generally 1 to 2 cm thick, and all mortar is removed in order to transfer the flat jack's pressure directly to the units. In those cases, steel shims are used to fill the void between the flat jack and the units. The use of steel shims was not necessary in the performance of the flat jack test in the cob walls. Cob is a homogenous material and, as the cuts made with the ring saw were of very good quality, the flat jack fitted nice and tightly into the slot occupying the entire thickness of the slot.

To measure the depth of the cut a template was fabricated with another piece of timber. As specified by the standards, the depth of the cut was measured at every 2 cm, thus obtaining an approximate profile of the cut. Long "*Vernier*" callipers (30 cm) were used to measure the depth of the cut (see Figure 5. 47). The thickness of the piece of timber was of 12.3 mm and the values measured with the calliper were corrected by subtracting this value from the measures.

Figure 5. 47. Timber template and calliper Vernier used to measure the depth of the cut.

A hand pump with manometer included, model SISGEO 0L10PM10000 (see Figure 5. 48 (a)), was used to perform both single and double flat jack tests in the first

wallette (W6). The pump had a limited capacity though, its reservoir had to be constantly monitored and refiled and a lot of work was required to achieve the necessary pressure increments. For the rest of the wallettes a more powerful pump, already available at the lab (see Figure 5. 48 (b)), was used. With the new hand pump the process was highly simplified and the test times significantly reduced which, according to the standards, improves the quality of the results.

(a) (b)

Figure 5. 48. Manual pumps.

Connection kits with ball valve and nylon tube, model SISGEO 0L10KITV380, were used to connect the pump to the flat jack. The manufacturer set-up for the single flat jack test is shown in Figure 5. 49 (a). This set-up was slightly modified to better suit the purpose of the test. The manometer was substituted with a pressure transducer, model Wykeham Farrance 28-WF6301, with a pressure range capacity of 0-2000 kPa. The pressure transducer was located just before the ball valve connected to the inlet of the flat jack instead of directly after the pump to try to avoid peak pressure values typically appearing while manually pumping the oil. Furthermore, a second ball valve was connected to the outlet of the flat jack to improve the purging of the system to reduce the amount of trapped air within it. The final set-up used is shown in Figure 5. 49 (b).

Finally, the wallettes were set-up as described in section 5.10 for the consolidation process in order subject them to a known external load. The load applied for the single flat jack test was of only 50 kN, 12.5 kN per threaded bar. If it is accepted that this load caused an overburden pressure σ'_{v0} and the consolidation load caused a pre-consolidation pressure $\sigma'_{p,}$ then the wallettes $OCR = 1.68$.

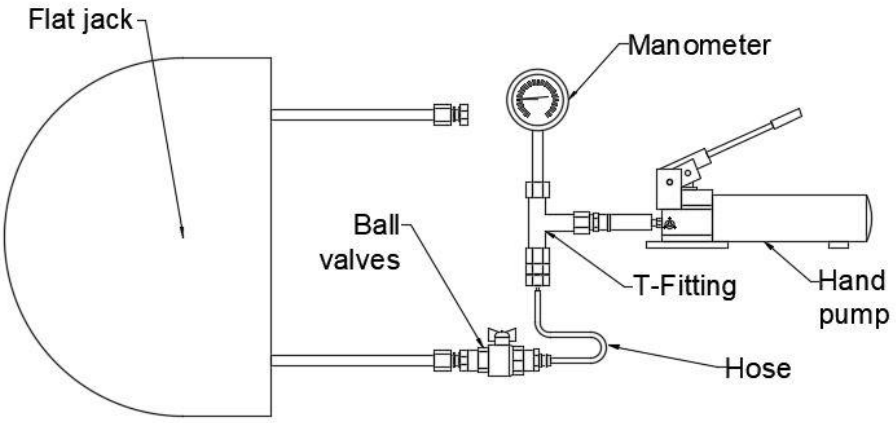

(a)

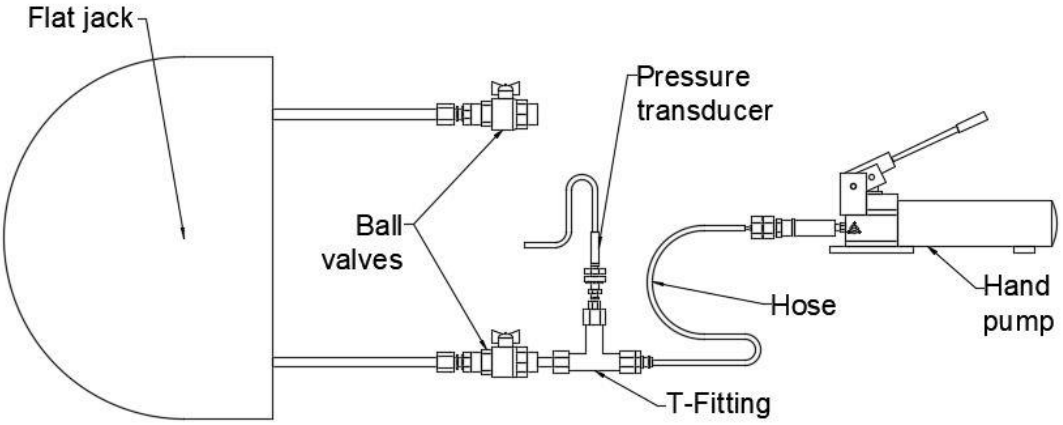

(b)

Figure 5. 49. (a) Initial system connection set-up proposed by flat jacks' manufacturer and (b) modified set-up used in this experimental campaign.

5.11.1 Testing of the first wallette

The wallettes were tested in a random order. The first one to be tested was wallette W6. The second step consisted of marking the location of the cut with sprayed paint using the template. Control points were fixed having this line as reference as indicated in Figure 5. 45. Before proceeding to cut the slot the initial distance between control points was measured (see Figure 5. 50). After this the cut was made. The ring saw was operated manually by the lab technician who had to kneel to make the cut (see Figure 5. 51 (a)). This position allowed him to use all his body as support to carry and stabilize the ring saw. During the execution of the cut he constantly monitored the bubble level to ensure horizontality. The result was a horizontal, well executed and very neat cut (see Figure 5. 51 (b)).

Figure 5. 50. Measurement of the initial distance between control points.

The slot was cleaned using the vacuum (see Figure 5. 52) and then the depth of the cut was measured by using the timber template and the long "*Vernier*" callipers (see Figure 5. 53). The timber template was nailed to the cob wallette and measurements were taken at every 2 cm. The depth recorded using the callipers was then corrected to take into account the thickness of the template (12.3 mm). After finishing the cut-depth measurements the template was removed and the distance between control points was measured again. The difference between this set of measurements and those taken before making the cut gave the deformation suffered by the material due to the release of stresses caused by the opening of the slot.

(a)

(b)

Figure 5. 51. (a) Technician performing the cut manually handling the ring saw and (b) good quality cut.

Figure 5. 52. Cleaning of the slot.

Figure 5. 53. Measurement of the cut depth.

After this, the flat jack, previously connected to the pump and pressure transducer as indicated in Figure 5. 49 (b) (see Figure 5. 54 (a)), was introduced into the slot. The cut was very well made and the flat jack occupied the entire thickness of the slot. In fact, the flat jack fit was so tight into the slot that a few centimetres were left outside the wallettes face as shown in Figure 5. 54 (b). From this point, the flat jack had to be gently pushed all the way through the slot by using a timber lever (see Figure 5. 54 (c)). The flat jack fit very tightly into the slot and there was no need to use steel shims to fill the extra space between the flat jack and the material.

(a)

(b)

(c)

Figure 5. 54. Insertion of the flat jack into the slot.

The system was then purged and the extra oil pumped into the system recovered in a bottle to be re-used in future tests (see Figure 5. 55). The ball valve installed at the end of the system enabled the closure of the system just after stop pumping in order to avoid the inclusion of air into the hydraulic system.

After some rough calculations it was estimated that the level of stress at the location where the cut was made would be of approximately 0.14 MPa. The standard's advice applying 50 % of the estimated pressure to allow the flat jack to seat into the slot. Nevertheless, a pressure of only 0.7 bars didn't seem to have any significant effect on the device. Thus, it was decided to apply 1.0 bars of pressure to allow the flat jack to seat correctly into the slot. This was also done taking into account that the standard recognizes

that the single flat jack test will overestimate the level of stress. Therefore, once the ball valve at the end of the system was closed, oil was pumped to increase the pressure in the flat jack until it reached 1.0 bar. At this point the pressure was fully released.

Figure 5. 55. System purged and ready to start applying pressure increments.

Pressure increments were then applied to the flat jack and the distance between control points was recorded at every step. Even though the standards specify a pressure increment of about 0.5 bars, for the application of the tests in masonry walls, it was decided to modify the procedure for its application in cob walls and increments of 0.25 bars were applied instead. This was decided based on the rough calculations performed to estimate the level of stress in the wallette. If increments of 0.5 bars were applied and the initial distance between control points turned out to be recovered at 1.5 – 2.0 bars, the plots would not show a clear trend if only 3 or 4 points were recorded.

At the point when the initial distance between control points was recovered it was observed that there was a small leakage of oil at the end ball valve (see Figure 5. 56). After further inspection it was observed that one of the fitting pieces connecting the outlet of the flat jack to the ball valve at the end of the system was damaged. Luckily, the leakage only appeared at the end of the test and it did not prevent the successful completion of the test. Finally, the pressure was released in the system and the flat jack was easily removed from the wallette.

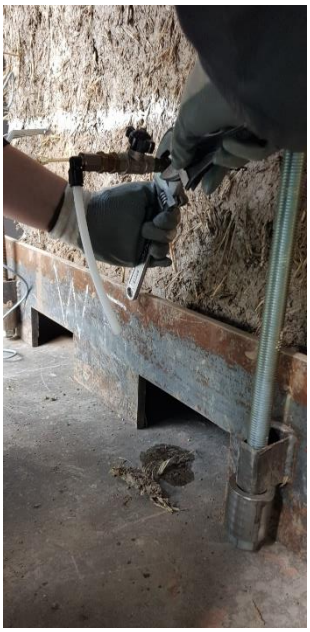

Figure 5. 56. Oil leakage from a fitting piece between the outlet of the flat jack and the ball valve.

5.11.2 Testing of the rest of the wallettes

The rest of the wallettes were tested in the following order: W1, W3, W5, W4 and W2. Randomization was used in order to avoid time related biases, i.e. drying of the material which may have resulted into higher values of strength. The single flat jack test in the rest of the wallettes was performed as per described in section 5.11.1 except for the following modifications:

- The fittings between the outlet of the flat jack and the ball valve at the end of the system were replaced for ones in a good sate and no more leakage was observed.
- As it was observed that the recovery pressure for W1 was of roughly 4 bars it was decided to apply pressure increments of 0.5 bars as this would be enough to identify clearly the trend of the plots.
- A seating pressures of 2 bars (50 % of the estimated recovery pressure) was implemented as per specified in the masonry standards.
- A bigger hand pump was used to optimize the process.
- The cut was made by attaching the ring saw to the timber frame supported in top of the pallets jack (see 5.12.2). This made it easier to ensure a neat horizontal cut.

5.11.3 Single flat jack tests' results summary

The complete data collected from the single flat jack tests are presented in Appendix C. In Figure 5. 57 a summary of the deformation recovery curves is shown. It can be observed that as the pressure was increased in the flat jack the average deformation of the control points, caused by the release of stresses when the cut was made, decreased. Increments of pressure were always applied until a negative value for the control points' average deformation was recorded. The recovery pressure for every wallette, p, was computed as the interpolation between the two pressure points that presented the last positive and first negative average deformation value respectively. The obtained recovery pressure values are presented in the second column of Table 5. 14. The mean recovery pressure was of 0.345 MPa with a SD of 0.0327 and a COV of only 9.48 %.

The values of the estimated stress in the wall at the location of the cut, f_m, were computed taking into account a total load imposed by; the volume of the wallette on top of the cut with a self-weight computed using the weights obtained after the wallettes' consolidation, the weight of the top steel cap and other pieces supported by the wallette (load cells, threaded bars, etc.) plus the average load recorded in the bars between the time period before the cut and the recovery of the initial distances between control points, divided by the measured cross section at the height of the cut. The f_m values computed are presented in the third column of Table 5. 14. The mean value estimated was of 0.14 MPa with a SD of 0.006 and a COV of only 4.52 %.

Dimensionless geometrical coefficients, K_a, for each wallette were determined by the ratio between the area of the flat jack and the area of the slot cut. The obtained values are presented in the fourth column of Table 5. 14. The mean value obtained was of 0.94 which testifies to the overall good quality of the cuts.

Finally, the dimensionless geometrical efficiency constant which takes into account the geometrical characteristics of the flat jack and its relative size with respect to the specimen, K_e, was computed using EQ. 24 and the obtained values are presented in the last column of Table 5. 14. The mean value obtained was of 0.48 with a SD of 0.0427 and a COV of only 8.84 %. Adopting a confidence level of 95 % and assuming our six samples as the total population a CI would give values of (0.45, 0.51). This value can be interpreted in the sense that levels of stress in a cob wall estimated with the use of the single flat jack test would be typically overestimated by a factor of 2. It is recommended

to adopt the upper value of the interval, thus respecting certain safety margin, to correct the average compressive stress values obtained with the use of the single at jack test in cob walls and obtain a more realistic estimation of the stress.

$$K_e = \frac{f_m}{K_m K_a p} \qquad \textit{EQ. 24}$$

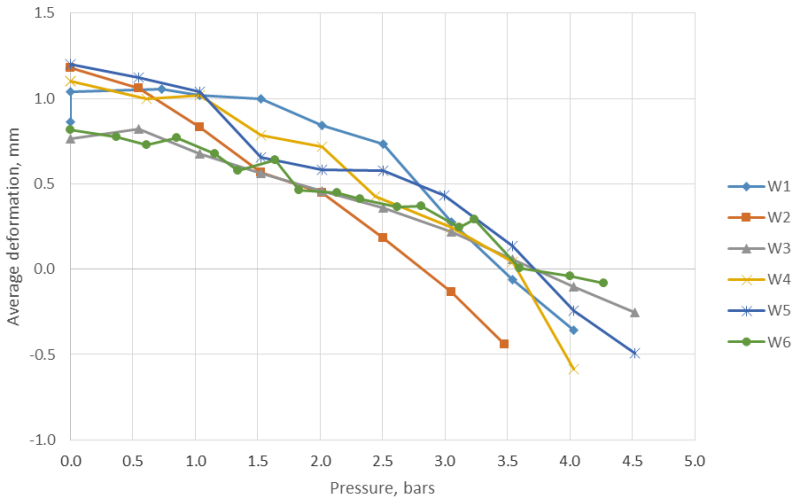

Figure 5. 57. Deformation recovery curves.

Table 5. 14. Recovery pressures, estimated stresses and dimensionless coefficients.

Wallette	p (MPa)	f_m (MPa)	K_a (-)	K_m (-)	K_e (-)
W1	0.35	0.14	0.97	0.92	0.47
W2	0.28	0.13	0.91	0.92	0.57
W3	0.37	0.14	0.92	0.92	0.46
W4	0.35	0.14	0.97	0.92	0.47
W5	0.36	0.14	0.94	0.92	0.47
W6	0.36	0.15	0.94	0.92	0.46

5.12 Double flat jack tests

Similar arrangements to those implemented for the single flat jack test were used for the double flat jack test. It is worth mentioning that even though no compression load is necessary to perform the double flat jack test, the level of load present in the wallette after the single test was finished was maintained. This was done with the purpose of providing enough resistance against lifting of the material in top of the second flat jack and to avoid the typical complications present in walls with a low load on top of the location of the test as highlighted by the standard RILEM MDT.D.4 (RILEM, 2004a). The main

difference in the set-up with respect to the single flat jack was the use of two flat jacks connected in series as shown in Figure 5. 58.

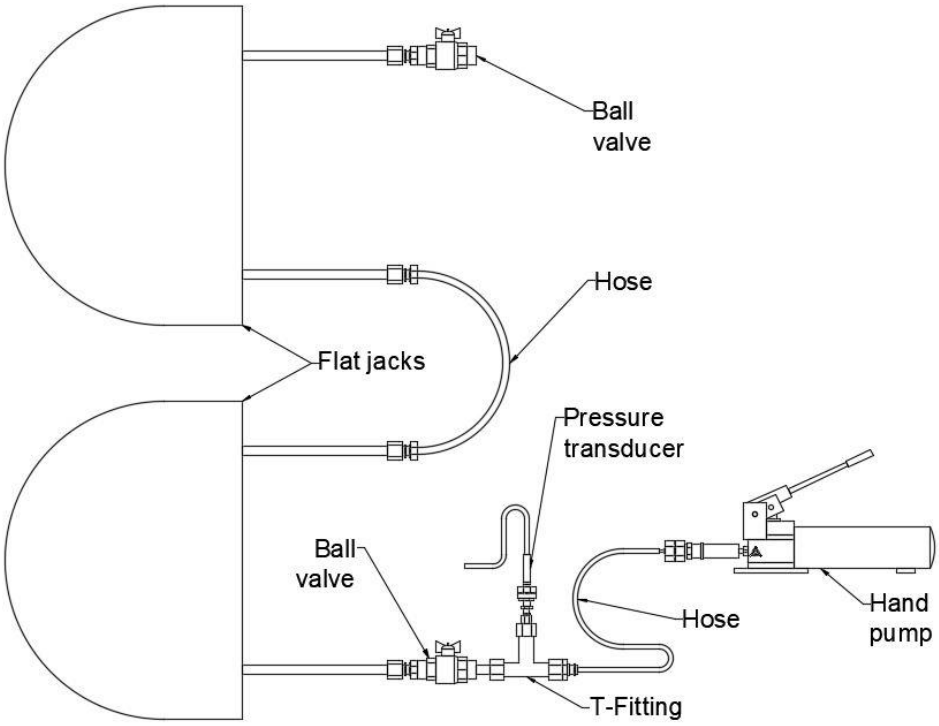

Figure 5. 58. Double flat jack test system connection set-up.

Then the control points were fixed in the wall approximately as shown in Figure 5. 59. For the double flat jack test four pairs of vertical control points and three pairs of horizontal control points were used. The points located on top of the slot made for the single flat jack test were used as the bottom control points for the pairs of vertical control points.

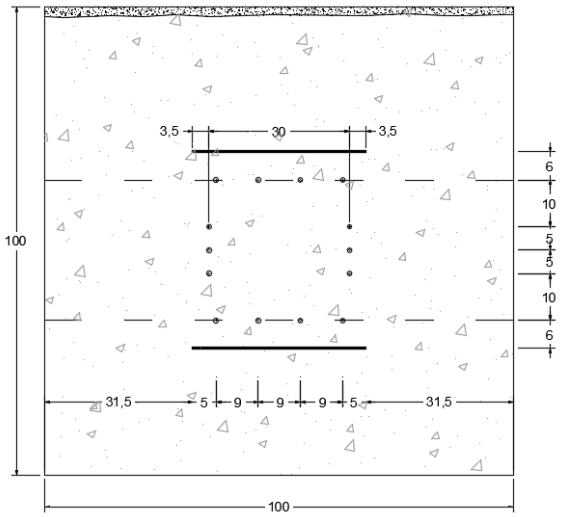

Figure 5. 59. Double flat jack test's sketch of control points' location (values in cm).

5.12.1 Testing of the first wallette

To perform the second cut in the wallette the technician kept operating the ring saw manually. This time the cut had to be made at a higher position and he had no longer the advantage of using his entire body to control the machine. He had to carry it in his arms, control the location of the cut and ensure horizontality all at the same time. This turned out to be too complicated and the result was a bad quality cut. The blade went sidewise, up and down and tilted while doing the cut. This produced a relatively thick, of about 1 cm, non-horizontal cut (see Figure 5. 61). The slot was cleaned and its depth was measured using the timber template and the long "*Vernier*" callipers at every 2 cm. Control points were fixed approximately at the locations indicated in the sketch shown in Figure 5. 59 (see Figure 5. 60).

Then two new flat jacks were introduced into the slots and connected to the manual pump and pressure transducer as indicated in Figure 5. 58. The system was purged and the extra oil recovered in a bottle for further use (see Figure 5. 62).

Rough calculations taking into account the compressive strength determined with the cob cylinders showed that a pressure of about 8 bars would be necessary to cause the failure in the specimen. Therefore, it was decided to apply a seating pressure of 4 bars. It was difficult to achieve this value as the flat jack inserted in the top slot, which was relatively thick in comparison with the thickness of the flat jack, deformed a lot without encountering any resistance from the material. Thus, a huge amount of oil (almost 3 l) had to be pumped. At this point it is worth mentioning that even though the standard advices the use of steel shims to fill the extra space between the flat jack and the material, in our case this was not feasible as the thickness of the cut was not even through its depth (see Figure 5. 63). Therefore, it was decided to neglect the initial void between flat jack and cob and proceed with the test under the described conditions.

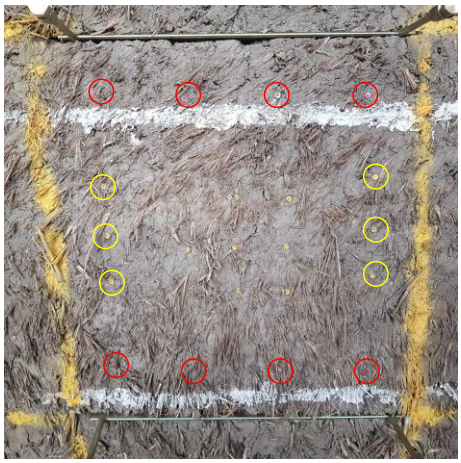

Figure 5. 60. Close up picture of installed control points in cob wallette (red circles indicate the location of the vertical control points whereas that yellow circles indicate the location of the horizontal control points.

Figure 5. 61. Second cut done in the first wallette.

Figure 5. 62. Purging of the system with both flat jacks connected.

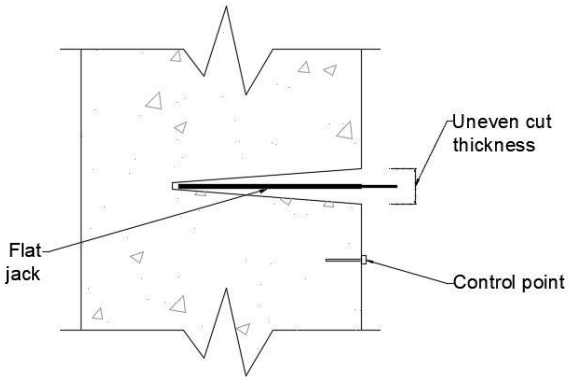

Figure 5. 63. Sketch showing the uneven slot thickness.

Once the seating pressure was reached it was subsequently removed from the system and the initial distance between control points was recorded by using the long "*Vernier*" callipers (as in this case the control points were located at a separation greater than 15 cm, which was the maximum distance the small digital callipers were able to measure). Then, pressure increments of roughly 0.5 bars were applied and at every pressure increment the distance between control points was recorded both for the vertical and horizontal control points (see Figure 5. 64).

The test had to stop at a pressure value of 7.0 bars as it seemed that the flat jack was deforming excessively without actually transferring adequately the pressure to the cob wallette. It was estimated that the increment of the pressure was mainly caused by the resistance of the flat jack placed in the upper slot as it had exceeded its elastic limit. It also seemed that the flat jack placed in the lower slot had started to deform beyond its elastic range as, when the test was stopped and the pressure was removed from the system, it was not possible to take it out from the slot. On the other hand, the uneven cut thickness allowed us to easily remove the flat jack from the upper slot and it was easy to appreciate the effect of its permanent deformation. Figure 5. 65 shows a comparison between the flat jack used for the single flat jack test and the flat jack introduce in the upper slot for the double flat jack test. The flat jack in the left practically recovered its original shape after the test was finished and the pressure had been removed whereas that the flat jack inserted in the thick slot kept much of its deformation, showing an inflated shape after removal from the slot.

Unfortunately, the test was unsuccessful and it was not possible to estimate the mechanical parameters of the wallette. It was believed that the cause of the failure was the poor quality of the second cut.

(a)

(b)

Figure 5. 64. Measurement of the distances between (a) vertical control points and (b) horizontal control points.

5.12.2 Testing of the rest of wallettes

To ensure consistency in the quality of the cuts, and to increase the levels of safety during the performance of the cut, it was decided to fabricate a timber frame to which the ring saw could be secured in a horizontal position. The timber frame was supported over the pallets jack and the cut was simply performed by sliding the pallets jack under the bottom steel pallet. The height of the cut was controlled by adding an extra timber box to the frame. In Figure 5. 66 (a) and Figure 5. 66 (b) the arrangement for the lower and upper cuts can be seen respectively.

Figure 5. 65. Flat jacks' comparison after test.

It was decided to implement pressure increments of 1 bar for the rest of the wallettes instead of the increments of 0.5 bars used in the first one. The rest of the process described in section 5.12.1 was also applied to the rest of cob wallettes. It is worth noting though that the test was performed relatively quickly in the last wallettes in comparison to the first one.

The rest of the wallettes were tested in the same order as per the single flat jack tests. A progressive reduction, from almost three hours to only an hour and a half, was achieved thanks to the level of practice acquired during the experimental campaign. Despite this reduction in the execution time of the test, no time-related variations were observed in the estimation of the mechanical parameters of the cob wallettes.

5.12.3 Double flat jack tests' results summary

The full data collected from the double flat jack tests is presented in Appendix D. In Figure 5. 67, a summary of the stress/strain curves obtained is shown. The positive values of strain represent a decrease of the distance between control points, whereas the negative values of strain represent a separation between control points. Therefore, the stress/strain curves plotted to the right of the zero value correspond to the strains of the vertical control points and those plotted to the left correspond to the horizontal control points. These curves were used to estimate the value of the mechanical parameters of the cob wallettes, namely, Young's modulus, Poisson's ratio and compressive strength. The obtained values

are presented in Table 5. 15 along with their basic statistics; mean, SD and COV. Finally, the failure patterns observed in the wallettes after completion of the double flat jack test, are presented in Figure 5. 68.

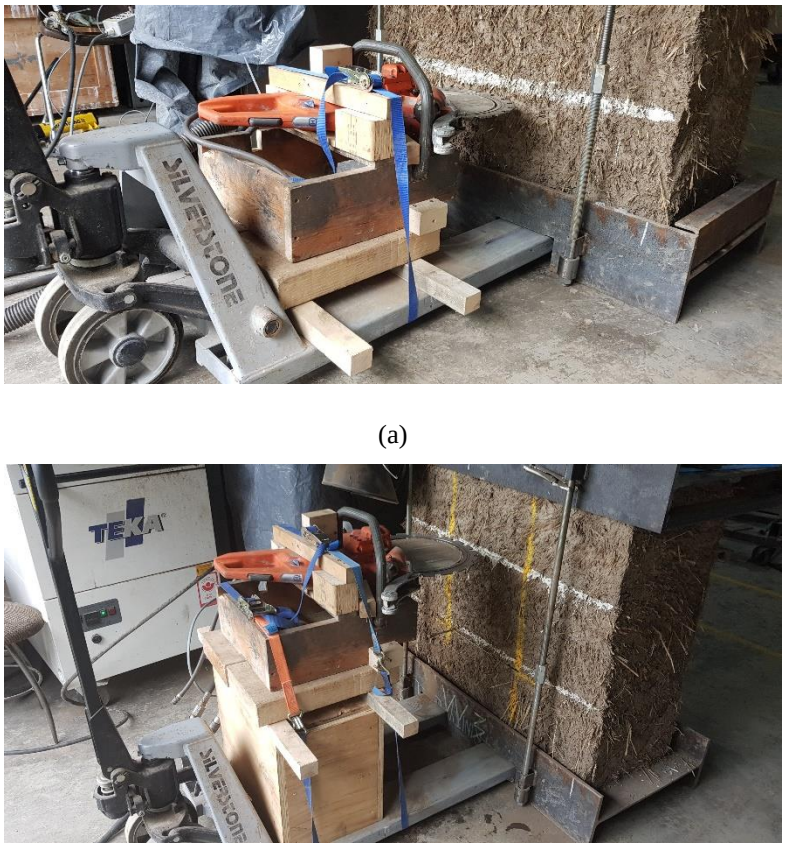

(a)

(b)

Figure 5. 66. Ring saw secured in the timber frame and at the appropriate height to perform (a) the lower cut and (b) the upper cut.

The dimensionless geometric coefficient, K_a, were calculated as the average of the ration between the area of the flat jack and the areas of the two slots. The value used for the dimensionless coefficient, K_m, was the one provided by the manufacturer of the flat jacks as new flat jacks were used for each wallette (the flat jack used for the single test of wallettes W1, W2, W3, W4 and W5 was reused for the double flat jack test as it recovered its original shape and was easily removed after completion of the single flat jack test from the slot). The values of stress, f_m, were computed using the formula provided in EQ. 25 in accordance with ASTM C 1197 (ASTM International, 2014) where p is the pressure recorded by the pressure transducer at every pressure increment.

$$f_m = K_m K_a p \qquad \textit{EQ. 25}$$

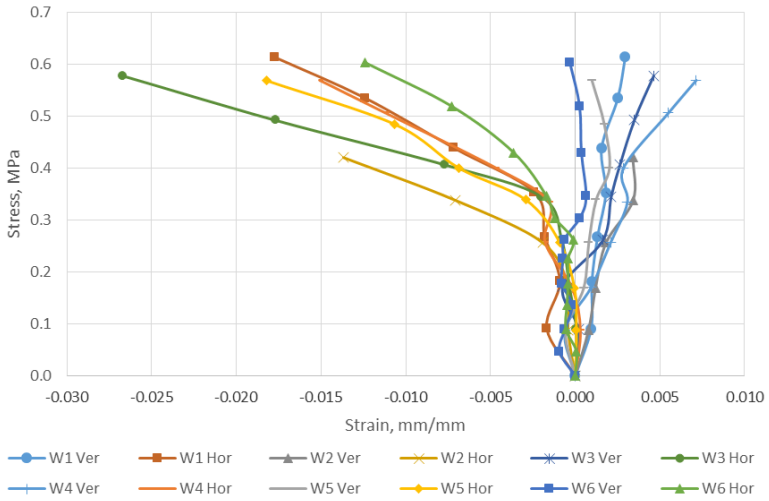

Figure 5. 67. Stress/strain curves obtained from the double flat jack tests.

Table 5. 15. Mechanical parameters estimated from the double flat jack tests.

Wallette	Slope Young's modulus (MPa)	Secant Young's modulus (MPa)	Secant Young's modulus corrected (MPa)	Poisson's ratio (-)	Compressive strength (MPa)
W1*	186.45	161.31	82.27	-	1.41
W2	136.57	125.63	64.07	0.35	0.73
W3	147.24	263.71	134.49	0.48	0.71
W4	103.86	137.92	70.34	0.20	0.76
W5	321.21	326.48	166.50	0.10	0.90
W6**	-	-	-	-	-
Mean	179.10	203.00	103.5	0.28	0.90
SD	84.80	87.90	44.8	0.17	0.29
COV	47.33	43.29	43.29	59.12	32.54

*None of the values obtained were within the feasible range, thus they were all discarded.

**Unsuccessful test due to the bad quality of the cut (see section 5.12.2).

It is worth noting that the strain values of the curves observed in Figure 5. 67 are counterintuitive. As pressure was applied vertically to the material between flat jacks one would expect to see bigger vertical strains, caused by the actual compression of the material than, horizontal strains, caused mainly by lateral bulging of the material due to Poisson's effect (for materials with Poisson's ratio between the range of 0.0 and 0.5). Nevertheless, after the apparent yielding point, horizontal strains increased non-linearly, whereas that the vertical strains seemed to keep following a linear relationship.

(a)

(b)

(c)

(d)

Figure 5. 68. Cob wallettes' failure patterns; (a) W1, (b) W2, (c) W3, (d) W4 and (e) W5.

(e)

Figure 5. 68. Cob wallettes' failure patterns; (a) W1, (b) W2, (c) W3, (d) W4 and (e) W5.

(continuation).

This phenomenon may be better understood if the relatively high stiffness of the flat jacks, in comparison with that of cob, is taken into account. When the pressure is increased by pumping oil in the system the flat jacks start to deform. Their deformation is not a uniform separation of the stainless-steel plates but more like a balloon inflation with bigger deformation at the centroid of the flat jack and practically negligible along its welded edges. The effect of this differential deformation is practically non-existent for small deformations, but becomes significant as deformations grow considerably, which happened while performing the double flat jack test on the cob wallettes of this experimental campaign.

The uneven deformation of the flat jacks causes the pressure to be transferred to the wallette in a non-uniform matter. The actual load in the wallette is actually more similar to a point load than to a uniformly distributed load. Furthermore, the almost zero deformation of the flat jacks along their edges, namely, at the wallettes' face, does not cause any restriction to the bulging of the material (see Figure 5. 69 (a)). Therefore, bulging compensates for some of the vertical deformation whereas that, at the same time, contributes to the further increment of the horizontal deformation of the material as shown in Figure 5. 69 (b). The bulging of the material between the flat jacks could be further investigated in a future work by developing a full 3D FEM model.

The Young's modulus values presented in the second column of Table 5. 15 represent the slope of a linear regression curve fitted between the points of the elastic range of the material, the values in the third column correspond to the secant modulus of elasticity calculated using EQ. 26 in accordance with ASTM C 1197 (ASTM International, 2014) and the values in the fourth column correspond to the corrected values computed in accordance with RILEM MDT.D.5 (RILEM, 2004b). The reason why

wallette W5 presents a relatively high stiffness in comparison to the rest of wallettes may be due to a bias in the selection points to which the regression equation has been fitted (see Appendix D).

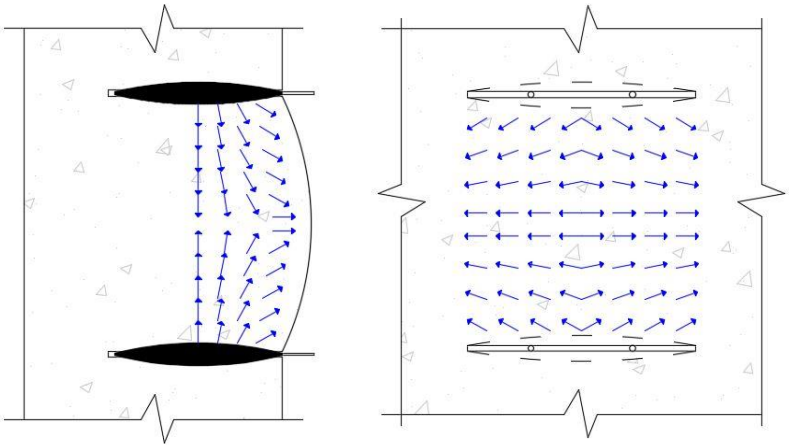

(a) (b)

Figure 5. 69. Idealized bulging (a) section view and (b) front view.

$$E_{si} = \frac{f_{mi}}{\varepsilon_{mi}} \qquad \textit{EQ. 26}$$

Where f_{mi} is the cumulative stress and ε_{mi} is the cumulative strain increment from zero. A value of 0.51, determined from the single flat jack tests' results of this experimental campaign, was used for K_e to correct the values presented in the third column. The values calculated taking into account the slope of the linear segment of the curve are in good agreement with the values obtained from the slope of the stress/strain consolidation curves. In fact, a 2-sample t-test comparing the means of both groups of values with a confidence level of 95 % and a null hypothesis H_0: $\mu_1 - \mu_2 = 0$ returned a P-Value of 0.419 (the 95 % CI contained 0) thus leading to the acceptance of the null hypotheses and concluding that there was not a statistically significant difference between the means of both groups.

On the other hand, the Young's modulus values corrected with the use of K_e, found after the single flat jack tests of this experimental campaign, turned out to be relatively small in comparison with the Young's modulus values found during the consolidation of the wallettes and with those obtained from the slope of the stress/strain curves linear segments. The referenced standard also mentions that the confinement provided by the adjacent material should be taken into account and this would imply even

a further reduction on the average value obtained thus increasing the difference. If the secant Young's modulus, or chord modulus as named in the American standard, is computed in accordance with ASTM C 1197 (ASTM International, 2014), then there is no need to use the dimensionless coefficient K_e to correct the values obtained by the ratio of cumulative stresses/strains. This formula would give an average Young's modulus of 203 MPa, which is in much better agreement with the value obtained from the slope of the stress/strain curves of both consolidation and double flat jack tests.

The values presented in the fourth column correspond to the estimation of cob's Poisson's ratio. Unfortunately, this property was not measured using any other testing method and it was not possible to make a comparison to verify the value obtained using the double flat jack test.

Finally, the last column of Table 5. 15 presents the values of the material's compressive strength obtained by fitting a logarithmic regression line into the stress/strain curve and subsequently extrapolating the value of the stress for a strain of approximately 2 %, strain value at which cob attains its peak strength according to Miccoli *et al*.(2014). These compressive strength results are in good agreement with the values obtained from the cob cylinders' compressive tests. In fact, a 2-sample t-test comparing the means of both groups of values with a confidence level of 95 % and a null hypothesis $H_0: \mu_1 - \mu_2 = 0$ returned a P-Value of 0.204 (the 95 % CI contained 0) thus leading to the acceptance of the null hypotheses and concluding that there was not a statistically significant difference between the means of both groups.

Regarding the failure patterns observed after the completion of the double flat jack tests (see Figure 5. 68), the presence of a consistent pattern in the form of a series of vertical cracks mainly concentrated at the centre of the material between the two horizontal flat jacks can be established. Nevertheless, it is necessary to note that establishing the actual location and extent of the cracks is not an easy, nor completely accurate task. As cracks, mainly caused by shrinkage, are present in the surface even before the wallette is subjected to any load it is not easy to differentiate the opening of new ones. The visual inspection was made more difficult by the typical irregularity of the wallettes' faces and by the presence of straw.

5.13 Conclusions

Six cob wallettes were successfully built in the laboratory using locally sourced materials and applying traditional construction methods. Furthermore, six cylinders were also prepared and tested under compression in order to provide an initial estimation of the mechanical properties of the material. The compression strength of cob was determined from the cob cylinders' compression tests and the values obtained are in good agreement, discrepancy of only 1 % for the average compressive strength, with values reported by Pullen and Scholz (2011) who applied similar testing methodology.

The importance of the consolidation of the wallettes highlighted by previous research (Lombillo, 2010) was verified in this thesis by comparing the stress/strain curves of the material before and after a six-days period of consolidation. Moreover, the stress/strain curves obtained from the second loading cycle of the wallettes allowed the estimation of the Young's modulus of the material.

After performing single flat jack tests on each one of the wallettes subjected to a known level of stress, a value of 0.51 was determined for the dimensionless coefficient K_e. It is advised to apply this coefficient value when investigation campaigns based on this minor destructive technique are performed on cob walls in order to obtain a more realistic value of the stresses to which the structure is being subjected to. This more realistic value would prevent the design and application of over invasive interventions that may endanger the value of the historical fabric.

The Young's modulus of the material estimated by taking into account the slope of the elastic range of the stress/strain curves was in good agreement with the values obtained from the slope of the consolidation process' stress/strain curves. As highlighted by the t-test, no statistically significant difference was observed between the mean values of both groups. On the other hand, the secant Young's modulus values obtained using EQ. 26 in accordance with RILEM MDT D.5 and corrected by using a value of $K_e = 0.51$ resulted to be roughly 50 % less than the values obtained from the slopes of the stress/strain curves. Therefore, it is advised not to correct the values obtained from the stress/strains ratios as per specified in ASTM C 1197, the uncorrected values give a more accurate estimation of cob's Young's modulus.

The values obtained for cob's Poisson's ratio by applying the double flat jack test are twice the values available in the literature. Unfortunately, no alternative measurement method was undertaken in this experimental campaign and the validity of the values obtained cannot be properly assessed.

The values of cob's mechanical properties obtained in this experimental campaign are summarised in Table 5.16. The determination of the mechanical properties of cob is of outmost importance for the conservation of cob historical buildings. The parameters determined with the application of the flat jack test may be used to define the constitutive material models, such as the ones explored in Chapter 4 of this thesis, needed to perform structural analysis of the structure. The quality of the diagnosis and, subsequently, of the design of interventions would be subjected to the amount of information available and to the quality of such information. Therefore, the methodology and the values presented in this chapter could greatly contribute to the conservation of cob buildings.

Table 5. 16. Cob's mechanical parameters values found in this experimental campaign.

Parameter	Value
Cylinders compressive strength (MPa)	0.697
Consolidation Young's modulus (MPa)	143.30
Dimensionless geometrical efficiency coefficient (-)	0.51
Flat Jack slope Young's modulus (MPa)	179.10
Flat Jack secant Young's modulus (MPa)	203.00
Flat Jack secant Young's modulus corrected (MPa)	103.50
Flat Jack Poisson's ratio (-)	0.28
Flat Jack compressive strength (MPa)	0.90

5.14 Workshops, public engagement and awareness increase

As this thesis aims at increasing awareness regarding the importance of conservation of vernacular architecture as identified on the ICOMOS Action Plan for the Future (ICOMOS, 2005), the experimental campaign was used to involve a great number of people and disseminate knowledge about the subject. Academics, technical staff, researchers, as well as undergraduate students and the general public participated in the different activities developed during this PhD related to the conservation of earthen vernacular buildings and the use of natural materials for sustainable construction purposes.

Several Professors and three Post-docs from the Department of CSEE actively participated with the author of this thesis in discussions and the progress of the experimental campaign. Eight international PhD students got involved in the construction of the wallettes. Furthermore, the project was explained to them and they were also asked about their previous experience with natural materials and traditional construction techniques on their own countries. The whole technical staff of the laboratory was greatly involved as well.

Two one-day workshops were run in the facilities of the Department of Civil, Structural and Environmental Engineering. In the first one undergraduate students from the department were invited to attend a morning presentation on the conservation of earthen vernacular buildings in Ireland and to participate in the construction of the wallettes of the experimental campaign. The second workshop was organized within the framework of the Trinity Green Week 2019. The Trinity Green Week is an annual environmentally themed event with a multitude of events to simulate the mind and engage the soul in creating better world citizens (Trinity College Dublin, 2019a). Both students and the general public were invited to participate in this second workshop. Participants to both workshops are shown in Figure 5. 70 (a) and Figure 5. 70 (b).

Finally, students of architecture from University College Dublin (UCD) and from the Dublin Technical University (DTU) were invited to the laboratory of TCD. The students were given a presentation on the aspects of this PhD thesis and of the experimental campaign performed. After this, a tour around the laboratory facilities was conducted where they could see the specimens that were built and tested along with the flat jack tests' equipment that was used in the experimental campaign (Figure 5. 70 (c)).

(a) (b) (c)

Figure 5. 70. Participants of (a) the undergraduate workshop, (b) the Trinity Green Week workshop and (c) UCD and DTU students of architecture.

Chapter 6: Learning from the past: parametrical analysis of cob walls

6.1 Introduction

We have much to learn from historic buildings. The fact that they are still standing is obvious, but unfortunately often not appreciated. Those buildings have resisted the forces of nature and decay for hundreds of years: something must have been done right and possibly could be replicated. Thus, the aim of this chapter is to analyse existing cob buildings to provide guidance for practitioners on the analysis of existent cob vernacular buildings and for the design of new sustainable and resilient ones.

Even though cob has a nonlinear structural behaviour, it presents an initial linear relationship between stress and strain up to a level of about 30 % of its peak strength (Miccoli *et al.*, 2014). This indicates that if the loads acting on the structure do not cause stresses beyond the linear elastic range of the material; cob structures may be studied with a simplified linear analysis. Linear analyses are easier and faster to perform than nonlinear analyses. Thus, it is of interest to find out up to what point the different values of the parameters influencing the response of the structure will allow to perform a simplified linear analysis with enough degree of accuracy. To verify this assumption and justify the use of linear analyses to study existent cob buildings, a linear parametric analysis has been performed. This analysis tries to identify the influence of geometric parameters, as well as external actions applied to the structure in the response of cob walls. The main objectives of this analysis are:

- To identify the levels assigned to the different parameters for which a linear analysis may still hold valid for the study of cob walls.
- To identify the possible failure modes of the walls if those limits are exceeded.

- To better understand the advantages and disadvantages of a simplified linear analysis for the study of cob walls.

Furthermore, the parametric analysis presented in this chapter could be used to verify whether the wall geometries used in practice are adequate and inform in the design of new cob buildings. The design of new cob buildings would not be further discussed since that topic is outside the scope of this thesis.

The models aim to cover representative remaining earthen vernacular buildings in Ireland, which typically are single storied, regular in plan, longer than wider and without rigid diaphragms to ensure a "*box-like*" structural behaviour. The methodology and results presented in this chapter could be extrapolated for its application on buildings with similar characteristics elsewhere. The influence of wall voids, gables, chimneys, or the variability on the mechanical properties of cob in the structural behaviour of the walls is not covered in this chapter, this may be addressed in further works.

6.2 Methodology

The methodology followed to perform the parametric analysis of cob walls consisted in three stages; parameters definition, analysis and interpretation of the results (see Figure 6. 1). Two analysis approaches were followed with the aim of exploring the pros and cons of each of them and provide alternatives to practitioners: linear elastic FEM analysis and macro elements kinematic limit analysis.

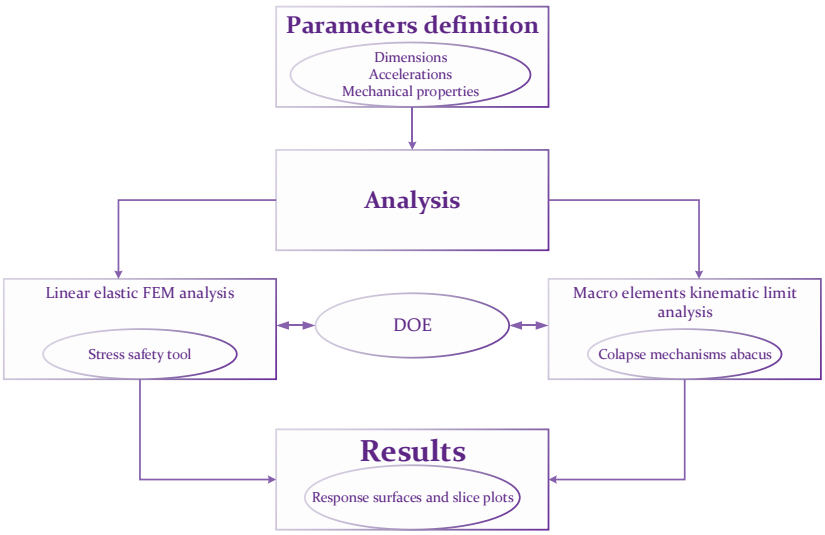

Figure 6. 1. Multilevel approach for the simplified analysis of cob walls.

6.2.1 Parameters

The parameters studied were the wall's dimensions and the accelerations to which cob walls may be subjected to during earthquakes. The "*best-guess*" fixed cob's mechanical properties values used in this parametric analysis correspond with those reported by Miccoli *et al*. (2014), as that was one of the most recent and complete studies done to determine cob's properties. The values are summarised in Table 6. 1 and Table 6. 2, respectively.

Table 6. 1. Cob's material properties.

Property	Value
Density (kg/m3)	1475
Young's modulus (Pa)	1.021×10^9
Poisson's ratio (-)	0.14

Table 6. 2. Cob's strength values.

Parameter	Tension	Compression
Yield strength (MPa)	0.062	0.477
Ultimate strength (MPa)	0.207	1.590

Currently in Ireland, a National Inventory of Architectural Heritage (NIAH) is being compiled. The aim of that work consists on "… *highlighting a representative sample of the architectural heritage of each county and to raise awareness of the wealth of architectural heritage in Ireland*" (NIAH, 2019). Unfortunately, the NIAH is limited to providing an overall description of the buildings and a summarised appraisal of their value; it does not record technical information which may be of interest for their study. Dimensions of traditional earthen vernacular buildings in Ireland are only generally recorded by several authors (Young, 1780, Danaher, 1957a, Gailey, 1984, Pfeiffer and Shaffrey, 1990, Keefe, 1993) and unfortunately there is not a comprehensive database containing such information. The geometric parameters adopted correspond to the values reported by such researchers based on studies of surviving cob buildings and records of historical cob buildings in Ireland. These values are summarized in Table 6. 3.

Table 6. 3. Cob walls geometric parameters values.

Parameter	Minimum value	Maximum value
Length (m)	3.0	9.0
Height (m)	1.8	3.05
Thickness (m)	0.4	0.9

Finally, regarding the dynamic actions acting on cob walls, Ireland is a region characterised by a low seismic activity. This fact may justify the use of simplified methods of analysis to describe cob buildings' structural behaviour as it is presumed that

the surviving vernacular cob buildings would not experience nonlinear behaviour caused by lateral accelerations. The same can also be said for newly constructed cob buildings (out of scope for this thesis though).

The Seismic Hazard Harmonization in Europe (SHARE) project produced a series of ground motion hazard maps for various spectral ordinates and exceedance probabilities in Europe. Figure 6. 2 shows the PGA (in g) map of Europe for a 10 % exceedance probability in 50 years. The acceleration values for a low seismicity area, and in this case the type of area correspondent to Ireland, can go from 0 to 0.10 g. The minimum and maximum values adopted for this parametric analysis were of 0.05 g and 0.10 g (0.4905 m/s^2 and 0.981 m/s^2), respectively. Even though these acceleration values seem to be quite small, damage in earthen structures has been reported at similar intensities (Webster, 2006). Furthermore, as it is intended that the methodology presented in this chapter could be interpolated and applied in other regions where buildings with similar characteristics exists, i.e. UK and North of France, it was considered as appropriate to explore the effect of earthquakes in cob structures.

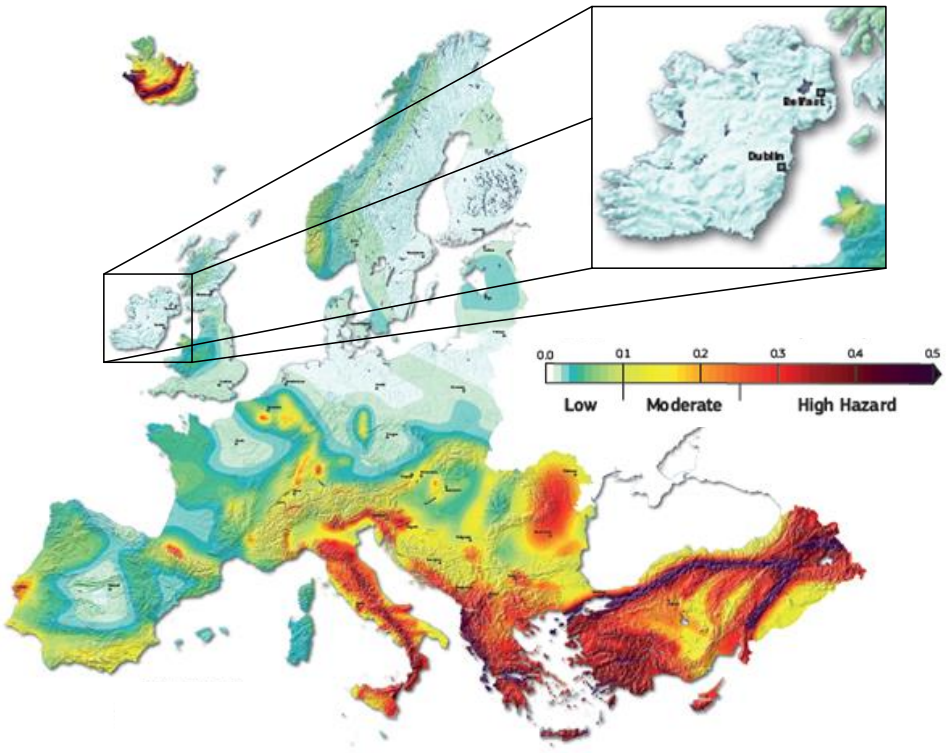

Figure 6. 2. PGA (in g) map of Europe for a 10 % exceedance probability in 50 years (Giardini et al., 2014).

The simplified models studied in this parametric analysis are static models. The dynamic accelerations caused by an earthquake in an existent cob structure were

simplified into static inertial forces by using D'Alembert's principle. This principle stablishes that "*a mass develops an inertial force proportional to its acceleration and opposing it*" (Clough Ray and Joseph, 1995).

It is also acknowledged that:

- Cob buildings in Ireland are subjected to lateral wind loads.
- This parametric analysis might give design guidance for/or rule out the suitability of cob in some earthquake prone regions.

Further work, not discussed within this thesis, would be needed to extend the scope of this parametric analysis and verify these two statements.

6.2.2 Linear elastic FEM analysis

A linear elastic FEM analysis was performed using ANSYS (ANSYS Inc., 2017). It was decided to study the response of the walls subjected to both in-plane as well as out-of-plane behaviour due to the multidirectional nature of dynamic actions. For either case, a free-standing cob wall fixed (translational degrees of freedom constrained) at its bottom was simulated. This assumption is justified by the fact that most earthen vernacular buildings in Ireland do not have rigid diagram roofs (lack of bond beam, roof trusses directly placed on top of cob wall). Thus, cob walls do not present a "*box-like*" behaviour and most of the time act individually to support the actions action upon them. Moreover, vertical cracks are quite common, especially at corners (see Figure 6.3), which would cause the detachment of perpendicular wall connections easing their out-of-plane overturning under horizontal loads.

These assumptions were adopted with the aim of simulating a general "*worst-case scenario*" in which a cob wall, part of a surviving cob building in Ireland, may be found. As discussed in previous chapters, a detailed study of the structure is desirable to avoid the design of over conservative interventions, which may endanger the historic fabric. Therefore, the assumptions adopted for specific case studies must be based in the results provided by a structural integrity inspection after which the following may be found:

- Wall interconnectivity (perpendicular walls providing out-of-plane support).
- Top restrain at roof level.

- *"Box-like"* behaviour (provided by a strengthening/retrofitting intervention).

Any of these factors would improve the structural response of the building and if they are neglected, the design of the intervention may result to be too invasive. On the other hand, wall voids and the presence of damage or decay would diminish the structure's capacity. To perform any detailed conservation study the iterative process presented in Figure 2. 2 must be followed.

(a) (b)

Figure 6. 3. Vertical cracks in a cob building located in County Kildare, Ireland (pay special attention to the cracks at the corners running all along the wall's height).

The walls were subjected to their own weight, to an external force at their top simulated as a concentrated mass, representing the loads transferred by the roof, and finally to a horizontal acceleration representing the effects of dynamic loads on the wall. The point mass at the top of the wall was assumed as that of a thatch roof with a thickness of 305 mm (including battens) and a self-weight of 450 N/m^2 (YS, 2019) with a tributary span of 3 m giving a value of 137.6 kg/m for every meter of wall length. The setup of the in-plane and of the out-of-plane models are shown in Figure 6. 4 (a) and Figure 6. 4 (b), respectively. The finite element used was the SOLID186 (ANSYS Inc., 2013d, 2013b) and the constitutive material model adopted was a simple linear elastic model.

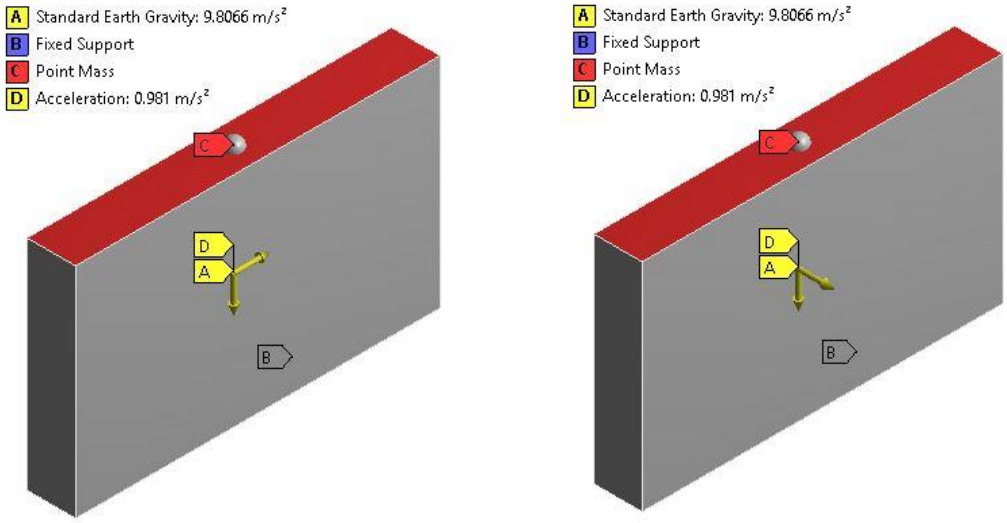

(a) (b)

Figure 6. 4. FEM model setup for (a) in-plane analysis and (b) out-of-plane analysis.

The response of the structure was monitored with the help of a Mohr-Coulomb stress safety tool. This tool is based on the Mohr-Coulomb theory for brittle materials and uses the principle stress values to determine the occurrence of failure. Safety factors for yielding, F_{ys}, and for the ultimate, F_{us}, capacity of the material are computed with EQ. 27 and EQ. 28, respectively (ANSYS Inc., 2013e).

$$F_{ys} = \left(\frac{\sigma_1}{S_{yt}} + \frac{\sigma_3}{S_{yc}}\right)^{-1} \qquad \textit{EQ. 27}$$

$$F_{us} = \left(\frac{\sigma_1}{S_{ut}} + \frac{\sigma_3}{S_{uc}}\right)^{-1} \qquad \textit{EQ. 28}$$

Where:

σ_1 and σ_3 = Maximum and minimum principal stresses.

S_{ut} and S_{uc} = Material ultimate tensile and compressive strengths.

S_{yt} and S_{yc} = Material yielding tensile and compressive strengths.

This stress tool evaluates EQ. 27 and EQ. 28 through the whole model taking into account the principle stresses, σ_1 and σ_3, developed at each particular location. Strictly speaking, the tool provides a distribution of safety factors throughout the model as it bases its calculations on the independent distributions of maximum and minimum stresses and not in the absolute principal stresses, developed most likely at two different

locations of the model. Therefore, the minimum value of such distribution is reported as the minimum factor of safety. The compressive strength of common brittle materials is usually much greater than their tensile strength. In this analysis, this assumption is considered to be valid for cob as well. In fact, it is assumed that cob's tensile ultimate strength corresponds to only 13 % of its compressive ultimate strength (Miccoli *et al.*, 2017). The Mohr-Coulomb stress safety tool takes direct account of this theory and is often considered to provide conservative results (ANSYS Inc., 2013e).

6.2.3 Macro elements kinematic limit analysis

A second method of analysis was implemented to compare the results obtained with the simplified FEM analysis. This method is based on the abacus of collapse mechanisms reported by the New Integrated Knowledge based approaches to the protection of cultural heritage from Earthquake–induced Risk (NIKER) European project (NIKER, 2013). The abacus of collapse mechanisms basically classifies the collapse mechanisms into two categories: in-plane and out-of-plane mechanisms.

The identified in-plane damage caused by horizontal loads consist mainly in rocking, sliding shear failure and diagonal cracking (see Figure 6. 5). On the other hand, the out-of-plane damages are mainly characterized by the development of vertical cracks. Vertical cracks may either start from the bottom or from the top of the wall and some run through the entire height of the wall. This causes the separation of important segments of the wall and can lead to the overturning of the element (see Figure 6. 6).

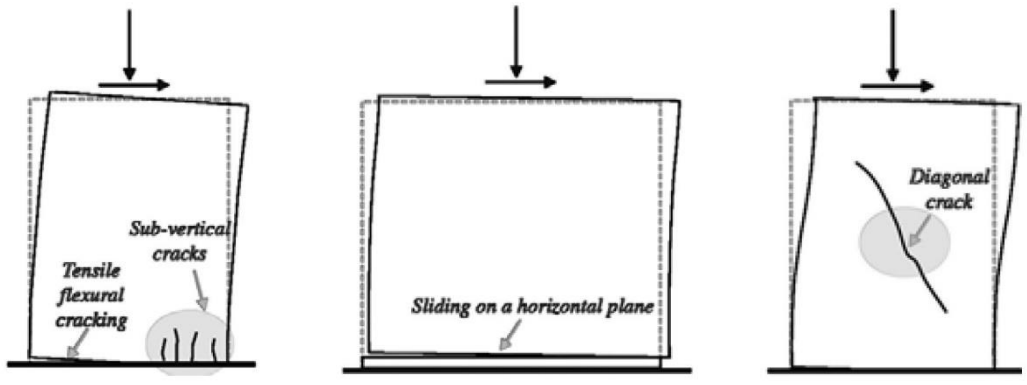

Figure 6. 5. In-plane typical damages caused by horizontal loads; (a) rocking, (b) sliding shear and (c) diagonal cracking (NIKER, 2010).

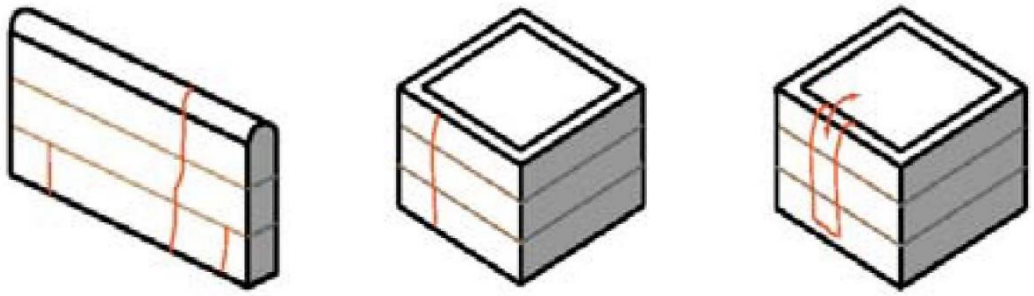

(a) (b) (c)

Figure 6. 6. Out-of-plane typical damages observed in cob walls (NIKER, 2010).

The macro elements kinematic limit analysis consists basically in finding the equilibrium condition under which, for a certain value of α coefficient, the studied collapse mechanism will form. Thus, α is defined (see EQ. 29) as the seismic mass multiplier that leads to the formation of the collapse mechanism assumed and eventually to the element failure (Valluzzi *et al.*, 2007):

$$\alpha = \frac{a}{g} \qquad \textit{EQ. 29}$$

Where:

a = Ground acceleration.

g = Gravity acceleration.

The out-of-plane mechanism considered in this parametric analysis is presented in Figure 6. 7. The thickness of the wall is represented by T_{wall}, its height by H_{wall} and its length by L_{wall}. It is assumed that cob has zero tensile strength and that no internal sliding would happen, in other words, the walls behave as rigid bodies and rotate while supported in two idealized pined supports. For the case shown in Figure 6. 7 (a), it was assumed that cob has infinite compressive strength and the bottom support is located at the edge of the wall. On the other hand, for the case presented in Figure 6. 7 (b) the compressive strength of the material, f_c, is taking into account and the bottom support is located at a distance t from the edge of the wall (this is a conservative assumption, a more realistic one would consider the location of the support at a distance of $t/3$ from the edge of the wall). The force *P* represents the self-weight of the wall and the force *N* the external loads transferred from the roof. To compute N a thatch roof with a thickness of 305 mm

(including battens) and a self-weight of 450 N/m^2 (YS, 2019) has been considered with a tributary span of 3 m giving a value of 1350 N/m for every meter of wall length.

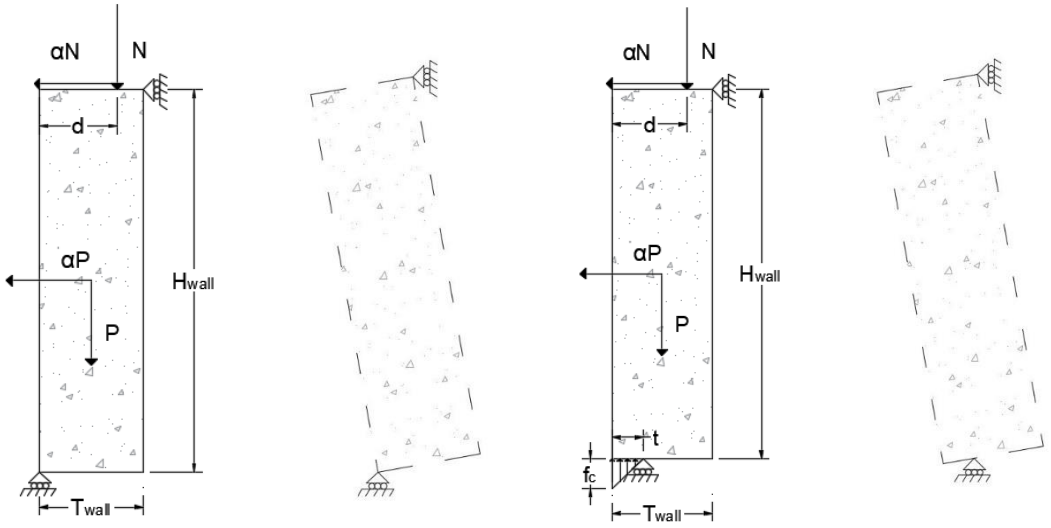

(a) (b)

Figure 6. 7. Out-of-plane mechanisms (a) assuming infinite compressive strength and (b) accounting for the compressive strength of the material, f_c.

The equilibrium condition of the rigid body for the case presented in Figure 6. 7 (a) is expressed in EQ. 30 from where the expression to compute the α coefficient is obtained (see EQ. 31). It is worth noting that for this parameter analysis the distance d was assumed to be half of the wall thickness, thus, placing the external loads over the centroid of the wall.

$$\alpha P\left(\frac{H_{wall}}{2}\right) + \alpha N(H_{wall}) - P\left(\frac{T_{wall}}{2}\right) - N(d) = 0 \qquad \textit{EQ. 30}$$

$$\alpha = \frac{P\left(\frac{T_{wall}}{2}\right) + N(d)}{P\left(\frac{H_{wall}}{2}\right) + N(H_{wall})} \qquad \textit{EQ. 31}$$

To find the equilibrium condition of the rigid body shown in Figure 6. 7 (b), it is necessary to find the value of t at which the support is located from the edge of the wall. This distance is obtained by equating the vertical forces acting on the wall with the force developed at the support as a function of the material compressive strength, f_c. Thus, for a unitary segment of wall (1 m length):

$$t = \frac{2(P+N)}{f_c * 1} \quad \textit{EQ. 32}$$

And the seismic mass multiplier is calculated using EQ. 33.

$$\alpha = \frac{P\left(\frac{T_{wall}}{2} - t\right) + N(d - T_{wall})}{P\left(\frac{H_{wall}}{2}\right) + N(H_{wall})} \quad \textit{EQ. 33}$$

The in-plane mechanism considered in this parametric analysis is presented in Figure 6. 8. It is the result of diagonal cracking on the cob wall. For the case shown in Figure 6. 8 (a) it was assumed that cob has infinite compressive strength (along with zero tensile strength and no internal sliding) and the bottom support is located at the edge of the wall whereas that for the case presented in Figure 6. 8 (b), the compressive strength of the material, f_c, is taken into account and the bottom support is located at a distance t from the edge of the wall (this is a conservative assumption, a more realistic one would consider the location of the support at a distance of $t/3$ from the edge of the wall). For the in-plane analysis the distance d was considered to be equal to half the distance between the wall supports.

The formulas used to calculate the seismic mass multiplier coefficient for case (a) and case (b) are presented in EQ. 34 and EQ. 36, respectively. The value of t was calculated using EQ. 35. These equations were obtained by applying equilibrium equations of the vertical stabilizing forces, P and N, and the horizontal destabilizing forces, αP and αN.

$$\alpha = \frac{N(d) + P\left(\frac{L_{wall}}{3}\right)}{NH_{wall} + P\left(\frac{2H_{wall}}{3}\right)} \quad \textit{EQ. 34}$$

$$t = \frac{P_2 + N}{\frac{T_{wall} f_c}{2} - H_{wall} T_{wall} \gamma_{cob} g + \frac{H_{wall} T_{wall} \gamma_{cob} g}{2}} \quad \textit{EQ. 35}$$

$$\alpha = \frac{N(d) + P_2\left(\frac{L_{wall} - t}{3}\right) - P_1\left(\frac{t}{2}\right)}{NH_{wall} + P_2\left(\frac{2H_{wall}}{3}\right) + P_1\left(\frac{H_{wall}}{2}\right)} \quad \textit{EQ. 36}$$

Where γ_{cob} represents cob's density. The values of α for the four mechanisms presented were computed using MATLAB (MATLAB, 2017) scripts.

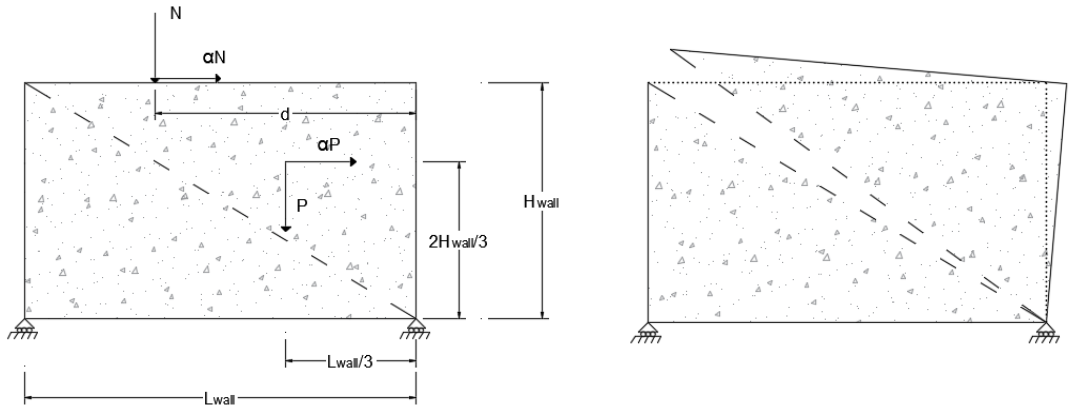

(a)

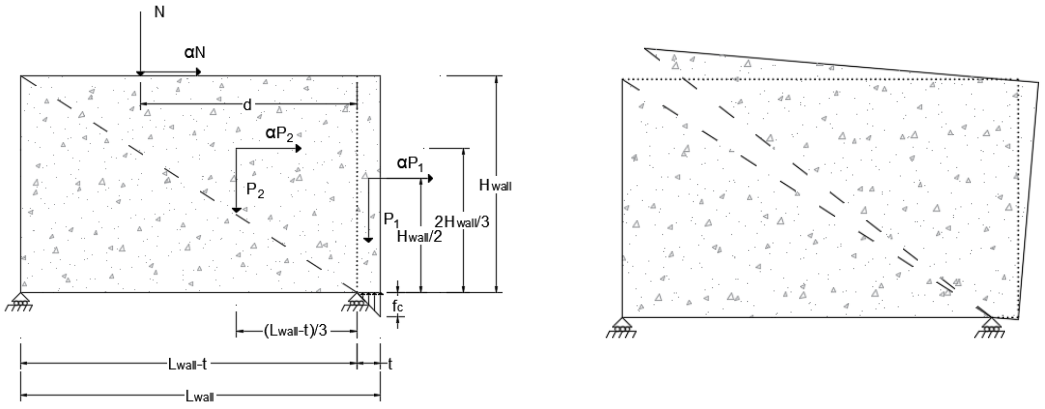

(b)

Figure 6. 8. In-plane mechanisms (a) assuming infinite compressive strength and (b) accounting for the compressive strength of the material, f_c.

6.2.4 Design of experiments

A DOE technique was used for both the linear elastic FEM analysis and the macro elements kinematic limit analysis to obtain meaningful results and, at the same time, to reduce the computational effort required. The DOE for the linear elastic FEM analysis was performed directly in ANSYS using the design exploration module (ANSYS Inc., 2013a), whereas the DOE for the macro elements kinematic limit analysis was performed using the statistics software Minitab (Minitab, 2013). Nevertheless, the same method was applied for both analyses.

The CCD method was implemented with the objective of studying the influence of the input parameters (geometric and accelerations for the FEM models and geometric

for the limit analysis models) in the responses of the models (F_{ys} and F_{us} for the FEM models and seismic mass multiplier for the limit analysis models). A full CCD was selected for the design type as this method is available as the default option in both applications and is the most commonly used method for the design of experiments to create response surfaces (Minitab, 2003). Adequate values for the distance of the star points were selected based on EQ. 37 in order to ensure rotatability and provide a constant prediction variance. The influence of this parameter in the design points generated by the CCD is shown in Figure 6.9 where the DOE of two factors with two levels each is illustrated. The blue points represent the cube design points, the red point is the centre point and the yellow points are the star points, also known as axial points.

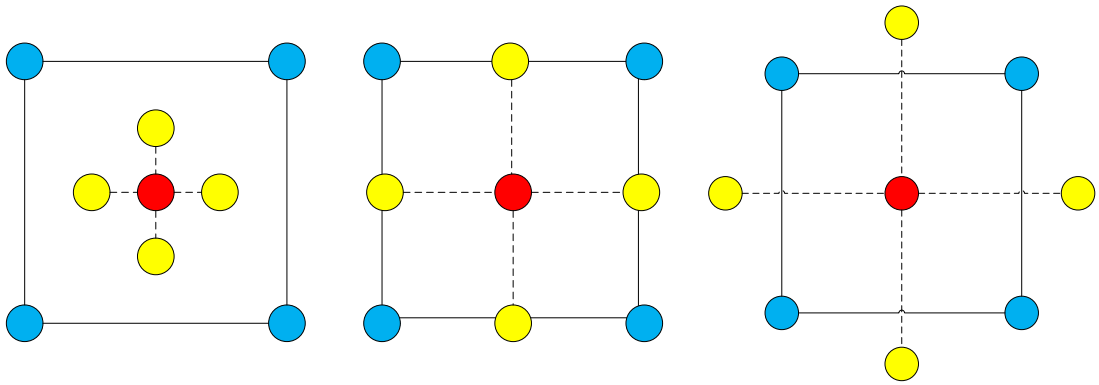

(a) (b) (c)

Figure 6. 9. Star points for values of (a) a_{CCD}<1, (b) a_{CCD} =1 and (c) a_{CCD} >1.

$$a_{CCD} = F_{CCD}^{1/4} \qquad \text{EQ. 37}$$

Where a_{CCD} is the axial spacing of the design points and F_{CCD} is the number of points in the factorial part of the design, usually $F_{CCD} = 2^k$, where k is the number of factors. More details about the CCD method can be consulted elsewhere (Montgomery, 2011).

Finally, the design points generated with the CCD were used to build the response surfaces by applying a full 2nd-order polynomial algorithm. Then, the main effect and interaction effect plots were analysed and a second response surface was created taking into account only those statistically significant terms (P-Value ≤ 0.05) to simplify the regression model.

For both FEM and macro elements models the mechanical properties of cob were maintained constant. The wall geometric parameters and the levels of acceleration were

used as input parameters for the FEM models in the DOE and the yield and ultimate safety factors computed were used as output parameters. On the other hand, only the geometric parameters were used as input parameters for the macro elements models and the computed α coefficients were the correspondent output parameters. The ranges adopted for the input geometric parameters were presented in Table 6. 3, whereas that the acceleration ranges adopted, which correspond to the low seismic hazard range, were obtained from Figure 6. 2.

6.3 Results and discussion

A free-standing wall fixed at its base and subjected to in-plane forces may be idealized as a plane-stress problem where the thickness of the wall could be neglected without significantly affecting the results. On the other hand, the same wall subjected to out-of-plane forces could be idealized as a plane strain problem, and in this case, the length of the wall would not affect the results. The results of the parametric analysis performed have confirmed these simple, but important, concepts and would are described in more detail in this section.

6.3.1 FEM out-of-plane analysis

The DOE using a CCD rotatability design with four factors (length, height, thickness and acceleration) generated 49 design points. The order in which the design points were generated by the CCD was random to avoid the effect of any nuisance variable in the output parameters (randomization is of paramount importance in the design of physical experiments, but it does not affect the numerical parametric analysis performed in this thesis). The values adopted in each one of these design points for each one of the parameters are presented in Table 6. 4. Table 6. 4 also presents the value calculated for both F_{ys} and F_{us} corresponding to each design point.

The minimum value computed for F_{ys} is equal to 3. This value was obtained for a wall with 4.5 m length, 2.74 m height, 0.53 m thickness, and subjected to a lateral acceleration of 0.86 m/s^2.

Almost all values computed for F_{us} are equal to 15, which is the cap value provided by ANSYS, and this means that the safety factor is equal or greater than 15.

Unfortunately, this cap value prevented the statistical analysis to develop any meaningful plots of the effect each input parameter has in F_{us}. The only useful conclusion that could be drawn from this situation is that within the rages explored of the input parameters the walls would not be subjected to stress values that may lead to their collapse.

Table 6. 4. Design points and computed responses' values for the out-of-plane FEM model.

Run Order	Length (m)	Height (m)	Thickness (m)	Acceleration (m/s^2)	F_{ys}	F_{us}
1	6.00	2.43	0.65	0.74	5.1	15.0
2	3.00	2.43	0.65	0.74	5.2	15.0
3	4.50	2.43	0.65	0.74	5.2	15.0
4	9.00	2.43	0.65	0.74	5.1	15.0
5	7.50	2.43	0.65	0.74	5.1	15.0
6	6.00	1.80	0.65	0.74	7.6	15.0
7	6.00	2.11	0.65	0.74	6.2	15.0
8	6.00	3.05	0.65	0.74	3.8	12.6
9	6.00	2.74	0.65	0.74	4.4	14.6
10	6.00	2.43	0.40	0.74	3.4	11.4
11	6.00	2.43	0.53	0.74	4.8	15.0
12	6.00	2.43	0.90	0.74	5.6	15.0
13	6.00	2.43	0.78	0.74	5.5	15.0
14	6.00	2.43	0.65	0.49	5.9	15.0
15	6.00	2.43	0.65	0.61	5.5	15.0
16	6.00	2.43	0.65	0.98	4.5	15.0
17	6.00	2.43	0.65	0.86	4.8	15.0
18	4.50	2.11	0.53	0.61	6.3	15.0
19	5.25	2.27	0.59	0.67	5.7	15.0
20	7.50	2.11	0.53	0.61	6.2	15.0
21	6.75	2.27	0.59	0.67	5.7	15.0
22	4.50	2.74	0.53	0.61	4.4	14.8
23	5.25	2.58	0.59	0.67	4.8	15.0
24	7.50	2.74	0.53	0.61	4.4	14.6
25	6.75	2.58	0.59	0.67	4.8	15.0
26	4.50	2.11	0.78	0.61	7.0	15.0
27	5.25	2.27	0.71	0.67	6.0	15.0
28	7.50	2.11	0.78	0.61	6.9	15.0
29	6.75	2.27	0.71	0.67	6.0	15.0
30	4.50	2.74	0.78	0.61	5.0	15.0
31	5.25	2.58	0.71	0.67	5.1	15.0
32	7.50	2.74	0.78	0.61	5.0	15.0
33	6.75	2.58	0.71	0.67	5.1	15.0
34	4.50	2.11	0.53	0.86	5.4	15.0
35	5.25	2.27	0.59	0.80	5.3	15.0
36	7.50	2.11	0.53	0.86	5.4	15.0

Table 6. 4. Design points and computed responses' values for the out-of-plane FEM model. (Continuation)

Run Order	Length (m)	Height (m)	Thickness (m)	Acceleration (m/s^2)	F_{ys}	F_{us}
37	6.75	2.27	0.59	0.80	5.3	15.0
38	4.50	2.74	0.53	0.86	3.0	10.0
39	5.25	2.58	0.59	0.80	4.5	14.9
40	7.50	2.74	0.53	0.86	3.1	10.3
41	6.75	2.58	0.59	0.80	4.5	14.9
42	4.50	2.11	0.78	0.86	6.3	15.0
43	5.25	2.27	0.71	0.80	5.6	15.0
44	7.50	2.11	0.78	0.86	6.2	15.0
45	6.75	2.27	0.71	0.80	5.6	15.0
46	4.50	2.74	0.78	0.86	4.4	14.7
47	5.25	2.58	0.71	0.80	4.8	15.0
48	7.50	2.74	0.78	0.86	4.3	14.5
49	6.75	2.58	0.71	0.80	4.7	15.0

If the values of the first five runs are analysed, where height, thickness, and acceleration are constant, and the length values varied, it can be observed that the values of F_{ys} are kept almost constant. A more effective way of interpreting the numbers presented in Table 6. 4 is by analysing the main effects and interaction effects plots presented in Figure 6. 10 and Figure 6. 11, respectively (only the plots for F_{ys} are presented and discussed). The main effect plots show that the value of F_{ys} are not influenced by the length of the wall (the first curve to the left of Figure 6. 10 is almost constant). On the other hand, height, thickness and acceleration proved to be parameters influencing F_{ys}.

It is expected that the higher and the thinner a wall is, the more critical it would be its safety when subjected to out-of-plane forces. This is confirmed by the results obtained from the parametric analysis as can be seen in the curves corresponding to wall height and wall thickness from Figure 6. 10. The higher is the value for the height parameter, the lower is F_{ys}. On the other hand, the higher is the thickness, the higher is F_{ys}. The second and third curves of Figure 6. 10, corresponding to the main effects of wall height and thickness, show a non-linear relationship with F_{ys} whereas that the relationship of the acceleration seems to be linear. Furthermore, F_{ys} also seems to be affected by the thickness/acceleration interaction since the three curves seem to converge for the higher values of thickness, as can be seen in the lower right curve of Figure 6. 11.

These observations regarding the influence of the input parameters on F_{ys} can be verified by analysing the P-Values obtained from the Analysis of Variance (ANOVA), which are presented Table 6. 5, of the fitted full 2nd-order polynomial model. At a significant level of 0.05, terms with a P-Value ≤ 0.05 are considered significant (Table 6. 5). Therefore, it can be observed that effectively the length of the wall does not affect the response of the wall (P-Value = 0.152), both height and thickness quadratic terms resulted to be significant (as previously highlighted based on the shape of the corresponding curves of Figure 6. 10), and finally, the only significant interaction term corresponds to the thickness/acceleration interaction (P-Value = 0.003).

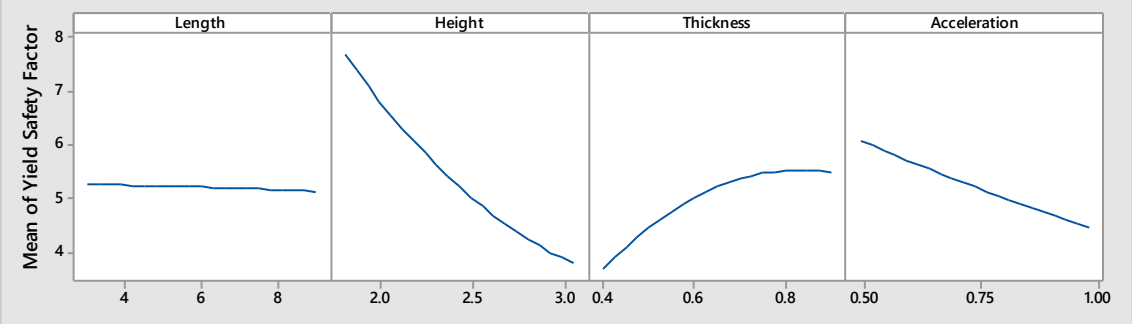

Figure 6. 10. Main effects plots for the out-of-plane FEM model.

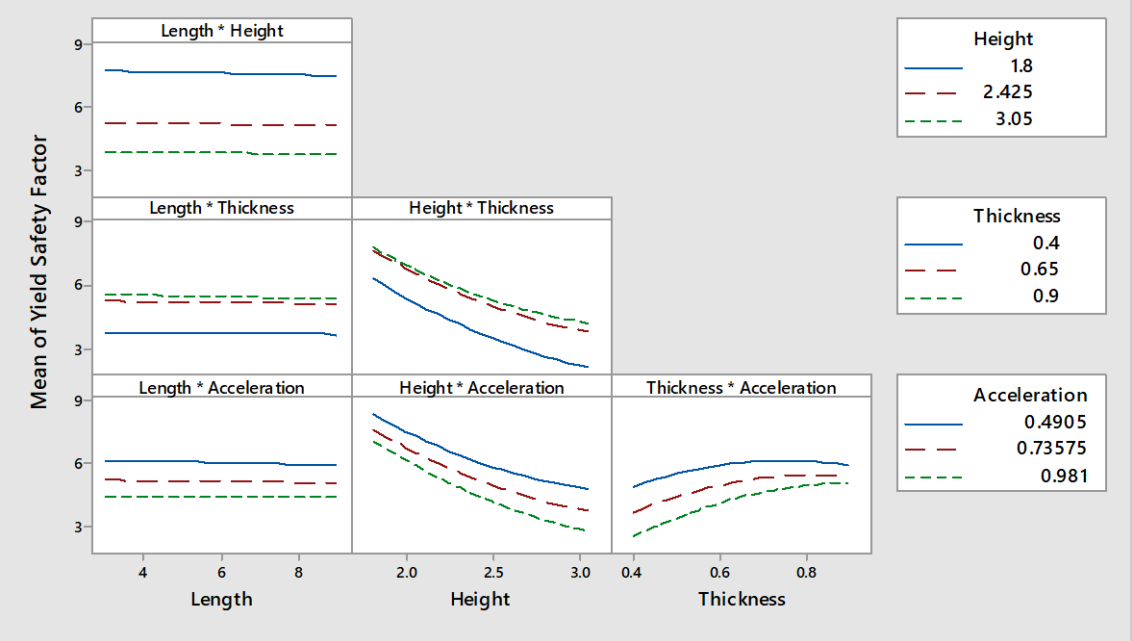

Figure 6. 11. Interaction effects plots for the out-of-plane FEM model.

The full quadratic model was refined by removing the non-significant terms. By taking into account only those statistically significant terms from Table 6. 5 the

expression shown in EQ. 38 was obtained (all coefficients of the refined regression model presented a VIF equal to one and the refined model summary properties are presented in

Table 6. 6.). EQ. 38 can be used to estimate the value of F_{ys} for every combination of wall height (H_{wall} in m), thickness (T_{wall} in m) and lateral acceleration (a in m/s^2) within the range of values explored by the analysis presented in this thesis. In this equation the length of the wall is not included, as its effect on the response is nonsignificant, and this confirms the comment made at the beginning of the section regarding the fact that the length of the wall was expected not to influence the out-of-plane response of the wall.

$$F_{ys} = 19.51 - 9.55H_{wall} + 11.76T_{wall} - 7.41a + 1.33H_{wall}^2 - 9.9T_{wall}^2 + 6.34T_{wall}a \qquad EQ.\ 38$$

If EQ. 38 is evaluated for a wall height of 3.05 m, a thickness of 0.40 m and an acceleration of 0.981 m/s^2, then, $F_{ys} = 1.1$. This indicates that even under the most adverse combination of values for the parameters explored, and based on the assumptions adopted, the material would not reach its yield point.

Table 6. 5. ANOVA for the out-of-plane FEM model.

Source	DF	Adj SS	Adj MS	F-Value	P-Value
Model	14	40.5502	2.8964	183.6900	0.0000
Linear	4	38.9268	9.7317	617.1600	0.0000
Length	1	0.0338	0.0338	2.1500	0.1520
Height	1	28.0922	28.0922	1781.5400	0.0000
Thickness	1	5.9092	5.9092	374.7500	0.0000
Acceleration	1	4.8916	4.8916	310.2100	0.0000
Square	4	1.3931	0.3483	22.0900	0.0000
Length*Length	1	0.0004	0.0004	0.0200	0.8760
Height*Height	1	0.5510	0.5510	34.9500	0.0000
Thickness*Thickness	1	0.7716	0.7716	48.9300	0.0000
Acceleration*Acceleration	1	0.0066	0.0066	0.4200	0.5220
2-Way Interaction	6	0.2302	0.0384	2.4300	0.0460
Length*Height	1	0.0029	0.0029	0.1900	0.6700
Length*Thickness	1	0.0022	0.0022	0.1400	0.7120
Length*Acceleration	1	0.0028	0.0028	0.1800	0.6740
Height*Thickness	1	0.0263	0.0263	1.6700	0.2050
Height*Acceleration	1	0.0355	0.0355	2.2500	0.1430
Thickness*Acceleration	1	0.1605	0.1605	10.1800	0.0030
Error	34	0.5361	0.0158		

Table 6. 6. Refined model summary for the out-of-plane FEM model.

S	R-sq	R-sq (adj)	R-sq (pred)
0.1241	98.43 %	98.2 %	97.08 %

EQ. 38 was also used to create the response surfaces shown in Figure 6. 12. Each one of the response surfaces show information regarding the effect of two input parameters, while the third one is kept constant at its more critical value, in the response, F_{ys}. These response surfaces reflect the quadratic effect the input parameters have in the response as initially observed in the main effect plots.

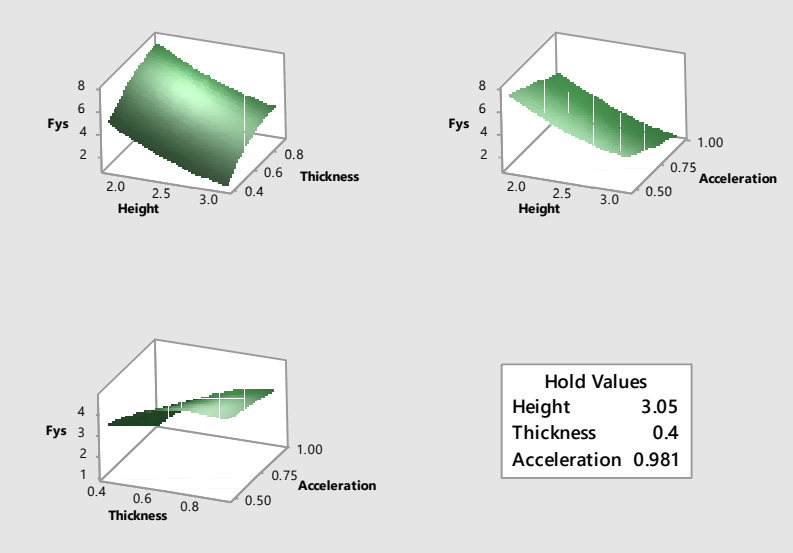

Figure 6. 12. Response surfaces for F_{ys} for the out-of-plane FEM model.

6.3.2 FEM in-plane analysis

The DOE using a CCD rotatability design with four factors (length, height, thickness and acceleration) generated 49 design points. The values adopted in each one of these design points for each one of the parameters are presented in Table 6. 7. Table 6. 7 also presents the values calculated for both F_{ys} and F_{us} corresponding to each design point.

The minimum value computed for F_{ys} is equal to 5.52. This value was obtained for a wall with 6 m length, 3.05 m height, 0.65 thickness, and subjected to an acceleration of 0.74 m/s^2.

As can be seen, all values computed for F_{us} are equal to 15, which is the automatic cap value used by ANSYS, and this prevented the statistical analysis to develop any meaningful plots of the effect each input parameter has in F_{us}. Once again, all that can be

said from those values is that within the rages explored of the input parameters the walls would not be subjected to stress values that may lead to their collapse.

Table 6. 7. Design points and computed responses' values for the in-plane FEM model.

Run Order	Length (m)	Height (m)	Thickness (m)	Acceleration (m/s^2)	F_{ys}	F_{us}
1	6.00	2.43	0.65	0.74	7.1	15.0
2	3.00	2.43	0.65	0.74	7.0	15.0
3	4.50	2.43	0.65	0.74	7.1	15.0
4	9.00	2.43	0.65	0.74	7.0	15.0
5	7.50	2.43	0.65	0.74	7.0	15.0
6	6.00	1.80	0.65	0.74	9.8	15.0
7	6.00	2.11	0.65	0.74	8.2	15.0
8	6.00	3.05	0.65	0.74	5.5	15.0
9	6.00	2.74	0.65	0.74	6.2	15.0
10	6.00	2.43	0.40	0.74	7.1	15.0
11	6.00	2.43	0.53	0.74	7.1	15.0
12	6.00	2.43	0.90	0.74	7.1	15.0
13	6.00	2.43	0.78	0.74	7.1	15.0
14	6.00	2.43	0.65	0.50	7.5	15.0
15	6.00	2.43	0.65	0.62	7.3	15.0
16	6.00	2.43	0.65	0.98	6.7	15.0
17	6.00	2.43	0.65	0.86	6.9	15.0
18	4.50	2.11	0.53	0.62	8.5	15.0
19	5.25	2.27	0.59	0.68	7.8	15.0
20	7.50	2.11	0.53	0.62	8.4	15.0
21	6.75	2.27	0.59	0.68	7.8	15.0
22	4.50	2.74	0.53	0.62	6.5	15.0
23	5.25	2.58	0.59	0.68	6.8	15.0
24	7.50	2.74	0.53	0.62	6.4	15.0
25	6.75	2.58	0.59	0.68	6.8	15.0
26	4.50	2.11	0.78	0.62	8.6	15.0
27	5.25	2.27	0.71	0.68	7.7	15.0
28	7.50	2.11	0.78	0.62	8.5	15.0
29	6.75	2.27	0.71	0.68	7.7	15.0
30	4.50	2.74	0.78	0.62	6.5	15.0
31	5.25	2.58	0.71	0.68	6.7	15.0
32	7.50	2.74	0.78	0.62	6.4	15.0
33	6.75	2.58	0.71	0.68	6.7	15.0
34	4.50	2.11	0.53	0.86	8.0	15.0
35	5.25	2.27	0.59	0.80	7.6	15.0
36	7.50	2.11	0.53	0.86	8.0	15.0
37	6.75	2.27	0.59	0.80	7.5	15.0
38	4.50	2.74	0.53	0.86	6.0	15.0

Table 6. 7. Design points and computed responses' values for the in-plane FEM model. (Continuation)

Run Order	Length (m)	Height (m)	Thickness (m)	Acceleration (m/s^2)	F_{ys}	F_{us}
39	5.25	2.58	0.59	0.80	6.6	15.0
40	7.50	2.74	0.53	0.86	6.0	15.0
41	6.75	2.58	0.59	0.80	6.6	15.0
42	4.50	2.11	0.78	0.86	8.1	15.0
43	5.25	2.27	0.71	0.80	7.5	15.0
44	7.50	2.11	0.78	0.86	8.0	15.0
45	6.75	2.27	0.71	0.80	7.5	15.0
46	4.50	2.74	0.78	0.86	6.0	15.0
47	5.25	2.58	0.71	0.80	6.5	15.0
48	7.50	2.74	0.78	0.86	6.1	15.0
49	6.75	2.58	0.71	0.80	6.6	15.0

If the values for run order 10 to 13 are analysed, where length, height, and acceleration are constant, and the thickness values varied, it can be observed that the values of F_{ys} are kept almost constant. This analysis suggests that the in-plane response is not influenced by the wall thickness, as expected based on the plane stress assumption. Also if the values of the first five runs are analysed, where height, thickness, and acceleration are constant, and the length values varied, it can be observed that the values of F_{ys} are kept almost constant, thus, not being influenced neither by the wall length. It would be expected that the length of the wall also played an important role in its in-plane behaviour. Bulky walls tend to fail by shear whereas that slender walls tend to top up or fail by crushing at their base. Nevertheless, as the boundary conditions adopted prevent the in-plane rotation of the wall and, furthermore, since the levels of stress created by the low levels of acceleration adopted do not exceed the yielding point of the material, the parametric analysis do not capture properly the effects of wall length. This is further confirmed by the main effect plots, shown in Figure 6. 13, which effectively show that the values of F_{ys} are neither influenced by the length or the thickness of the wall (the first and third curves from the left of Figure 6. 13 are almost constant). On the other hand, height and acceleration seem to be parameters influencing F_{ys}.

The taller is a wall and the higher is the acceleration to which it is subjected, the more probabilities of damage are expected. Effectively, the trend depicted by the main effects plots show that a lower F_{ys} is obtained for the upper values of both height and acceleration. Furthermore, it can also be observed that the interaction between parameters is negligible as none of the curves shown in Figure 6. 14 seem to intersect each other.

These observations regarding the influence of the input parameters on F_{ys} can be verified by analysing the P-Values obtained from the Analysis of Variance (ANOVA), which are presented in Table 6. 8. Length and thickness, as well as all interaction terms, turn out to be not significant (both have P-Values > 0.05). The only significant quadratic term is the one of height. And finally, length and thickness terms are neglected as their P-Value is greater than 0.05.

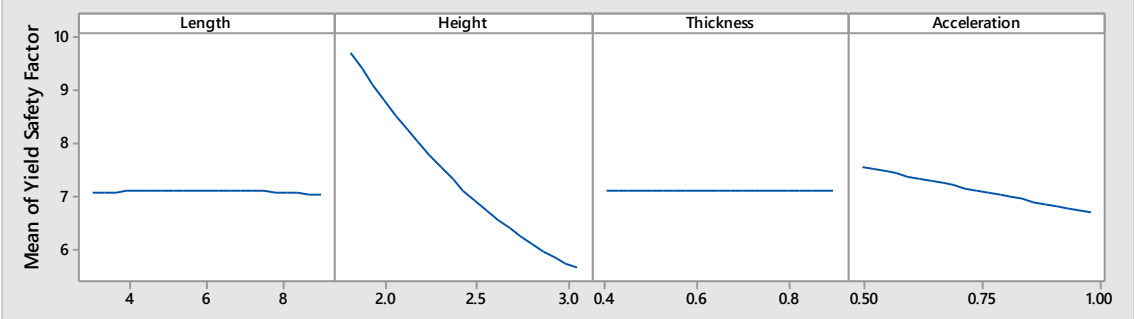

Figure 6. 13. Main effects plots for the in-plane FEM model.

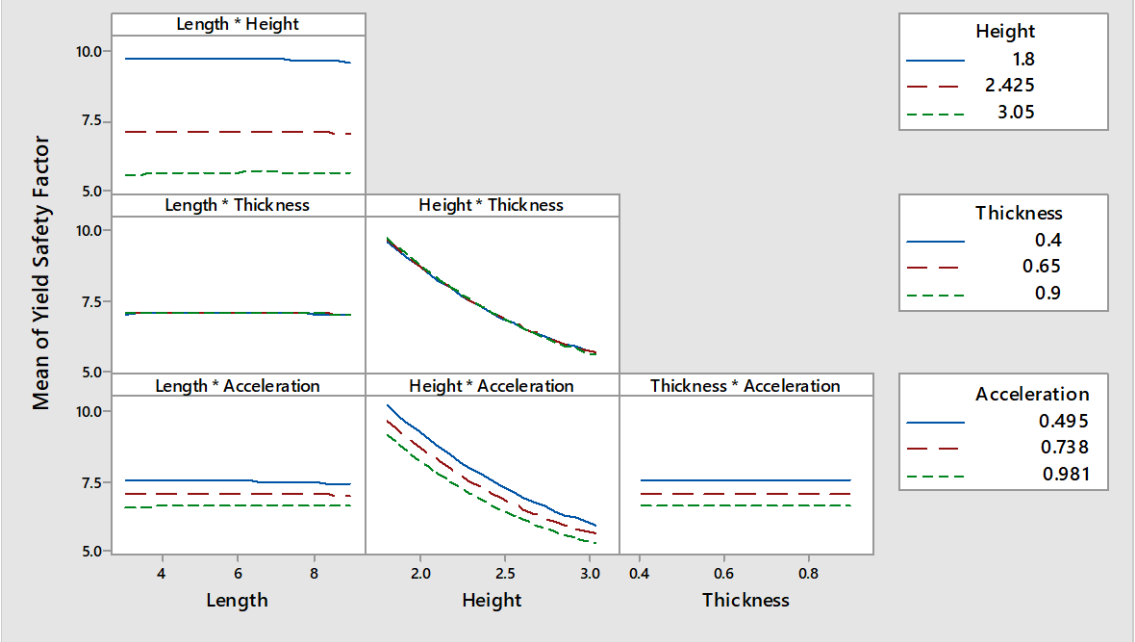

Figure 6. 14. Interaction effects plots for the in-plane FEM model.

The full quadratic model was refined by removing the non-significant terms. By taking into account only those statistically significant terms from Table 6. 8 the expression shown in EQ. 39 was obtained (all coefficients of the refined regression model presented a VIF equal to one and the refined model summary properties are presented in Table 6. 9). EQ. 39 can be used to estimate the value of F_{ys} for every combination of wall height (H_{wall} in m) and lateral acceleration (α in m/s^2) within the range of values

explored by the analysis presented in this thesis. In this equation the length and the thickness of the wall are not included, as their effect on the response is nonsignificant, and this confirms the comment made at the beginning of the section regarding the fact that the thickness of the wall was expected not to influence the in-plane response of the wall.

$$F_{ys} = 24.799 - 10.239H_{wall} - 1.7982a + 1.4394H_{wall}^2 \qquad EQ.\ 39$$

If EQ. 39 is evaluated for a wall height of 3.05 m and an acceleration of 0.981 m/s^2, then, $F_{ys} = 5.19$. This indicates that even under the most adverse combination of values for the parameters explored, and based on the assumptions adopted, the material would not reach its yield point. Furthermore, it can be seen that the out-of-plane model is more critical than the in-plane model as the critical value of F_{ys} obtained for the out-of-plane model was of only 1.093.

Table 6. 8. ANOVA for the in-plane FEM model.

Source	DF	Adj SS	Adj MS	F-Value	P-Value
Model	14	33.2066	2.3719	1146.2100	0.0000
Linear	4	32.5336	8.1334	3930.4200	0.0000
Length	1	0.0026	0.0026	1.2700	0.2680
Height	1	31.0986	31.0986	15028.2200	0.0000
Thickness	1	0.0004	0.0004	0.1800	0.6770
Acceleration	1	1.4320	1.4320	692.0200	0.0000
Square	4	0.6552	0.1638	79.1600	0.0000
Length*Length	1	0.0100	0.0100	4.8500	0.0350
Height*Height	1	0.6342	0.6342	306.4600	0.0000
Thickness*Thickness	1	0.0002	0.0002	0.1100	0.7450
Acceleration*Acceleration	1	0.0001	0.0001	0.0700	0.7890
2-Way Interaction	6	0.0177	0.0030	1.4300	0.2330
Length*Height	1	0.0025	0.0025	1.1900	0.2840
Length*Thickness	1	0.0000	0.0000	0.0000	0.9500
Length*Acceleration	1	0.0022	0.0022	1.0700	0.3090
Height*Thickness	1	0.0037	0.0037	1.7600	0.1930
Height*Acceleration	1	0.0093	0.0093	4.5200	0.0410
Thickness*Acceleration	1	0.0000	0.0000	0.0200	0.8900
Error	34	0.0704	0.0021		
Total	48	33.2769			

EQ. 39 was also used to create the response surfaces shown in Figure 6. 15. This response surface shows the way in which F_{ys} varies based on the values of height and

acceleration. This response surfaces reflects the quadratic effect the height has in the response as initially observed in the main effect plots.

Table 6. 9. Refined model summary for the in-plane FEM model.

S	R-sq	R-sq (adj)	R-sq (pred)
0.0475	99.69 %	99.67 %	99.48 %

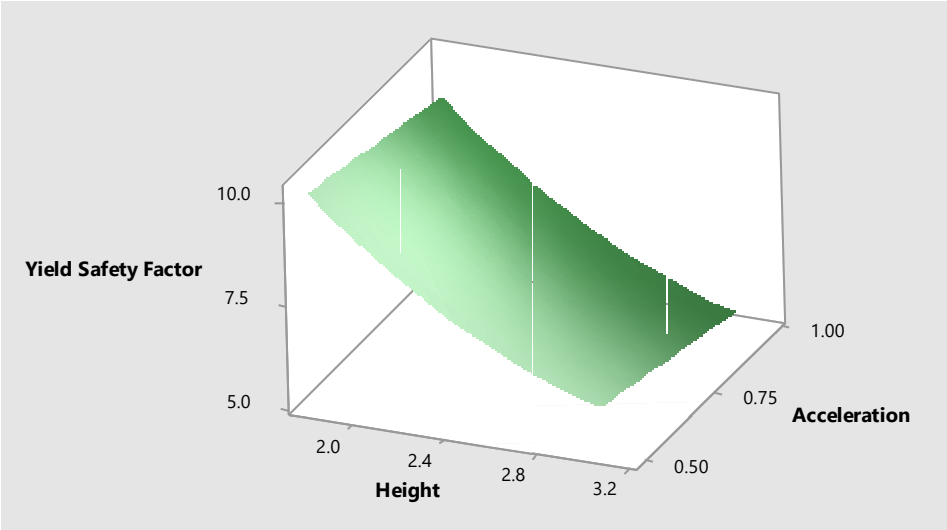

Figure 6. 15. Response surface for the Yield Safety Factor for the in-plane FEM model.

6.3.3 Macro elements out-of-plane analysis assuming infinite compressive strength

The design points generated with Minitab using a CCD with three factors (length, height and thickness) consisted in eight cube points, six centre cube points and six axial points. It used a value for the distance of the axial points equal to 1.68179 to ensure rotatability and generated 20 design points. The values adopted in each one of these design points for every parameter are presented in Table 6. 10. Table 6. 10 also presents the value calculated for the seismic mass multiplier, α, and the corresponding values of acceleration.

The minimum value computed for α is equal to 0.08. This value was obtained for a wall with 6.0 m length, 2.43 m height and 0.23 m thickness (a thickness of 0.23 m is outside the range of values adopted, it is automatically generated by dividing the minimum value of 0.4 m by the specified value $a_{CCD} = 1.68179$ for the axial spacing). A mass seismic multiplier of 0.08 corresponds to a lateral acceleration of 0.7848 m/s^2 or to a PGA of 0.08 g. This level of acceleration corresponds to the upper range values for low seismic hazard areas (see Figure 6. 2)

As previously discussed in previous sections of this chapter, it is expected that the higher and the thinner a wall is, the more critical it would be its safety when subjected to out-of-plane forces. This assumption is verified by the data generated with this parametric macro elements out-of-plane analysis. The non-influence of wall length in the values computed for the seismic mass multiplier, as it would be in the case of a plane strain simplified model, is explained by the fact that this parameter is not part of EQ. 33.

The data points generated can be better interpreted if the main and interaction effects plots, shown in Figure 6. 16 and Figure 6. 17 respectively, are analysed. The main effect plots showed that the value of the response, α, was quasi-constant for the different values of length explored, thus it can be concluded that α is not influenced by the length of the wall. On the other hand, the seismic mass multiplier is greatly influenced by height and thickness (see the central and right curves of Figure 6. 16). The seismic mass multiplier presents an inversely proportional relationship with the wall height. Moreover, this relationship seems to be non-linear. On the other hand, α presents a directly proportional relationship with the wall thickness. Furthermore, it can be observed that the interaction between parameters was negligible except for the height-thickness parameters interaction as it seems that the curves shown in the lower right corner of Figure 6. 17 tend to approach.

Table 6. 10. Design points for the out-of-plane mechanism assuming infinite compressive strength.

Run Order	Length (m)	Height (m)	Thickness (m)	α (-)	Acceleration (m/s^2)
1	3.00	3.05	0.40	0.12	1.18
2	6.00	1.37	0.65	0.43	4.22
3	6.00	2.43	0.65	0.25	2.45
4	6.00	2.43	0.65	0.25	2.45
5	6.00	2.43	0.23	0.08	0.78
6	9.00	3.05	0.90	0.29	2.84
7	6.00	2.43	0.65	0.25	2.45
8	6.00	2.43	1.07	0.43	4.22
9	6.00	2.43	0.65	0.25	2.45
10	9.00	3.05	0.40	0.12	1.18
11	9.00	1.80	0.40	0.20	1.96
12	3.00	3.05	0.90	0.29	2.84
13	3.00	1.80	0.40	0.20	1.96
14	11.05	2.43	0.65	0.25	2.45
15	3.00	1.80	0.90	0.47	4.61
16	6.00	2.43	0.65	0.25	2.45
17	6.00	2.43	0.65	0.25	2.45
18	6.00	3.48	0.65	0.18	1.77
19	9.00	1.80	0.90	0.47	4.61
20	0.95	2.43	0.65	0.25	2.45

These observations regarding the influence of the input parameters on α can be verified by analysing the P-Values obtained from the ANOVA, which are presented in Table 6. 11, of the fitted full 2nd-order polynomial model. It can be observed that effectively the length of the wall does not affect the response of the wall (P-Value = 1.0), both length and thickness quadratic terms resulted to be nonsignificant (as previously highlighted based on the shape of the corresponding curves of Figure 6. 16), similarly interaction terms length-height and length-thickness could be neglected (P-Value > 0.05) and finally, the rest of terms turn out to be significant (P-Value < 0.05).

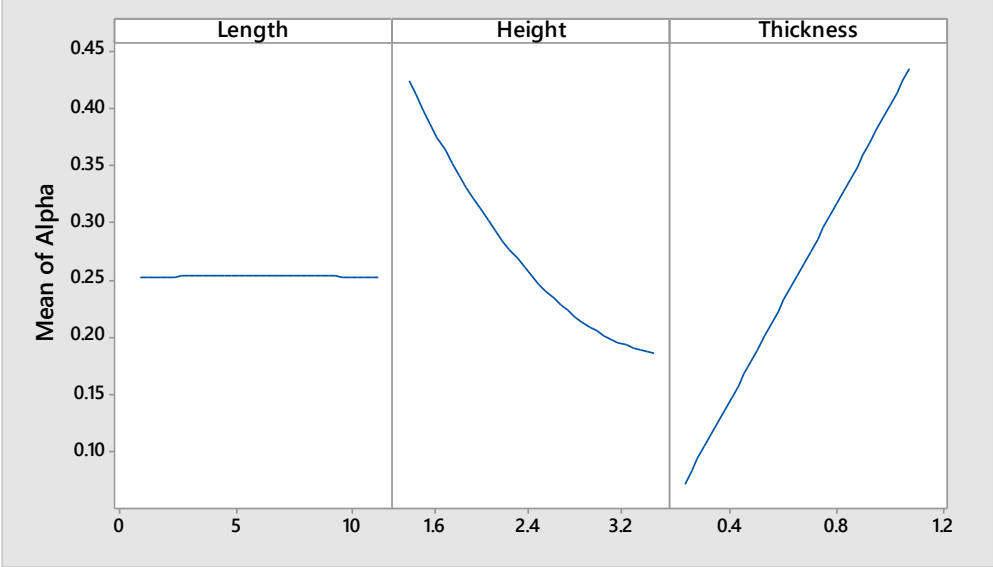

Figure 6. 16. Main effects plots for the out-of-plane mechanism assuming infinite compressive strength.

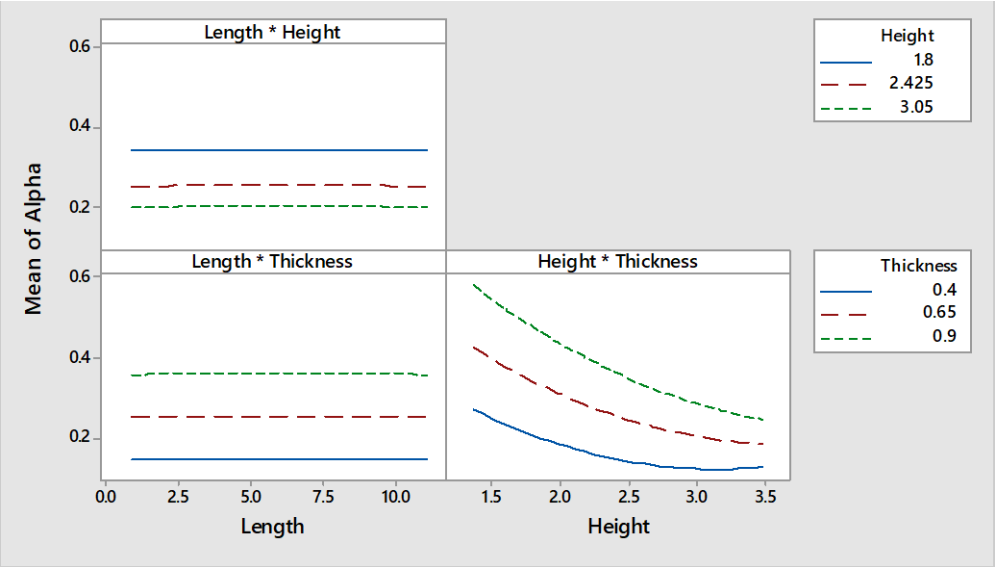

Figure 6. 17. Interaction plots for the out-of-plane mechanism assuming infinite compressive strength.

The full quadratic model was refined by removing the non-significant terms. By taking into account only those statistically significant terms from Table 6. 11 the expression shown in EQ. 40 was obtained (all coefficients of the refined regression model presented a VIF equal to one and the refined model summary properties are presented in

Table 6. 6.). EQ. 40 can be used to estimate the value of α for every combination of wall height (H_{wall} in m) and thickness (T_{wall} in m) within the range of values explored by the analysis presented in this thesis. In this equation the length of the wall is not included, as its effect on the response is nonsignificant, and this is in agreement with the comment made at the beginning of the section regarding the fact that the length of the wall was expected not to influence the out-of-plane response of the wall.

Table 6. 11. ANOVA for the out-of-plane mechanism assuming infinite compressive strength.

Source	DF	Adj SS	Adj MS	F-Value	P-Value
Model	9	0.2327	0.0259	588.1300	0.0000
Linear	3	0.2217	0.0739	1681.0500	0.0000
Length	1	0.0000	0.0000	0.0000	1.0000
Height	1	0.0668	0.0668	1520.0300	0.0000
Thickness	1	0.1549	0.1549	3523.1100	0.0000
Square	3	0.0048	0.0016	36.2100	0.0000
Length^2	1	0.0000	0.0000	0.0700	0.7960
Height^2	1	0.0047	0.0047	105.9100	0.0000
Thickness^2	1	0.0000	0.0000	0.0100	0.9200
2-way interaction	3	0.0062	0.0021	47.1300	0.0000
Length*Height	1	0.0000	0.0000	0.0000	1.0000
Length*Thickness	1	0.0000	0.0000	0.0000	1.0000
Height*Thickness	1	0.0062	0.0062	141.3900	0.0000
Error	10	0.0004	0.0000		
Lack-of-fit	5	0.0004	0.0000		
Pure error	5	0.0000	0.0000		
Total	19	0.2331			

Table 6. 12. Refined model summary for the out-of-plane mechanism assuming infinite compressive strength.

S	R-sq	R-sq (adj)	R-sq (pred)
0.0054	99.81 %	99.76 %	99.38 %

If EQ. 40 is evaluated for a wall height of 3.05 m and a thickness of 0.40 m, then, $\alpha = 0.1232$. This indicates that under the most adverse combination of values for the geometric parameters explored, and based on the assumptions adopted, a cob wall would have to be subjected to an acceleration of 1.21 m/s^2 or 0.12 g so that the out-of-plane mechanism is generated. This level of acceleration corresponds to the lower range values for a moderate seismic hazard area. As Ireland is located in the low seismic hazard area (see Figure 6. 2) it can be concluded that the out-of-plane mechanism analysed would not form in Irish surviving cob walls. On the other hand, this level of acceleration can be

expected to affect similar cob buildings in other regions, such as the UK and North of France, and the methodology presented in this chapter could be implemented to evaluate the safety level of those buildings.

$$\alpha = 0.2383 - 0.2199H_{wall} + 0.8586T_{wall} + 0.0462H_{wall}^2 - 0.1784H_{wall}T_{wall} \quad \textit{EQ. 40}$$

EQ. 40 was also used to create the response surfaces shown in Figure 6. 18. The response surface shows information regarding the effect of two input parameters, wall height and thickness, in the response, α. These response surfaces reflect the quadratic effect the input parameters have in the response as initially observed in the main effect plots.

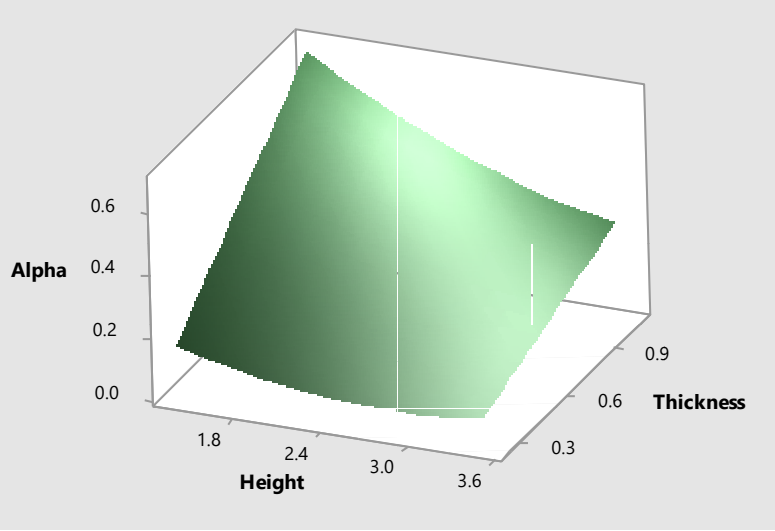

Figure 6. 18. Response surface for the out-of-plane mechanism assuming infinite compressive strength.

6.3.4 Macro elements out-of-plane analysis taking into account the compressive strength of the material

As it was observed in the parametric analysis of section 6.3.3 the length of the wall does not influence its out-of-plane response (the results of that parametric analysis confirmed the expected behaviour based on the plane strain assumption) it was decided to ignore that parameter for the macro elements out-of-plane analysis taking into account the compressive strength of the materials. The compressive strength of the material was introduced as a categorical parameter with two levels representing both the yield and the ultimate compressive strength of cob (see Table 6. 2). Therefore, the DOE using a CCD with two continuous factors (height and thickness) and one categorical factor

(compressive strength) consisted in eight cube points, ten centre cube points and eight axial points. It used a value for the distance of the axial points equal to 1.41421 to ensure rotatability and generated 26 design points. The values adopted in each one of these design points for each one of the parameters are presented in Table 6. 13. Table 6. 13 also presents the values calculated for the seismic mass multiplier, α, and the corresponding values of acceleration.

The minimum value computed for α is equal to 0.07. This value was obtained for two parameter combinations: a wall with 2.43 m height, 0.30 m thickness (a thickness of 0.30 m is outside the range of values adopted, it is automatically generated by dividing the minimum value of 0.4 m by the specified value $a = 1.41421$ for the axial spacing) and a compressive strength of 0.48 MPa; and for a wall with 3.05 m height, 0.4 m thickness and a compressive strength of 0.48 MPa. A mass seismic multiplier of 0.07 corresponds to a lateral acceleration of 0.6867 m/s^2 or to a PGA of 0.07 g. This level of acceleration corresponds to the upper range values for low seismic hazard areas (see Figure 6. 2).

Table 6. 13. Design points for the out-of-plane mechanism accounting for the compressive strength of cob.

Run Order	Height (m)	Thickness (m)	Compressive strength (MPa)	α (-)	Acceleration (m/s2)
1	1.80	0.40	0.48	0.15	1.47
2	1.54	0.65	1.59	0.36	3.53
3	2.43	0.65	1.59	0.23	2.26
4	3.31	0.65	1.59	0.16	1.57
5	2.43	0.65	1.59	0.23	2.26
6	2.43	1.00	0.48	0.28	2.75
7	1.54	0.65	0.48	0.31	3.04
8	2.43	0.65	1.59	0.23	2.26
9	2.43	0.65	1.59	0.23	2.26
10	3.05	0.90	1.59	0.25	2.45
11	2.43	1.00	1.59	0.36	3.53
12	2.43	0.30	0.48	0.07	0.69
13	2.43	0.65	1.59	0.23	2.26
14	3.05	0.40	1.59	0.11	1.08
15	2.43	0.65	0.48	0.17	1.67
16	2.43	0.30	1.59	0.10	0.98
17	2.43	0.65	0.48	0.17	1.67
18	3.05	0.40	0.48	0.07	0.69
19	1.80	0.90	1.59	0.44	4.32
20	2.43	0.65	0.48	0.17	1.67
21	2.43	0.65	0.48	0.17	1.67
22	2.43	0.65	0.48	0.17	1.67
23	1.80	0.90	0.48	0.36	3.53
24	1.80	0.40	1.59	0.18	1.77
25	3.31	0.65	0.48	0.19	1.86
26	3.05	0.90	0.48	0.18	1.77

The data points generated can be better interpreted if the main and interaction effects plots, shown in Figure 6. 19 and Figure 6. 20 respectively, are analysed. The main effect plots showed that the seismic mass multiplier is greatly influenced by height and thickness (see the left and central curves of Figure 6. 19). The seismic mass multiplier presents an inversely proportional relationship with the wall height. Moreover, this relationship seems to be non-linear. On the other hand, α presents a directly proportional linear relationship with the wall thickness.

As the higher is the compressive strength of the material the smaller would be the value of t, it was expected that the response would be as well influenced by this parameter. Effectively, as can be observed in the right curve of Figure 6. 19, a directly proportional relationship exists between cob's compressive strength and α. Furthermore, the interactions between parameters height-thickness and thickness-compressive strength seem to be significant whereas that the height-compressive strength appears to be non-significant (see Figure 6. 20).

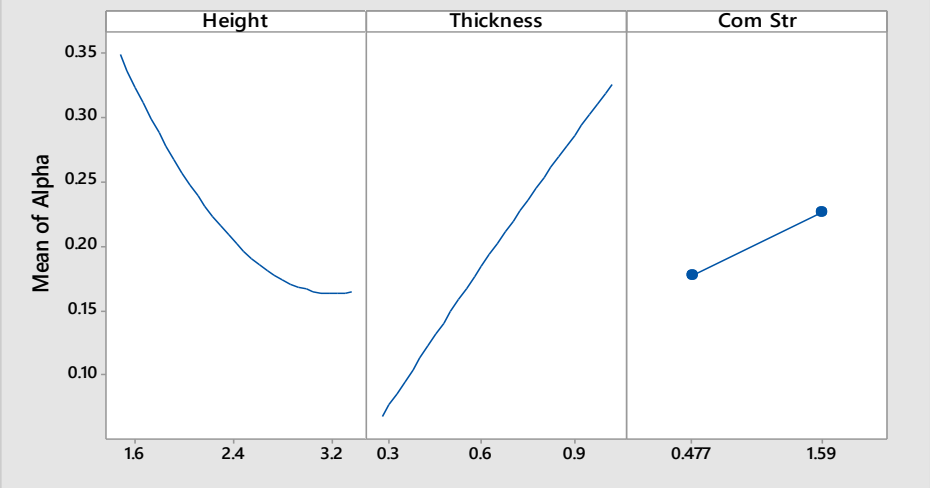

Figure 6. 19. Main effects plots for the out-of-plane mechanism accounting for the compressive strength of cob.

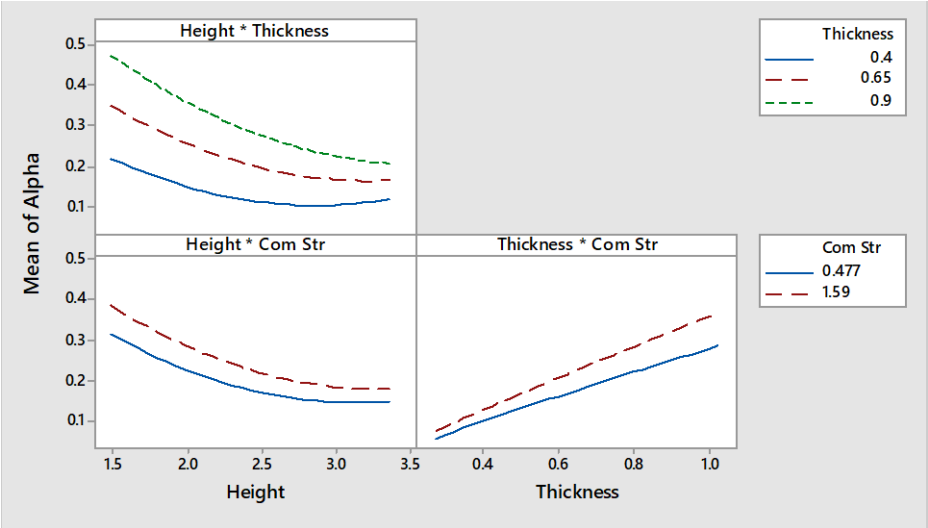

Figure 6. 20. Interaction plots for the out-of-plane mechanism accounting for the compressive strength of cob.

These observations regarding the influence of the input parameters on α can be verified by analysing the P-Values obtained from the ANOVA, which are presented in Table 6. 14, of the fitted full 2nd-order polynomial model. It can be observed that effectively the quadratic thickness term and the height-compressive strength terms resulted non-significant (P-Value > 0.05) whereas that the rest of terms were significant.

The full quadratic model was refined by removing those non-significant terms. Thus, the expression shown in EQ. 41 was obtained for a compressive strength of 0.48 MPa and the expression shown in EQ. 42 was obtained for a compressive strength of 1.59 MPa (all coefficients of the refined regression model presented a VIF equal to one and the refined model summary properties are presented in Table 6. 15). EQ. 41 and EQ. 42 can be used to estimate the value of α for every combination of wall height (H_{wall} in m) and thickness (T_{wall} in m) within the range of values explored by the analysis presented in this thesis based on the different compressive strengths mentioned. In these equations the length of the wall is not included, as its effect on the response is non-significant, and this is in agreement with the comment made at the beginning of the section regarding the fact that the length of the wall was expected not to influence the out-of-plane response of the wall.

Table 6. 14. ANOVA for the out-of-plane mechanism accounting for the compressive strength of cob.

Source	DF	Adj SS	Adj MS	F-Value	P-Value
Model	8	0.2132	0.0266	150.4500	0.0000
Linear	3	0.1957	0.0652	368.3200	0.0000
Height	1	0.0607	0.0607	342.8300	0.0000
Thickness	1	0.1191	0.1191	672.2800	0.0000
Com Str	1	0.0159	0.0159	89.8600	0.0000
Square	2	0.0087	0.0043	24.5200	0.0000
Height*Height	1	0.0082	0.0082	46.5100	0.0000
Thickness*Thickness	1	0.0001	0.0001	0.4700	0.5030
2-Way Interaction	3	0.0088	0.0029	16.5300	0.0000
Height*Thickness	1	0.0062	0.0062	35.1900	0.0000
Height*Com Str	1	0.0008	0.0008	4.2800	0.0540
Thickness*Com Str	1	0.0018	0.0018	10.1300	0.0050
Error	17	0.0030	0.0002		
Lack-of-Fit	9	0.0030	0.0003		
Pure Error	8	0.0000	0.0000		
Total	25	0.2162			

Table 6. 15. Refined model summary for the out-of-plane mechanism accounting for the compressive strength of cob.

S	R-sq	R-sq (adj)	R-sq (pred)
0.0142	98.22 %	97.66 %	95.83 %

$$\alpha_{0.48MPa} = 0.3078 - 0.2885H_{wall} + 0.7359T_{wall} + 0.0631H_{wall}^2 - 0.1786H_{wall}T_{wall} \quad \textit{EQ. 41}$$

$$\alpha_{1.59MPa} = 0.3022 - 0.2885H_{wall} + 0.8206T_{wall} + 0.0631H_{wall}^2 - 0.1786H_{wall}T_{wall} \quad \textit{EQ. 42}$$

If EQ. 41 and EQ. 42 are evaluated for a wall height of 3.05 m and a thickness of 0.40 m, then, $\alpha_{0.48MPa} = 0.0913$ and $\alpha_{1.59MPa} = 0.1196$. This indicates that under the most adverse combination of values for the geometric parameters explored, and based on the assumptions adopted, a cob wall would have to be subjected to an acceleration of 0.913 m/s^2 or 0.09 g so that the out-of-plane mechanism is generated if the yield compressive strength value is taken into account, and would have to subjected to an acceleration of 1.196 m/s^2 or 0.1196 g so that the out-of-plane mechanism is generated if the ultimate compressive strength value is taken into account. The decision as to what equation should be used would depend on the degree of damage that is considered acceptable for the structure. The yield of the materials could be adopted for a Serviceability Limit State (SLS) whereas that the ultimate strength of the materials would be adequate for an Ultimate Limit State (ULS) scenario. Nevertheless, as this level of

acceleration corresponds to the lower range values for a moderate seismic hazard area, and since Ireland is located in the low seismic hazard area (see Figure 6. 2), it can be concluded that the out-of-plane mechanism analysed would not form in Irish surviving cob walls. On the other hand, this level of acceleration can be expected to affect similar cob buildings in other regions, such as the UK and North of France, and the methodology presented in this chapter could be implemented to evaluate the safety level of those buildings.

EQ. 41 and EQ. 42 were also used to create the response surfaces shown in Figure 6. 21 and Figure 6. 22 for values of compressive strength of 0.48 and 1.59 MPa respectively. The response surface shows information regarding the effect of two input parameters, wall height and thickness, in the response, α. These response surfaces reflect the quadratic effect the input parameters have in the response as initially observed in the main effect plots.

The results of these macro elements out-of-plane analyses are in agreement with the results obtained with the FEM out-of-plane analysis. The expected negligible influence of the wall length on the response was confirmed by both analyses approaches. Furthermore, both analyses results demonstrated that the cob wall, even under the "*worst-case scenario*" assumptions adopted, would not be damaged when subjected to the range of lateral accelerations expected in Ireland.

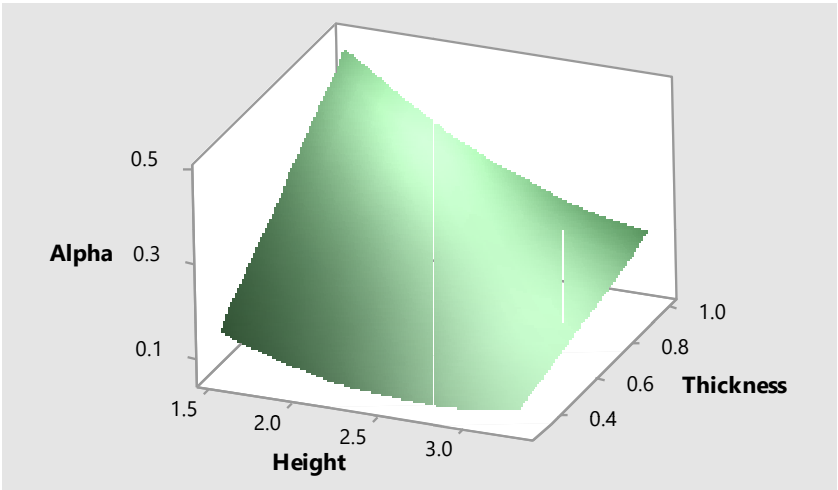

Figure 6. 21. Response surface for the out-of-plane mechanism for a compressive strength of cob of 0.48 MPa.

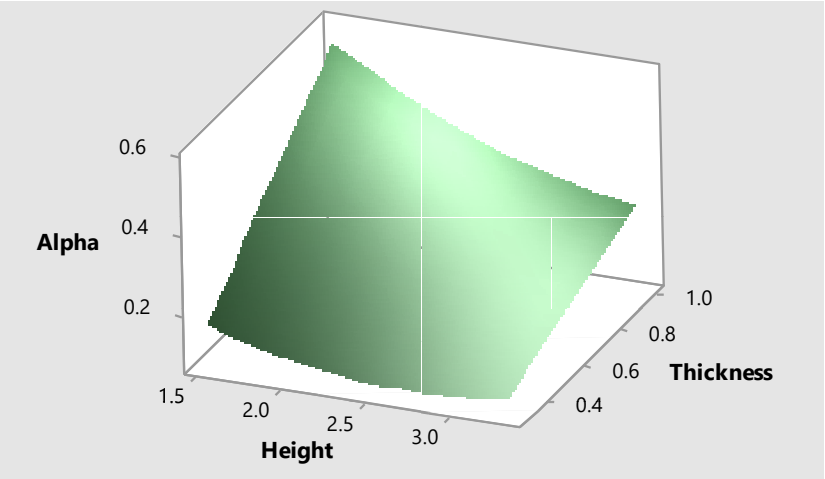

Figure 6. 22. Response surface for the out-of-plane mechanism for a compressive strength of 1.59 MPa.

6.3.5 Macro elements in-plane analysis assuming infinite compressive strength

The design points generated with Minitab using a CCD with three factors (length, height and thickness) consisted in eight cube points, six centre cube points and six axial points. It used a value for the distance of the axial points equal to 1.68179 to ensure rotatability and generated 20 design points. The values adopted in each one of these design points for every parameter are presented in Table 6. 16. Table 6. 16 also presents the value calculated for the seismic mass multiplier, α, and the corresponding values of acceleration.

The minimum value computed for α is equal to 0.20. This value was obtained for a wall with 0.95 m length, 2.43 m height and 0.65 m thickness (a length of 0.95 m is outside the range of values adopted, it is automatically generated by using the axial spacing value adopted). A mass seismic multiplier of 0.20 corresponds to a lateral acceleration of 1.96 m/s^2 or to a PGA of 0.2 g. This level of acceleration corresponds to the upper range values for moderate seismic hazard areas (see Figure 6. 2)

Table 6. 16. Design points for the in-plane mechanism assuming infinite compressive strength.

Run Order	Length (m)	Height (m)	Thickness (m)	α (-)	Acceleration (m/s2)
1	9.00	3.05	0.90	1.48	14.52
2	6.00	2.43	0.65	1.24	12.16
3	0.95	2.43	0.65	0.20	1.96
4	9.00	1.80	0.90	2.50	24.53
5	6.00	2.43	0.65	1.24	12.16
6	6.00	2.43	0.65	1.24	12.16
7	6.00	3.48	0.65	0.86	8.44
8	3.00	3.05	0.40	0.49	4.81
9	6.00	2.43	0.65	1.24	12.16
10	3.00	1.80	0.40	0.83	8.14
11	6.00	2.43	0.65	1.24	12.16
12	6.00	2.43	0.23	1.24	12.16
13	11.05	2.43	0.65	2.28	22.37
14	9.00	1.80	0.40	2.50	24.53
15	6.00	1.37	0.65	2.18	21.39
16	3.00	1.80	0.90	0.83	8.14
17	6.00	2.43	1.07	1.24	12.16
18	6.00	2.43	0.65	1.24	12.16
19	3.00	3.05	0.90	0.49	4.81
20	9.00	3.05	0.40	1.48	14.52

As previously discussed in previous sections of this chapter, it is expected that the higher a wall is, the more critical it would be its safety when subjected to in-plane forces. The length of the wall is also expected to influence in the failure of the wall subjected to in-plane forces; bulky walls tend to fail by shear, whereas that slender walls tend to rock and fail by crushing at their base. The effect of both parameters in the wall's response is verified by the data generated with this parametric macro elements in-plane analysis. The non-influence of wall thickness in the values computed for the seismic mass multiplier, as would be the case for a plane stress simplified problem, is explained by the fact that this parameter is not part of EQ. 34.

The data points generated can be better interpreted if the main and interaction effects plots, shown in Figure 6. 23 and Figure 6. 24, respectively, are analysed. The main effect plots showed that the value of the response, α, was quasi-constant for the different values of thickness explored; thus, it can be concluded that α is not influenced by the thickness of the wall. On the other hand, the seismic mass multiplier is greatly influenced by length and height (see the left and central curves of Figure 6. 23). The seismic mass multiplier presents an inversely proportional relationship with the wall height. Moreover, this relationship seems to be non-linear. On the other hand, α presents a directly proportional relationship with the wall length. One of the assumptions of the macro elements limit analysis consist of the neglect of internal sliding of the element, in other words, no shear failure can be detected with this simplified model. If the length of the

wall increases it is expected that its rotation, the mechanism that is being studied, would become less critical and a higher acceleration would be needed to initiate it but, in reality, this would not mean that the wall is safe from shearing failure. The lack of capability to detect that type of failure is one of the main shortcomings of the simplified model adopted in this parametric analysis.

Furthermore, it can be observed that the interaction between parameters was negligible except for the length-height parameters interaction as it seems that the curves, shown in the upper left corner of Figure 6. 24, tend to approach at the lower values of length.

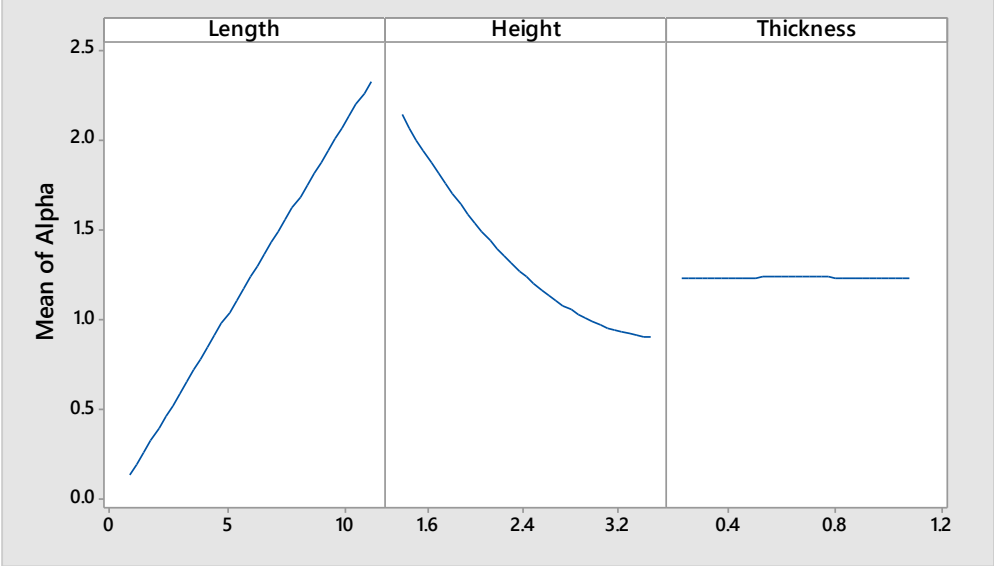

Figure 6. 23. Main effects plots for the in-plane mechanism assuming infinite compressive strength.

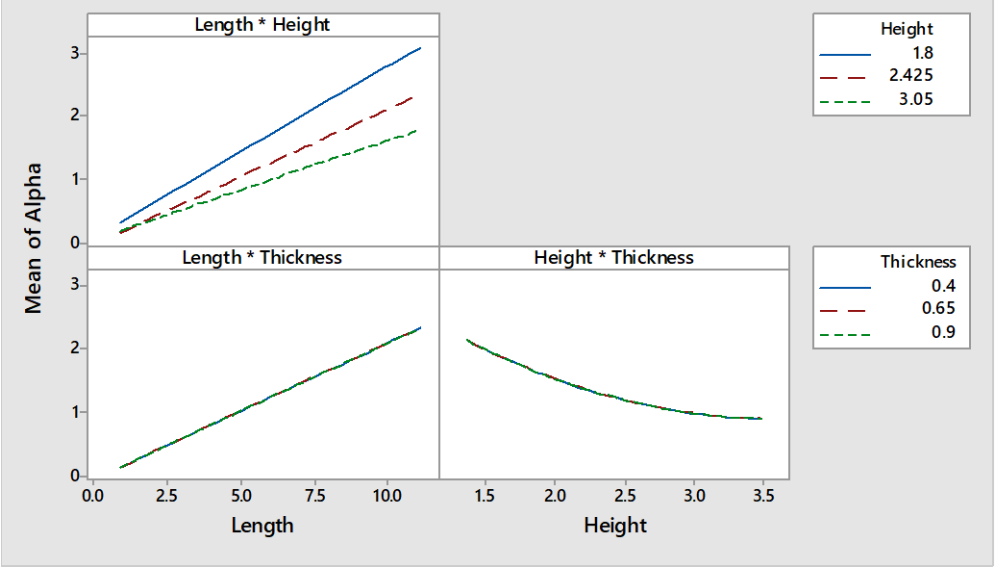

Figure 6. 24. Interaction plots for the in-plane mechanism assuming infinite compressive strength.

These observations regarding the influence of the input parameters on α can be verified by analysing the P-Values obtained from the ANOVA, which are presented in Table 6. 17, of the fitted full 2nd-order polynomial model. It can be observed that effectively the thickness of the wall does not affect the response of the wall (P-Value = 1.0), both length and thickness quadratic terms resulted to be nonsignificant, similarly interaction terms length-thickness and height-thickness could be neglected (P-Value > 0.05) and finally, the rest of terms turn out to be significant (P-Value < 0.05).

Table 6. 17. ANOVA for the in-plane mechanism assuming infinite compressive strength.

Source	DF	Adj SS	Adj MS	F-Value	P-Value
Model	9	7.8438	0.8715	557.5000	0.0000
Linear	3	7.4667	2.4889	1592.1000	0.0000
Length	1	5.6701	5.6701	3627.0500	0.0000
Height	1	1.7966	1.7966	1149.2400	0.0000
Thickness	1	0.0000	0.0000	0.0000	1.0000
Square	3	0.1438	0.0479	30.6600	0.0000
Length*Length	1	0.0001	0.0001	0.0700	0.7950
Height*Height	1	0.1396	0.1396	89.3000	0.0000
Thickness*Thickness	1	0.0001	0.0001	0.0700	0.7950
2-Way Interaction	3	0.2333	0.0778	49.7500	0.0000
Length*Height	1	0.2333	0.2333	149.2500	0.0000
Length*Thickness	1	0.0000	0.0000	0.0000	1.0000
Height*Thickness	1	0.0000	0.0000	0.0000	1.0000
Error	10	0.0156	0.0016		
Lack-of-Fit	5	0.0156	0.0031		
Pure Error	5	0.0000	0.0000		
Total	19	7.8594			

The full quadratic model was refined by removing the non-significant terms. By taking into account only those statistically significant terms from Table 6. 17, the expression shown in EQ. 43 was obtained (all coefficients of the refined regression model presented a VIF equal to one and the refined model summary properties are presented in Table 6. 18). EQ. 43 can be used to estimate the value of α for every combination of wall height (H_{wall} in m) and length (L_{wall} in m) within the range of values explored by the analysis presented in this thesis. In this equation the thickness of the wall is not included, as its effect on the response is non-significant, and this is in agreement with the comment made at the beginning of the section regarding the fact that the thickness of the wall was expected not to influence the in-plane response of the wall.

$$\alpha = 1.5160 + 0.4357L_{wall} - 1.2620H_{wall} + 0.2533H_{wall}^2 - 0.0911L_{wall}H_{wall} \quad \text{EQ. 43}$$

If EQ. 43 is evaluated for a wall height of 3.05 m and a length of 3.00 m, then, $\alpha = 0.4968$. This indicates that under the most adverse combination of values for the geometric parameters explored, and based on the assumptions adopted, a cob wall would have to be subjected to an acceleration of 4.968 m/s^2 or 0.4968 g so that the in-plane mechanism studied is generated. This level of acceleration corresponds to the upper range values for a high seismic hazard area. As Ireland is located in the low seismic hazard area (see Figure 6. 2), it can be concluded that the in-plane mechanism analysed would not form in Irish surviving cob walls.

Table 6. 18. Refined model summary for the in-plane mechanism assuming infinite compressive strength.

S	R-sq	R-sq (adj)	R-sq (pred)
0.0325	99.80 %	99.74 %	99.35 %

EQ. 43 was also used to create the response surfaces shown in Figure 6. 25. The response surface shows information regarding the effect of two input parameters, wall height and length, in the response, α. These response surfaces reflect the quadratic effect the input parameters have in the response as initially observed in the main effect plots.

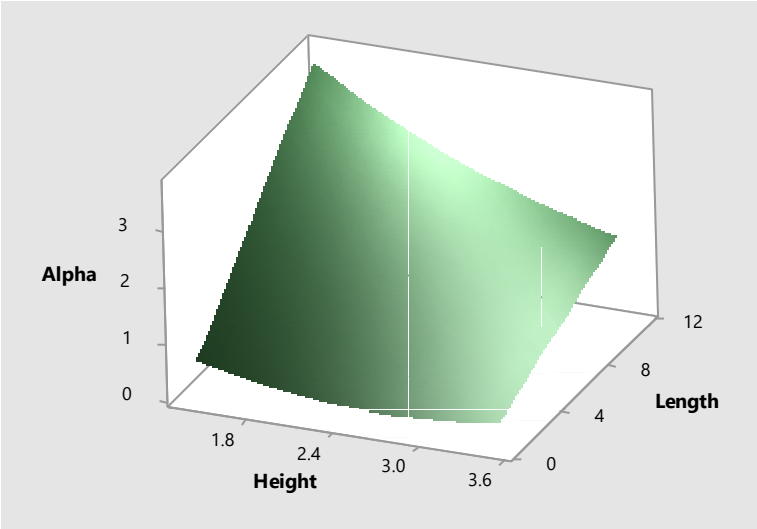

Figure 6. 25. Response surface for the in-plane mechanism assuming infinite compressive strength.

6.3.6 Macro elements in-plane analysis taking into account the compressive strength of the material

As it was observed in the parametric analysis of section 6.3.5 that the thickness of the wall does not influence its in-plane response (the results of that parametric analysis confirmed the expected behaviour based on the plane stress assumption), it was decided to ignore that parameter for the macro elements in-plane analysis taking into account the

compressive strength of the materials. The compressive strength of the material was introduced as a categorical parameter with two levels representing both the yield and the ultimate compressive strength of cob (see Table 6. 2). Therefore, the DOE using a CCD with two continuous factors (height and length) and one categorical factor (compressive strength) consisted in eight cube points, ten centre cube points and eight axial points. It used a value for the distance of the axial points equal to 1.41421 to ensure rotatability and generated 26 design points. The values adopted in each one of these design points for each one of the parameters are presented in Table 6. 19. Table 6. 19 also presents the values calculated for the seismic mass multiplier, α, and the corresponding values of acceleration.

The minimum value computed for α is equal to 0.31. This value was obtained for a wall with 2.43 m height, 1.76 m length (a length of 1.76 m is outside the range of values adopted, it is automatically generated by using the specified axial spacing value) and a compressive strength of 0.48 MPa. A mass seismic multiplier of 0.31 corresponds to a lateral acceleration of 3.0411 m/s^2 or to a PGA of 0.31 g. This level of acceleration corresponds to the lower range values for high seismic hazard areas (see Figure 6. 2)

The data points generated can be better interpreted if the main and interaction effects plots, shown in Figure 6. 26 and Figure 6. 27 respectively, are analysed. The main effect plots showed that the seismic mass multiplier is greatly influenced by height and length (see the left and central curves of Figure 6. 26). The seismic mass multiplier presents an inversely proportional relationship with the wall height. Moreover, this relationship seems to be non-linear. On the other hand, α presents a directly proportional linear relationship with the wall length.

As the higher is the compressive strength of the material, the smaller would be the value of t, it was expected that the response would be as well influenced by this parameter. Effectively, as can be observed in the right curve of Figure 6. 26, a directly proportional relationship exists between cob's compressive strength and α. Furthermore, the interactions between parameters length-height and length-compressive strength seem to be significant whereas that the height-compressive strength appears to be non-significant (see Figure 6. 27).

Table 6. 19. Design points for the in-plane mechanism accounting for the compressive strength of cob.

Run Order	Length (m)	Height (m)	Compressive strength (MPa)	α (-)	Acceleration (m/s2)
1	3.00	3.05	1.59	0.47	4.61
2	6.00	2.43	0.48	1.04	10.20
3	6.00	2.43	1.59	1.18	11.58
4	6.00	2.43	0.48	1.04	10.20
5	1.76	2.43	1.59	0.35	3.43
6	6.00	2.43	0.48	1.04	10.20
7	6.00	1.54	1.59	1.89	18.54
8	9.00	1.80	1.59	2.42	23.74
9	6.00	2.43	1.59	1.18	11.58
10	6.00	2.43	1.59	1.18	11.58
11	6.00	3.31	1.59	0.85	8.34
12	9.00	3.05	0.48	1.18	11.58
13	6.00	2.43	1.59	1.18	11.58
14	3.00	1.80	0.48	0.74	7.26
15	9.00	3.05	1.59	1.40	13.73
16	6.00	3.31	0.48	0.71	6.97
17	9.00	1.80	0.48	2.21	21.68
18	1.76	2.43	0.48	0.31	3.04
19	6.00	1.54	0.48	1.75	17.17
20	3.00	3.05	0.48	0.39	3.83
21	10.24	2.43	1.59	2.02	19.82
22	3.00	1.80	1.59	0.81	7.95
23	6.00	2.43	0.48	1.04	10.20
24	6.00	2.43	0.48	1.04	10.20
25	10.24	2.43	0.48	1.78	17.46
26	6.00	2.43	1.59	1.18	11.58

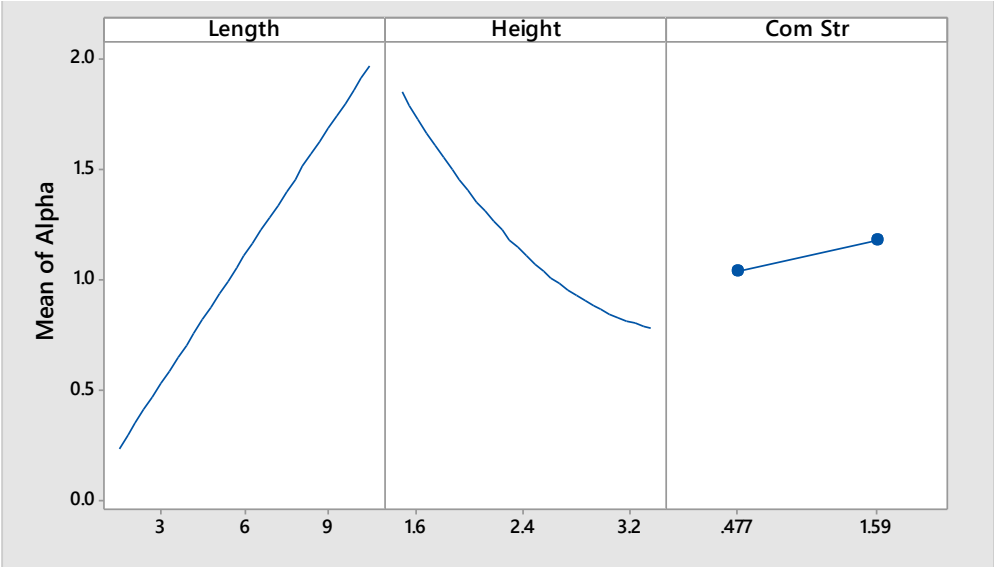

Figure 6. 26. Main effects plots for the in-plane mechanism accounting for the compressive strength of cob.

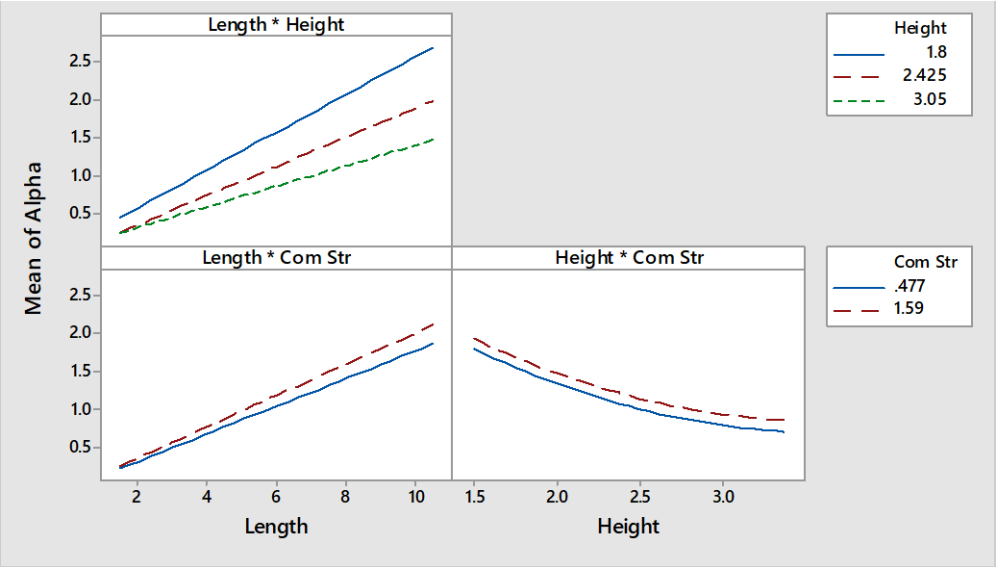

Figure 6. 27. Interaction plots for the in-plane mechanism accounting for the compressive strength of cob.

These observations regarding the influence of the input parameters on α can be verified by analysing the P-Values obtained from the ANOVA, which are presented in Table 6. 20, of the fitted full 2nd-order polynomial model. It can be observed that effectively the quadratic length term and the height-compressive strength terms resulted non-significant (P-Value > 0.05) whereas that the rest of terms were significant.

Table 6. 20. ANOVA for the in-plane mechanism accounting for the compressive strength of cob.

Source	DF	Adj SS	Adj MS	F-Value	P-Value
Model	8	7.8811	0.9851	1595.9700	0.0000
Linear	3	7.5060	2.5020	4053.3900	0.0000
Length	1	5.3593	5.3593	8682.3900	0.0000
Height	1	2.0186	2.0186	3270.1800	0.0000
Com Str	1	0.1281	0.1281	207.6000	0.0000
Square	2	0.1211	0.0606	98.1200	0.0000
Length*Length	1	0.0000	0.0000	0.0600	0.8030
Height*Height	1	0.1185	0.1185	191.9300	0.0000
2-Way Interaction	3	0.2539	0.0846	137.1300	0.0000
Length*Height	1	0.2342	0.2342	379.4200	0.0000
Length*Com Str	1	0.0197	0.0197	31.9200	0.0000
Height*Com Str	1	0.0000	0.0000	0.0400	0.8370
Error	17	0.0105	0.0006		
Lack-of-Fit	9	0.0105	0.0012		
Pure Error	8	0.0000	0.0000		
Total	25	7.8916			

The full quadratic model was refined by removing those non-significant terms. Thus, the expression shown in EQ. 44 was obtained for a compressive strength of 0.48 MPa and the expression shown in EQ. 45 was obtained for a compressive strength of 1.59 MPa (all coefficients of the refined regression model presented a VIF equal to one

and the refined model summary properties are presented in Table 6. 21). EQ. 44 and EQ. 45 can be used to estimate the value of α for every combination of wall height (H_{wall} in m) and length (L_{wall} in m) within the range of values explored by the analysis presented in this thesis based on the different compressive strengths mentioned. In these equations the thickness of the wall is not included, as its effect on the response is non-significant, and this is in agreement with the comment made at the beginning of the section regarding the fact that the thickness of the wall was expected not to influence the in-plane response of the wall.

$$\alpha_{0.48MPa} = 1.3980 + 0.4025L_{wall} - 1.1692H_{wall} + 0.2368H_{wall}^2 - 0.0912L_{wall}H_{wall} \quad \textit{EQ. 44}$$

$$\alpha_{1.59MPa} = 1.3980 + 0.4259L_{wall} - 1.1692H_{wall} + 0.2368H_{wall}^2 - 0.0912L_{wall}H_{wall} \quad \textit{EQ. 45}$$

If EQ. 44 and EQ. 45 are evaluated for a wall height of 3.05 m and a length of 3.00 m, then, $\alpha_{0.48MPa} = 0.4078$ and $\alpha_{1.59MPa} = 0.4780$. This indicates that under the most adverse combination of values for the geometric parameters explored, and based on the assumptions adopted, a cob wall would have to be subjected to an acceleration of 4.00 m/s^2 or 0.4078 g so that the out-of-plane mechanism is generated if the yield compressive strength value is taken into account, and would have to subjected to an acceleration of 4.69 m/s^2 or 0.4780 g so that the out-of-plane mechanism is generated if the ultimate compressive strength value is taken into account. The decision as to what equation should be used was discussed in section 6.3.4. As these levels of acceleration correspond to the upper range values for a high seismic hazard area, and since Ireland is located in the low seismic hazard area (see Figure 6. 2), it can be concluded that the in-plane mechanism analysed would not form in Irish surviving cob walls.

Table 6. 21. Refined model summary for the in-plane mechanism accounting for the compressive strength of cob.

S	R-sq	R-sq (adj)	R-sq (pred)
0.0236	99.87 %	99.82 %	99.66 %

EQ. 44 and EQ. 45 were also used to create the response surfaces shown in Figure 6. 28 and Figure 6. 29 for values of compressive strength of 0.48 and 1.59 MPa respectively. The response surface shows information regarding the effect of two input parameters, wall height and length, in the response, α. These response surfaces reflect the

quadratic effect the input parameters have in the response as initially observed in the main effect plots.

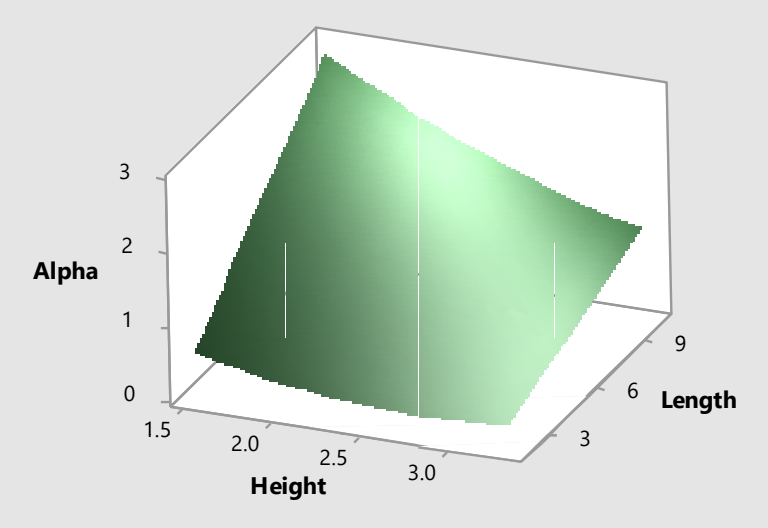

Figure 6. 28. Response surface for the in-plane mechanism for a compressive strength of cob of 0.48 MPa.

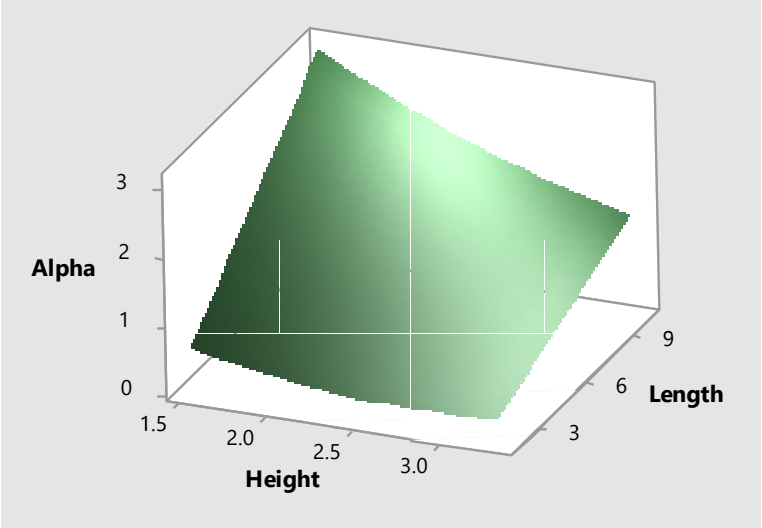

Figure 6. 29. Response surface for the in-plane mechanism for a compressive strength of cob of 1.59 MPa.

The results of these macro elements in-plane analyses are in agreement with the results obtained with the FEM in-plane analysis. The expected negligible influence of the wall thickness on the response was confirmed by both analysis approaches. Furthermore, both analyses results demonstrated that the cob wall, even under the "*worst-case scenario*" assumptions adopted, would not be damaged when subjected to the range of lateral accelerations expected in Ireland.

Walls are structural elements with higher inertia in their plane than in their out-of-plane direction. Therefore, walls can resist relatively high lateral forces within their plane in comparison to lateral forces out of their plane. The parametric analyses performed and presented in this chapter are in agreement with this fact. The values presented in the last column of Table 6. 22 show the response values computed using the corresponding equations (and the critical values for the input parameters) for every parametric analysis performed. The safety factors obtained for the in-plane FEM analyses are higher than for the out-of-plane FEM analyses, which indicates that higher acceleration values would be required to cause damage to the wall for the in-plane than for its out-of-plane behaviour conditions studied. Similarly, higher values for the in-plane seismic mass multipliers are required to develop the in-plane mechanism than for the development of the out-of-plane mechanism according to the macro elements limit analyses results obtained.

Table 6. 22. Critical response values obtained with the different parametric analysis performed.

Analysis type	Behaviour/Mechanism	Response	Value
FEM	In-plane	F_{ys}	5.19
		F_{us}	15.0*
	Out-of-plane	F_{ys}	1.093
		F_{us}	15.0*
Macro elements	In-plane	α	0.4968
		$\alpha_{0.48MPa}$	0.4078
		$\alpha_{1.59MPa}$	0.4780
	Out-of-plane	α	0.1232
		$\alpha_{0.48MPa}$	0.0913
		$\alpha_{1.59MPa}$	0.1196

*Cap value used by the software.

6.4 Conclusions

The results obtained with the macro elements models are in agreement with those of the FEM analyses. The expected negligible influence of the wall length on the wall's out-of-plane response was confirmed by both analyses approaches. Similarly, the expected negligible influence of the wall thickness on the wall's in-plane response was also confirmed by both analyses approaches. Furthermore, both analyses results demonstrated that the cob wall, even under the "*worst-case scenario*" assumptions adopted, would not be damaged when subjected to the range of lateral accelerations expected.

Since the values for yield safety factors found were greater than one for all parameters combinations, it can be concluded that the linear analysis would be valid for

the analysis of surviving cob walls in Ireland within the range of geometric parameters explored, at least for walls in similar conditions to the assumptions adopted. This may not hold true for decayed cob walls whose compressive strength is smaller than the values adopted based on those reported by the referenced authors (Miccoli *et al.*, 2014) or for walls with relatively high void/surface ratios.

It was identified that the possible failure modes the cob walls may develop, in case the studied parameters ranges were exceeded, would be related to the out-of-plane behaviour/mechanisms. This fact was expected beforehand and confirmed by comparing the response parameters values found for each parametric analysis performed. Those values were summarized in Table 6. 22.

The advantages of the simplified FEM linear models used in the parametric analyses presented, as per comparison to the non-linear models studied in Chapter 4, in this thesis were:

- Easy model definition (no need for calibration of parameters to describe the complex stress-strain relationship characteristic of cob).
- Faster solution of the model, which allowed to run several simulations in a relatively short period of time to evaluate the design points and generate the response surfaces.
- Easier interpretation of the results, based in two response parameters, yield safety factor, F_{ys}, and ultimate safety factor, F_{us}.

Based on the results obtained with both simplified analyses traditional cob walls in Ireland could be described structurally as very robust. It was observed that relatively high acceleration values, unlikely to happen in a low seismic hazard region such as Ireland, would be needed to start the collapse mechanisms studied or cause yielding in typical vernacular cob walls. Due to the characteristics of the vernacular architecture typologies in the island (single story buildings with regular rectangular plans), low seismicity hazard levels and relatively thick walls, needed in principle for construction purposes, it can be concluded that cob walls would very rarely fail under the seismic loads that they may normally be subjected to. Proof of this fact are the many remaining cob buildings which, providing they had been adequately protected against rain and raising damp, have survived for hundreds of years in a relatively good state.

The equations generated with the refined regression models, based solely in the geometry of the walls and acceleration values, can be used by practitioners as a first approach to estimate the safety levels of existing cob buildings in Ireland as well as in other countries where buildings with similar characteristics exists, such as in the UK and North of France. Nevertheless, it must be borne in mind that the assumptions adopted and the analyses performed to obtain them are of conservative nature. If their application results in the design of an over invasive intervention it is advisable to carry out a more sophisticated analysis in order to try to preserve, as much as possible, the value of the structure and its original fabric.

The logical line of extension for the results presented in this thesis would consist on the study of different conditions that would affect the walls' responses, i.e. voids, lateral and top movement restrictions, wind load, etc. The results obtained from the parametric analysis of walls fixed at their base and lateral ends, assuming good interconnectivity with return perpendicular walls could provide lateral support, are presented in Appendix F. Furthermore, the simple methodology adopted to generate the parametric analysis presented in this thesis could be also used as part of a more complex seismic vulnerability analysis in countries located in moderate or high seismic hazard areas as it provides an efficient and relatively fast way to obtain an estimate of the building's structural response.

Chapter 7: Conclusions, future work and list of publications

Remaining earthen buildings in Ireland are of vernacular nature and are mainly represented by the construction technique known as cob. Cob walls were usually built over a stone plinth to protect them from the decay caused by raising damp and rain splashing. Furthermore, they were roofed with thatch, which commonly had an important amount of overhanging over the eaves in order to prevent direct rain from causing damages to the earthen walls. As an extra measurement of protection, cob walls were sometimes clay-plastered and ubiquitously lime washed.

Typical dwellings were characteristically rectangular in plan, single story, longer than wider, with solid load bearing walls and either hipped or gabled roofed. Traditionally they have served as accommodation for their dwellers and also for agricultural and animal husbandry purposes.

Earthen vernacular buildings in Ireland were built during a "*meitheal*" in which men, women and children participated in the communal construction while alternating working with singing and dancing to the rhythm of one or two fiddlers. This socio-cultural characteristic allowed that the construction techniques, skills and know-how were shared among most members of the society and inherited from generation to generation. The selection of the construction place was determined by a folklore tradition related to fairy paths and skulls would be buried to provide the dwellers with good luck.

A dualist perception exists with respect to the remaining vernacular earthen buildings in Ireland. Part of the population associate them with negative concepts such as poverty, evictions, squalor and starvation whereas that other part of the population confers these buildings with positive attributes such as cosiness, beauty, comfort and cultural value. Moreover, the remaining Irish cob buildings poses economic, environmental and sustainable values. They contribute to the housing stock of the country, were built with recyclable materials and are deemed to provide comfort to their inhabitants.

7.1 Conclusions

7.1.1 Completed work

The first stage of this work consisted of the identification of the Irish earthen vernacular architecture's characteristics. A thorough literature review process on the remaining earthen vernacular buildings in Ireland was carried out. The historical and geographical context in which these types of buildings developed was identified as well as their social, cultural and economic aspects have been described in this thesis. Typical traditional Irish farm and dwelling layouts were described. Based on this information, the authenticity of this group of historical buildings was defined. Furthermore, the main factors threatening vernacular architecture and the principal motivations for its conservation were highlighted.

The next step of the research focused on the assessment of the suitability of currently available simulation methods and material constitutive models to describe cob's structural behaviour. The numerical simulations carried out in this thesis were based on the experimental campaign reported by Miccoli *et al*., in which they performed a series of simple and diagonal compression tests on cob wallettes. The results obtained with the simulations of this thesis were compared with those reported by these authors in terms of cob's peak strength, stress/strain curves and failure modes. Two different numerical methods were implemented; FEM and DLO.

It was decided to use FEM as this is one of the most important and widely used simulation tools in engineering. The FEM simulations were carried out using two of the most commonly used FEM programs in the market, ANSYS and ABAQUS. Three material constitutive models were tested in ANSYS, namely, MISO, CONCR and DMGI/DMGE, whereas in ABAQUS the selected material constitutive models that were tested were the CDP and the CSC models. Furthermore, a mesh size sensitivity analysis was performed following a mesh refinement approach. Pros and cons of different available constitutive material models were identified and discussed.

The purpose of finding a suitable non-linear model to describe cob's structural behaviour was to reproduce cob's pre-peak and post-peak behaviour and to identify its peak strength. By doing so, a better safety evaluation of existent cob buildings could be performed, thus avoiding the implementation of over conservative intervention measures

that may cause the loss of their authenticity. Non-linear models also hold the promise of potentially describing the behaviour of cob structures under the action of earthquakes or other extreme loading events.

The FEM simulations performed are novel work. Neither ANSYS nor ABAQUS had been previously used to describe cob's structural behaviour. Furthermore, the simulations reproduced the referenced simple compression and diagonal compression tests, both in 2D and 3D models (numerical results reported by Miccoli *et al.* only covered a simplified plane stress model of the diagonal compression test).

Alternative simulations were performed using DLO. This method was explored as an alternative to the detailed, non-linear and computationally expensive FEM models. The DLO models were created using the software LimitState GEO and two different simulation refinement levels were tested, namely, medium and very fine nodal density. The main advantages of DLO, with respect to FEM, are the identification of singularities without difficulties, the faster solution of the problem and the easy interpretation of the results, which are explicitly identified by the method. Fast results (less than 60 s for both simple and diagonal compression with very refined number of nodes) where obtained from the DLO simulations. On the other hand, the accuracy of the models to predict the failure load was quite poor as the software is only suitable to perform plain strain analysis and not 3D or plane stress analysis as for the case of the simulated wallettes. The DLO simulations performed to reproduce cob's structural behaviour contribute to the novel work presented in this thesis.

Another important part of this research comprised the application of the MDT technique known as the flat jack test, used to determine in-situ the levels of stress and the mechanical properties of walls. The technique was applied to a series of cob wallettes built in the laboratory of CSEE at TCD. The experimental campaign performed produced the first results ever obtained from the application of the flat jack test in cob walls. Thus, all the results obtained are part of the novel work contributed by this thesis.

Values for the dimensionless coefficient, K_e, were obtained by performing single flat jack tests in the cob wallettes subjected to a known level of stress and comparing such level with the corrected recovery pressure obtained by the test. Furthermore, the values of the mechanical properties of the cob wallettes, namely, Young's modulus, Poisson's ratio and compressive strength, were obtained after performing the double flat jack tests

in the same cob wallettes. Cob's compressive strength and Young's modulus were as well estimated by subjecting a series of cob cylinders, prepared with the same cob mix of the wallettes, to compressive tests and during the consolidation of the cob wallettes respectively. The values obtained with the double flat jack tests were compared to those estimated with the alternative methods and proved to be in good agreement.

Furthermore, at the time this thesis was written, no record of the application in Ireland of flat jack tests to any kind of wall typology was available. The flat jack tests performed in the cob wallettes are therefore the first application of this MDT test in Ireland. The laboratory of CSEE at TCD is, at the time this thesis was written, the only one in the country with the required equipment to perform this type of MDT test in the country. Novel test guidelines to perform this test were also produced and can be consulted in Appendix E.

As one of the aims of the research was to increase awareness regarding the importance of conservation of vernacular architecture the experimental campaign performed in this PhD project was used to get a great number of people involved and disseminate knowledge about the subject among them. Academics, technical staff and researchers, as well as undergraduate students and the general public participated in different activities related to the conservation of earthen vernacular buildings and the use of natural materials for sustainable construction purposes.

Several Professors and three Post-docs from the Department of CSEE actively participated with the author of this thesis in discussions along the progress of the experimental campaign. Eight international PhD students got involved in the construction process of the wallettes. Furthermore, after the project was explained to them, they were also asked about their previous experience with natural materials and traditional construction techniques on their own countries. The technical staff of the laboratory was greatly involved throughout the whole process as well.

Two one-day workshops were run in the facilities of the Department of CSEE. In the first one undergraduate students from the department were invited to attend a morning presentation on the conservation of earthen vernacular buildings in Ireland and to participate in the construction of the wallettes of the experimental campaign. The second workshop was organized within the framework of the Trinity Green Week 2019 and both students and the general public were invited to participate.

For the last dissemination activity organized during this PhD students of architecture from UCD and from the DTU were invited to the laboratory of TCD. The students were given a presentation on the aspects of this PhD thesis and of the experimental campaign performed. After this, a tour around the laboratory facilities was conducted where they could see the specimens that were built and tested along with the flat jack tests' equipment that was used during the experimental campaign. The discussion that took place during and after the visit proved to be extremely rich, especially due to its multidisciplinary character and the different backgrounds and previous experiences of the participants of the event.

Finally, a parametric analysis of cob walls was performed with the aim of assessing the effect geometric parameters and levels of acceleration have on the response of existent cob walls. The main objectives of this analysis were:

- To identify the levels assigned to the different parameters for which a linear analysis may still hold valid for the study of cob walls.
- To identify the possible failure modes of the walls if those limits are exceeded.
- To better understand the advantages and disadvantages of a simplified linear analysis for the study of cob walls.

It was decided to study the response of the walls subjected to both in-plane as well as out-of-plane behaviour due to the multidirectional nature of dynamic actions. For either case, a free-standing cob wall fixed (translational degrees of freedom constrained) at its bottom was simulated. These assumptions were adopted with the aim of simulating a general "*worst-case scenario*" in which a cob wall, part of a surviving cob building in Ireland, may be found. Both in-plane and out-of-plane cob wall conditions were studied using two different approaches, namely, linear elastic FEM analysis and macro elements kinematic limit analysis. The "*best-guess*" fixed cob's mechanical properties values used in this parametric analysis correspond with those reported by Miccoli *et al*. (2014). The geometric parameters adopted corresponded to the values reported by researchers based on studies of surviving cob buildings and records of historical cob buildings in Ireland. The minimum and maximum values adopted for the lateral accelerations of the parametric analysis were of 0.05 g and 0.10 g (0.4905 m/s^2 and 0.981 m/s^2) respectively. These values were taken from the Seismic Hazard Harmonization in Europe map of ground

motion hazard for a 10 % exceedance probability in 50 years. The simplified models studied in the parametric analysis were static. The dynamic accelerations caused by an earthquake in an existent cob structure were simplified into static inertial forces by using D'Alembert's principle.

The walls were subjected to their own weight, to an external force at their top simulated as a concentrated mass, representing the loads transferred by the roof, and finally to a horizontal acceleration representing the effects of dynamic loads on the wall. Yielding and ultimate safety factors were obtained from the linear elastic analysis, whereas the macro elements kinematic limit analysis provided the minimum values needed for the seismic mass multiplier, α, to form the proposed collapse mechanisms.

A DOE technique was used for both the linear elastic FEM analysis and the macro elements kinematic limit analysis to obtain meaningful results and, at the same time, to reduce the computational effort required. A full CCD was selected for the design type as this method is available as the default option in both applications and is the most commonly used method for the design of experiments to create response surfaces. Adequate values for the distance of the star points were selected in order to ensure rotatability and provide a constant prediction variance. The design points generated with the CCD were used to build the response surfaces by applying a full 2nd-order polynomial algorithm. Then, the main effect and interaction effect plots were analysed and a second response surface was created taking into account only those statistically significant terms to simplify the regression model.

7.1.2 Main findings

Regarding cob's numerical modelling

The results obtained with ANSYS and ABAQUS (simulations performed to model the simple compression and diagonal compression tests of cob wallettes in both 2D and 3D models) are one of the main findings of this thesis and represent novel work.

MISO was the simpler material constitutive model studied. The values of the material's Young's modulus, Poisson's ratio, density, and compressive stress/ strain relationship were used as reported by the referenced authors. It was not necessary to perform any calibration as the material was completely defined with those parameters.

Unfortunately, Miccoli *et al*. calibrated their stress/strain curve assuming a plane stress behaviour of the cob wallettes and it turn out to be inadequate for the 3D simulations. 3D models, not only for the MISO but also for the CDP and CSC for which the stress/strain curve was used, gave higher values of peak strength in comparison to the reference value reported by Miccoli *et al*. from the experimental testing of the cob wallettes. A plane stress simplified model usually gives accurate enough results when the thickness of the element is relatively small to its other two dimensions. In the case of the cob wallettes tested by Miccoli *et al*. the T_{wall}/L_{wall} (thickness/length) and T_{wall}/H_{wall} (thickness/height) ratios gave values of 0.27. Based on the results observed in the MISO models, as well as in the CDP and CSC models, it can be concluded that this ratio is not small enough to adopt a plane stress simplification. The thickness of the wallettes provided enough confinement to the material out of its plane as to create a significant difference between the plane stress and the 3D models. Furthermore, the MISO constitutive model does not have the capability of defining a post-peak loss of strength. Therefore, the MISO models were not capable of reproducing the port-peak loss of strength observed from the experimental campaign. Moreover, the MISO model is not suitable for reproducing the behaviour of materials with different compressive/tensile strengths (cob's tensile strength is between a tenth and a sixteenth of its compressive strength). For all these reasons, the MISO material constitutive model is considered to be inadequate to reproduce cob's structural behaviour.

The model that best represented the behaviour of cob in ANSYS was the 3D CONCR with a 10 mm mesh size. The discrepancy values (difference in percentage between the reproduced peak strength and the reference peak strength taken from Miccoli *et al*. experimental campaign) for both simple and diagonal compression peak strengths are smaller than 10 %. Moreover, the cracks obtained in the model are in good agreement with the typical failure pattern presented in these types of experimental tests. Nevertheless, caution should be exercised while interpreting results when CONCR is used to model cob structural behaviour under different conditions from those studied in this paper as it was noticed that the model is sensible to the mesh size that is implemented. Furthermore, the CONCR model is one of the more complex models studied in this thesis as it requires the use of snippets in Workbench and the calibration of several parameters for its definition which may limit its application to advanced users of the software. Moreover, this material constitutive model can only be used in combination with the

element SOLID65 which is a legacy element. Currently the software documentation advices the use of the current-technology SOLID185 element and the SOLID65 may no longer be able in future versions of the software.

The DMGI/DMGE models with a Hashin failure criteria and continuum damage mechanics approach adopted did not reproduced accurately enough cob's structural behaviour.

The model that best represented the behaviour of cob in ABAQUS was the 2D CDP with a 10 mm mesh size. The discrepancy values for both simple and diagonal compression peak strengths are smaller than 10 %. Besides, the maximum strain plots obtained in the model are in good agreement with the typical failure pattern presented in these types of experimental tests. Moreover, the CDP material constitutive model is of special interest as according to the software documentation this model is suitable for reproducing the cyclic and dynamic behaviour of the material and this capability could be further explored in future research. The CSC model on the other hand, presented quite limited capabilities in comparison with the CDP model. Based on a comparison of the results obtained with both material constitutive models, the use of CDP would be advised over the use of CSC to model cob walls in ABAQUS.

Regarding the mesh size sensitivity (h-refinement) the MISO stress/strain curves obtained show that a finer mesh would provide larger strain values. This may have been caused by the presence of stress concentrations between the contacts of the cob wallette with the steel plates. The plasticity of the material would affect the four corners in a small element whereas that for larger elements it would be averaged and slightly reduced as some corners in the element may not have reached the plasticity point. The mesh sensitivity was negligible for the simulation of the simple compression test using the CONCR constitutive model whereas that for the simulation of the diagonal compression test an important difference, between coarser and the 10 mm mesh model, was observed in the shear stress/shear strain curves obtained. Similarly, the DMGI/DMGE models did not show significant difference for the simple compression simulations whereas that for the diagonal compression simulations the finest mesh presented larger strain values in comparison to the coarser ones. The participation of the shear induced stresses in the material would influence on the failure of the material, which concentrated in a smaller element, would cause the lager values of strain observed. Regarding the ABAQUS models, the symmetric simplification adopted, to reduce the size of the 3D models, may

have caused that the 10 mm models present smaller strain values than the coarser ones for the cases of CDP and CSC simple compression and CSC diagonal compression.

The alternative DLO simulations performed provided practically identical failure modes, as those experimental results reported by Miccoli's *et al*. (2014), for the medium refined model. On the other hand, a symmetrical failure mode was obtained from the refined models (symmetry that was not capture in the experimental results due to imperfections in the material and experimental setup as noted by Miccoli *et al*. (2019)). Failure loads were computed as 17.78 kN/m2 and 1.46 kN/m2 for the simple and diagonal simulations respectively. Unfortunately, as GEO can only be used to solve geotechnical problems (plane strain), the failure loads obtained from the simulations are meaningless.

Regarding the use of flat jacks on cob walls

The flat jack test is one of the most applied investigation techniques in the area of cultural heritage conservation, where the information obtained with this method is used, to assist in the structural safety evaluation of existent structures. Originally developed to be implemented in the field of rock mechanics, it has been adopted and used during the last four decades to determine in-situ the levels of stress and the mechanical properties of different types of masonry (ashlar, brick, stone) and earthen (adobe and rammed earth) walls. Despite its popularity and widely spread use by conservation engineers, there were no results available in the literature reporting the application of the at jack test in cob walls. The experimental campaign carried out and presented in this thesis provided the first results of a flat jack test ever performed in a cob wall, thus, it represents one of the main contributions of this thesis.

First of all, the importance of the consolidation of the wallettes highlighted by previous research (Lombillo, 2010) was verified in this thesis by comparing the stress/strain curves of the material before and after a six-day period of consolidation. Moreover, the stress/strain curves obtained from the second loading cycle of the wallettes allowed the Young's modulus of the material to be estimated.

Then, after performing single flat jack tests in each one of the wallettes subjected to a known level of stress a value of 0.51 was determined for the dimensionless coefficient K_e. It is advisable to apply this coefficient when investigation campaigns based on this minor destructive technique are performed on cob walls in order to obtain a more realistic

value of the stresses to which the test piece is being subjected to. This more realistic value would prevent the design and application of over invasive interventions that may place in danger the value of the historical fabric.

The double flat jack tests allowed the mechanical parameters of the material to be calculated. The Young's modulus of the material estimated by taking into account the slope of the elastic range of the stress/strain curves was in good agreement with the values obtained from the slope of the consolidation process' stress/strain curves. On the other hand, the secant Young's modulus values obtained in accordance with RILEM MDT D.5 and corrected by using a value of $K_e = 0.51$ resulted to be roughly 50 % smaller than the ones obtained from the slopes of the stress/strain curves. Therefore, it is advised not to correct the values obtained from the stress/strains ratios as per specified in ASTM C 1197, this would result into a more accurate estimation of cob's Young's modulus.

The values of cob's mechanical properties obtained in this experimental campaign are summarised in Table 7. 1 (repeated). The determination of the mechanical properties of cob is of outmost importance for the conservation of cob historical buildings. The parameters determined with the application of the flat jack test may be used to define the constitutive material models, such as the ones explored in Chapter 4 of this thesis, needed to perform structural analysis of the structure. The quality of the diagnosis and, subsequently, of the design of interventions would be subjected to the amount of information available and to the quality of such information. Therefore, the methodology and the values obtained in this thesis could greatly contribute to the conservation of cob buildings.

Table 7. 1, Cob's mechanical parameters values found in this experimental campaign (repeated).

Parameter	Value
Cylinders compressive strength (MPa)	0.70
Consolidation Young's modulus (MPa)	143.30
Dimensionless geometrical efficiency coefficient (-)	0.51
Flat Jack slope Young's modulus (MPa)	179.10
Flat Jack secant Young's modulus (MPa)	203.00
Flat Jack secant Young's modulus corrected (MPa)	103.50
Flat Jack Poisson's ratio (-)	0.28
Flat Jack compressive strength (MPa)	0.90

Regarding the parametric analysis of cob walls

The results obtained with the macro elements models were in general agreement with those of the FEM analyses. The expected negligible influence of the wall length on the

wall's out-of-plane response was confirmed by both analyses approaches. Similarly, the expected negligible influence of the wall thickness on the wall's in-plane response was also confirmed by both analyses approaches. Furthermore, both analyses results demonstrated that the cob wall, even under the "*worst-case scenario*" assumptions adopted, would not be damaged when subjected to the range of lateral accelerations expected.

Since the values for yield safety factors found were greater than one for all parameters combinations it can be concluded that the linear analysis would be valid for the analysis of surviving cob walls in Ireland, within the range of geometric parameters explored, at least for walls in similar conditions to the assumptions adopted. This may not hold true for decayed cob walls whose compressive strength is smaller than the values adopted based on those reported by the referenced authors (Miccoli *et al.*, 2014) or for walls with relatively high void/surface ratios.

It was identified that the possible failure modes the cob walls may present in case the studied parameters ranges were exceeded would be related to the out-of-plane behaviour/mechanisms. This fact was expected beforehand and confirmed by comparing the response parameters values found for each parametric analysis performed. Those values are presented in Table 7. 2 (repeated).

Table 7. 2. Critical response values obtained with the different parametric analysis performed (repeated).

Analysis type	Behaviour/Mechanism	Response	Value
FEM	In-plane	F_{ys}	5.2
		F_{us}	15.0*
	Out-of-plane	F_{ys}	1.1
		F_{us}	15.0*
Macro elements	In-plane	α	0.5
		$\alpha_{0.48MPa}$	0.4
		$\alpha_{1.59MPa}$	0.5
	Out-of-plane	α	0.1
		$\alpha_{0.48MPa}$	0.1
		$\alpha_{1.59MPa}$	0.1

*Cap value used by the software.

The advantages of the simplified FEM linear models used in the parametric analyses presented, as per comparison to the non-linear models studied in Chapter 4, in this thesis were:

- Easy model definition (no need for calibration of parameters to describe the complex stress-strain relationship characteristic of cob).

- Faster solution of the model, which allowed to run several simulations in a relatively short period of time to evaluate the design points and generate the response surfaces.
- Easier interpretation of the results, based in two response parameters, yield safety factor, F_{ys}, and ultimate safety factor, F_{us}.

Based on the results obtained with both simplified analyses traditional cob walls in Ireland could be described structurally as very robust. Due to the characteristics of the vernacular architecture typologies on the island (single story buildings with regular rectangular plans), low seismicity hazard levels and relatively big wall thicknesses, needed in principle for construction purposes, it was observed that cob walls would very rarely fail under the loads that they are normally subjected to. Proof of this fact are the many remaining cob buildings which, providing they had been adequately protected against rain and raising damp, have survived for hundreds of years in a relatively good state.

Equations derived solely on the geometry of the walls and the PGA values and presented after the results obtained from the parametrical analyses performed can be used by practitioners as a first approach to estimate the safety levels of existing cob buildings in Ireland as well as in other countries where buildings with similar characteristics exists such as in the UK and North of France. Nevertheless, it must be borne in mind that the assumptions adopted and the analyses performed to obtain them are of conservative nature. If their application resulted in the design of an over invasive intervention it is advised to carry out a more sophisticated analysis in order to try to obtain more accurate results, reduce the level of invasibility of the intervention and consequently preserve as much as possible the value of the structure and its original fabric.

Furthermore, the simple, but effective, methodology adopted to generate the parametric analysis presented in this thesis could be also used as part of a more complex seismic vulnerability analysis in countries located in moderate or high seismic hazard areas as it provides an efficient and relatively fast way to obtain an estimate of cob building's structural response.

Regarding the conservation of earthen vernacular architecture in Ireland

Traditional earthen vernacular buildings in Ireland serve as historical evidence of its past and have important socio-economic as well as intangible values attached to them. Unfortunately, little or no value is placed on their conservation and there is little academic or technical research to provide assistance for their conservation in Ireland.

Interventions on vernacular buildings should follow a conservative and sympathetic approach in agreement with the principles and guidance stablished on international conservation charters and research results published by several authors.

Conservation proposals by the authorities encompass the use of tourism, the reinforcement of the current preservation legislation, the creation of museums, and the reconstruction of houses belonging to historical characters. Hopefully with the adoption of the new national heritage plan, Heritage Ireland 2030, (which was being developed at the moment this thesis was written) the Government will increase and respect its commitment towards heritage conservation thus recognising the paramount role of heritage in the community, the economy and the society.

7.2 Future work

As a general extension/direct application of the novel work done and presented in this thesis: detailed cob's structural behaviour non-linear FEM simulations, cob's mechanical properties determined from the application of flat jack tests, and the information obtained from the parametric FEM and macro elements analyses, it could be used as the base to develop, or inform the development of, a code of practice for the conservation of cob buildings and the design of new cob walls. Moreover, the novel information generated during this research project can assist on the design of interventions and in the development of risk assessment procedures for cob structures situated in high seismic hazard regions.

A series of specific future work proposals are presented under three different headings: experimental work, numerical simulation, and sustainability and conservation.

7.2.1 Experimental work

- The experimental campaign performed in this thesis focused on the study of the flat jack technique to study cob walls. Other MDT techniques (see Table 2. 1 and Table 2. 2) have been developed and are currently used by conservators around the world to study masonry and earthen walls. Most of those techniques have never been experimentally validated to explore cob walls' properties. Thus, the possibility of exploring them in future projects is available. The implementation of several investigation techniques during the research stage of the conservation process would provide useful information to the conservators and guide them to better diagnose the causes of deterioration of historical structures.
- Experimental validation is also required for the assessment of repairing, strengthening and retrofitting interventions in cob walls. The efficiency of traditional intervention methods presented by several authors (Smith and Redman, 2009, Bhattacharya *et al.*, 2014, Ortega *et al.*, 2017), and already applied in different walls typologies, could also be tested for cob walls.
- The values obtained for cob's Poisson's ratio by applying the double flat jack test are twice the values available in the literature. Unfortunately, no alternative measurement method was undertaken in this experimental campaign and the validity of the values obtained cannot be properly assessed.
- Cob holds the promise of being a sustainable material. Studies regarding the thermal, hygroscopic and specially the embodied energy and the life cycle properties of cob walls need to be performed in order to verify this assumption. Besides from helping the conservation of the remaining historical cob buildings, those studies could foster the use of cob in contemporary and future sustainable architectural projects. In this regard, need for the development of a building code for cob is clear.

7.2.2 Numerical simulation

- The capabilities of the CDP material constitutive model explored in ABAQUS could be further explorer by studying the dynamic response of

cob walls in future research. Also a typology performance study of the remaining cob buildings in Ireland could be done to better assess their seismic behaviour as per indicated by Ortega *et al*. (2015). Very few resources are available in the published literature regarding cob's dynamic behaviour thus making this field a very good option to develop new contributions to the state of knowledge.

- As per the experimental case, numerical simulations could also be used to assess the efficiency of available repairing, strengthening and retrofitting interventions in cob walls.
- To use DLO for the study of cob buildings it would be necessary to adapt the method to solve plane stress and 3D problems and to extend the software capabilities. Nowadays, FEM remains the most valuable simulation tool for the study of cob structures but DLO definitely has lots of potential as stated by its developers.
- The bulging of the material between the flat jacks could be further investigated in a future work by developing a full 3D FEM model.
- Nevertheless, this material constitutive model can be defined in different terms, i.e. using a maximum stress or maximum strain criteria along with a continuum damage mechanics or with a material property degradation approach, and those approaches may provide better results. The DMGI/DMGE would have to be further study in future works before providing a definitive recommendation for its use to model cob structural behaviour.

7.2.3 Sustainability and conservation

The achievement of the UN SDGs is seriously compromised as highlighted in the last progress report at the time this thesis was being written (United Nations, 2019a). An overview on the progress of SDG 11 is shown in Figure 7. 1. Of special concern is the situation of Target 11.4: Strengthen efforts to protect and safeguard the world's cultural and natural heritage. No data exist to measure Indicator 11.4.1, which consists in the total expenditure per capita spent on the preservation, protection and conservation of all

cultural and natural heritage, consequently the progress on the achievement of Target 11.4 is not even being tracked nor discussed in the latest report presented by the UN.

If SDG 11, and specially Target 11.4, is to be achieved, the collaboration between member states and their contribution should be improved. Budget and infrastructure should be allocated to support the conservation of cultural heritage in their development plans. Local governments should support citizens and communities by implementing policies that allow to localise the global agenda by boosting policy initiatives, planning and infrastructural development towards the conservation of cultural heritage.

Figure 7. 1. Progress overview on the achievement of SDG 11: Make cities and human settlements inclusive, safe, resilient and sustainable (United Nations, 2019a).

A lot of work is required to ensure the constant protection of cultural heritage. Some activities specifically related to the conservation of earthen vernacular architecture in Ireland could be:

- Technical training, which is of paramount importance to avoid the disappearance of the Irish vernacular tradition and with it, irreplaceable knowledge and skills, should be taught and researched in a modern context in the universities of the country.

- Documentation and dissemination activities should be encouraged in order to increase awareness among the population regarding the importance of conservation of the remaining earthen vernacular buildings in the country.
- The creation and approval of a specialised conservation standard dealing specifically with cob would be of great help to protect and preserve such rich cultural heritage.

7.3 Publications

During this PhD project a series of publications were prepared. Some of which have already been published, whereas others have been recently submitted for publication. Journal papers are presented in Table 7. 3, papers included in conference proceedings and other publications are presented in Table 7. 4 and Table 7. 5, respectively.

Table 7. 3. Journal papers.

Reference
Jimenez, A. R., & O'Dwyer, D. (2019). Numerical modelling of cob´s non-linear monotonic structural behaviour. *International Journal of Computational Methods*. 1940013. https://doi.org/10.1142/S0219876219400139
Jiménez, A. R., & O'Dwyer, D. (Under review). Experimental validation for the application of the flat jack in cob walls. *Construction and Building Materials*.
Jiménez, A. R., & O'Dwyer, D. (Under review). Cob cylinders drying monitoring and compressive strength test data. *Data in Brief*.
Jiménez, A. R., & O'Dwyer, D. (Under review). Cob wallettes consolidation dataset. *Data in Brief*.
Jiménez, A. R., & O'Dwyer, D. (Under review). Data collected from the application of single flat jack tests in cob walls. *Data in Brief*.
Jiménez, A. R., & O'Dwyer, D. (Under review). Data collected from the application of double flat jack tests in cob walls. *Data in Brief*.
Jiménez, A. R., & O'Dwyer, D. (Under review). Adaptations of the flat jack test for its application in cob walls. *MethodsX*.
Jimenez, A. R., & O'Dwyer, D. (In preparation) Learning from the past: parametrical analysis of cob walls. *International Journal of Architectural Heritage*.

Table 7. 4. Conference papers.

Reference
Jimenez, A. R., Grimes, M. & O'Dwyer, D. (2020). *Experimental campaign on the use of the flat jack test in cob walls.* Abstract submitted to the 12 th International Conference on Structural Analysis of Historical Constructions (2020). Barcelona, Spain.
Jimenez, A. R., & O'Dwyer, D. (2018). *External post-tensioning system for the strengthening of historical stone masonry bridges.* Paper presented at the 11th International Conference on Structural Analysis of Historical Constructions. Cuzco, Peru.
Jiménez, A. R., & O'Dwyer, D. (2018). *Earhen buildings in Ireland*. Paper presented at the 6th International Congress on Construction History. Brussels, Belgium.
Jiménez, A. R., & O'Dwyer, D. (2018). *FEM non-linear modelling of cob using ANSYS.* Paper presented at the 9th International Conference on Computational Methods. Rome, Italy.

Table 7. 5. Other publications.

Reference
Jimenez, A. R. (2019). *Reuse and redevelopment proposal of Newtownbutler Market House and Lanesborough Hotel*. Poster presented at the 3rd Biennial Cross-Border "Conservation without Frontiers" Conference. Counties Fermanagh, Northern Ireland and Cavan, Ireland.
Jiménez, A. R. (2019), Cob wallettes' consolidation data, *Mendeley Data*, v1 http://dx.doi.org/10.17632/twbf86wxtx.1
Jiménez, A. R. (2019), Cob cylinder's data, *Mendeley Data*, v1 http://dx.doi.org/10.17632/h8ksd6mvkj.1

Appendices

The appendices referenced in this thesis can be found in the CD attached to the hard copy of this document.

- Appendix A: First findings on the analysis of cob using DLO.
- Appendix B: Data collected from the cob wallettes' consolidation process.
- Appendix C: Data collected from the single flat jack tests.
- Appendix D: Data collected from the double flat jack tests.
- Appendix E: Maximum principal strain and crack development figures for the different element sizes of the constitutive material models explored in Chapter 4.
- Appendix F: Parametric analysis of a cob wall supported at its base and lateral ends subjected to an out-of-plane acceleration.
- Appendix G: Flat jack test laboratory guidelines.

References

Aalen, Fred HA, Kevin Whelan and Matthew Stout (1997). *Atlas of the Irish rural landscape*, University of Toronto Press.

Aalen, Frederick HA (1966). "*The evolution of the traditional house in western Ireland*." The Journal of the Royal Society of Antiquaries of Ireland **96**(1): 47-58.

Aalen, Frederick Herman Andreasen (1978). *Man and the Landscape in Ireland*, Academic Press.

Abdunur, C (1983). *Stress and deformability in concrete and masonry*. IABSE Symposium on Strengthening of Building Structures-Diagnostic and Therapy, Venice, Italy.

Akinkurolere, OO, Cangru Jiang, AT Oyediran, OI Dele-Salawu and AK Elensinnla (2006). "*Engineering properties of cob as a building material*." Journal of Applied Sciences **6**(8): 1882-1885.

Almeida, C, J P Guedes, A Arêde, C Q Costa and A Costa (2012). "*Physical characterization and compression tests of one leaf stone masonry walls*." Construction Building Materials **30**: 188-197.

Amaco (2014). *Developing and understanding building materials*. France.

ANSYS Inc. (2013a). *ANSYS Design Exploration User's Guide*. Canonsburg, PA, ANSYS Inc.

ANSYS Inc. (2013b). *ANSYS Mechanical APDL Element Refernece*. Canonsburg, PA, ANSYS Inc.

ANSYS Inc. (2013c). *ANSYS Mechanical APDL Material Reference*. Canonsburg, PA, ANSYS Inc.

ANSYS Inc. (2013d). *ANSYS Mechanical APDL Theory Reference*. Canonsburg, PA, ANSYS Inc.

ANSYS Inc. (2013e). *ANSYS Mechanical User's Guide*. Canonsburg, PA, ANSYS Inc.

ANSYS Inc. (2017). *ANSYS® Academic Research Mechanical, Release 17.0*, ANSYS, Inc.

ASTM International (2009). *C 1196-09 Standard Test Method for In Situ Compressive Stress Within Solid Unit Masonry Estimated Using Flatjack Measurements*.

ASTM International (2010). *E2392/E2392M-10 Standard Guide for Design of Earthen Wall Building Systems*. United States, ASTM International**:** 10.

ASTM International (2011). *ASTM D6432-11, Standard Guide for Using the Surface Ground Penetrating Radar Method for Subsurface Investigation*. West Conshohocken, PA.

ASTM International (2012). *Standard Test Methods for Conducting Strength Tests of Masonry Wall Panels*.

ASTM International (2013a). *ASTM C1583 / C1583M-13, Standard Test Method for Tensile Strength of Concrete Surfaces and the Bond Strength or Tensile Strength of Concrete Repair and Overlay Materials by Direct Tension (Pull-off Method)*. West Conshohocken, PA.

ASTM International (2013b). *ASTM D4788-03(2013), Standard Test Method for Detecting Delaminations in Bridge Decks Using Infrared Thermography*. West Conshohocken, PA.

ASTM International (2013c). *ASTM E837-13a, Standard Test Method for Determining Residual Stresses by the Hole-Drilling Strain-Gage Method*.

ASTM International (2014). *C 1197-04 Standard Test Method for In Situ Measurement of Masonry Deformability Properties Using the Flatjack Method*.

ASTM International (2015a). *ASTM C1383-15, Standard Test Method for Measuring the P-Wave Speed and the Thickness of Concrete Plates Using the Impact-Echo Method*. West Conshohocken, PA.

ASTM International (2015b). *ASTM E494-15, Standard Practice for Measuring Ultrasonic Velocity in Materials*. West Conshohocken, PA.

ASTM International (2015c). *Standard Test Method for Diagonal Tension (Shear) in Masonry Assemblages*

ASTM INternational (2016). *ASTM C1531-16, Standard Test Methods for In Situ Measurement of Masonry Mortar Joint Shear Strength Index*. West Conshohocken, PA.

Astudillo, R. Pastor and P. Ruiz Garcia (1995). "*El ensayo de gato plano como técnica para la auscultación in situ de obras de fábrica*." Ingeniería Civil(98).

Aubert, Jean-Emmanuel, P Maillard, JC Morel and M Al Rafii (2016). "*Towards a simple compressive strength test for earth bricks?*" Materials and structures **49**(5): 1641-1654.

Avrami, Erica, Hubert Guillaud and Mary Hardy (2008). *Terra literature review An overview of research in earthen architecture conservation*. Los Angeles, USA, The Getty Conservation Institute.

Baker, Rafael and Sam Frydman (2009). "*Unsaturated soil mechanics: Critical review of physical foundations*." Engineering Geology **106**(1-2): 26-39.

Barbero, Ever J. and Mehdi Shahbazi (2017). "*Determination of material properties for ANSYS progressive damage analysis of laminated composites*." Composite structures **176**: 768-779.

Barroso, Cristina Alexandra de Jesus (2017). *Reforço sísmico inovador de construção de taipa*.

Bartoli, Gianni, Michele Betti and Saverio Giordano (2013). "*In situ static and dynamic investigations on the "Torre Grossa" masonry tower*." Engineering structures **52**: 718-733.

Bhattacharya, Subhamoy, Sanket Nayak and Sekhar Chandra Dutta (2014). "*A critical review of retrofitting methods for unreinforced masonry structures*." International Journal of Disaster Risk Reduction **7**: 51-67.

Binda, L, A Saisi, S Messina and S Tringali (2001). *Mechanical damage due to long term behaviour of multiple leaf pillars in Sicilian Churches*. III International Seminar on Structural Analysis of Historical Constructions, University of Minho.

Binda, Luigia, Antonella Saisi and Luigi Zanzi (2003). "*Sonic tomography and flat-jack tests as complementary investigation procedures for the stone pillars of the temple of S. Nicolò l'Arena (Italy)*." NDT & E International **36**(4): 215-227.

Binda, Luigia and Claudia Tiraboschi (1999). "*Fiat-Jack Test: A slightly destructive technique for the diagnosis of brick and stone masonry structures/Flachpressenprüfung: Eine zerstörungsarme Methode zur Untersuchung von Ziegel-und Natursteinmauenverk*." Restoration of buildings and monuments **5**(5): 449-472.

Boffill, Yosbel, Haydee Blanco, Ignacio Lombillo and Luis Villegas (2019). "*Device for continuous assessment of uniaxial stress of existing masonry structures: Laboratory validation*." Structural Control and Health Monitoring **26**(5): e2344.

Bosiljkov, Vlatko, Mojmir Uranjek, Roko Žarnić and Violeta Bokan-Bosiljkov (2010). "*An integrated diagnostic approach for the assessment of historic masonry structures*." Journal of Cultural Heritage **11**(3): 239-249.

BOVIAR (2012). *Diagnostica delle strutture, martinetti piatti*. BOVIAR. Italy.

Brencich, Antonio and Donato Sabia (2008). "*Experimental identification of a multi-span masonry bridge: The Tanaro Bridge*." Construction Building Materials **22**(10): 2087-2099.

Briceño, Carolina, Susana Moreira, Maria F. Noel, Mauricio Gonzales, Eduarda Vila-Chã and Rafael Aguilar (2018). "*SEISMIC VULNERABILITY ASSESSMENT OF A 17th CENTURY ADOBE CHURCH IN THE PERUVIAN ANDES*." International Journal of Architectural Heritage: 1-13.

British Standard (1990). *BS 1377-2:1990 Methods of Test for Soils for Civil Engineering Purposes - Part 2: Classification Tests*. United Kingdom, British Standard**:** 64.

British Standard (1999). *BS EN 1052-1:1999 Methods of test for masonry - Part 1: Determination of compressive strength*, BSI.

British Standard (2009a). *BS EN 12390-2:2009 Testing of hardening concrete, Part 2: Making and curing specimens for strength tests*.

British Standard (2009b). *BS EN 12390-3:2009 Testing of hardening concrete, Part 3: Compressive strength of test specimens*.

British Standard (2013). *Guide to the conservation of historic buildings*, British Standard.

British Standard (2016a). *BS 1377-1:2016 Methods of Test for Soil for Civil Engineering Purposes - Part 1: General Requirements and Sample Preparation*. United Kingdom, British Standard**:** 48.

British Standard (2016b). *Methods of test for mortar for masonry. Determination of adhesive strength of hardened rendering and plastering mortars on substrates*.

British Standard (2018a). *BS 1377-3:2018 Methods of Test for Soils for Civil Engineering Purposes - Part 3: Chemical and electro-chemical tests*. United Kingdom, British Standard**:** 98.

British Standard (2018b). *BS EN ISO 14688-1:2018 Geotechnical investigation and testing. Identification and classification of soil. Identification and description.*, BSI.

British Standard (2018c). *BS EN ISO 14688-2:2018 Geotechnical investigation and testing. Identification and classification of soil. Principles for a classification*, BSI.

British Standard (2018d). *BS EN ISO 17892-12:2018 Geotechnical investigation and testing - Laboratory testing of soil. Part 12: Determination of liquid and plastic limits.*, BSI.

Buson, Márcio, Nuno Lopes, Humberto Varum, Rosa Maria Sposto and Paulo Vila Real (2012). *Evaluation of performance under fire of compressed earth blocks*. 15th International Conference on Experimental Mechanics (ICEM15).

Cancino, Claudia, Dina D'Ayala, Sara Lardinois, Carina Fonseca Ferreira, Daniel Torrealva Dávila, Erika Vicente Meléndez and Luis Villacorta Santamato (2013). *Seismic retrofitting project: assessment of prototype buildings*, Getty Conservation Institute.

Carpinteri, A, S Invernizzi and G Lacidogna (2009). "*Historical brick-masonry subjected to double flat-jack test: Acoustic emissions and scale effects on cracking density*." Construction and building materials **23**(8): 2813-2820.

Carter, Michael and Stephen P Bentley (2016). *Soil properties and their correlations*, John Wiley & Sons.

Casarin, Filippo, Meir Ronen, Yaacov Schaffer, Raffaele Italia, Massimo dalla Benetta, Matthew R Kyler and Elvis Cescatti (2019). *Mechanical Characterization of Masonry Typologies in Israel via Flat Jack Tests*. Structural Analysis of Historical Constructions, Springer**:** 625-633.

CEN (2004). *BS EN 1998-1: 2004 Eurocode 8: Design of structures for earthquake resistance - Part 1: General rules, seismic actions and rules for buildings*.

CEN (2017). *EN 16853:2017 Conservation of cultural heritage - Conservation process - Decision making, planning and implementation*, British Standard.

Chesi, Claudio, Antonio Ingrassia and Valentina Sumini (2019). *Seismic Pounding Analysis of Palazzotto Borbonico "Vecchio" and "Nuovo" in Naples*. Structural Analysis of Historical Constructions, Springer**:** 1480-1488.

Chiu, Rebecca LH (2004). "*Socio-cultural sustainability of housing: a conceptual exploration*." Housing, theory and society **21**(2): 65-76.

Choi, HwanSuk Chris and Ercan Sirakaya (2006). "*Sustainability indicators for managing community tourism*." Tourism management **27**(6): 1274-1289.

Cid, J., F. R. Mazarron and I. Canas (2011). "*The earth building normative documents in the world*." Informes de la Construccion **63**(523): 159-169.

Circular Ecology. (2019). "*Embodied energy and carbon - The ICE database.*" Retrieved 05/10/2019, 2019, from http://www.circularecology.com/embodied-energy-and-carbon-footprint-database.html#.

Clough Ray, W and Penzien Joseph (1995). "*Dynamics of structures*." Computers & Structures, Inc.

Cloughjordan Ecovillage. (2019). "*Cloughjordan Ecovillage.*" Retrieved 15/04/2019, 2019, from http://www.thevillage.ie/.

Cob Research Institute (2019). *Proposal RB299-19 - Appendix U Cob Construction (Monolithic Adobe)*. Online, CRI.

Correia, Mariana, Gilberto Carlos and Sandra Rocha (2013). *Vernacular heritage and earthen architecture*, CRC Press.

Correia, Mariana, Letizia Dipasquale and Saverio Mecca (2014). *VERSUS: Heritage for Tomorrow*, Firenze University Press.

Correia, Mariana R, Paulo B Lourenço and Humberto Varum (2015). *Seismic Retrofitting: Learning from Vernacular Architecture*, CRC Press.

Council of Europe (1985). *Convention for the Protection of the Architectural Heritage of Europe*. C. o. Europe. Granada, Spain, Council of Europe**:** 8.

Cox, Ronald and Philip Donald (2013). *Ireland's Civil Engineering Heritage*, Cork: The Collins Press.

CSO. (2019). "*Population at Each Census 1841 to 2016 (Number) by Sex, County and Census Year*." Retrieved 06/08/2019, 2019, from https://www.cso.ie/px/pxeirestat/Statire/SelectVarVal/saveselections.asp.

Cundall, P. A. and O. D. L. Strack (1979). "*A discrete numerical model for granular assemblies*." Geotechnique **29**(1): 47-65.

Danachair, Caoimhin ó (1964). "*The combined byre-and-dwelling in Ireland*." Folk Life **2**(1): 58-75.

Danaher, Kevin (1957a). "*Materials and methods in Irish traditional building*." Royal Society of Antiquaries of Ireland **87**(1): 61-74.

Danaher, Kevin (1957b). "*Some distribution patterns in Irish folk life*." Bealoideas **25**: 108-123.

Danaher, Kevin (1970). *The pleasant land of Ireland*. Cork, Ire., Mercier Press.

Danaher, Kevin and Irish Tourist Board (1975). *Ireland's traditional houses*. Dublin, Bord Filte.

Dassault Systemes (2013). *Abaqus/CAE 6.13-1*. Providence, RI, USA, Dassault Systems Simulia Corp.

Dassault Systemes (2014). *ABAQUS analysis user's guide*. Providence, RI, Dassault Systemes Simulia Corp.

DCHG, Department of Culture Heritage and the Gaeltacht (1954). *National Monuments (Amendment) Act, 1954*. Ireland, DCHG, Department of Culture Heritage and the Gaeltacht.

DCHG, Department of Culture Heritage and the Gaeltacht (1987). *National Monuments (Amendment) Act, 1987*. Ireland, DCHG, Department of Culture Heritage and the Gaeltacht.

DCHG, Department of Culture Heritage and the Gaeltacht (1994). *National Monuments (Amendment) Act, 1994*. Ireland, DCHG, Department of Culture Heritage and the Gaeltacht.

DCHG, Department of Culture Heritage and the Gaeltacht (2004). *National Monuments (Amendment) Act, 2004*. Ireland, DCHG, Department of Culture Heritage and the Gaeltacht.

DCHG, Department of Culture Heritage and the Gaeltacht (2019). *Heritage Ireland 2030, Public Consultation*. Ireland, DCHG, Department of Culture Heritage and the Gaeltacht.

de Vekey, R. C. and J. S. Skandamoorthy (1997). "*Measurement of stress in Sandstone blockwork using flat jacks*." Masonry International **11**(2): 56-59.

de Vekey, RC (1995). *Thin stainless steel flat-jacks: calibration and trials for measurement of in-situ stress and elasticity of masonry*. Proc 7th Canadian Masonry Symposium, Hamilton.

Della Torre, Stefano, Lorenzo Cantini and Rossella Moioli (2019). *Stone masonry with brick stripe courses: study on a historical building technique diffused in Brianza district*. Structural Analysis of Historical Constructions, Springer**:** 275-284.

DIANA (2014). *TNO DIANA*. Delft, The Netherlands, TNO DIANA BV.

Doat, Patrice (1979). *Construire en terre*, CRAterre.

Dobson, Stephen (2000). *Continuity of tradition: new earth building*. Terra 2000**:** 275.

Domingos, Carlos Manuel Neves (2010). *Caracterização de edifícios antigos: edifícios pré-pombalinos*, Faculdade de Ciências e Tecnologia.

Dowling, DM, J Diaz and B Samali (2004). *Horizontal shear testing of mudbrick masonry mortar joints*. Australasian Masonry Conference, The University of Newcastle, NSW.

Dowling, DM, H Price and B Samali (2005). *Shear strength of adobe-mudbrick mortar joints*. Australian Structural Engineering Conference 2005, Engineers Australia.

DTTS (2015). *People, place and policy growing tourism to 2025*, Department of Transport, Tourism and Sport**:** 104.

ECORYS (2011). *Economic Value of Ireland's Historic Environment*. Online, Heritage Council.

English Heritage (2013). *English Heritage practical building conservation*. London Farnham, Surrey, English Heritage.

Epperson, Gary Stuart and Daniel Paul Abrams (1990). *Nondestructive evaluation of masonry buildings*, University of Illinois at Urbana-Champaign.

Fanale, Lorenzo, Dante Galeota and Antonio Pietrucci (2019). *Case Study: Assessment of the Load-Carrying Capacity of Multi-span Masonry Ancient Roman Arch Bridge Situated in "Campana", Near L'Aquila City (IT)*. Structural Analysis of Historical Constructions, Springer**:** 1027-1035.

Figueiredo, Bruno, Luis Lamas and Jose Muralha (2010). *Determination of in situ stresses using large flat jack tests*. ISRM International Symposium 2010 and 6th Asian Rock Mechanics Symposium - Advances in Rock Engineering. New Delhi, India.

Filipe, Marco Gonçalves (2012). *Caracterização de alvenarias antigas-ensaios de Flat Jack*, Universidade de Aveiro.

Forest Service (2008). *Irish forests, a brief history*, Department of Agriculture, Fisheries and Food.

Fredlund, Delwyn (2006). "*Unsaturated soil mechanics in engineering practice*." Journal of geotechnical geoenvironmental engineering **132**(3): 286-321.

Gailey, Alan (1984). *Rural houses of the north of Ireland*. Edinburgh, Donald.

Gandreau, David and Leticia Delboy (2012). *World Heritage Inventory of Earthen Architecture*. Grenoble, France, CRATerre-ENSAG.

Gelmi, A, C Modena, PP Rossi and A Zaninetti (1993). *Mechanical characterization of stone masonry structures in old urban nuclei*. Proc. of the 6th North American Masonry Conference, Philadelphia, Pennsylvania, USA.

GEO (2017). *LimitState GEO*. Sheffield, UK.

Geological Survey Ireland. (2019). "*Volcanoes.*" Natural Hazards Retrieved 05/04/2019, 2019.

Giamello, M, F Fratini, S Mugnaini, E Pecchioni, F Droghini, F Gabbrielli, E Giorgi, E Manzoni, F Casarin and A %J J. Mater. Environ. Sci Magrini (2016). "*Earth Masonries in the Medieval Grange of Cuna–Siena (Italy)*." **7**(10): 3509-3521.

Gilbert, Matthew and Colin C. Smith (2007). *Discontinuity layout optimization: A new numerical procedure for upper bound limit analysis*. IX International Conference on Computational Plasticity. E. Oñante and D. R. J. Owen. Barcelona, CIMNE.

GLÖTZL Baumeßtechnik (2003). *Flat Jack*. G. Baumeßtechnik. Germany.

Goodhew, Steven and Richard Griffiths (2005). "*Sustainable earth walls to meet the building regulations*." Energy Buildings **37**(5): 451-459.

Greer, Matthew James Addison (1996). "*The effect of moisture content and composition on the compressive strength and rigidity of cob made from soil of the Breccia measures near Teignmouth, Devon*."

Gregorczyk, Paweł and Paulo B Lourenço (2000). "*A review on flat-jack testing*." Engenharia Civil.

Guillaud, Hubert (2010). *Presentation Simplifiée Bilan sur le Fonctionnement 2002-2009 et Perspectives de Developpement 2010-2014*. Chaire UNESCO Architecture de Terre, Cultures Constructives et Developpement Dutable. France, CRATerre-ENSAG**:** 9.

Hamard, Erwan, Bogdan Cazacliu, Andry Razakamanantsoa and Jean-Claude Morel (2016). "*Cob, a vernacular earth constuction process in the context of modern sustainable building*." Building and environment **106**: 103-119.

Harries, R, D Clark and L Watson (2000). *A rational return to earth as a contemporary building material*. Terra 2000. J. Fidler. Devon, UK. **426:** 452.

Henry, Paul (1930). *A Connemara Village*. Online, National Gallery of Ireland.

Heritage Care (2017a). *General methodology for the preventive conservation of cultural heritage buildings***:** 165.

Heritage Care (2017b). *Survey of construction systems, type of damages and deterioration processes within the SUDOE territory.***:** 165.

Heritage Care (2017c). *Technical requirements for the tools to develop on the HeritageCare project***:** 165.

Heyman, Jacques (1982). *The masonry arch*. Chichester, Horwood.

Heyman, Jacques (1995). *The stone skeleton : structural engineering of masonry architecture*. Cambridge, Cambridge University Press.

Hillel, Daniel and Jerry L Hatfield (2005). *Encyclopedia of Soils in the Environment*, Elsevier Amsterdam.

Hillerborg, Arne, Mats Modéer and P-E Petersson (1976). "*Analysis of crack formation and crack growth in concrete by means of fracture mechanics and finite elements*." Cement and concrete research **6**(6): 773-781.

Historic England (2015). *Practical building conservation*. Farnham, Ashgate.

Hutton, Arthur Wollaston, Ed. (1892). *Arthur Young's tour in Ireland (1776-1779)*. London, George Bell.

ICOMOS (1931). *The Athens Charter for the Restoration of Historic Monuments*, ICOMOS.

ICOMOS (1964). *Decisions and Resolutions of the Second Congress of Architects and Specialists of Historic Buildings*. Second Congress of Architects and Specialists of Historic Buildings. Venice, ICOMOS.

ICOMOS (1980). *ICOMOS 1965-1980*. L. Hinsch. Oslo, Norway, ICOMOS**:** 30.

ICOMOS (1994). *The Nara Document on Authenticity*. Nara, Japan, ICOMOS.

ICOMOS (1999). *Charter on the built vernacular heritage*. Mexico, ICOMOS.

ICOMOS (2003a). *Guidelines for the Analysis, Conservation and Structural Restoration of Architectural Heritage*. Victoria Falls, Zimbabwe, ICOMOS.

ICOMOS (2003b). *Principles for the Analysis, Conservation and Structural Restoration of Architectural Heritage*. Vicoria Falls, Zimbabwe ICOMOS.

ICOMOS (2005). *The World Heritage List, Filling the Gaps - An Action Plan for the Future*. Monuments and Sites. J. Jokilehto, H. Cleere, S. Denyer and M. Petzet. Frnace, ICOMOS. **XII:** 109.

ICOMOS (2008). *Eger-Xi'an Principles for the International Scientific Committees of ICOMOS*. China, ICOMOS.

ICOMOS (2009). *Dubrovnik-Valletta Principles for the ICOMOS National Committees*. Online, ICOMOS**:** 6.

ICOMOS (2013). *The Australia ICOMOS Charter for Places of Cultural Significance*. Burra, Australia, ICOMOS.

ICOMOS (2018). *ICOMOS International Scientific Committees* Online, ICOMOS.

ICOMOS Ireland (1984). *Memorandum of Association of ICOMOS Ireland*.

ICOMOS Ireland. (2019). "*National Scientific Committees.*" Retrieved 05/01/2019, 2019, from http://www.icomos.ie/index.php/committees/vernacular.

ICOMOS UK Earth Structures Committee (2000). *Terra britannica; a celebration of earthen structures in Great Britain and Ireland*. London, UK, ICOMOS UK.

ISO (2010). *Bases for Design of Structures – Assessment of Existing Structures* Switzerland, ISO.

Jaquin, Paul and Charles Augrade (2012). *Earth building : history, science and conservation*. Bracknell, IHS BRE Press.

Jones, Craig (2019). *ICE (Inventory of Carbon and Energy)*. C. Ecology. Online.

Keefe, Laurence (1993). "*The cob buildings of Devon 1 & 2*." DHBT Devon.

Keefe, Laurence (2012). *Earth building : methods and materials, repair and conservation*, Routledge.

Köppen, Wladimir, Esther Volken and Stefan Brönnimann (2011). "*The thermal zones of the earth according to the duration of hot, moderate and cold periods and to the impact of heat on the organic world (Translated from: Die Wärmezonen der Erde, nach der Dauer der heissen, gemässigten und kalten Zeit und nach der Wirkung der Wärme auf*

die organische Welt betrachtet, Meteorol Z 1884, 1, 215-226)." Meteorologische Zeitschrift **20**(3): 351-360.

Kutarna, Matthew, Kevin Li and Ntokozo Radebe (2013). "*An investigation into the use of cob and/or straw bale construction in non-residential buildings*."

Laborel-Preneron, Aurélie, Jean-Emmanuel Aubert, Camille Magniont, Christelle Tribout and Alexandra Bertron (2016). "*Plant aggregates and fibers in earth construction materials: A review*." Construction and building materials **111**: 719-734.

Lagomarsino, Sergio, Andrea Penna, Alessandro Galasco and Serena Cattari (2013). "*TREMURI program: an equivalent frame model for the nonlinear seismic analysis of masonry buildings*." Engineering structures **56**: 1787-1799.

Ley, Tony and Mervyn Widgery (1997). "*Devon Earth Building Association: cob and the Building Regulations*." Structural Survey **15**(1): 42-49.

Lombillo, I, H Blanco, L Villegas, Y %J Construction Boffill and Building Materials (2018). "*Laboratory validation of the hole-drilling technique on the most common load-bearing walls used in heritage constructions*." **168**: 280-294.

Lombillo, I, L Villegas, E Fodde, C %J Construction Thomas and Building Materials (2014). "*In situ mechanical investigation of rammed earth: Calibration of minor destructive testing*." **51**: 451-460.

Lombillo, I, L Villegas, Enrico Fodde, Dina %J International Journal for Housing Science D'Ayala and Its Applications (2013). "*EXPERIMENTAL DIAGNOSIS OF EARTHEN CONSTRUCTION: CHARACTERIZATION AND IN-SITU ESTIMATION*." **37**(4).

Lombillo, Ignacio Vozmediano (2010). *Investigación teórico-experimental sobre ensayos ligeramente destructivos (MDT) utilizados para la caracterización mecánica in-situ de estructuras de fábrica del patrimonio construido.* PhD, Universidad de Cantabria.

Lourenço, P. B., Federica Greco, Alberto Barontini, Maria Pia Ciocci and Giorgos Karanikoloudis (2018). *Modeling of prototype buildings*, Getty Publications.

Lourenço, P. B. and Joao M. Pereira (2018). *Recommendations for advanced modeling of historic earthen sites*, Getty Publications.

Lourenço, P. B., G. Vasconcelos and L. Ramos (2001). "*Assessment of the stability conditions of a Cistercian cloister*." Studies in Ancient Structures: 669-678.

Lourenço, Paulo B (2002). "*Computations on historic masonry structures*." Progress in Structural Engineering Materials and structures **4**(3): 301-319.

Lourenço, Paulo B, Luís F Ramos, Graça Vasconcelos and Fernando Peña (2008). *Monastery of Salzedas (Portugal): Intervention in the cloister and information management*. Structural Analysis of Historic Construction: Preserving Safety and Significance, CRC Press**:** 106-119.

Lucy, L. B. (1977). "*A numerical approach to the testing of the fission hypothesis*." The Astronomical Journal **32**(12): 1013-1024.

Macdonald, Frank and Peigín Doyle (1997). *Ireland's earthen houses*. Ireland, A. & A. Farmar.

Maguire, Donal (2019). *Shaping Ireland: Landscapes in Irish Art*, National Gallery of Ireland.

Maheri, Mahmoud R, Alireza Maheri, Saeed Pourfallah, Ramin Azarm and Akbar Hadjipour (2011). "*Improving the durability of straw-reinforced clay plaster cladding for earthen buildings*." International Journal of Architectural Heritage **5**(3): 349-366.

Manzoni, Elena, Filippo Casarin, Silvia Dandria, Alberto Dusi, Marco Giamello, Elisabetta Giorgi, Fabio Gabbrielli, Andrea Magrini and Fausto Randazzo (2019). *The Medieval Grange of Cuna–Siena (Italy)-Interdisciplinary Studies on Masonry Structures*. Structural Analysis of Historical Constructions, Springer**:** 2350-2358.

MATLAB (2017). *MATLAB R2017b*. US, The MathWorks Inc.

McPadden, James and Sara Pavía (2016). *An assessment of raw materials for earth construction in County Offaly, Ireland.* REHABEND 2016. Burgos, Spain.

Miccoli, Lorenzo, Urs Müller and Patrick Fontana (2014). "*Mechanical behaviour of earthen materials: a comparison between earth block masonry, rammed earth and cob*." Construction and building materials **61**: 327 - 339.

Miccoli, Lorenzo, Rui A Silva, Daniel V Oliveira and Urs Müller (2019). "*Static Behavior of Cob: Experimental Testing and Finite-Element Modeling*." Journal of Materials in Civil Engineering **31**(4): 04019021.

Miccoli, Lorenzo, Rui Silva, Angelo Garofano and Daniel Oliveira (2017). *In-plane behaviour of earthen amterials: a numerical comparison between adobe masonry, rammed earth and cob.* 6th ECCOMAS Thematic Conference on Computational Methods in Structural Dynamics and Earthquake Engineering M. Papadrakakis and M. Fragiadakis. Rhodes Island, Greece.

MIDAS (2006). *MIDAS FEA Advanced Nonlinear and Detail Analysis System*, MIDAS Information Technology Co., Ltd.

Mileto, Camilla, Fernando Vegas, L García Soriano and Valentina Cristini (2014). *Vernacular architecture: Towards a sustainable future*, CRC Press.

Minitab (2013). *Minitab® 17.1.0*. Coventry, UK, Minitab Inc.

Minitab, INC (2003). "*MINITAB User's guide 2: data analysis and quality tools*." 2003.

Minke, Gernot (2000). *Earth construction handbook : the building material earth in modern architecture*. Southampton, Wit.

Minke, Gernot (2012). *Building with earth: design and technology of a sustainable architecture*, Walter de Gruyter.

Moevus, Mariette, Romain Anger and Laetitia Fontaine (2012). *Hygro-thermo-mechanical properties of earthen materials for construction: a literature review*. Terra 2012.

Montgomery, Douglas C. (2011). *Applied statistics and probability for engineers*. Hoboken, N.J., John Wiley.

Moquin, Michael (1994). "*Ancient solutions for future sustainability: Building with adobe, rammed earth, and mud*." CIB TG **16**: 543-552.

Motisi, Marco, Filippo Casarin, Gionata Rizzi, Franco Pianon, Alessandro Zamara and Lucia Gomez-Robles (2019). *The Bahrain Pearling Path: Urban Planning, Structural Investigation and Design of the Strengthening Interventions*. Structural Analysis of Historical Constructions, Springer**:** 1830-1838.

Nash, Clare (2016). *Contemporary vernacular design, how British housing can rediscover its soul*. Newcastle, UK, RIBA.

Neves, Célia Maria Martins (2003). *Técnicas de construcción con tierra*, PROTERRA, Proyecto XIV. 6, Tecnología de Construccíon con Tierra.

Ng, Charles Wang Wai and Bruce Menzies (2014). *Advanced unsaturated soil mechanics and engineering*, CRC Press.

NIAH. (2019). "*National Inventory of Architectural Heritage.*" Retrieved 15/05/2019, 2019, from http://www.buildingsofireland.ie/.

Nicholson, Asenath (1847). *Ireland's Welcome to the Stranger: Or An Excursion Through Ireland, in 1844 & 1845, for the Purpose of Personally Investigating the Condition of the Poor*, Baker and Scribner.

NIKER. (2013). "*NIKER Project.*" Retrieved 17/05/2019, 2019, from http://www.niker.eu/.

NOVATEST (2018). *Martinetti piatti, rectangolari e semicircolari*. NOVATEST. Italy.

NZS (1998a). *NZS 4297:1998 Engineering design of earth buildings*. Wellington, New Zealand, Standards New Zealand**:** 56.

NZS (1998b). *NZS 4298:1998 Materials and workmanship for earth buildings*. Wellington, New Zealand, Standards New Zealand**:** 82.

NZS (1998c). *NZS 4299:1998 Earth buildings not requiring specific design*. Wellington, New Zealand, Standards New Zealand**:** 122.

O'Reilly, Barry and Colm Murray (2005). *Traditional Buildings on Irish Farms*, The Heritage Council.

O'Riordan, Colum. (2014). "*An experiment in sustainable architecture.*" Retrieved 11/04/2019, 2019, from https://iarc.ie/blog/page/2/.

O'Rourke, Mona (2016). *Legislative Protection for the Built Heritage in Ireland***:** 20.

Oireachtas (1995). *Heritage Act, 1995*. H. Minister of Arts, Gaeltacht and the Islands. Ireland.

Oireachtas (1999). *Architectural Heritage (National Inventory) and Historic Monuments (Miscellaneous Provisions) Act, 1999*. H. Minister of Arts, Gaeltacht and the Islands. Ireland.

Oireachtas (2000). *Planning and Development Act, 2000*. Ireland, Oireachtas.

Oireachtas (2002). *Planning and Development (Amendment) Act, 2002*. Ireland, Oireachtas.

Oireachtas (2006). *Planning and Development (Strategic Infrastructure) Act, 2006*. Ireland, Oireachtas.

Oireachtas (2010). *Planning and Development (Amendment) Act, 2010*. Ireland, Oireachtas.

Oireachtas (2015). *Planning and Development (Amendment) Act, 2015*. Ireland, Oireachtas.

Oireachtas (2016). *Planning and Development (Housing) and Residential Tenancies Act, 2016*. Ireland, Oireachtas.

Oliver, Paul (2007). *Built to meet needs: Cultural issues in vernacular architecture*, Routledge.

Onsiteformasonry Project (2005). *On-site investigation techniques for the structural evaluation of historic masonry buildings Onsiteformasonry, Recommendations for the end users.* Florence, Italy, ZAG, BAM, SLG, POLIMI and RT.

Ortega, J, G Vasconcelos, PB Lourenço, H Rodrigues and H Varum (2015). "*Seismic behaviour assessment of vernacular isolated buildings*." Seismic retrofitting: learning from vernacular architecture. 1st ed. London: Taylor & Francis: 203-212.

Ortega, Javier, Graça Vasconcelos, Hugo Rodrigues, Mariana Correia and Paulo B Lourenço (2017). "*Traditional earthquake resistant techniques for vernacular architecture and local seismic cultures: A literature review*." Journal of Cultural Heritage **27**: 181-196.

Pacheco-Torgal, F and Said Jalali (2012). "*Earth construction: Lessons from the past for future eco-efficient construction*." Construction and building materials **29**: 512-519.

Parsekian, Guilherme, Douglas Barreto, Marcos Carilho, Vera Domschke and Fernando Fonseca (2019). *The Sobrado Vallim Rehabilitation Project*. Structural Analysis of Historical Constructions, Springer**:** 2285-2294.

Pfeiffer, Walter and Maura Shaffrey (1990). *Irish cottages*. London, Weidenfeld & Nicolson.

Piesik, Sandra (2017). *Habitat: Vernacular Architecture for a Changing Planet*. UK, Thames & Hudson Ltd.

Pullen, Quinn M and Todd V Scholz (2011). "*Index and Engineering Properties of Oregon Cob*." Journal of Green Building **6**(2): 88-106.

Quagliarini, Enrico and Gianluca Maracchini (2018). "*Experimental and FEM Investigation of Cob Walls under Compression*." Advances in Civil Engineering **2018**.

Rael, Ronald (2009). *Earth architecture*, Princeton architectural press.

Rafi, Muhammad Masood and Sarosh Hashmat Lodi (2017). "*Comparison of dynamic behaviours of retrofitted and unretrofitted cob material walls*." Bulletin of Earthquake Engineering **15**(9): 3855-3869.

Rafi, Muhammad Masood, Sarosh Hashmat Lodi and Saad Ahmed Qazi (2018). "*Dynamic Testing of Seismic Resistant Cob Structure for Post-Earthquake Reconstruction*." Journal of Earthquake Engineering: 1-22.

Rapoport, Amos (1969). *House form and Cultua*, New Delhi: Prentice-hall of India Private Ltd.

Reardon, Chris (2013). *Your Home: Australia's Guide to Environmentally Sustainable Homes*. Australia, Department of Industry.

Reddy, BV Venkatarama and KS Jagadish (2003). "*Embodied energy of common and alternative building materials and technologies*." Energy Buildings **35**(2): 129-137.

Reeners, Roberta (2003). *A Wexford farmstead, the conservation of an 18th-century farmstead at Mayglass*. Ireland, Criterion Press.

RILEM (1994a). *Compendium comp012 : RILEM Recommendations for the Testing and Use of Constructions Materials*. LUM.C.1 Compressive strength of walls and other elements, E & FN SPON**:** 490 - 492.

RILEM (1994b). *Compendium comp012 : RILEM Recommendations for the Testing and Use of Constructions Materials*. LUM C2 Full-scale wall out-of-plane flexural test, 1991, E & FN SPON**:** 493 - 496.

RILEM (1994c). *Compendium comp012 : RILEM Recommendations for the Testing and Use of Constructions Materials*. LUM C3 Cyclic shear test for masonry panels designed to resist seismic forces, 1991 E & FN SPON**:** 497 - 500.

RILEM (1997). "*RILEM Recommendation TC 127-MS, "MS.D.1 Measurement of mechanical pulse velocity for masonry"*." Materials and structures **30**: 463-466.

RILEM (2004a). *RILEM Recomendations MDT. D. 4. In-situ stress tests based on the flat-jack*. Masonry durability and on-site testing**:** 491 - 496.

RILEM (2004b). *RILEM Recommendation MDT. D. 5: In-situ stress-strain behavior tests based on the flat jack*. Masonry durability and on-site testing**:** 497-501.

Ritchie, Colin and Feile Butler. (2019). "*Mud and Wood.*" Retrieved 11/04/2019, 2019, from http://www.mudandwood.com/index.html.

Rizza, Michael Scoles and Hana Mori Böttger (2013). *Effect of Straw Length and Quantity on Mechanical Properties of Cob*, University of San Francisco Press.

Roca, Pere, Miguel Cervera and Giuseppe Gariup (2010). "*Structural analysis of masonry historical constructions. Classical and advanced approaches*." Archives of Computational Methods in Engineering **17**(3): 299-325.

Rossi, Pier Paolo (1980). "*Prove distruttive e non distruttive per la caratterizzazione meccanica dei materiali*." ISMES Bollettino(130).

Rossi, Pier Paolo (1982a). *ANALYSIS OF MECHANICAL CHARACTERISTICS OF BRICK MASONRY BY MEANS OF NON-DESTRUCTIVE'IN-SITU' TESTS*. Proc. 6 th Int. Brick Masonry Conf.(6 th I. B. Ma. C.) held in Rome, 16-19 May, 1982. Rome.

Rossi, Pier Paolo (1982b). "*Analysis of mechanical characteristics of brick masonry by means of non-destructive in-situ tests*." Proc. 6th LBMaC, Roma.

Rossi, Pier Paolo (1987a). *Flat jack test for the analysis of mechanical behaviour of brick masonry structures*, ISMES.

Rossi, Pier Paolo (1987b). *Recent developments of the flat-jack test on masonry structures*, ISMES.

Rossi, Pier Paolo (1995). *Analisi delle condizioni statiche della Basilica di San Marco in Venezia*, Convegno per il IX centenario della Dedicazione della Basilica di S. Marco ….

Rossi, Pier Paolo, Alberto Peano and Edmondo Carabelli (1982). *Determinazione sperimentale delle caratteristiche meccaniche delle murature*. Comportamento statico delle strutture murarie**:** 89-131.

Rossi, Pier Paolo and M. Vavassori (1992). *Il sistema di monitoraggio delle torri e del Duomo di Pavia*. SAIE 1992. Bologna, Italy.

Rossi, Pier Paolo and S Zaldivar (1996). *Testing and monitoring for the restoration of the Metropolitan Cathedral in Mexico City*. Int. Conference, Napoli.

Rudofsky, Bernard (1964). *Architecture without architects: a short introduction to non-pedigreed architecture*, UNM Press.

Rufo, Rafael José Gonçalves (2010). *Ensaios de caracterização mecânica das alvenarias de adobe: flat-jack testing*, Universidade de Aveiro.

Saisi, Antonella, Stefania Terenzoni, Antonello Ruccolo and Carmelo Gentile (2019). *Safety of the Architectural Heritage: Structural Assessment of the Zuccaro's Tower in Mantua*. Structural Analysis of Historical Constructions, Springer**:** 2422-2430.

Saxton, R. H. (1995). "*Performance of cob as a building material*." Structural Engineer **73**(7): 111-115.

Schroeder, Horst (2016). *Sustainable building with earth*, Springer.

SEAI (2016). *Ireland's Energy Targets: Progress, Ambition & Impacts*, The Sustainable Energy Authority of Ireland.

Seo, Seongwon and Yongwoo Hwang (2001). "*Estimation of CO2 emissions in life cycle of residential buildings*." Journal of Construction Engineering Management **127**(5): 414-418.

Shaffrey, Patrick and Maura Shaffrey (1985). *Irish countryside buildings : everyday architecture in the rural landscape*. Dublin, The O'Brien Press.

Shukla, Shivangi (2016). *Seismic strengthening of rammed earth constructions using reinforced coatings*.

Siano, Rossella, Vincenzo Sepe, Guido Camata, Enrico Spacone, Pere Roca and Luca Pelà (2017). "*Analysis of the performance in the linear field of Equivalent-Frame Models for regular and irregular masonry walls*." Engineering structures **145**: 190-210.

Simões, A., R. Bento, A. Gago and M. Lopes (2016). "*Mechanical characterization of masonry walls with flat-jack tests*." Experimental Techniques **40**(3): 1163-1178.

SISGEO (2015). *Flat jacks testing accessories, pressure and load cells*. SISGEO. Italy.

Smith, Andrew and Thomas Redman (2009). *A critical review of retrofitting methods for unreinforced masonry structures*. EWB-UK research conference, Citeseer.

Solomos, G., A. Pinto and S. Dimova (2008). *A review of the seismic hazard zonation in national building codes in the context of Eurocode 8*. JRC Scientific and Technical Reports. J. E. Commission. Italy.

Stokes, Alan (2008). *Cob dwellings, compliance with the building regulations 2000 (as amended)*. Online, Devon Earth Buildings Association**:** 21.

Sumitro, S, K Hida and T Le Diouron (2003). *Structural health monitoring paradigm for concrete structures*. 28th Conference on Our World In Concrete & Structures, Singapore.

Szczecina, Michal and Andrzej Winnicki (2015). *Calibration of the CDP model parameters in ABAQUS*. 2015 World Congress on Advances in Structural Engineering and Mechanics, ASEM15. Incheon, Korea.

Tacas Guillen, Kiyoshi (2018). *Ensayo de flat jack como herramienta para la determinación del comportamiento mecánico de construcciones de adobe*, Pontificia Universidad Católica del Perú.

Tacas, Kiyoshi, Mauricio Gonzales and Rafael Aguilar (2019). *Mechanical Characterization of Adobe Constructions Using Flat Jack Tests: Case Study of the Virgen de la Asunción de Sacsamarca Church*. Structural Analysis of Historical Constructions, Springer**:** 706-715.

Tecchio, G, F Da Porto, P Zampieri, C Modena and C Bettio (2012). *Static and seismic retrofit of masonry arch bridges: case studies*. Proceedings of the 6th International Conference on Bridge Maintenance and Safety (IABMAS'12), Lake Maggiore, Italy.

Teixeira, Tania, Corinna Konig and Ulrike Schwantner (2018). *BASEhabitat Summer School 2018 Handbook*. Linz, Austria, BASEhabitat.

Terra Incognita (2011). *Terra Europae, Earthen Architecture in the European Union*

Terzaghi, Karl, Ralph B Peck and Gholamreza Mesri (1996). *Soil mechanics in engineering practice*, John Wiley & Sons.

The Hollies. (2019). "*The Hollies: Centre for Practical Sustainability.*" Retrieved 11/04/2019, 2019, from https://www.thehollies.ie/.

Tolles, E Leroy, Edna E Kimbro and William S Ginell (2003). *Planning and engineering guidelines for the seismic retrofitting of historic adobe structures*, Getty Publications.

Torrealva, Daniel, Erika Vicente and Tim Michiels (2018). *Testing of materials and building components of historic adobe buildings in Peru*, Getty Publications.

Trinity College Dublin. (2019a). "*Green week.*" Retrieved 01/07/2019, 2019, from https://www.tcd.ie/provost/sustainability/greenweek/.

Trinity College Dublin. (2019b). "*Postgraduate Diploma in Applied Building Repair and Conservation.*" Retrieved 05/01/2019, 2019, from https://www.tcd.ie/civileng/diploma-in-applied-building-repair-and-conservation/.

UNESCO (1956). *UNESCO 9th General Conference*. New Delhi, UNESCO**:** 6.

UNESCO (1972). *Convention Concerning the Protection of the World Cultural and Natural Heritage*. France, UNESCO**:** 16.

UNESCO (2005). *The 2005 Convention on the Protection and Promotion of the Diversity of Cultural Expressions*. France, UNESCO**:** 52.

UNESCO (2007). *World Heritage 31 COM WHC-07/31.COM/21C*. Christchurch, New Zealand, UNESCO. **31:** 8.

UNESCO (2010). *UNESCO at a glance*. UNESCO website. UNESCO. Online, UNESCO.

UNESCO (2013). *The Hangzhou Declaration*. UNESCO. Hangzhou, People's Republic of China, UNESCO.

UNESCO. (2019). "*World Heritage List Statistics.*" Retrieved 08/07/2019, 2019, from https://whc.unesco.org/en/list/stat.

UNESCO WHC (2008). *World Heritage Information Kit*. France, UNESCO WHC**:** 30.

UNESCO WHC (2016). *Operational Guidelines for the Implementation of the World Heritage Convention*. France, UNESCO WHC**:** 167.

UNESCO WHC. (2019). "*Brú na Bóinne - Archaeological Ensemble of the Bend of the Boyne.*" Retrieved 06/01/2019, from http://whc.unesco.org/en/list/659/.

United Nations (2015a). *Paris agreement*.

United Nations (2015b). *A/RES/10/1 Transforming Our World: the 2030 Agenda for Sustainable Development*, United Nations. **70:** 35.

United Nations. (2018a). "*Sustainable Development Goals.*" Retrieved 13/11/2018, 2018, from https://www.un.org/sustainabledevelopment/.

United Nations (2018b). *Tracking Progress Towards Inclusive, Safe, Resilient and Sustainable Cities and Human Settlements, SDG 11 Synthesis Report*. High Level Political Forum 2018, United Nations**:** 114.

United Nations (2019a). *The Sustainable Development Goals Report 2019*. Online, United Nations.

United Nations. (2019b). "*UNdata a World of Information.*" Retrieved 03/04/2019, 2018, from http://data.un.org/en/iso/ie.html.

Valluzzi, MR, Marco Munari, Claudio Modena, Luigia Binda, Giuliana Cardani and A Saisi (2007). "*Multilevel Approach to the Vulnerability Analysis of Historic Buildings in Seismic Areas Part 2: Analytical Interpretation of Mechanisms for Vulnerability Analysis and Structural Improvement/Ansatz zur Analyse der Empfindlichkeit historischer Gebäude in Erdbeben gefährdeten Zonen auf mehreren Ebenen; Teil 2: Analytische Interpretation der Mechanismen für eine Empfindlichkeitsanalyse und für das Ertüchtigen von Tragwerken*." Restoration of buildings and monuments **13**(6): 427-442.

Vinceslas, Théo, Erwan Hamard, Andry Razakamanantsoa and Fateh Bendahmane (2018). "*Further development of a laboratory procedure to assess the mechanical performance of cob*." Environmental Geotechnics: 1-8.

Walsh, Seamus (2012). *A summary of climate averages for Ireland 1981-2010*. Dublin, Ireland, Met Eireann.

Watson, L. and K. McCabe (2011). "*The cob building technique. Past, present and future*." Informes de la construcion **63**(523): 59-70.

Webster, Frederick A (2006). *Application of stability-based retrofit measures on some historic and older adobe buildings in California*. Proceedings of the Getty Seismic Adobe Project 2006 Colloquium, Getty Center, Los Angeles, April 11–13.

Wilkinson, Brian (2009). "*A Study of Turf: Historic Rural Settlements in Scotland and Iceland*." Architectural Heritage: 15-31.

William, K. and E. Warnke (1974). *Constitutive model for the triaxial behaviour of concrete*. IABSE reports of the working commissions = Rapports des commissions de travail AIPC = IVBH Berichte der Arbeitskommissionen. Seminar on concrete structures subjected to triaxial stresses. Bergamo, Italy**:** 1-30.

Wilson, Alex (1998). "*Thermal mass and R-value: making sense of a confusing issue*." Environmental Building News **7**(4).

Winston, Nessa (2012). *Sustainable housing: A case study of the Cloughjordan Eco-village*, Emerald, Bingley, UK.

Wu, Zheng Ping and YuanTong Gu (2011). "*Prediction of structural integrity, robustness, and service life using advanced finite element methods*." International Journal of Computational Methods **8**(04): 787-800.

Xavier, Rui Pedro Mendes (2011). *Ensaios de caracterização de alvenarias de adobe*, Universidade de Aveiro.

Young, Arthur (1780). *A tour in Ireland; : with general observations on the present state of that kingdom, made in the years 1776, 1777, and 1778, and brought down to the end of 1779, / by Arthur Young, Esq; F.R.S***:** 0-9.

YS. (2019). "*Typical weights of building materials.*" Retrieved 17/05/2019, 2019, from https://www.yourspreadsheets.co.uk/typical-weights-of-building-materials.html.

Zami, Mohammad Sharif and Angela Lee (2010). "*Economic benefits of contemporary earth construction in low-cost urban housing–state-of-the-art review*." Journal of Building Appraisal **5**(3): 259-271.

Ziegert, C. (2003). *Lehmwellerbau: Konstruktion, Schäden und Sanierung*, Fraunhofer-IRB-Verlag.

Zienkiewicz, O. C. (2013). *The finite element method : its basis and fundamentals*. Oxford, Butterworth-Heinemann.